INVESTIGATION OF CANDIDATE BIOMARKERS IN GRAVES' DISEASE AND THYROID-ASSOCIATED OPHTHALMOPATHY

by

MATTHEW ROSS EDMUNDS

A thesis submitted to the
University of Birmingham
for the degree of
DOCTOR OF PHILOSOPHY

Academic Unit of Ophthalmology
School of Immunity and Infection
College of Medical and Dental Sciences
University of Birmingham

July 2014

Abstract

Thyroid-Associated Ophthalmopathy (TAO) is a debilitating inflammatory condition of the orbit occurring in 30-50% of Graves' Disease (GD) patients. It is not currently possible to predict which GD patients will develop TAO or the severity of their eventual ophthalmic manifestations. The aim of this thesis was to evaluate novel biomarkers for this purpose.

I developed two immunoassays to detect serum antibodies to insulin-like growth factor-1 receptor (IGF-1R-Ab) in GD, TAO and healthy controls (HC). Assays were validated to measure commercial monoclonal IGF-1R-Ab but no study group differences, or correlation with clinical activity or severity, were noted with sera.

Differential IGF-1R expression on peripheral blood CD4+ and CD8+ T lymphocyte memory subsets was observed, although without variance between groups. However, T cell differentiation was perturbed, with elevated proportions of naïve, and reduced cytokine-producing effector memory T cells, in GD and TAO compared to HC.

Nuclear magnetic resonance-based serum metabolomic analysis differentiated GD and TAO subjects, and varying TAO clinical activity, with good uncorrected sensitivity and specificity. Distinguishing metabolites included lactate, isopropanol, methylguanidine and pyruvate.

Collectively these data cast doubt on a simple model of IGF-1R-Ab being responsible for orbital inflammation in GD, but highlight the biomarker potential of metabolomics in TAO.

Dedication

In memory of

Linda Joyce Harry (née Martin)

12.09.1954 – 12.08.2001

Acknowledgements

First, I would like to thank my supervisors, Dr. John Curnow and Mr. Omar Durrani for making this project possible. Their support, advice and guidance through all aspects of my PhD – assisting with the ethics process, imparting clinical and immunological knowledge and directing research methodology - has been invaluable. I am also very grateful to the Wellcome Trust for generously sponsoring my fellowship.

I am extremely grateful to my many collaborators and co-investigators, including: Ali Bodla, Kristien Boelaert, Robert Barry, Rachel Bayley, Hema Chahal, Alastair Denniston, Lindsay Durant, Rebecca Ford, Martin Fitzpatrick, Jayne Franklyn, Julia Hale, Peter Hampson, Ghaniah Hassan-Smith, Julie Huntbach, Katherine Howlett, Philip Murray, Peter Nightingale, Siobhan Restorick, Jane Smith, Saaeha Rauz, Sue Southworth, Marie Voice, Graham Wallace, Geraint Williams, Emma Yates and Stephen Young, who have been enormously generous with their time and efforts in supporting my endeavours. I would also like to thank the many, many patients who have been so generous and giving of their time.

Finally, and most important, I would like to thank my wife Jenny for her amazing, unwavering support and encouragement throughout. She, and our lovely children Jacob and Isobel, have given me focus and purpose, particularly at difficult times, and have always been a pleasure to return home to after a tough day in the lab.

Graves' Disease and Thyroid-Associated Ophthalmopathy:

A Historical Perspective

I have lately seen three cases of violent and long-continued palpitations in females, in each of which the same peculiarity presented itself – viz., enlargement of the thyroid gland; the size of this gland, at all times considerably greater than natural, was subject to remarkable variations in every one of these patients.

In one, the beating of the heart could be heard during the paroxysm at some distance from the bed – a phenomenon I had never before witnessed, and which strongly excited my attention and curiosity…….. I could distinctly hear the heart beating when my ear was distant at least four feet from her chest!

A lady, aged twenty, became affected with some symptoms which were supposed to be hysterical. This occurred more than two years ago; her health previously had been good. After she had been in this nervous state about three months, it was observed that her pulse had become singularly rapid. This rapidity existed without any apparent cause, and was constant, the pulse being never under 120, and often much higher. She next complained of weakness on exertion, and began to look pale and thin. Thus she continued for a year, but during this time she manifestly lost ground on the whole, the rapidity of the heart's action having never ceased.

In a few months, the action of the heart continuing with unceasing violence, a tumour, of a horseshoe shape, appeared on the front of the throat and exactly in the situation of the thyroid gland. This was at first soft, but soon attained a greater hardness, though still elastic. From the time it was first observed, it has increased little, if at all, in size and is now about thrice the natural bulk of the fully developed gland in a female after the age of puberty.

It was now observed that the eye assumed a singular appearance, for the eyeballs were apparently enlarged, so that when she slept, or tried to shut her eyes, the lids were incapable of closing. When the eyes were open, the white sclerotic could be seen, to a breadth of several lines, all round the cornea.

Graves RJ. Newly observed affection of the thyroid gland in females. From the clinical lectures delivered by Robert J. Graves, MD, at the Meath Hospital, during the session of 1834-35. London Medical and Surgical Journal 1835; 7:516-517.

Cited by Major RH. Classic descriptions of disease with biographical sketches of the authors. Springfield, IL: CC Thomas, 1978: 279-281.

Table of Contents

List of Figures

List of Tables

List of Common Abbreviations Used

AITD	Autoimmune Thyroid Disease
APC	Allophycocyanin
BMEC	Birmingham and Midland Eye Centre
cAMP	Cyclic Adenosine Monophosphate
CAS	Clinical Activity Score
CBZ	Carbimazole
CD	Cluster of Differentiation
CM	Central Memory
CO_2	Carbon Dioxide
CTLA-4	Cytotoxic T Lymphocyte Associated Antigen-4
Cy5	Cyanine 5
Cy7	Cyanine 7
EDTA	Ethylene Diamine Tetra Acetic acid
EM	Effector Memory
EMRA	Effector Memory RA
EOM	Extraocular Muscle
ERK	Extracellular Signal-Regulated Kinases
EUGOGO	European Group on Graves' Orbitopathy
FCS	Foetal Calf Serum
FoxP3	Forkhead Box Protein 3
FITC	Fluorescein Isothiocyanate
GAG	Glycosaminoglycan
GD	Graves' Disease
GPS	L-glutamine, benzylpenicillin, streptomycin
GPx	Glutathione Peroxidase
HC	Healthy Controls
HIFCS	Heat-Inactivated Foetal Calf Serum
HOAT	Human Orbital Adipose Tissue
HLA	Human Leucocyte Antigen
^{131}I	Radioiodine or Radioactive Iodine

Ig	Immunoglobulin
IL	Interleukin
IFN-γ	Interferon-γ
IGF-1R	Insulin-like Growth Factor-1 Receptor
IGF-1R-Ab	Insulin-like Growth Factor-1 Receptor Antibody
MFI	Median Fluorescence Intensity
MHC	Major Histocompatibility Complex
MMZ	Methimazole
MS	Multiple Sclerosis
NMR	Nuclear magnetic resonance
PBMC	Peripheral Blood Mononuclear Cells
PCA	Principal Components Analysis
PE	Phycoerythrin
PETR	Phycoerythrin Texas Red
PGE-2	Prostaglandin E-2
PGHS	Prostaglandin Endoperoxide-H Synthase-2
PLS-DA	Partial Least Squares Discriminant Analysis
PMA	Phorbol 12-Myristate 13-Acetate
PTU	Propylthiouracil
RA	Rheumatoid Arthritis
RANTES	Regulated on Activation, Normal T Expressed and Secreted
ROS	Reactive Oxygen Species
RPMI 1640	Roswell Park Memorial Institute Medium 1640
SLE	Systemic Lupus Erythematosus
SOD	Superoxide Dismutase
TAO	Thyroid-Associated Ophthalmopathy
TBII	Thyroid Stimulating Hormone Binding Inhibitory Immunoglobulin
TC	Thionamide Control
TCR	T Cell Receptor
TG	Thyroglobulin
Th	T helper
TNF	Tumour Necrosis Factor

TPO	Thyroid Peroxidase
Treg	Regulatory T Cell
TRAb	Thyroid Stimulating Hormone Receptor Antibody
TSAb	Thyroid Stimulating Hormone Antibody
TBAb	Thyroid Stimulating Hormone Blocking Antibody
TSH	Thyroid Stimulating Hormone
TSH-R	Thyroid Stimulating Hormone Receptor
TSI	Thyroid-Stimulating Immunoglobulin

1 GENERAL INTRODUCTION

1.1 Thyroid-Associated Ophthalmopathy and Graves' Disease

Thyroid-Associated Ophthalmopathy (TAO), also known as Thyroid Eye Disease (TED), Graves' Orbitopathy (GO), Graves' Ophthalmopathy, Endocrine Orbitopathy and Ophthalmic Graves' Disease, is an inflammatory condition of the orbit, associated with autoimmune thyroid diseases (AITD), particularly Graves' disease (GD).[1] TAO constitutes a major clinical and therapeutic challenge and is the commonest and most important extrathyroidal manifestation of GD.[2]

Figure 1.1: Typical clinical features in a variety of TAO patients demonstrating the heterogeneous nature of ophthalmic manifestations. Patients with moderate disease severity but clinically inactive TAO (A & B) and severe, sight-threatening and active TAO (C). Clinical features include eyelid retraction, proptosis (asymmetrical in each of these subjects), conjunctival injection and caruncular swelling (Images used with the permission of the patients and of Mr. O. Durrani, Consultant Ophthalmologist, Birmingham & Midland Eye Centre).

GD is an autoantibody-mediated, multisystem, autoimmune disorder affecting the thyroid gland, with additional connective tissue manifestations of the orbital tissues and, more rarely, the pre-tibial skin and the acra of the finger.[3] The orbital manifestations (**Figure 1.1**) of GD do not appear to be a direct effect of hyperthyroidism, rather a reflection of the underlying autoimmunity, as patients need not be thyrotoxic to develop TAO.[4]

1.2 Graves' Disease

In GD, IgG antibodies (GD-IgG) bind to the thyroid-stimulating hormone receptor (TSH-R) on thyroid epithelial cells. These TSH-R antibodies (TRAb) modulate thyroid function in a number of different ways, with either thyroid-stimulating antibodies (TSAb), thyroid-blocking antibodies (TBAb) or antibodies with neutral properties.[5]

TSAb mimic the actions of thyroid stimulating hormone (TSH) but are not subject to negative feedback by the hypothalamic-pituitary-thyroid axis. This results in TSH-R activation with overproduction of thyroid hormone, leading to increased thyroid gland size (goitre) and overproduction of thyroid hormones.[6,7] Histological changes in the thyroid gland in GD include follicular hyperplasia and hypertrophy, vascular congestion, reduction in follicular colloid, with colloid droplets and scalloping and a predominant T cell infiltrate.[8] This may result in hyperthyroidism, with high serum free tetraiodothyronine (T4, also known as thyroxine) and triiodothyronine (T3) and low or undetectable TSH. T3 and T4 activate the sympathetic nervous system, so typical symptoms of GD include palpitation (due to tachycardia or arrhythmia), tremor, weight loss, sweating, anorexia, heat intolerance, disruption of the menstrual cycle in women, difficulty swallowing (or perhaps breathing) due to retrosternal goitre (causing extrinsic compression of the oesophagus or trachea).

Importantly, thyrotoxicosis refers to the biochemical and physiological manifestations of excessive thyroid hormone whereas hyperthyroidism is the over production of thyroid hormone by the thyroid gland. In addition to TRAb, antibodies generated to

thyroid peroxidase (TPO-Ab) or thyroglobulin (TG-Ab) can also be detected, in around 70% of patients with GD.[9-11]

Although many manifestations of GD can be attributed to TSAb, the pathogenic basis for extrathyroidal manifestations, including TAO, remain poorly understood and, to some extent, controversial. It is generally agreed that autoimmunity to thyroid-related antigens occurs in the context of both genetic susceptibility and environmental risk factors but the exact molecular basis for the extrathyroidal manifestations of GD, including TAO, are not known.

Overall, 90% of patients with TAO are hyperthyroid at presentation, with 6% presenting as euthyroid, 3% with another form of AITD, Hashimoto's thyroiditis,[12] and 1% with primary hypothyroidism.[13-16] Of all orbital conditions, TAO is one of the most common, accounting for 15-28% of unilateral proptosis and 80% of bilateral proptosis.[17-19] TAO may precede the onset of hyperthyroidism in 20% of cases, although more commonly it presents at the same time or following onset of hyperthyroidism.[20] Regardless of whether thyroid dysfunction or TAO develops first, the other becomes apparent within 18 months in 85% of patients.[9,21] It is unclear why anatomically unrelated tissues undergo coinciding immune infiltration and inflammation in GD, but thyroid dermopathy, a nodular or diffuse thickening of the pre-tibial skin, is diagnosed in only 13% of patients with severe TAO.[22] In addition, approximately 20% of patients with thyroid dermopathy have thyroid acropachy, which manifests as clubbing of the fingers (**Figure 1.2**).[22]

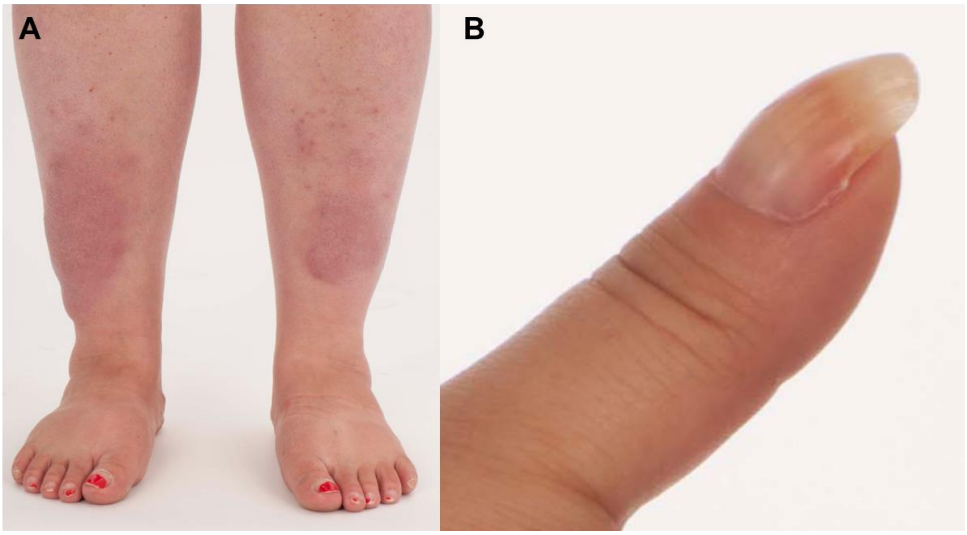

Figure 1.2: Extrathyroidal manifestations of GD. TAO patient with additional evidence of pre-tibial myxoedema (A), characterised by waxy, erythematous, indurated skin on the anterior aspect of both lower legs; thyroid acropachy (B), 'clubbing' and swelling of the fingers (and sometimes the toes), characterised by subperiosteal new bone formation.

1.3 Epidemiology of GD and TAO

The prevalence of GD is 1.85 – 2.7% and is the underlying cause of 50-80% of hyperthyroidism.[23,24] TAO is clinically apparent in approximately 30-50% of patients with GD, but is detected in 70-80% of GD patients who undergo orbital imaging.[25] TAO has an incidence of 2.9 to 16.0 cases per 100,000 population per year and, from studies 10 years ago, was thought to affect an estimated 400,000 individuals in the United Kingdom (based on a population of 59 million people).[26] Extrapolating from a presumed GD prevalence of 1%,[27] Putta-Manohar and Perros made the assumption that if TAO occurs in 40% of those with GD, then the prevalence of TAO is 0.4%, or 3 million in Europe, 1.2 million in the US and 27 million worldwide.[28]

TAO is the most common cause of orbital inflammation, accounting for approximately 40% of all orbital disease.[1] TAO may affect any age and ethnic group,[28] although there appears to be a bimodal age distribution of TAO presentation, with peak

incidence in those aged 40-44 years and 65-69 years.[14] It has been established that the age of onset tends to be higher in males.[28] Women are 5 to 7 times more likely to develop the condition than men, although men are generally felt to have more severe manifestations, particularly with increasing age.[29] Studies attempting to determine ethnic differences in TAO have found that the prevalence of TAO, and overall risk of TAO development in Europeans, were 6.4 times higher than that of Asian (Indian subcontinent) patients, although other groups have found similar prevalence of TAO in Asian (Malay, Chinese, and Indian) patients with GD as compared with Caucasian GD patients.[30,31] However, more recent studies have found no independent association of ethnicity with the severity of TAO.[32]

TAO progresses to sight-threatening disease in 3-5%, usually occurring in the context of compression of the optic nerve at the orbital apex by intraorbital tissues, known as dysthyroid optic neuropathy (DON), or corneal exposure with ocular surface breakdown and subsequent perforation.[9] Rarely, other factors may threaten sight including eyeball subluxation and choroidal folds.[2] Patients with TAO are 5 times more likely to be smokers than non-smokers. TAO patients who smoke are also more severely affected, in a dose-dependent fashion.[26,29,33-35]

1.4 Clinical Features of TAO

The symptoms of TAO include change of appearance (including “staring” appearance), excessive watering of the eyes, double vision, dry, gritty, red eyes with retrobulbar aching sensation and reduced vision. These features are due to the

classical clinical signs of TAO (**Figures 1.1 and 1.3**), which consist of a variable combination of unilateral or bilateral ocular protrusion (known as proptosis or exophthalmos), upper and perhaps lower eyelid retraction, eyelid swelling and erythema, periorbital oedema, conjunctival and canalicular injection, swelling or chemosis, lagophthalmos, ocular surface exposure and disruption (with the possibility of corneal abrasion, ulceration and perforation), impaired ocular motility and optic nerve compression.[36] TAO is bilateral in 85-95%.[37] Although clinically unilateral TAO may occur, orbital imaging generally confirms the presence of asymmetric bilateral disease.[9,22] Interestingly, euthyroid and hypothyroid patients have been shown to have milder and more asymmetric TAO.[38]

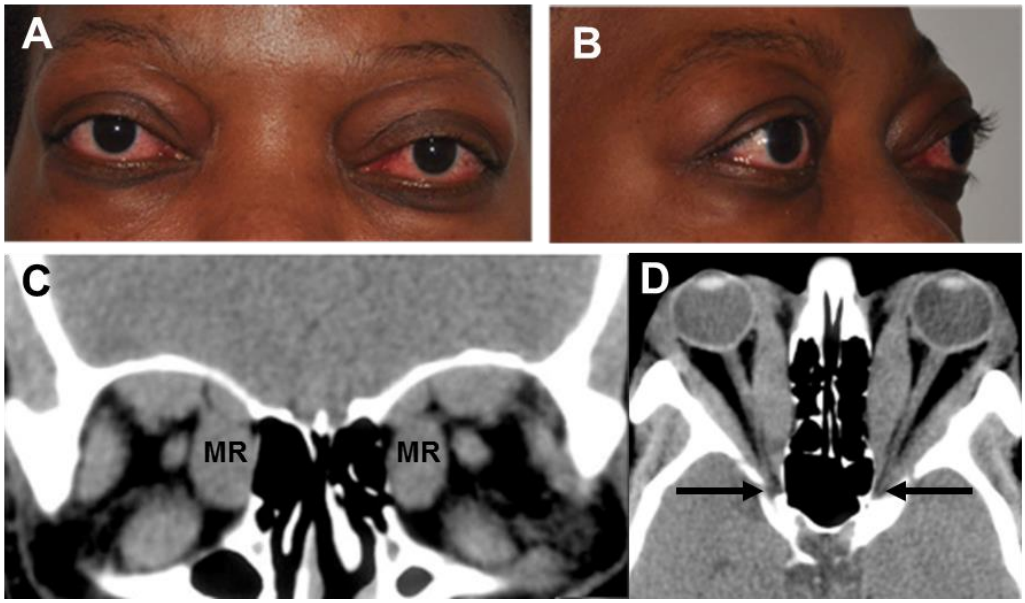

Figure 1.3: Correlation of clinical signs of TAO with orbital imaging. Typical TAO patient displaying cardinal signs of TAO including proptosis, periocular swelling and conjunctival injection (A & B). Coronal (C) and axial (D) computed tomography images of the same patient demonstrating enlargement of the extraocular muscles, particularly medial rectus (MR), and impingement of the optic nerve at the orbital apex, representing dysthyroid optic neuropathy (demonstrated with black arrows).

1.5 Rundle's Curve in TAO

For the majority of those with TAO the clinical course is relatively predictable and can be described by 'Rundle's Curve', first described in 1945 (**Figure 1.4**). There is an initial 6 to 12 months of increasing periorbital and orbital inflammatory activity, around a year of persistent but static inflammation and finally a 'burnt out', inactive phase.[15]

TAO is generally self-limiting, with resolution of inflammation within 18-24 months of onset.[9,39] Indeed, a series of 120 TAO patients determined that 74% needed no treatment or only supportive measures.[15] In a series of 59 patients with mild TAO observed for a median of 12 months, 64.4% improved spontaneously, while only 13.5% worsened.[40] This highlights the importance of early diagnosis. Studies have demonstrated that in those TAO patients who have early diagnosis and adequate treatment there is more likely to be a self-limiting course of the disease and at least partial remission in 65%.[41]

The factors involved in the resolution of TAO are, as yet, not fully identified. Theories include a decline in autoantigen or decreased autoantigen presentation as well as consumption of tissue substrate.[9] The targets of other autoimmune diseases, such as synovial tissue in rheumatoid arthritis (RA) show recognisable lymphoid structures that provide the basis for sustained immune reactions.[9] In AITD the thyroid gland has been shown to show a lymph node-like structure, with germinal centres (regions of secondary lymphoid tissue that promote B cell immunity) that may function to support maturation of memory B cells and plasma cells, perpetuating thyroid autoantibody production.[42] However, no such structures have been detected in the

orbit in TAO.[9] It is unexplained as to why there may be late reactivation of TAO (defined as recurrence of orbital inflammatory activity more than five years after quiescence) in around 5% of patients.[39]

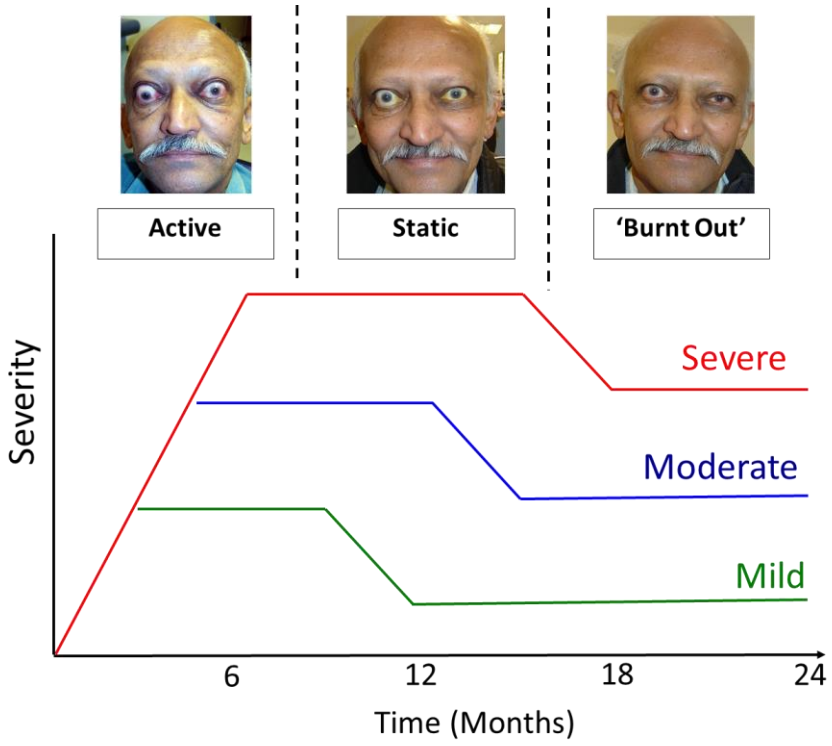

Figure 1.4: Rundle's Curve demonstrating active, static and resolution ('burnt out') phases of TAO. Length of the disease phases vary, but the active phase is usually 6 – 12 months, static phase 12-18 months and the resolution phase continuining for an indeterminate period. Medical intervention is undertaken during the period of disease activity with the aim of converting the patient to a state of lesser clinical activity and subsequent lesser clinical severity.

1.6 Clinical Activity and Severity Scoring in TAO

Classification of clinical activity and severity in TAO is extremely challenging and all measures currently in use are felt to be suboptimal.[43] Several classification systems have been developed to assess the heterogeneous nature of TAO, although these should be separated into strategies to assess disease activity and those to assess disease severity.

The NO SPECS system was perhaps the first to be introduced, with the mnemonic representing different symptoms and signs which are either present or absent. N; No symptoms or signs, O; Only signs (of upper eyelid retraction, with or without lid lag), S; Soft tissue involvement (periocular and conjunctival injection and chemosis), P; Proptosis, E; EOM involvement (precipitating diplopia), C; Corneal involvement, S; Sight loss. This grading system has a number of disadvantages, mainly in failing to differentiate clinical activity from severity. This was therefore amended to provide more subdivisions of abnormality, for example with S; Soft tissue involvement being either absent, minimal, moderate or marked and C; Corneal involvement being represented by either absence of abnormality, stippling of cornea, ulceration or clouding, necrosis and perforation.[44]

Since the late 1980's the Clinical activity score (CAS), devised by Mourits et al (1989), has been widely used, principally because it aims to assess the activity of TAO and the likelihood of a patient responding to immunosuppressive treatment.[45] Certainly, CAS has been shown to correlate with levels of serum autoantibodies.[46] In CAS a point is given to each parameter and a score equal to, or greater than, 3 indicates active TAO. However, CAS has been criticised as it is felt to only truly be valid for the active phase of TAO. CAS has therefore been amended by the European Group on Graves' Orbitopathy (EUGOGO), a multidisciplinary group of European GD and TAO clinicians.[2] EUGOGO themselves define TAO as mild; requiring no treatment, moderate-to-severe; requiring intervention with immunosuppressants or radiotherapy, and sight-threatening; patients with DON or

severe corneal exposure with ulceration and perforation. Most recently, the VISA classification has been proposed, with V; Vision (presence or absence of DON), I; Inflammatory (signs such as conjunctival injection and chemosis), S; Strabismus (or ocular motility) and A; Appearance (such as lid retraction and proptosis).[47] As yet it remains unclear which system is the optimum but, in keeping with the majority of studies, CAS is used throughout this thesis (**Figure 1.5**).

Pain	Painful, oppressive feeling on or behind the eyes (4 weeks) Pain on attempted eye movements (4 weeks)
Redness	Eyelid(s) red Diffuse conjunctival injection at least one quadrant of eyeball
Swelling	Swollen eyelid(s) Swollen caruncle(s) Conjunctival oedema (chemosis)
Loss of Function	Proptosis increasing >2 mm (1-3 months) Reduced eye movements >5' in any direction (1-3 months) Reduced visual acuity (1 line on Snellen chart (1-3 months)

Figure 1.5: The CAS score for assessment for disease activity, but not necessarily disease severity, in TAO.[48] A point is given to each parameter present and a score ≥3 indicates active TAO. EUGOGO have adapted the activity measures to be scored out of 7 rather than 10, with removal of whether proptosis has increased, whether eye movements or visual acuity have reduced over the preceding 1-3 months from the assessment.

1.7 Medical and Surgical Management of TAO

A consensus statement by EUGOGO was produced in 2008. This document recommends the review of TAO patients in combined thyroid-eye clinics and highlights that many TAO patients never reach combined clinics, or are referred too late to benefit from treatment.[2]

The management of TAO depends on the disease activity and severity.[2] All cigarette smoking patients should be encouraged to quit. Underlying thyroid function should be controlled tightly, whether through anti-thyroid drug treatment such as methimazole (MMZ), carbimazole (CBZ, a pro-drug subsequently converted to MMZ *in vivo.* Both MMZ and CBZ function through thyroid peroxidase inhibition) or propylthiouracil (PTU), radioiodine (^{131}I) or thyroidectomy. Regular administration of selenium is advocated in mild TAO, given its anti-inflammatory properties related to inhibition of NF-κB activation, C-reactive protein production and modulation of selenoprotein gene expression.[49,50] Simple measures for those with mild TAO and ocular surface symptoms include cool compresses and topical lubricants, particularly for nocturnal use if there is incomplete eyelid closure. For diplopia, orthoptic assessment, Fresnel prisms or botulinum toxin injection into the relevant EOM(s) may be necessary.

If there is active or sight-threatening disease then high-dose corticosteroids may be required.[2] There is significant debate about the optimal dosing regimen and subsequent efficacy of oral and intravenous steroids,[51] whether with or without combined radiotherapy,[52] but response rates of 77% and 51% have been reported for intravenous and oral treatments, respectively.[53] Immunosuppressants such as azathioprine,[54] ciclosporin,[55] and methotrexate have been advocated.[56] It may be necessary to progress to orbital radiotherapy, usually a cumulative dose of 20 Gray per orbit, with ten doses in a two week period, if response to immunosuppression is poor, and particularly if ocular motility disruption is a prominent feature.[57,58] Urgent orbital decompression surgery may be necessary if there is DON or intractable

corneal exposure. Rehabilitative surgery should always start with orbital decompression, followed by squint surgery, with periocular and eyelid surgery last.[2]

The use of “biologic” agents such as infliximab and etanercept (anti-TNF-α antibodies) in TAO have previously been described in isolated case reports and small case series.[59,60] However outcomes of the treatment of TAO with rituximab, an anti-CD20 monoclonal antibody, has been more widely reported. The rationale for the use of rituximab in TAO is that B cell depletion might disrupt autoantibody generation, antigen presentation and pro-inflammatory cytokine production.[61] Certainly, the germinal centres found in GD thyroid tissue, and proposed to perpetuate autoimmunity in GD,[42] have been shown to be eliminated within one week of rituximab therapy.[62] Indeed, sera of GD patients treated with rituximab have been shown to stimulate less cyclic adenosine monophosphate (cAMP) production in TSH-R-transfected Chinese Hamster Ovary (CHO) cells as compared to sera from GD patients not treated with rituximab, suggesting reduced TSAb activity.[63] These findings are consistent with previous data demonstrating a significant reduction in thyroid autoantibodies in GD patients following rituximab therapy.[64-66] Rituximab has also been confirmed to reduce T and B lymphocytes in orbital tissues.[67,68] A number of series, limited to relatively small numbers of TAO patients, have subsequently shown that rituximab may be efficacious in TAO, particularly those with steroid-resistant disease. However, side effects such as hypotension, nausea, fever, joint pain and sinus tachycardia have been described in up to 50% of patients.[64,65,69-71] A recent Cochrane review determined, due to lack of randomised controlled trials, that there is currently insufficient evidence to justify rituximab use in TAO patients.[72]

1.8 Long-term Psychosocial and Occupational Impact of TAO

While psychological stress has been proposed to be a precipitant for GD,[73,74] TAO is also known to cause significant long-term psychosocial morbidity.[75] Specific, validated TAO quality of life questionnaires (e.g. GO-QoL, TED-QoL) have been developed to more fully assess this.[76,77] TAO patients tend to have significantly poor self-image when compared with control groups.[75] This is related to physical discomfort and visual dysfunction from the underlying disease process, but also to disfigurement. Unfortunately, exophthalmos is known to persist in the majority of patients. In a study of 122 patients with exophthalmometry measurements over 3-19 years, even after correction of thyrotoxicosis, exophthalmos remained stable in 78.7%, improved in 5.7% and worsened in 15.6%.[78] Even after 10 years, between 61 and 90% of patients report a change in their appearance as a result of TAO, 38% state that they are unhappy because of it and 63% feel that disfigurement significantly interferes with their psychosocial functioning.[76,79,80] Certainly, in a cohort of 250 TAO patients, 45% felt constrained in their daily activities, 36% were on sick leave and 28% were disabled. Furthermore, 5% had retired early, and 3% had lost their job because of TAO.[81]

In a separate study, the mean duration of sickness absence for TAO patients was 22 days per year, as compared to the equivalent national average of almost 12 days per year. This was estimated to represent a cost of 3,301€ - 6,683€ per patient per year. Duration of sick leave was found to correlate significantly with TAO severity, while work disability correlated with diplopia.[81]

1.9 Genetics of TAO

A genetic component in TAO is suggested by a 35% concordance rate for GD in monozygotic twins.[82] A family history of thyroid disease, especially in maternal relatives, is associated with increased incidence of GD and younger age at onset.[83] Nevertheless, it has been proposed that 79% of the risk of developing GD is due to genetic factors, with 21% of the susceptibility due to environmental factors.[82]

A number of susceptibility genes have been proposed to be involved in GD.[9] These include MHC class II HLA-DR genes,[84] MHC class I HLA-C genes,[85] CD40,[86] CTLA-4 (2q33),[87] the protein tyrosine phosphatase (PTPN22) region on chromosome 1p13,[88,89] tumour necrosis factor (TNF) (6p21.3),[90] interferon-γ (IFN-γ) (12q14),[91] ICAM-1 (19p13),[92] the IL-2Rα/CD25 region on chromosome 10p15[93] and TSH-R (14q31) itself.[94] In particular, a PTPN22 single nucleotide polymorphism (SNP), known as R620W, is associated with GD. This SNP, which codes for a variant of the protein tyrosine phosphatase Lyp, involved in the regulation of signalling through immune cell receptors, has also been associated with a range of other autoimmune diseases including type 1 diabetes mellitus, myasthenia gravis, RA, multiple sclerosis (MS) and systemic lupus erythematosus (SLE).[95-97]

The IL-23R gene, which has also been associated with several autoimmune diseases including inflammatory bowel diseases[98] and RA,[99] has also been found to be implicated in GD and TAO.[100] This may have particular aetiological significance in

TAO as IL-23 and IL-23R are known to be required for T cell differentiation toward certain possibly pathogenic T cell phenotypes.[100] The gene locus for FoxP3, a key gene in the development of regulatory T cells (Treg) has also been analysed in separate Japanese and Caucasian cohorts. While no association was found between FoxP3 polymorphisms and AITD in a Japanese cohort, there was a significant association in the Caucasian group.[101] However, no genetic study has identified markers that distinguish between GD with and without TAO.[102,103]

1.10 Environmental Factors and TAO

1.10.1 Smoking and TAO

Cigarette smoking is considered to have a strong, consistent, independent association with TAO. There is evidence that individuals with GD who smoke are more likely to have increased risk of TAO, more severe disease and a poorer prognosis, with a dose-response relationship.[2,29,34,104,105] Patients who smoke cigarettes are less likely to respond to therapy.[33,104] In addition, smoking increases the risk for progression of TAO after radioiodine therapy (discussed in **Chapter 1.10.3**) and decreases the efficacy of measures felt to reduce the risk of such radioiodine-related progression.[29,106-108] Furthermore, it has been proposed that smoking cessation is associated with improved TAO outcome.[2]

The prevalence of TAO in the United Kingdom may be decreasing. In one study the prevalence of TAO among GD patients was 57% in 1960 and 37% in 1990.[109]

However, the prevalence of TAO in some Eastern European countries has increased. These phenomena have been hypothesised to be due to rates of smoking, which are reducing in the United Kingdom but increasing in Eastern Europe.[110]

The mechanism by which smoking initiates or aggravates TAO is, as yet, unknown. Nicotine and benzpyrene components increase sympathetic nervous system activity, and the latter is known to increase thyroid hormone secretion from thyroid follicular cells.[111] Smoking has also been shown to increase the production of pro-inflammatory cytokines such as IL-1 from mononuclear cells.[105] Salvi et al (2000) found increased serum concentrations of pro-inflammatory IL-6 in TAO patients, irrespective of thyroid function tests or whether they were on treatment with anti-thyroid medications, compared with controls.[112] However, serum IL-6 receptors (IL-6R) were significantly affected by treatment and were significantly higher in those patients with active TAO than inactive TAO. Serum IL-1Ra concentrations were not affected by the presence of TAO and did not differ in treated and untreated GD patients. Furthermore, smoking did not affect serum levels of IL-6, sIL-6R, TNF-α, IL-1β and IL-6Ra, even in the presence of active TAO or presence of TRAb or TPO-Ab.

Another hypothesis is that smoking causes tissue hypoxia, resulting in oxidative stress and inducing release of superoxide free radicals, which have previously been shown to cause orbital fibroblasts from TAO patients to proliferate and produce glycosaminoglycans (GAG) *in vitro* in a dose-dependent manner.[105,113]

1.10.2 TAO and Control of Thyroid Function

Those TAO patients with poorly controlled thyroid function, irrespective of whether hyperthyroid or hypothyroid, are more likely than euthyroid patients to have severe TAO.[114] However, no advantage or disadvantage is conferred on TAO patients if they are treated with either anti-thyroid drugs (of whatever regimen) or thyroidectomy (total or sub-total), and neither medical nor surgical management necessarily changes the course of TAO.[107,115,116]

1.10.3 TAO and Radioiodine

Radioiodine (also known as radioactive iodine or ^{131}I) is used to treat hyperthyroidism arising from GD. About 15% of GD patients develop new TAO or experience progression of pre-existing TAO within the six months following radioiodine treatment. However, this risk is “almost eliminated” by a short (three month) course of oral glucocorticoids following radioiodine, particularly if post-treatment hypothyroidism is avoided,[117,118] if patients are non-smokers and do not have high levels of thyroid autoantibody.[106,107] It is known that radioiodine causes a prolonged release of serum antibodies such as TSH-R and TPO-Ab, but the mechanism for this is not known.[119,120] It is proposed that this is secondary to damage to thyroid follicular cells, leading to liberation of thyroid antigens.[121]

1.11 Pathogenesis of TAO

The pathogenesis of TAO remains unclear. There is not, as yet, a definitive, unified model for the disease. The association between thyroid dysfunction and orbitopathy is still not fully understood. The most widely-held hypothesis has been that there is cross-reactivity between orbital and thyroid antigens with a loss of peripheral immune tolerance to TSH-R.[122,123]

The currently accepted immunological model of the pathophysiology of TAO (**Figure 1.6**) indicates that the disease is triggered by the binding and activation of antigens on orbital fibroblasts by autoantibodies (e.g. those to TSH-R and insulin-like growth factor-1 receptor).[124] The activated fibroblasts release cytokines and chemokines such as IL-16 and RANTES (regulated upon activation, normal T-cell expressed and secreted), also known as CCL5, which recruit T cells into the orbit. Subsequent, reciprocal activation of T cells and orbital fibroblasts, through CD40-CD40L interaction, further promotes cytokine production (e.g. IFN-γ, PGD2, IL-8, IL-1α, IL-1β, CD154, IL-6).[125] These cytokines, in turn, activate pro-inflammatory genes such as those encoding prostaglandin endoperoxide H synthase-2 (PGHS-2), IL-6, IL-8, hyaluronan synthase (HAS), and UDP glucose dehydrogenase, inducing fibroblasts to proliferate, produce hydrophilic GAG and differentiate toward either fat-forming adipocytes or scar-forming myofibroblasts, resulting in the underlying pathological and clinical features of TAO.[9,124]

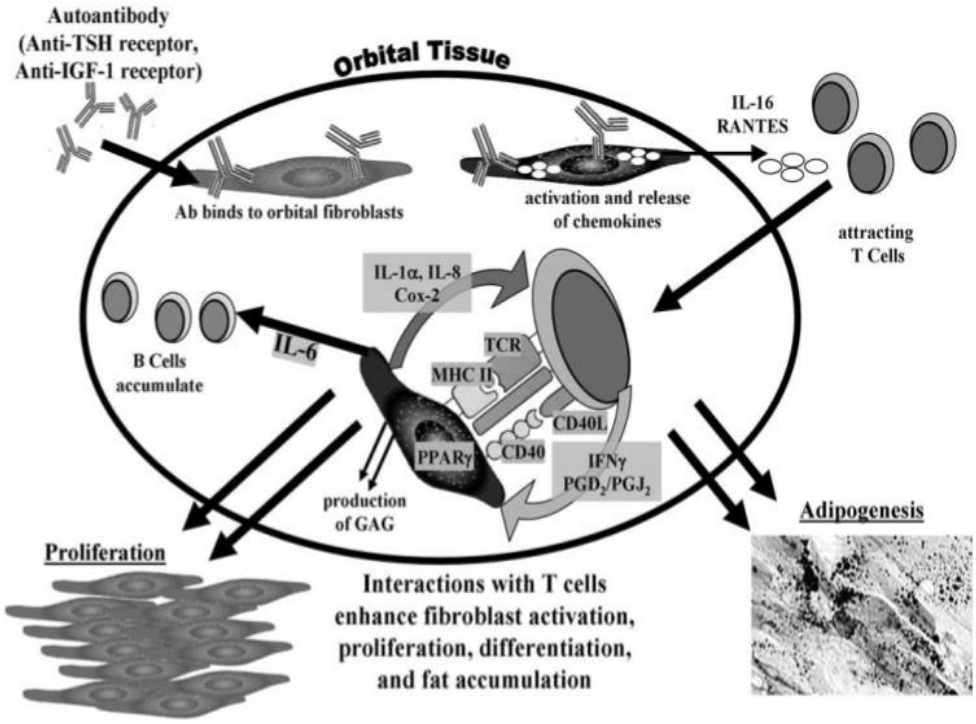

Figure 1.6: Currently accepted immunological model of TAO with immunoglobulin-mediated fibroblast activation resulting in chemokine release and subsequent T cell recruitment. This promotes cytokine production and activates pro-inflammatory pathways, causing fibroblasts to proliferate, produce hydrophilic glycosaminoglycans and differentiate toward either fat-forming adipocytes or scar-forming myofibroblasts (taken from Lehmann et al 2008).[124]

The TSH-R is an autoantigen firmly established in the pathogenesis of GD.[126] Indeed, the clinical presentation has previously been shown to be influenced by the presence of circulating antibodies against TSH-R.[127] Levels of TSH-R antibodies correlate positively with clinical features of TAO and influence the eventual prognosis.[128] TSH-R is considered to be a shared antigen in GD and TAO, and to have a role in the pathogenesis of the latter.[129] There will be further discussion of TSH-R as an autoantigen later in this thesis (**Chapter 1.18**)

1.12 Gross Features of TAO

The hallmark pathological features of TAO are an increase in orbital connective tissues, with (1) production and deposition of excess hydrophilic extracellular matrix components such as GAG, particularly hyaluronic acid (hyaluronan, HA – a negatively charged, hydrophilic molecule which binds water approximately 1000 times greater than albumin), mononuclear cell infiltration, fibroblast proliferation and differentiation with (2) *de novo* adipogenesis and subsequent expansion of orbital adipose tissues and extraocular muscles (EOM).[130,131] Indeed, orbital GAG content in TAO is about 70% higher than healthy controls.[131] This increased tissue volume and remodelling within the unyielding confines of the bony orbit results in protrusion of the globe (known as proptosis or exophthalmos), restriction of ocular movements, increased intraorbital pressure, reduced orbital venous drainage and microcirculation and the subsequent TAO phenotype.[36]

1.13 Subtypes of TAO

Variations in the clinical manifestations of TAO have been observed to exist. In a study of 95 untreated TAO patients, expansion of orbital fat, without EOM expansion, occurred in 5.3%.[36] Some authors contend that this variation represents different configurations of orbital size and shape.[132] However, others postulate that TAO can be subdivided into distinct types depending on differing tissue expansion patterns. On this basis, TAO has been subdivided into Type 1 and Type 2 (**Figure 1.7**).

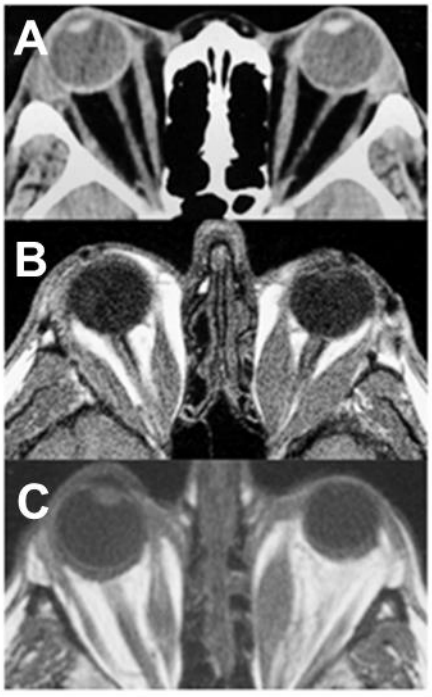

Figure 1.7: Computed tomography features of different TAO subtypes. A: Predominant fat expansion and Type 1 phenotype; B: Predominant EOM expansion and Type 2 phenotype. C: Combined fat and muscle compartment expansion.[26]

Type 1 TAO is felt to be more common, primarily affecting women (M:F 8.5:1) with a wide age range, but mean of 36 years. This subtype is represented by predominant fat compartment hypertrophy, with only mild-to-moderate EOM enlargement. In contrast, Type 2 TAO tends to have a more equal sex distribution (M:F 1.5:1) and to preferentially affect older age groups, with a mean of 52 years. This subtype is primarily represented by expansion and dysfunction of the EOMs.[133] There is also proposed to be Type 3 TAO, representing an expansion of both EOMs and orbital adipose tissue. Of the EOMs affected, inferior rectus is the most common, followed by medial rectus, then superior rectus and finally lateral rectus.[8]

1.14 Extraocular Muscles in TAO

Although EOM volumes are increased in TAO, electron microscopic examination demonstrates that the muscle fibres themselves remain intact, at least in early disease.[134] There is, however, infiltration of T cells, mast cells and B cells, as well as expansion of the perimysial connective tissue between EOM fibres. This has been interpreted to suggest that the connective tissue, rather than the muscle itself, is the autoimmune target.[135] Later in the TAO disease process, there is fibrosis and fatty infiltration of EOMs, correlating with later deficiencies in ocular motility.[125]

1.15 Oxidative Stress Model of TAO

The generation of reactive oxygen species (ROS) has been proposed to occur in GD and TAO, both as a cause and a consequence of systemic and orbital inflammatory activity.[136] Hyperthyroidism, with subsequent sympathetic nervous system hyperactivity, stimulation of cellular functions requiring mitochondrial activity, and consequent increased oxygen consumption, is known to increase ROS production. This, combined with orbital infiltration of immune cells, production of pro-inflammatory cytokines, altered orbital blood flow, cigarette smoking and treatment with anti-thyroid, immunosuppressant drugs and administration of orbital radiotherapy, may all alter metabolic processes in patients with GD and TAO.[137,138] Indeed, tissue damage related to hyperthyroidism is manifest in such features of GD as thyrotoxic myopathy and cardiomyopathy.[139]

ROS are molecules with unpaired electrons, such as hydrogen peroxide (H_2O_2) and superoxide anions (O_2^-), which damage proteins, lipids, nucleic acids and cellular structures. Usually a 'scavenging' system of enzymes (e.g. superoxide dismutase (SOD), catalase, glutathione peroxidase (GPx) and glutathione reductase, as well as other vitamins (e.g. ascorbic acid) or molecules (e.g. glutathione) protect against ROS-mediated damage. However, any increase in ROS production or decrease in constituents of the ROS scavenging system results in oxidative stress.[136]

Superoxide free radicals have been shown to cause orbital fibroblasts from TAO patients to proliferate and produce GAG *in vitro* in a dose-dependent manner.[113] Further *in vitro* studies have demonstrated that subjecting orbital fibroblasts to H_2O_2 results in increased expression of proteins involved in T cell recruitment and antigen recognition such as HLA-DR and heat shock protein-72, features inhibited by pre-treatment of fibroblast monolayers with the anti-thyroid drugs MMZ and PTU.[140]

In untreated hyperthyroid GD patient serum, changes related to ROS metabolism have been identified as compared to controls. For example, increased products of lipid peroxidation have been noted, which correlate with serum thyroid hormone concentrations. In addition, increased thiobarbituric acid-reacting substances (TBARS) and SOD activity have been found, along with reduced anti-oxidant enzymes such as GPx.[141,142] These oxidative stress markers normalise when the euthyroid state is returned, although more effectively due to antithyroid drugs than radioiodine.[143,144] In addition, the aetiology of the hyperthyroidism may have an influence on the normalisation of oxidative parameters. For example, differences

have been found in autoimmune hyperthyroid (GD) patients as opposed to those with non-autoimmune (toxic multinodular goitre) hyperthyroidism, as well as GD patients with and without orbital manifestations.[145,146]

This data relating to oxidant status in GD and TAO has been corroborated by clinical trial data. A large, randomised, double-blind placebo-controlled trial of 159 patients with mild TED found that at 6 and 12 months those who took the antioxidant selenium (100 µg, twice daily), although not the anti-inflammatory drug pentoxifylline, for six months had comparatively better quality of life, less ophthalmic involvement and reduced TED progression, with no adverse effects.[49]

1.16 Microarray Studies in TAO

There have been five microarray studies evaluating gene expression in orbital tissue from TAO subjects as compared to healthy controls.[147-151] In one study, 25 known genes were increased in expression (>4-fold) in TAO orbital tissues and 11 genes were decreased (>4-fold).[149] Separately, microarray studies have identified upregulation of several adipocyte regulatory genes (e.g. PPAR-γ, apolipoprotein E and adiponectin)[149] and immediate early genes (e.g. cysteine-rich, angiogenic inducer, 61 [CYR61], cyclo-oxygenase-2 [COX-2]), as well as CYR61-responsive genes participating in inflammation such as IL-1β, matrix metalloproteinase-3 (MMP-3) and vascular endothelial growth factor (VEGF).[148] Upregulation of the gene for secreted frizzled-related protein-1 (sFRP1), an inhibitor of the complex wingless-type (Wnt) signalling which, when active, inhibits adipogenesis, has been described.[149]

Likewise, other Wnt signalling genes (DKK3, sFRP4, Wnt5a) have been found to be downregulated in TAO by microarray[150] and others (sFRP1 in chronic TAO and sFRP3 in active TAO) downregulated only when evaluated by RT-PCR.[151] Although of uncertain significance, lysosome-related genes, such as CLN2, CLN3, and HEXB have also been implicated.[147]

More recently, dysregulated expression of genes related to IGF-1 binding and signalling in TAO has been demonstrated. Ezra et al (2012) showed that the most differentially expressed genes between TAO and control orbital fat were IGF-1 and IGF-1R signalling and binding genes (e.g. SOCS3, IRS2) and downstream signalling and transcriptional regulators (e.g.SGK, c-JUN). However, only two of these (DKK3 downregulated and SOCS3 upregulated) with expression change >4-fold.[150]

The number of TAO subjects in each of these studies have been generally low, with the largest cohort being 20 patients with euthyroid, severe TAO[149] and one of the studies including only two TAO patients.[147] In addition, in four of the five studies, some of the TAO subjects had received immunomodulatory treatment prior to removal of orbital tissue for analysis. The majority of the studies have also been undertaken in severe TAO states, with selection bias meaning that the samples examined have not represented the majority of TAO cases with more mild disease.[150]

1.17 Autoantigens in TAO

Infiltration of orbital tissues by lymphocytes is characteristic of TAO.[22] However, why immunocompetent cells are directed into the orbit is unclear. A number of potential autoantigens have been proposed to have a role in TAO, although these remain poorly understood. It is felt that T cells infiltrate the orbit and respond to orbital autoantigens that are either identical to, or share epitopes with, a thyroid autoantigen.[152]

Initially, the autoantigens were felt to be EOM-related antigens such as the 63 kDa calcium-binding skeletal muscle protein calequestrin, the 67 kDa flavoprotein subunit of the mitochondrial enzyme succinate dehydrogenase; G2s, a 141 amino acid fragment of the winged-helix transcription factor FoxP1 and collagen XIII, a connective tissue protein in orbital fibroblast cell membranes.[153,154] However, these are now felt to be non-pathogenic and instead represent proteins released during tissue destruction rather than being a cause of the initial pathological process itself.[155] TG and TPO have also been proposed, but the levels of anti-TG and anti-TPO antibodies do not correlate with the presence, CAS scores or severity of TAO.[9]

The autoantigens currently felt to be principally involved in GD and TAO are TSH-R and insulin-like growth factor-1 receptor (IGF-1R). It is important to note that the published data on TSH-R and IGF-1R is interwoven, often with that related to fibroblasts, meaning that autoantigen and fibroblast data frequently overlaps.

1.18 Thyroid Stimulating Hormone Receptor (TSH-R)

TSH-R is an autoantigen firmly established in the pathogenesis of GD.[126] However, the role of TSH-R autoantibodies in TAO is less certain as there is no direct evidence of a link between TSH-R and TAO pathogenesis.[156,157] The observation that GD and TAO occur concomitantly has lead to the hypothesis that there must be a shared antigen between the thyroid and the orbit that is responsible for autoimmunity in these anatomically distinct sites. TSH-R is considered to be a shared antigen in GD and TAO, and to have a role in the pathogenesis of the latter, but this remains, as yet, unproven.[129]

1.18.1 TSH-R and TSH-R Antibodies and TAO

There are a number of indirect pieces of evidence for a role of TSH-R in TAO. Levels of TSH-R antibodies correlate positively with clinical features of TAO and influence the eventual prognosis.[128,158-160] Even in patients with euthyroid TAO it has been determined that TRAb are present in the vast majority.[4] Furthermore, the prevalence of TAO in untreated GD patients increases with higher TSH-binding inhibitory immunoglobulins (TBII) in a dose-dependent manner, with those patients with TBII 2-10 U/L having a 14% prevalence and TBII >40 U/L a 38% prevalence of GD.[161] As already discussed, TRAb rise by 70% in the six months following radioiodine, while TSH-R decrease after anti-thyroid drug treatment or thyroidectomy.[162,163]

In animal studies, BALB/c mice immunised with human TSH-R A-subunit plasmids by *in vivo* muscle electroporation developed clinical and histological features of TAO,

whereas those injected with control plasmids did not. Furthermore, all animals had high levels of predominantly stimulatory TSH-R antibodies, which persisted up to 15 weeks after plasmid immunisation.[164]

The evidence against a role of TSH-R in TAO is the absence of a definite case of neonatal TAO. There is an entity of neonatal hyperthyroidism, due to trans-placental passage of maternal immunoglobulins and rare forms of non-immune neonatal hyperthyroidism due to molecular abnormalities of TSH-R. Such babies may have eyelid retraction but no cases of true neonatal TAO have been reported.[165,166] Nevertheless, new autoimmune disease, including GD, may be induced, likely due to adoptive immunity following bone marrow transplantation from a GD donor to a non-autoimmune individual.[167]

1.18.2 Structure and Function of TSH-R

The thyroid gland functions under the control of TSH, released from the anterior portion of the pituitary gland. TSH-R is expressed on the surface of thyroid epithelial cells and binds TSH, regulating the synthesis and secretion of thyroid hormones. TSH binding to TSH-R activates mainly the adenylate cyclase pathway, via the stimulatory G protein (G_s), resulting in an increase in intracellular cAMP. However, TSH-R may also interact with $G_{q/11}$, which activates phosphatidylinositol signalling, phospholipase C (PLC) and protein kinase A signal transduction systems.[168] Indeed, it is known that TSH-R signals via cAMP, as well as PI3K/pAkt/mTOR (phosphatidyl inositol 3-kinase/pAkt/mammalian target of rapamycin).[169] Following this, genes

related to thyroid hormone synthesis are activated. TG is iodinated and converted to T4 through the action of TPO. T4 is then deiodinated to T3.[170,171] Chronic over-stimulation of TSH-R results in thyroid hyperplasia, hyperthyroidism and GD.[170]

TSH-R is a G protein-coupled receptor, with seven membrane-spanning segments, three extracellular and intracellular loops, a large ligand binding extracellular domain (α subunit) linked by disulfide bonds to the membrane-domain and an intracellular carboxy terminal (β subunit).[170,171] TSH-R α subunit is responsible for initiating or augmenting immune responses,[172] although TSH-R has been shown to dimerise, potentially modulating the actions of TSH.[173] TSH-R is encoded by ten exons on the TSH-R gene on chromosome 14q31. This encodes an 84-87 kDa protein consisting of 764 amino acids, although SDS-PAGE sometimes reveals an apparent molecular weight of 95–100 kDa.[168] This discrepancy is thought to be due to receptor shedding of the α subunit.[168]

1.18.3 Expression of TSH-R in the Orbit and Extra-Thyroidal Tissues

TSH-R was cloned in 1989 and,[174] other than the thyroid, has also been shown to be expressed in a number of extra-thyroidal sites,[175] such as human skin,[176] abdominal adipose tissue,[177] brain,[178] lacrimal gland,[129] heart,[179] bone,[180] testis,[181] thymus and lymphocytes.[182,183] It has also been found on cells in the bone marrow.[184] TSH-R mRNA and protein has also been detected in cultured fibroblasts from pre-tibial dermopathy tissues.[185,186] Subsequently, TSH-R mRNA and protein has been detected in orbital tissues and orbital fibroblasts, albeit at extremely low levels.[185,187-

[195] TSH-R have since been found to be expressed on orbital differentiating preadipocytes.[188,196] Indeed, elevated TSH-R expression is observed in orbital tissues, particularly newly differentiated adipocytes, in TAO, with the highest levels in those with clinically active disease.[126,148,197-199]

TSH-R immunoreactivity therefore unifies thyroid, orbit and pre-tibial tissues in TAO, but any role for TSH-R in TAO would appear to require differentiation of fibroblasts to adipocytes in the first instance. TSH-R expression is generally increased during adipogenesis, meaning that it is unknown whether this is a primary or secondary effect. In contrast, thyrocytes require no such adipocytic differentiation to express TSH-R or to be activated by TSH or TRAb.[148,187,188,197,200,201] It has therefore been proposed that TSAb may not necessarily cause TAO but are implicated in disease progression.[187]

Evidence supporting the involvement of cytokines in the TAO disease process is their effect on TSH-R expression in TAO orbital tissue[202,203] and their possible actions on orbital fibroblasts.[204,205] Certainly, IL-6 is elevated in the circulation of GD patients and has been found to stimulate TSH-R expression *in vitro* in orbital fibroblasts.[112,206] It has therefore been proposed that IL-6 may play a role in TAO by stimulating TSH-R expression in orbital tissues. However, it is uncertain whether IL-6 also stimulates adipogenesis in the orbit.[126] Indeed, other cytokines, including IFN-γ and TGF-β, inhibit TSH-R expression and adipogenesis by orbital fibroblasts.[126] The initiation and subsequent clinical severity of TAO may therefore be influenced by competing inhibitory and stimulatory cytokine-related effects occurring within orbital tissues.

1.19 The Insulin-Like Growth Factor-1 Receptor (IGF-1R)

The IGF-1 axis is a prime candidate involved in TAO and it has been speculated that stimulating antibodies to IGF-1R (IGF-1R-Ab) are involved in TAO development. However, despite a wide and growing body of evidence for the involvement of IGF-1R in TAO, this remains controversial.[122]

1.19.1 Structure and Function of IGF-1R

The IGF-1R, also known as CD221,[207] is a heterotetrameric transmembrane glycoprotein of approximately 150-200 kD molecular weight,[208,209] that is highly expressed in all mammalian cell types and tissues.[210,211] The receptor consists of two α and two β subunits, with the N-terminus α subunit being extracellular and highly glycosylated, while the β subunit has an extracellular domain, a transmembrane domain and an intracellular, cytoplasmic tyrosine kinase domain (**Figure 1.8**). The extracellular domain may be divided into six discrete regions: at the N terminus is a receptor L domain (L1), a cysteine-rich repeat (CRR) domain, another receptor L domain (L2) and three type III fibronectin domains – FnIII-1, FnIII-2, FnIII-3. It is FNIII-2 that constitutes the division between IGF-1R α and β chains. The IGF-1R extracellular domain, particularly an interface that includes L1, L2, FnIII-1 and FnIII-2, constitutes the binding region for ligand. Following the extracellular regions is a transmembrane portion and a cytoplasmic tyrosine kinase signalling domain.[212] The IGF-1R gene maps to chromosome 15q26.3, with both the α and β subunits being encoded within a single precursor cDNA, encoding a 1,368 amino acid proreceptor

polypeptide that is proteolytically cleaved and disulfide-linked to yield the mature receptor.[213]

IGF-1R acts as a receptor tyrosine kinase, influencing cellular processes including cell migration, metabolism, survival, proliferation and differentiation.[121,130] IGF-1R mediates tumour proliferation and inhibition of apoptosis, including through the PI3K/Akt/FRAP/mTOR/p70s6k pathway.[214,215] It is therefore important in signalling pathways controlling tissue growth and development.[216] In particular, it has been shown to stimulate the growth of some types of cancer, including breast, prostate, pancreatic, hepatocellular and lung cancers,[217,218] and a number of IGF-1R-specific therapeutic antibodies are currently under investigation in clinical trials.[219-222]

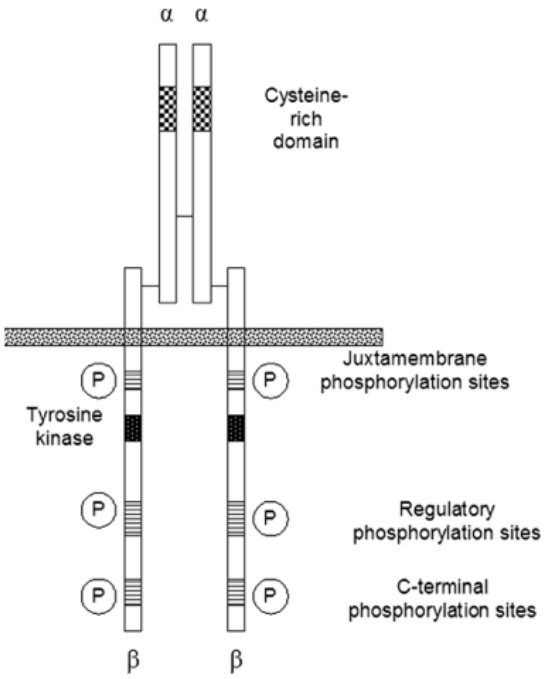

Figure 1.8: Schematic diagram of the IGF-1R demonstrating α and β subunits, the cysteine-rich domain as well as phosphorylation domain distribution on α and β chains and the location of α-α and α-β disulfide bonds (taken from Smith 2010).[213]

In addition to its role in oncogenesis, IGF-1R also has immune-mediating roles. It has diverse roles in thymic development and immune function,[223] including stimulating cytokine production by T cells and monocytes.[224,225] It also increases B cell antibody production.[226,227] IGF-1 is important in fetal and neonatal growth as well as being implicated in adipogenesis.[228]

There is around 85% homology between IGF-1R and the insulin receptor in terms of sequence and structure. In addition, IGF-1R ligands IGF-1 and IGF-2 share 50% homology to insulin.[208,213] This has been proposed to lead to difficulties in accurately detecting and targeting IGF-1R.

1.19.2 Insulin-Like Growth Factor-1

Essentially all of the biological activities of IGF-1 (also known as somatomedin) have been shown to be mediated via IGF-1R, with IGF-1R binding IGF-1 with high affinity and IGF-2 and insulin with much lower affinity.[213] IGF-1, a single-chain polypeptide of 70 amino acids, derives from two distinct sources: the liver (80%) generates IGF-1 as a component of the growth hormone (GH) axis; IGF-1 is also produced locally by many peripheral tissue cell types, such as skeletal muscle, both in the resting state and in response to inflammatory mediators.[213] IGF-1 secretion is primarily regulated by GH. Through a negative feedback loop, IGF-1 then inhibits the release of GH releasing hormone (GHRH) in the hypothalamus, reducing GH levels. The IGF-1

principally produced by such tissues as skeletal muscles has been shown to act locally in a paracrine fashion.[229]

Normal serum levels of IGF-1 have been established, with lower levels being associated with increased mortality.[230,231] Human sera contains IGF-1 concentrations of around 200 µg/L in normal individuals. However, in GH deficiency it may be around 100 µg/L and in acromegaly 1000 µg/L.[232] Acromegaly is a disease characterised by GH excess, usually due to a GH-secreting pituitary adenoma, that results in tissue overgrowth, including coarsening of the facial features, large hands and feet and associated cardiovascular and endocrine complications.[229] Analysis of serum IGF-1 is are therefore important in acromegaly diagnosis and monitoring.

Free IGF-1 is regulated by a family of six IGF binding proteins (IGFBP) which act as transporters of IGF-1 and prevent IGF-1 degradation. IGFBP undergo proteolysis by IGFBP proteases such as serine proteases, PSA, cathepsins and matrix metalloproteinases (MMP). The majority (80%) of IGF-1 in serum is bound to IGFBP-3, a 264 amino acid protein, and the remainder to other IGF1BPs, with less than 1% being unbound.[213,233] This unbound component has a half-life of only 10 minutes, although the complex of IGF-1/IGFBP-3 has a half-life of 16 hours.[229] The half-life of GH is only 30 minutes, its secretion is pulsatile and daytime levels, although diurnal, are low or essentially undetectable. GH levels are also altered with such factors as age, gender, exercise and stress. As IGF-1 levels are less likely to undergo such fluctuations it is tested for in preference to GH itself.

1.19.3 IGF-1R-Mediated Cell Signalling

IGF-1R signal transduction takes place following a conformational change induced by receptor ligation. Tyrosine autophosphorylation of the Src homology and collagen domain protein p66, Shc, and insulin receptor substrate (IRS) -1, -2, -3 and -4 (which serve as docking proteins) activates multiple pathways, including PI3K/Akt and mitogen-activated protein kinase (MAPK)/ extracellular-signal-regulated kinases (ERK1/2). However, “cross-talk” between IGF-1 and other growth factors makes the IGF-1 signalling cascade even more complicated (**Figure 1.9**).[210,234] As already described, there are at least six IGF-1 binding proteins (IGFBP) which modulate the effects of IGF-1 by acting as transporter proteins and storage pools.[210] The concentrations of IGFBP are different in different body compartments.[210]

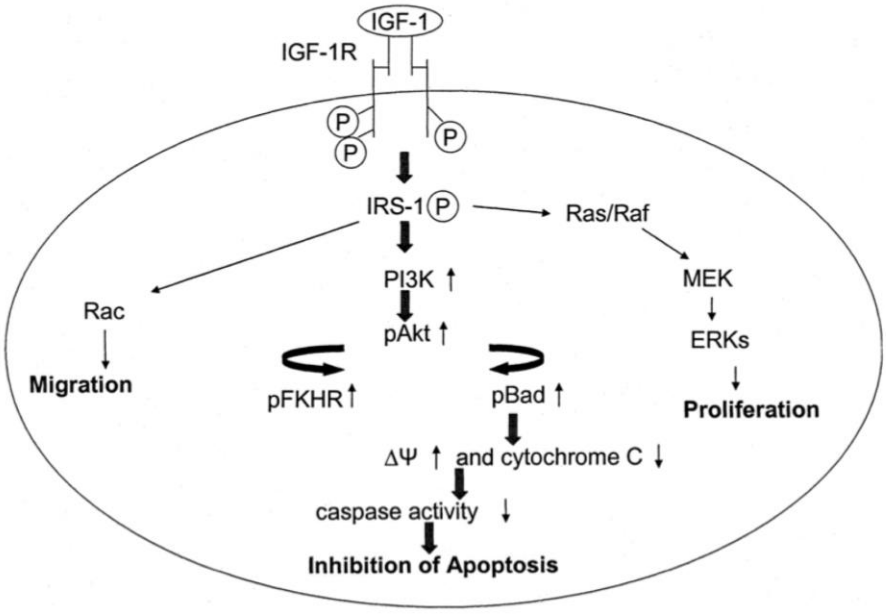

Figure 1.9: IGF-1 signal transduction demonstrating IGF-1R tyrosine kinase autophosphorylation activity, catalysing phosphorylation of cellular proteins (e.g. IRS-1, insulin-receptor substrate-1) which go on to interact with signalling molecules such as PI3K (phosphatidyl inositol 3-kinase) and MAPK (mitogen-activated protein kinase) (taken from Delafontaine et al 2004).[210]

IGF-1 is thought to have a regulatory role in the immune system, particularly in human T lymphocyte development and function, including chemotaxis and proliferation.[223] IGF-1 has also been shown to have a role in innate immunity. In particular, NK cells produce IGF-1, and IGF-1 itself is able to modulate the cytotoxicity of NK cells.[235] IGF-1, even in nanomolar concentrations *in vitro*, leads to growth of a number of cell types, including hepatocytes, pancreatic β cells, epithelial cells and fibroblasts.[236] Peripheral blood T and B cells and monocytes from healthy donors express low levels of IGF-1R *in vivo*.[237] However, IGF-1R appears to be overexpressed on a number of cell types in GD and TAO, including orbit, skin and thyroidal fibroblasts.[238,239], T cells[240] and B cells.[3] It is therefore hypothesised that increased immune cells expressing IGF-1R in GD and TAO may be responsible for the connective tissue manifestations in GD and TAO.[3,240]

1.19.4 IGF-1R and Cancer

IGF-1R has been implicated in a number of forms of human cancer.[241] Indeed, IGF-1R was identified on neoplastic tissues as early as 1987.[242] IGF-1R is known to be important in tumour biology and malignant transformation. For example, IGF-1R activity has been shown to promote growth and survival of cancer cells and has also been associated with survival of metastases.[212] Many tumour cell lines have increased expression of IGF-1 or IGF-1R.[243,244] Furthermore, fibroblasts lacking IGF-1R are unable to undergo malignant transformation, an ability restored when IGF-R expression is reinstated to these cells by transfection.[245] Inhibition of IGF-1R has been found to decrease tumour size and reduce tumour growth.[222]

Mitsiades et al (2004) found that IGF-1R is expressed in numerous malignant cell types, both haematologic (multiple myeloma, lymphoma, leukaemia) and solid tumours (breast, prostate, lung, colon, thyroid, renal, adrenal, retinoblastoma, sarcoma).[207] Specifically, increased plasma IGF-1 and reduced IGF-1BP3 concentrations have been associated with increased risk of breast, prostate, lung and colorectal cancer.[246-251] Indeed, serum IGF-1 measurement has been proposed as a possible predictor of risk in several types of cancer, even if IGF1BP-3 levels are taken into account. For example, a four-fold increase in the risk of prostate cancer has been determined in men whose serum IGF-1 levels are the highest population quartile.[249] Likewise, a seven-fold increased breast cancer risk, at least in pre-menopausal women was found in women with higher serum IGF-1 levels.[248] Finally, a relative risk of 2.5 was found for colorectal cancer in patients who had IGF-1 levels in the highest quintile.

1.19.5 Therapeutic Antibodies to IGF-1R

From the above data it is clear that IGF-1R is an important therapeutic target. As a result, a number of IGF-1R monoclonal antibodies have been developed. Dalotuzumab (MK0646), Figitumumab (CP-751871), Cixutumumab (IMC-A12), Ganitumab (AMG-479), Teprotumumab (RV001) have each been used in clinical trials. Indeed, Teprotumumab is being used in a current phase 2 clinical trial in TAO patients (NCT01868997). Examples of other situations in which IGF-1R monoclonal antibodies have been used include small cell lung cancer and Ewing's sarcoma.[252,253]

1.19.6 Colocalisation of TSH-R and IGF-1R

A functional link between IGF-1R and TSH-R has been suggested since initial studies demonstrating IGF-1 enhancement of TSH action in an *in vitro* model.[254,255] Precedents for such an interaction already exist. For example, there is known to be cross-talk between IGF-1R and epidermal growth factor receptor (EGFR).[256]

Previous studies have shown that TSH-R levels are 11-fold higher on thyrocytes than on TAO or control fibroblasts. In contrast, IGF-1R levels are 3-fold higher on TAO as compared to control fibroblasts.[187] However, it may be that TSH-R and IGF-1R form a functional complex, as immunoprecipitation studies on fibroblasts, thyrocytes and thyroid tissue demonstrate that specific antibodies against either IGF-1R or TSH-R bring both proteins out of solution. Furthermore, confocal microscopy shows IGF-1R and TSH-R colocalisation to perinuclear and cytoplasmic compartments in fibroblasts and thyrocytes, with similar findings in TAO orbital tissue. Finally, treatment of thyrocytes with recombinant human TSH results in rapid (presumably IGF-1R-mediated) ERK phosphorylation which can be abrogated by IGF-1R blocking antibody, suggesting that IGF-1R may be involved in TSH signalling pathways.[187]

In a separate study, Kumar et al (2012) noted stimulation of the production of hyaluronan in six euthyroid TAO orbital fibroblast cultures with bovine TSH, IGF-1 and M22, a high-affinity, human, monoclonal, stimulatory TSH-R antibody which has previously been shown to increase adipogenesis in TAO orbital fibroblasts by PI3K

activation.[257,258] These findings were somewhat in contrast to van Zeijl et al (2010 and 2011) who found that GD-IgG and recombinant human TSH did not increase hyaluronan production by undifferentiated orbital fibroblasts, although using orbital fibroblasts that had differentiated into adipocytes it was found that GD-IgG, but not recombinant human TSH, did stimulate hyaluronan synthesis.[201,259] In the study of Kumar et al (2012), hyaluronan synthesis by M22 was inhibited by the IGF-1 blocking monoclonal antibody, 1H7 (in serum free media). In addition, M22-induced hyaluronan synthesis was abrogated by LY294002 (PI3K inhibitor) or rapamycin (mTOR inhibitor) but not protein kinase inhibitor, reinforcing that M22 stimulates hyaluronan synthesis in TAO orbital fibroblasts via PI3K/pAkt/mTOR signalling.

It is noteworthy that neither of the colocalisation studies of Tsui et al (2008) and Kumar et al (2012) utilised GD-IgG to stimulating TAO orbital fibroblasts. The authors concede that using M22, a very definite stimulatory antibody, may be different to the constituents of GD-IgG, which may be stimulatory, inhibitory or neutral.

1.19.7 IGF-1R and IGF-1R Autoantibodies in TAO

The rationale for a role of IGF-1R as an autoantigen in TAO has arisen from a significant body of research. The first description of the presence of excess IGF-1 in orbital tissues was by Hansson et al in 1986.[260] This group took samples of formalin-fixed orbital tissue from two patients with ‘endocrine exophthalmos’ an ‘unexplained complication of thyrotoxicosis’, and demonstrated IGF-1 immunoreactivity along the plasma membranes of muscle and adipose cells, greater than that present in control

tissue of the temporal muscle of the same subject. In the same year, Tramontano et al (1986) found that IGF-I and TSH each produced dose-dependent enhancement of DNA synthesis and cell proliferation in a rat thyroid follicular epithelium cell line. When added together, IGF-I and TSH were synergistic in stimulating DNA synthesis. Importantly, this synergistic effect was also noted when IGF-I was utilised in association with GD-IgG.[254]

However, the initial proposal for the presence of IGF-1R autoantibodies (IGF-1R-Ab) in TAO was from Weightman et al (1993). This group noted that TAO is characterised by hypertrophy of EOMs and intraorbital adipose tissue, suggesting the involvement of growth factors. IGF-1 is known to induce hypertrophic changes in muscle and fat cells.[260] They therefore investigated the effect of IgG extracted from the sera of patients with GD (with or without TAO) on [^{125}I]-IGF-1 binding sites on human orbital fibroblasts grown from EOM explants.[261] In this study, IgG prepared from 12 out of 23 (52%) GD subjects was shown to significantly inhibit [^{125}I]-IGF-1 binding to orbital fibroblasts, when compared with IgG prepared from healthy individuals.[261]

It has subsequently been shown that IGF-1R is overexpressed on cultured retro-orbital fibroblasts from TAO patients.[239] A functional effect of GD-IgG directed against IGF-1R is indicated by both GD-IgG and recombinant IGF-1 itself resulting in increased stimulation of hyaluronan production by cultured orbital fibroblasts, as well as the production of T cell chemoattractants such as IL-16 and RANTES from GD and TAO subjects, but not controls.[238,239] This *in vitro* effect is reduced by inclusion of a transwell, suggesting necessity for cell-to-cell (T cell to fibroblast) contact, and

diminished by the blocking IGF-1 monoclonal antibody 1H7, indicating that this effect is likely IGF-1-mediated.[238,239]

Furthermore, T cells from peripheral blood and orbital tissue in patients with GD are skewed toward the CD3+IGF-1R+ phenotype, particularly in the CD45RO+ memory T cell population.[240] However, expression of IGF-1R on CD45RA+ "naïve" T cells is similar between GD and controls.[240] IGF-1R appears important in T cell proliferation and survival, with addition of IGF-1 or GD-IgG enhancing T cell proliferation (as measured by BrdU incorporation) and reducing T cell apoptosis (as measured by high Annexin-V but low 7-AAD expression).[240]

Even in healthy subjects, T cells internalise IGF-1R from their cell membrane soon after activation with IGF-1, down-regulating IGF-1R expression between 1 and 6 hours after stimulation, followed by re-expression, *de novo* synthesis and IGF-1R up-regulation, peaking at 48 hours after activation, subsequently reaching levels higher than baseline.[262] The group undertaking these studies suggest that this indicates a role for IGF-1R on lymphocytes in supporting the expansion of memory T cells in GD. Taking this further, McCoy et al (2014) studied 8 patients with moderate-to-severe TAO treated with rituximab. It was determined that clinical indices improved for these individuals and that reduced IGF-1R+CD3+ and IGF-1R+CD4+ and IGF-1R+CD8+ T cells were noted 4-6 weeks after treatment. Likewise, the phenotype of B cells from GD subjects is skewed toward CD19+IGF-1R+ in peripheral blood and orbital tissue.[3]

This also affects the function of B cells, with increased B cell antibody production (IgG but not IgM) from those with GD as compared with controls.[3]

It has been proposed that increased IGF-1R expression in GD is acquired rather than purely genetic. In 18 pairs of monozygotic twins (seven pairs with only one of the twins with GD (i.e. “discordant”) four pairs with both twins having GD (i.e. “concordant”) and seven healthy pairs), those individuals with GD had increased IGF-1R+ T cells (both naïve and memory CD4+ and CD8+ cells) and B cells, compared to those without GD. However, in twin pairs discordant for GD, the affected twin had higher IGF-1R+ cells as compared to their healthy twin.[216] The resulting implication is that IGF-1R expression is an acquired factor in a genetically susceptible individual.[216]

1.20 T Cell Differentiation and Plasticity

To comprehend the possible importance of particular T lymphocyte subsets in GD and TAO it is necessary to discuss current understanding of T cell phenotypes in health and disease.

T lymphocytes are components of the adaptive immune response. T cells are produced in the thymus, where gene segment rearrangement takes place to produce an antigen-specific T cell receptor (TCR), a heterodimer of αβ or γδ chains. T cells are separated on the basis of CD4+ and CD8+ expression, with CD8+ T cells being cytotoxic (producing such lytic materials as perforin and granzyme, which induce apoptosis of a targeted cell) and CD4+ T helper (Th) cells assisting other cells in immune responses.[263] CD8+ and CD4+ T cells recognise peptides derived from protein antigens presented on MHC Class I and II by antigen presenting cells (e.g. macrophages, dendritic cells), respectively, and become activated. In the thymus T lymphocytes undergo a process to ensure that they can sufficiently recognise peptide-MHC complexes while at the same time not recognising self-peptide, hence inducing autoimmunity. Within the thymus, T cells initially express both CD4 and CD8. Prior to exiting the thymus each T cell downregulates either CD4 or CD8 to become a CD4+ or CD8+ cell, and leaves as a naïve T cell, circulating between blood and secondary lymphoid organs.[264]

Initially, CD4+ T helper cells were felt to be divided into two major phenotypic subsets, Th1 and Th2.[265] This paradigm was accepted for many years. Indeed, Th1 cells were thought to be responsible for many organ-specific autoimmune diseases,

whereas Th2 cells were felt to be responsible for asthma and other allergic reactions.[263] However, many different subsets have now been discovered (**Figure 1.10**), the most pertinent for discussion in the context of TAO being Th17, Treg and Tfh. In addition, there is now understood to be significant plasticity of T cell lineages.

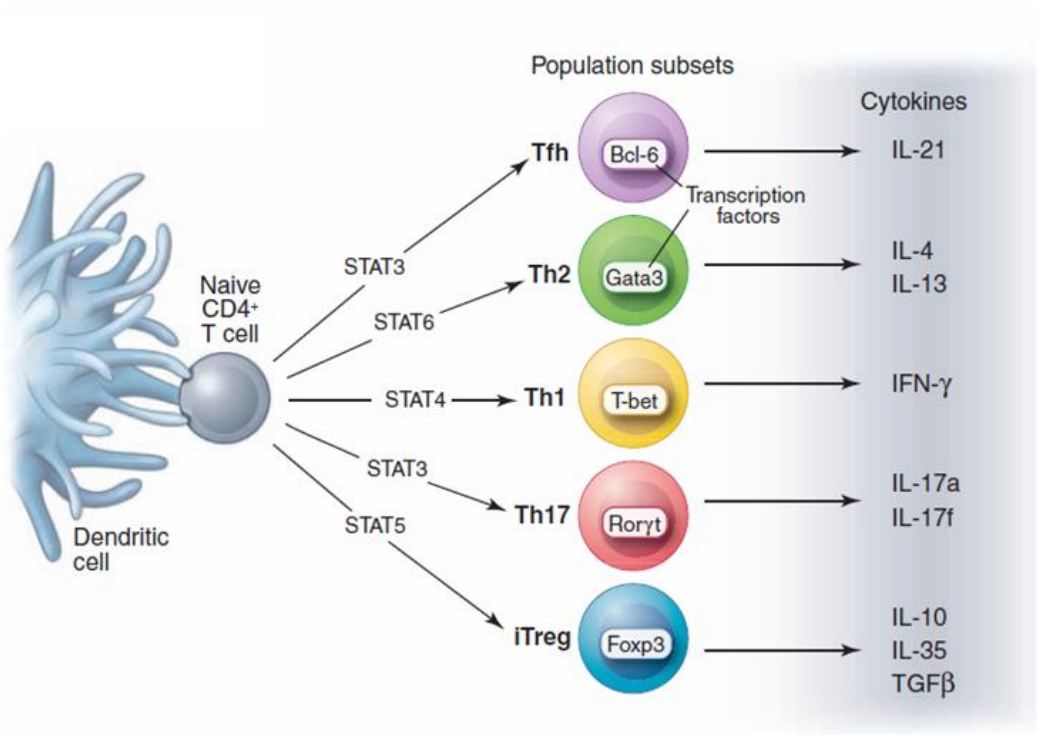

Figure 1.10: Proposed Th cell lineages including lineage-defining transcription factors and cytokines produced. CD4+ Th cells can be divided into at least four lineages: Th1, Th2, Th17 and Treg. Other subtypes including Tfh, Th9 Th3 and Tr1 also exist but Tfh cells also produce Th1, Th2, Th17 or Treg cytokines and some Th1, Th2, Th17 and Treg subsets secrete Th9, Tr1 or Th3 cytokines (taken from O'Shea et al 2010).[266]

1.20.1 T Helper 1 (Th1)

Th1 CD4+ cells are characterised by IFN-γ secretion and are important for macrophage activation and clearance of intracellular pathogens. They are defined by the transcription factor T-bet, a member of the T-box transcription factors. Th1 cells

are induced by IFN-γ and IL-27, and particularly IL-12, which bind to their respective receptors on undifferentiated naïve CD4+ T cells.[266]

1.20.2 T Helper 2 (Th2)

Th2 CD4+ cells are critical for IgE production, eosinophil recruitment and clearance of extracellular parasites. GATA-3 is the transcription factor defining the Th2 phenotype. Th2 cells are induced by either an IL-4-dependent or IL-4-independent pathway and subsequently produce cytokine such as IL-4, IL-5, IL-10 and IL-13.[267]

1.20.3 T Helper 17 (Th17)

Th17 cells are critical for immune responses against extracellular bacteria and fungi, and produce many cytokines including IL-17A, IL-17F, IL-22 and IL-21. Although IL-17A and IL-17F are isoforms of the same cytokine they have different immunological effects, with only IL-17A being able to activate macrophages.[268] RORC is the Th17 transcription factor in humans (RORγt in mice).[267] Th17 have been linked with autoimmune diseases such as RA, MS and Crohn's disease, which were initially thought to be controlled by an IL-12-mediated response.[269] However, IL-23 shares a receptor subunit (p40) with IL-12 (with a separate p19 subunit being attached rather than the p35 subunit that IL-12 possesses). From this it became clear that a number of autoimmune diseases, earlier attributed to Th1, might instead involve other IL-23-responsive Th cells, namely Th17 cells.[267,269]

1.20.4 T Follicular Helper (Tfh)

These cells, which express CXCR5 and ICOS (inducible T-cell costimulatory or CD278), play a role in B cell activation and immunoglobulin class switching, helping B cells produce antibody responses through the chemokine receptor CXCL13. Tfh produce cytokines of other lineages, such as Th1, Th2 and Th17, but particularly IL-21. Bcl6 is considered to be the master regulator of Tfh, acting as a transcriptional repressor to prevent the activity of other lineage-defining transcription factors (e.g. T-bet or GATA-3). Although it is uncertain whether Tfh cells are a separate lineage to Th1, Th2, and Th17, they have been shown to be involved in the generation and maintenance of germinal centres.[266]

1.20.5 Regulatory T Cells (Treg)

Treg are a CD4+ subset that suppress otherwise pathogenic immunity by inducing self-tolerance.[270] They comprise 5-10% of the CD4+ T cell population and can be produced in the thymus (nTreg) or induced in the periphery (iTreg or pTreg).[271] Treg are characterised by expression of the Forkhead Box P3 (FoxP3) gene, IL-2 receptor α chain ($CD25^{High}$) and low expression of CD127 ($CD127^{Low}$).[271] Treg utilise different mechanisms to suppress effector T cell activation including (1) production of immunosuppressive cytokines such as IL-10 and TGF-β, (2) release of protease enzymes (e.g. granzyme), with destruction of effector cells and (3) CTLA-4 binding to CD80/86, thereby affecting dendritic cell maturation and preventing effector cell proliferation.[267,270,271] Indeed, dysfunction of FoxP3 can result in IPEX (immunodysregulation polyendocrinopathy enteropathy X-linked) syndrome.

1.21 Defining CD4+ and CD8+ Memory T Cell Populations

It is possible to define distinct T cell populations on their basis of particular surface markers. The common leucocyte antigen CD45 has a variety of isoforms depending on alternative splicing of a single complex gene composed of 33 exons,[272] with the subsequent products ranging in molecular weight from 180 to 220 kDa. Naïve T cells are defined by their expression of one of the largest and glycosylated of these isoforms, CD45RA, while memory T cells express the shortest isoform, CD45RO. Indeed, there is a reciprocal relationship of these two CD45 isoforms with CD45RA+ lymphocytes being CD45RO- and vice versa.[272] One of the constituents of CD45 is an intracellular tyrosine phosphatase, which facilitates signalling by T lymphocytes following TCR binding. The shorter, CD45RO, isoform of CD45 is more permissive for binding to the TCR-MHC complex.

Sallusto et al (1999) demonstrated that CCR7, a chemokine receptor, controls homing of T cells to secondary lymphoid organs.[273] Once activated, T cells lose CCR7 expression. Therefore, on the basis of the expression of CCR7, memory T cells (defined by either CD45RO positivity or CD45RA negativity) may be divided into functionally distinct “central memory” (CM) (CCR7+) or “effector memory” (EM) (CCR7-) (**Figures 1.11 and 1.12**). In addition, particularly in CD8+ T cells, there is a population of “effector memory RA” (EMRA), “revertant” cells (CD45RO- or CD45RA+ and CCR7).[273] These EMRA cells are antigen experienced are therefore able to produce IFN-γ.[274] It has been found that this may be driven by chronic viral infection, particularly Cytomegalovirus (CMV).[275]

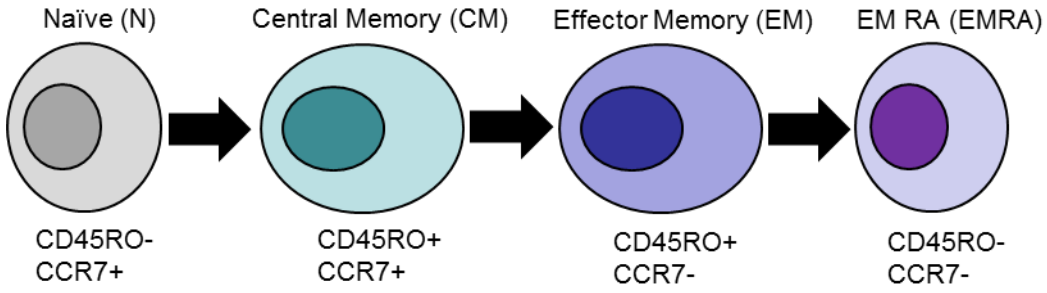

Figure 1.11: Linear model of T lymphocyte differentiation, with development of CD4+ and CD8+ T cells from naïve to central and effector memory status followed by the effector memory RA phenotype (adapted from Wikén et al 2011).[276]

	Naive	CM	EM	EMRA
CD3	+	+	+	+
CD45RA	+	-	-	+
CD45RO	-	+	+	-
CD28	+	+	-	-
CD62 Ligand	+	+	-	-
CD27	+	+	-	-
CCR7	+	+	-	-
Cytokines	IL-2	IL-2	IL-2, IFN-γ, IL-4 or IL-5	IL-2 +/- IFN-γ

Figure 1.12: Markers of T cell Memory Status. CD4+ and CD8+ T cell memory subsets can be defined by expression of a number of markers including isoforms of the CD45 common leucocyte antigen: CD45RA (higher molecular weight) and CD45RO (lower molecular weight), as well as the lymphocyte homing marker, CCR7 (CM: Central Memory, EM: Effector Memory, EMRA: Effector Memory RA).

1.22 CD4+ and CD8+ Memory T cell Populations in GD and TAO

Several groups have produced evidence of a deviation in the distribution of CD4+ and CD8+ T cell memory subsets in the peripheral blood of patients with GD and

TAO. However, these have generally not been consistent findings (**Table 1.1**). The reasons postulated for the differing results may include methodological variations, differences in patient cohorts in terms of extent and duration of thyroid dysfunction, differing drugs or medical treatment strategies and differing TAO clinical activity. In particular, previous groups did not differentiate patients with TAO from those with GD and also did not take account of treatment differences between patients, particularly if they were on thionamide drugs such as CBZ and PTU.

Table 1.1: Summary of previous studies investigating T cell subset distributions in TAO. Adapted from Vaidya et al (2005).[277]

Study	TAO/ HC	CD4+	CD8+	CD4+/CD8+ Ratio	Memory T Cells	Naïve T Cells
Van der Gaag et al, 1984	54/13	⇓	⇑	NS	(-)	(-)
Felberg et al, 1985	45/24	NS	⇑¶	⇓¶	(-)	(-)
Tyuntyunikov et al, 1992	47/27	⇑†	NS	⇑†	(-)	(-)
Vaidya et al, 2005	26/24	⇑	NS	⇑	⇑	⇓

¶Only in a subgroup of TAO patients with chemosis. †Only in patients with active and severe TAO, not in mild and stable disease. NS: Not significantly different from healthy controls. (-): Not done.

Certain factors need to be taken into consideration when interpreting these previous studies. In particular, some of the studies included hyperthyroid patients. This is significant as it has been shown that even the treatment of hyperthyroid GD, with thionamide drugs such as CBZ or PTU, can alter the distribution of peripheral T cell subsets.[278,279] The actual TAO disease activity and severity has also been

demonstrated to affect peripheral T cell subsets, with more active, severe subjects being those with an increased proportion of CD4 T cells.[280] Also of significance is that no group, so far, has differentiated GD subjects without inflammatory ocular and orbital manifestations from those with TAO.

1.23 Orbital Infiltration of T cells in TAO

There is known to be a diffuse infiltrate of T cells in the EOM interstitial tissue and orbital adipose tissue but it is not clear if true autoreactive T cells are present, or if this represents non-specific recruitment of recently activated T cells.[1,281,282] Both CD4+ (Th1 and Th2) and CD8+ T cells are present in TAO retro-orbital tissues, but there have been contradictory findings regarding whether CD4+ or CD8+ lymphocytes are the most prevalent and which T lymphocyte subsets predominate.[281] Some groups have found CD4+ T cells to predominate[283-285] while others have found a majority of CD8+ T cells.[286] Still others have hypothesised that the predominant T cell subset in the orbital tissue in TAO may change over the course of the disease,[287], with Th1 clones predominating in cultures from patients with recent onset (<2 years) TAO and predominantly Th2-type clones in cultures from patients more remote from TAO onset (>2 years).[203,281,283,288]

1.24 Orbital Fibroblasts and TAO

Orbital fibroblasts are felt to be the focus of the autoimmunity in TAO, rather than EOMs.[125] Indeed, the activation, differentiation and proliferation of orbital fibroblasts

is currently regarded as a key event in the pathogenesis of TAO [289]. Certainly, orbital fibroblasts are present in orbital adipose tissue as well as in the interstitial space between EOM cells.[290] Orbital fibroblasts also express important surface molecules and cytokines relevant to TAO.[238,239,291-293]

For example, it is known that hyaluronan synthesis by orbital fibroblasts *in vitro* is stimulated by several cytokines and growth factors, including IL-1,[294] IFN-γ,[295] and platelet-derived growth factor.[296] Specifically, in orbital fibroblast cultures from patients with GD and TAO, IGF-1 and GD-IgG provoke T cell chemoattractant (IL-16 and RANTES) and hyaluronan production.[238,239,296] This production is exaggerated as compared to control orbital fibroblasts.[205,291,297] Likewise, treatment with CD154 upregulates the expression of IL-6, IL-8, and monocyte chemoattractant protein-1 (MCP-1) in TAO fibroblasts but not in control cultures. IL-1β also induces greater MCP-1, IL-6, and IL-8 in TAO-derived fibroblasts as compared to controls.[291]

TAO orbital fibroblasts also have exaggerated production of prostaglandin E-2 (PGE-2) in response to IL-1β, CD154 and leukoregulin as a result of induction of pro-inflammatory genes such as PGHS-2, IL-1α, IL-1β, IL-6, RANTES, and IL-16 and microsomal PGE-2 synthase genes, resulting in increased synthesis and accumulation of hyaluronan.[298] PGE-2 has also been shown to bias the differentiation of naïve T cells to the Th2 phenotype at the expense of Th1 responses.[125,299]

It has been proposed that orbit (and pre-tibial) fibroblasts have distinct susceptibility factors to local cytokines, so that while T cell recruitment in GD and TAO may be generalised, the clinical manifestations are predominantly noted in the orbit.[125] This can be explained by an overexpression of putative autoantigens, particularly IGF-1R, by orbital fibroblasts, although detectable levels of TSH-R are only produced when orbital fibroblasts are induced to become adipocytes.[187,188]

The major factor thus far identified as explaining the site-specific, exaggerated responses of orbital fibroblasts to cytokines is the low levels of soluble IL-1 receptor antagonist (sIL-1RA) expressed by orbital fibroblasts as compared to non-orbital fibroblasts. This results in poorly-opposed IL-1β signalling. In addition, IL-4 and IL-13 induce 15-lipoxygenase exclusively in orbital fibroblasts from patients with GD, perhaps accounting for the different patterns of inflammation found in TAO.[125,300]

Fibroblasts, through increased CD40 expression, allow T cell co-stimulation via interactions with CD154, resulting in clonal expansion of T cells, once again enhancing pro-inflammatory cytokine production (e.g. IL-1, IL-6 and IL-8). These, in turn, cause increased expression of PGHS-2, HAS and UGDH genes which leads to further inflammation and connective tissue production.[9,125,293] These features are similar to those described in cultured human thyrocytes.[301] TAO orbital fibroblasts, but not those of HC, can be induced to differentiate to adipocytes by IL-1β and IL-6, leading to increased TSH-R on orbital fibroblasts.[302] However, TNF-α and IFN-γ inhibit adipocyte differentiation, possibly acting within the TAO orbital tissues to modulate expression of TSH-R.[302,303]

Autologous T cells have been shown to drive orbital fibroblast proliferation in mixed culture, dependent on MHC class II and CD40-CD40L signalling.[304] Other data demonstrate that activated T cells from TAO patients can stimulate differentiation of fibroblasts to adipocytes through lymphocyte-derived PGD2, presumably mediated through PPAR-γ.[305] Furthermore, retrobulbar CD8+ T cells from TAO patients recognise autologous orbital fibroblasts, but not EOM extracts, in a MHC class-1 restricted manner.[286] These T cells also proliferate in response to autologous proteins from orbital fibroblasts (but not orbital myoblasts).[282]

Lastly, there is also heterogeneity of the orbital fibroblast population in TAO, with divergent potential for differentiation, providing the basis for clinical variations in TAO phenotype. For example, the expression of CD90 (Thy-1) has been used to differentiate the phenotype and function of orbital fibroblast subsets. Orbital tissue contains both Thy-1+ and Thy-1- fibroblasts. Thy-1+ fibroblasts differentiate into scar-forming, fibrosis-generating myofibroblasts when treated with TGF-β.[125] Meanwhile, Thy-1- fibroblasts differentiate into adipocytes when treated with PPAR-γ agonists.[300,306] Interestingly, PPAR-γ agonists such as thiazolidinediones (e.g. pioglitazone), commonly administered to diabetic patients, have been shown to increase expansion of orbital tissue in those with coexisting TAO.[307-309] While both Thy-1+ and Thy-1- subsets produce IL-6 following stimulation with IL-1β or CD154, Thy-1+ fibroblasts produced higher levels of PGHS-2 and PGE-2. In contrast, Thy-1- orbital fibroblasts produced more IL-8, and when treated with IFN-γ.[291,292]

TSH-R function has been demonstrated, with increased cAMP production from TAO orbital fibroblasts, when stimulated with recombinant human TSH and GD-IgG, leading to differentiation into mature adipocytes and to increased hyaluronic acid production, mainly through upregulation of HAS-1 and HAS-2.[188,257,259,297,310] Some of these observations are abrogated by a small molecule antagonist of TSH-R activation.[311] Interestingly, IGF-1 alone did not increase HAS-2 mRNA in orbital preadipocytes, with an increase in transcripts only when IGF-1 was used in combination with rapamycin.[312]

Another unique finding of orbital fibroblasts was described by Hoa et al (2012), who demonstrated that IGF-1 and GD-IgG cause accumulation of a 110 kDa fragment of IGF-1R in the cell nucleus of TAO fibroblasts, where it colocalises with chromatin. This observation was blocked by the IGF-1R blocking monoclonal antibody, 1H7. [^{125}I]-IGF-1 cross-links with surface IGF-1R and the complex accumulates in TAO orbital fibroblasts. This requires phosphorylation of IGF-1R and ADAM17, a membrane-associated metalloproteinase. This same accumulation in the orbital fibroblast cell nucleus was not observed in HC orbital fibroblasts.[209]

1.25 Fibrocytes in TAO

Recent studies have raised the possibility that CD34+ fibroblasts, originating from bone-marrow derived fibrocytes, may infiltrate the orbit and differentiate into orbital adipose cells.

Fibrocytes can originate from monocyte or B cell precursors and represent a subset of peripheral blood mononuclear cells (PBMC), constituting 0.5% of circulating leucocytes, although frequencies may vary in a number of diseases.[313] Fibrocytes have been described as 'pluripotent monocyte lineage progenitor cells' but their function within bone marrow, and beyond, is uncertain.[314] Fibrocytes have been shown to be able to differentiate into a wide variety of cell types, depending on the cytokine milieu in which they find themselves.[315] They are CD45+ and have markers representative of bone marrow origin, including being CD34+CD11b+ and CXCR4+. They have phenotypic features in common with both fibroblasts (produce Col I and α-SMA) and haematopoietic cells (CD45+ and CD34+).[157]

Fibrocytes migrate to, and infiltrate, connective tissues (particularly sites of injury) using the CXCL12/CXCR4 pathway,[316] and perform functions such as wound healing, inflammation, angiogenesis and tissue remodelling.[317] They have a number of attributes which exemplify their ability to mediate chronic inflammatory disease processes.[318,319] Fibrocytes have the potential to be involved in antigen-specific T cell activation in that they constitutively express MHC class II.[320] They also synthesise collagen I (Col I),[321] and are able to differentiate into either adipocytes (when stimulated by PPAR-γ agonists) or myofibroblasts (when stimulated by TGF-β).[322] Fibrocytes have therefore been implicated in fibrotic processes such as those in lung,[316,323,324] liver,[325] and kidney.[326] They may also be involved in RA.[327] It is interesting, therefore, that a series of articles have recently built a range of evidence for the role of fibrocytes in the pathogenesis of GD and TAO, particularly because fibrocytes could represent a therapeutic target in these conditions.

Recent studies have found significantly more (mean of five-fold increase) peripheral fibrocytes in cultured PBMC of 70, predominantly euthyroid, GD subjects when compared with controls.[157] Fifty-one of the GD patients had manifestations of TAO, 16 with active disease as defined by CAS≥3.[157] Subsequent studies have shown that these CD34+CXCR4+Col I+ cells appear morphologically similar to orbital fibroblasts. Moreover, these cells express putative autoantigens such as IGF-1R, TG and TSH-R, with TSH-R expression on peripheral fibrocytes being increased in GD as compared to controls.[157,314,328] However, CD34+ cells are only found in GD orbital tissue, not in healthy controls. While GD orbital fibroblasts consist of a mixture of CD34+ and CD34- cells, TG and TSH-R mRNA levels are only found in CD34+ cells.[328] These CD34+ cells subsequently express TSH-R to high levels, higher than orbital fibroblasts, and are induced by TSH and the monoclonal TSH-R antibody M22 to produce pro-inflammatory cytokines such as IL-1, IL-6, IL-8 and TNF-α as well as RANTES and MCP-1.[123,157,314,329] However, there was no difference in GD patients with and without TAO in terms of fibrocyte yields, nor any difference between those with active versus inactive TAO, degree of exophthalmos, thyroid function, smoking, nor duration of TAO.[157,314] Clearly the presumption of the groups publishing this work is that orbital CD34+ cells are derived from circulating fibrocytes.

In an attempt to link autoimmune processes in the thyroid and the orbit, Smith et al (2013) characterised CD34+ fibrocytes in thyroid tissue. CD34+Col I+CXCR4+TSH-R+ cells were identified in thyroid tissue from GD, Hashimoto's thyroiditis and

'normal' thyroids. However, while thyroid fibroblasts were Col I+CXCR4+TSH-R+ and produced IL-6 and IL-8 when treated with TSH, they were CD34-.

The balance between IL-1 and IL-1RA, hypothesised to be important in GD and TAO,[330] as well as other diseases, particularly SLE,[331] has also been investigated in fibrocytes. IL-1β, a proinflammatory cytokine, is detected in TAO orbital tissues, especially in more active TAO.[193] In a study by Li et al (2013), in keeping with previous studies, orbital fibroblasts treated with IL-1β go on to display more pro-inflammatory IL-1α, IL-1β and PGHS-2 mRNA than fibrocytes, whereas fibrocytes exhibit higher levels of IL-1 receptor antagonist mRNA (IL-1RA), both secreted (sIL-1RA) and intracellular (icIL-1RA), which are known to competitively bind IL-1 receptor and inhibit downstream signalling.[332] Furthermore, when fibrocytes are treated with IL-1β they upregulate sIL-1RA whereas fibroblasts treated in the same way upregulated only icIL-1RA. It is sIL-1RA, responsible for controlling IL-1 activities between cells, which is the IL-1RA which is the more important modulator of IL-1. In contrast, icIL-1RA is felt to regulate intracellular activities.[332] In animal models of rheumatoid arthritis and osteoarthritis, sIL-1RA has even been postulated to have therapeutic potential.[333] The hypothesis from this is that the hyperactive response of orbital fibroblasts in TAO is because they do not produce the potent antagonist of IL-1β, sIL-1RA, due to a shift from sIL-1-RA to icIL-1RA as they change from fibrocytes to CD34+ fibroblasts, presumably within the TAO orbit. In addition, although fibrocytes initially produce sIL-1RA, they go on to lose this ability as they transform to orbital fibroblasts.[332]

Lastly, the IGF-1R monoclonal blocking antibody Teprotumumab (RV001, R1507), a fully humanised monoclonal antibody that binds to the ligand-binding extracellular alpha subunit of IGF-1R, and currently undergoing a phase 2 clinical trial (NCT01868997) in patients with moderate-to-severe, active TAO, inhibits the expression and action (as defined by reduced pAkt levels induced by TSH or IGF-1 and the production of IL-6 and IL-8 mRNA and protein induced by TSH) of TSH-R and IGF-1R in fibrocytes, supporting the rationale for blocking IGF-1R in TAO.[334] This is also in accordance with with findings of other studies which determined reduced TSH-R-related signalling in TAO orbital fibroblasts with another IGF-1R blocking monoclonal antibody, 1H7.[258,335]

Until recently it has been uncertain how such anatomically distinct sites should be involved in the same disease process, how the autoimmune thyroid disease in GD links with the orbital inflammation in TAO. The authors of these various papers postulate that fibrocytes may migrate from bone marrow to be recruited to, and infiltrate, thyroid and orbital tissues in GD, as well as other distinct soft tissues such as the pre-tibial region (thyroid dermopathy) and acra of the finger (thyroid acropachy), thus providing a potential link between the pathological glandular and extra-thyroidal manifestations of GD. However, the link between bone marrow and thyroid autoimmunity remains uncertain. Certainly, evidence exists that fibrocytes express potential autoantigens, are able to present these antigens in association with MHC class II, produce cytokines and GAG and are known to be involved in fibrotic reactions in other diseases. It is noteworthy that none of the fibrocyte studies so far

have used GD-IgG. It is uncertain whether this is because the experiments have not yet been performed or whether results have proven inconclusive.

A number of putative autoantigens associated with autoimmune endocrine disease other than GD and TAO have been shown to be expressed on human fibrocytes. For example, fibrocytes express islet cell antigens implicated in type 1 diabetes mellitus, namely ICA512 (IA-2) and ICA69, although in healthy individuals, GD and MS patients as well as those with type 1 diabetes mellitus.[336]

1.26 Animal Models of TAO

Until recently it was felt that there was no existing robust animal model for TAO. None of the models previously developed were felt to exhibit the full spectrum of GD, recapitulating the characteristic features of orbital remodelling or demonstrating a primary role for the TSH-R as an orbital target antigen.[164] In addition, a number of these models proved difficult to replicate.[337-339]

A number of TSH-R induced murine models were attempted, with either transfer of TSH-R-primed T cells to naïve syngeneic recipients, the use of a TSH-R fusion protein or genetic immunisation with a plasmid encoding the TSH-R to generate TSH-R-primed T cells.[338] Thyroiditis was transferred to NOD (non-obese diabetic) and BALB/c mice, but this was associated with only low titres of TSH-R antibodies (which were predominantly inhibitory rather than stimulatory) and there was no evidence of orbital disease in a significant proportion of the mice.[337] However,

examination of the orbits in 17 of 25 of animals showed lymphocytic and mast cell infiltration, accumulation of adipose tissue, dissociation of muscle fibres and evidence of TSH-R immunoreactivity, whereas control mice showed no such ocular pathology.[337,340-342] This was a predominantly Th2-mediated thyroiditis, with the extent of the orbital changes correlating with the extent of the Th2 response in the thyroid immune infiltrate. It has been observed, however, that different methods of TSH-R vaccination may lead to Th1 responses in which IFN-γ, rather than autoantibody, lead the immune response.[337,338] It has been argued that differences in orbital anatomy may underpin the lack of proptosis that occurs in mice in the models attempted.

More recently, all 22 female BALB/c mice immunised with human TSH-R A-subunit plasmids by *in vivo* muscle electroporation resulted in the clinical and histopathological features of TAO, with evidence of asymmetric but bilateral enlarged EOM, proptosis and indications of orbital congestion, clinically and on *in vivo* MRI, as compared with those injected with control plasmids.[164] In addition, histopathology of orbital tissue demonstrated infiltration of CD3+ T lymphocytes, macrophages and mast cells, as well as GAG deposition, although no B lymphocytes. The histological findings were heterogeneous, with some mice manifesting predominantly EOM abnormalities, with interstitial inflammatory infiltrate or otherwise adipogenesis with expansion of retro-ocular adipose tissue. Furthermore, all animals had high levels of TSH-R antibodies, predominantly with stimulatory function, which persisted up to 15 weeks after plasmid immunisation. The majority also had IGF-1R antibodies. However, the animals with evidence of TAO were predominantly hypothyroid (2/8

having significantly depressed T4 and 5/8 showing lower T4), with one mouse having evidence of hyperthyroidism, and the majority of these mice (6/7) also having evidence of hypothyroid histological appearances, with only one mouse demonstrating histological changes of hyperthyroidism. There was no thyroiditis in either group. Interestingly, those mice injected with an IGF-1Rα plasmid (n=3) did not lead to any histological changes in thyroid or orbital tissues.[164]

These findings differed somewhat to a previous study by the same group using the same hTSH-R A-subunit plasmid, with only one out of eight animals developing hyperthyroidism in the most recent study as compared with eight out of 12 in their previous study.[343] The previous study resulted in a high frequency of TSH-R and IGF-1R antibodies but no evidence of orbital inflammation. The hypothesis raised by this group was that a variation in plasmid injection technique, with a deeper injection over a larger muscle area, was responsible as a result of improved transfection efficiency during electroporation.[164]

1.27 Immune Reconstitution and TAO

An intriguing observation exists relating to secondary AITD, felt to represent GD, following the treatment of patients with relapsing-remitting MS with Campath-1H (Alemtuzumab), a humanised anti-CD52 monoclonal antibody which depletes T cells. Coles et al (1999) noted that a third of MS patients treated with Campath-1H 12-24 mg/day for 5 days developed TSH-R antibodies and AITD. In addition, the reconstituted T cells had decreased proliferation and IFN-γ secretion *in vitro*.[344] Of 27

patients, 9 developed GD and 2 of these had evidence of TAO.[344] None of these patients had any particular genetic polymorphisms associated with AITD. Interestingly, there have apparently been no reports of AITD development when Campath-1H has been used in any other of its medical indications (e.g. RA).[344] Further studies have determined that this phenomenon is driven by higher serum levels of IL-21 and that patients who went on to develop secondary AITD had more than two-fold greater levels of serum IL-21 than the non-AITD group.[345] Immune reconstitution GD may also occur in other instances, such as following bone marrow transplantation from a donor with GD and during the phase of CD4+ expansion in patients with human immunodeficiency virus (HIV) infection treated with highly-active anti-retroviral therapy (HAART).[167,346]

The increased serum IL-21 levels related to immune reconstitution GD may provide an avenue for study in the context of follicular helper T cells (Tfh). As detailed in **Chapter 1.20.4**, these cells are felt to be a distinct CD4+ Th subset which are present in B cell follicles of secondary lymphoid organs and identified by constitutive expression of CXCR5.[347] Tfh mediate antigen-specific B cell activation, triggering germinal centre formation, probably through expression of CD40L and the secretion of IL-21 and IL-4.[347] It is therefore possible that Tfh may be involved in GD and TAO.

1.28 Current Difficulties in Predicting TAO Onset, Activity and Severity – The Need For A Biomarker in TAO

1) Predicting TAO Disease Onset and Severity: Although it is known that 30-50% of patients with GD will go on to develop TAO and that 85% of these will do so within

18 months of their initial diagnosis it is, at present, not possible to determine exactly which GD patients will subsequently be affected. In addition, it is currently not feasible to ascertain which of those who acquire TAO will be in the minority (3-5%) who develop severe, sight-threatening manifestations, which may be recalcitrant to conventional immunosuppressant treatment. If it were possible to differentiate these patients on the basis of particular biomarkers of acceptable sensitivity and specificity it would permit the evidence-based targeting of more intensive medical and ophthalmic monitoring of, and resource allocation to, those at greatest risk as well as the focusing of specific interventions and treatment strategies (e.g. smoking cessation, tight control of thyroid function, avoidance of radioiodine).

2) Providing Definite, Objective Diagnostic Criteria for TAO: While diagnosing TAO in a patient with GD would appear to be straightforward, this is certainly not always the case, particularly in early stages of disease. TAO diagnosis can be extremely challenging, as GD itself has some ocular manifestations (e.g. lid lag and lid retraction) which do not necessarily represent TAO but are actually manifestations of thyrotoxicosis and resulting sympathetic nervous system overactivity. Likewise, many of the most severely affected, sight-threatened TAO patients are those who do not present with classical proptosis or overt inflammatory signs, but who insidiously lose vision from unrecognised optic nerve compression. In both cases, the ability to differentiate on the basis of an objective biomarker would be extremely beneficial.

3) Following Responses to Therapy: With increasing utilisation of diverse immunosuppressant (e.g. azathioprine) and monoclonal antibody (e.g. rituximab)

therapies in TAO, and the advent of “personalised medicine”, it is crucial to have robust, impartial methods for determining responses to treatment. The clinical methods we utilise at present are adequate, but imperfect, and require objective and complementary assessments. Likewise, in planning the development and deployment of future novel treatments developed from clinical trials we require more concrete outcome measures to determine the efficacy of a particular candidate treatment, and to compare the utility of a novel therapy with established treatments.

4) Establishing the Optimum Time to Perform Rehabilitative Surgery for TAO: It is currently often difficult to discern if patients with TAO have persisting active, inflammatory disease (characterised by conjunctival injection and chemosis) or “burnt-out” disease with signs of venous congestion (also characterised by conjunctival injection and chemosis). Again, the clinical activity and severity scores we utilise at present are suboptimal. This is important, as we need to identify the correct time to undertake rehabilitative surgery for TAO. In the absence of sight-threatening TAO, the usual strategy is to wait until the active phase of disease has ended before proceeding to surgery. However, if this is performed too early then a patient may go on to require further surgery that should not have been necessary.

As already described, previous studies have investigated the epidemiology, inflammatory mechanisms and genetics of both GD and TAO in large cohorts of patients and through a diverse range of statistical methods and laboratory techniques. Many of these studies have aimed to identify particular risk factors or markers of the likelihood of developing severe TAO. From these it is clear that TAO

is a complex disorder associated with a number of genetic polymorphisms (e.g. PTPN22, CTLA-4) and candidate molecules of interest (e.g. IGF-1R) but also with a number of patient-specific factors such as cigarette smoking, uncontrolled thyroid function and treatment with radioiodine. The interaction between these multiple factors means that analysing the effect of a single possible biomarker that predicts TAO onset and prognosticates the course and severity of the ensuing orbital disease, while controlling for so many other variables, is extremely difficult.

1.29 PhD Hypotheses

There is a significant body of evidence for the involvement of IGF-1R in TAO pathogenesis. This is underlined by the influence of GD-IgG on production of T cell chemoattractants and GAG by orbital fibroblasts, abrogated by IGF-1R monoclonal blocking antibody.

I hypothesise that:

1) Autoantibodies to IGF-1R (IGF-1R-Ab) are present in sera of patients with GD with (GD+TAO+) and without (GD+TAO-) orbital manifestations and can be detected by immunoassay. IGF-1R-Ab titres correlate with TAO activity and may act as a biomarker for those individuals most likely to develop severe orbital disease.

2) IGF-1R-Ab skew T cell memory populations, with preferential accumulation of naïve T cells over cytokine-producing effector memory T cells as a result of the role

of IGF-1R in cell proliferation and survival, combined with data demonstrating differential expression of IGF-1R on memory CD4+ and CD8+ T lymphocytes,

3) Finally, although TAO arises from both genetic and environmental risk factors, the downstream metabolites produced from this complex interaction can be measured in GD+TAO+ and GD+TAO- sera and permit differentiation of the two groups when analysed by metabolomic techniques.

1.30 PhD Aims and Objectives

In order to address my hypothesis I have sought to undertake three principle objectives during this thesis:

Part 1: Develop, optimise and validate assays to detect and quantify IGF-1R-Ab, utilise these assays in GD+TAO+ and GD+TAO- subject sera and correlate IGF-1R-Ab titres with clinical phenotype;

Part 2: Characterise the memory and T helper phenotype of CD4+ and CD8+ T lymphocytes in GD+TAO+ and GD+TAO- subjects and correlate with clinical phenotype;

Part 3: Undertake metabolomic analysis of the sera of GD+TAO+ and GD+TAO subjects, identify metabolites of importance and determine the sensitivity and specificity by which these groups may be differentiated.

2 MATERIALS AND METHODS

General details of reagents and experimental techniques are described in this chapter. Specific adaptations, details of optimisation and subsequent amendments are described in each of the relevant results chapters.

2.1 Ethical Approval

Clinical data collection and patient sampling was undertaken following ethical approval in accordance with the Declaration of Helsinki. Successful acquisition of favourable opinion for collection of peripheral blood from patients with GD or TAO, and healthy controls, was gained from Birmingham East, North and Solihull Research Ethics Committee (Reference: 10/H1206/70; UKCRN number 10073).

2.2 Multiple-Site Research & Development Approval

Research and development approval was gained from three distinct sites: Sandwell and West Birmingham Hospitals NHS Trust (which encompasses Birmingham and Midland Eye Centre, BMEC), University Hospital Birmingham NHS Trust (UHB), and the University of Birmingham (UoB).

2.3 Definition of Study Groups

Three separate study groups were identified:

GD+TAO+: Diagnosis of GD made on the basis of initial biochemical hyperthyroidism (raised serum free T4 (fT4) and/or free T3 (fT3) concentrations and undetectable serum TSH), presence of goitre and identification of high titre of TPO-Ab (>59 IU/ml). Patients were hyperthyroid, euthyroid or hypothyroid.

References ranges for thyroid function tests:

fT4 10 – 22 pmol/L

fT3 3.1 – 6.8 pmol/L

TSH 0.30 – 4.50 mIU/L

In addition, these subjects had presence of ocular or orbital manifestations of TAO, as previously described. TAO subjects were from different phases in the disease – some in the early, active phase (CAS≥3), while others were 'inactive' as defined by EUGOGO (CAS<3) and some had no clinical evidence of inflammatory activity at the time of their assessment.

GD+TAO-: Diagnosis of GD made on the basis of initial biochemical hyperthyroidism (as described above) together with the presence of a palpable diffuse goitre and a significant titre of TPO-Ab, as previously described.[348] At the time of recruitment, patients may have been hyperthyroid, euthyroid or hypothyroid. However, subjects had no evidence of ocular or orbital manifestations of TAO.

Healthy Controls (HC): No previous or current thyroid dysfunction, no known underlying autoimmune disease and on no immunomodulatory drugs.

Both the GD+TAO- and GD+TAO+ subjects were heterogeneous groups in terms of thyroid status at the time of sampling, thionamide treatment, radioiodine or thyroidectomy treatment and cigarette smoking status. Despite all GD+TAO+ and GD+TAO- subjects having been TPO-Ab positive at the time of their GD diagnosis, I also measured their serum TRAb levels at the time at which they were recruited in to the study with a commercial TRAb ELISA (ElisaRSRTM TRAb 3rd Generation, Cardiff, UK). This assay had a cut-off for TRAb positivity of ≥0.4 uL.

2.4 Patient Identification, Assessment and Sample Collection

Study participants were identified and recruited on their attendance to either a tertiary referral endocrinology clinic at UHB (for GD+TAO+ and GD+TAO- subjects) or a tertiary referral orbital diseases clinic at BMEC (for GD+TAO+ subjects). HC subjects were recruited from a combination of UHB and BMEC. All subjects were carefully age- and sex-matched. A comprehensive medical history was taken from each subject, including age, sex, current and previous medications and smoking history, and all underwent a full ophthalmic, neuro-ophthalmic and orbital assessment. TAO disease activity was determined by CAS score (described in **Figure 1.5**) with active TAO defined by a CAS score of ≥3.

All peripheral blood sampling from GD+TAO+ and GD+TAO- patients and HC subjects in UHB and BMEC clinics was undertaken by myself. Samples from the different groups were analysed in mixed batches. Experiments never took place with samples from just one of the investigated groups.

2.5 Alphabetical List of Reagents, Media and Solutions

Reagent	Source
Brefeldin A	Sigma-Aldrich, Dorset, UK
BSA	Sigma-Aldrich, Dorset, UK
CFSE	Caltag/Invitrogen, Paisley, UK
Compensation Particles Set	BD Biosciences, Oxford, UK
Counting Beads	Caltag/Invitrogen, Paisley, UK
Des(1-3)IGF-1	IBT Systems, Reutlingen, Germany
EDTA	Sigma-Aldrich, Dorset, UK
Ficoll-Paque Plus	GE Healthcare, Amersham, UK
GPS	Sigma-Aldrich, Dorset, UK
HEPES	Sigma-Aldrich, Dorset, UK
HIFCS	Sigma-Aldrich, Dorset, UK
Human T-Activator CD3/CD28 Beads	Caltag/Invitrogen, Paisley, UK
IGF-1	Peprotech, London, UK
IGF-1R Duoset	R&D Systems, Abingdon, UK
Ionomycin	Sigma-Aldrich, Dorset, UK
IL-6 Monoclonal Antibody	R&D Systems, Abingdon, UK
$KHCO_3$	Sigma-Aldrich, Dorset, UK
Lightcycler 480 Genotyping Master Mix	Roche, Switzerland
Lightning Link Biotinylation Kit	Innova Biosciences, Cambridge
NH_4Cl	Sigma-Aldrich, Dorset, UK
PBS	Oxoid, Cambridge, UK
Phosflow Fixation Buffer	BD Biosciences, Oxford, UK
Phosflow Permeabilisation Buffer (III)	BD Biosciences, Oxford, UK
Phosflow Stain Buffer	BD Biosciences, Oxford, UK
PMA	Sigma-Aldrich, Dorset, UK
PTPN22 Anchor & Sensor Probes	TIB MOLBIOL, Germany
PTPN22 Forward & Reverse Primers	TIB MOLBIOL, Germany
Quickgene DNA Whole Blood Kit	Fujifilm, Japan
RPMI Medium 1640	Sigma-Aldrich, Dorset, UK
Tween 20	Sigma-Aldrich, Dorset, UK

2.6 List of Antibodies for Surface Staining Studies

Antibody	Channel	Isotype	Dilution	Source
CD3	eFluor780 (APC Cy7)	Mouse IgG1	1/50	eBioscience, Hatfield, UK
CD4	PE Cy7	Mouse IgG1	1/10	BD Pharmingen, Oxford, UK
CD8β	PE Cy5	Mouse IgG1	1/40	Beckman Coulter, High Wycombe, UK
CD8	V500 (Violet 2)	Mouse IgG1	1/20	BD Biosciences, Oxford, UK
CD69	FITC	Mouse IgG1	1/20	eBioscience, Hatfield, UK
CD71	FITC	Mouse IgG1	1/20	eBioscience, Hatfield, UK
CD154	FITC	Mouse IgG1	1/20	Biolegend, Cambridge, UK
CD25	PECy5	Mouse IgG1	1/10	Biolegend, Cambridge, UK
CD127	FITC	Mouse IgG1	1/20	eBioscience, Hatfield, UK
CD45RO	PETR	Mouse IgG1	1/50	Beckman Coulter, High Wycombe, UK
CD45RA	PETR	Mouse IgG1	1/80	Beckman Coulter, High Wycombe, UK
CCR7	FITC	Mouse IgG2a	1/20	R&D Systems, Abingdon, UK
CCR7	AlexaFluor 488 (FITC)	Mouse IgG2a	1/20	Biolegend, Cambridge, UK
IGF-1Rα	PE	Mouse IgG1	1/10	Santa Cruz Biotech, UK
CXCR5	AlexaFluor 647 (APC)	Rat IgG2b	1/160	BD Biosciences, Oxford, UK

2.7 List of Antibodies for Intracellular Cytokine Staining Studies

Antibody	Channel	Isotype	Dilution	Source
IFN-γ	eFluor450 (Violet 1)	Mouse IgG1	1/80	eBioscience, Hatfield, UK
IL-5	PE	Rat IgG2a	1/20	BD Pharmingen, Oxford, UK
IL-17A	PerCP Cy5.5	Mouse IgG1	1/20	eBioscience, Hatfield, UK
IL-21	eFluor 660 (APC)	Mouse IgG1	1/20	eBioscience, Hatfield, UK

2.8 List of Antibodies for Phosflow Studies

Surface Antibody	Channel	Isotype	Dilution	Source
Phospho-Akt	PE	Mouse IgG1	1/5	BD Biosciences, Oxford, UK
Phospho-ERK1/2	PE	Mouse IgG1	1/5	BD Biosciences, Oxford, UK

2.9 Preparation of Peripheral Blood

Peripheral blood was collected in EDTA vacutainer tubes and stored at 4^{o}C until use in experiments, within four hours of sampling. It was decided to perform T cell phenotype studies using both PBMC and lysed blood. The latter was used in order to analyse any differences in neutrophil and monocytes between the groups studied. Preparation of lysed blood and peripheral blood mononuclear cells were as follows:

2.9.1 Whole Blood Lysis

Peripheral blood was centrifuged and resuspended at a 1/10 dilution (1 ml of peripheral blood) of filter-sterilised red cell lysis buffer (8.29 g NH_4Cl, 1 g $KHCO_3$ and 37.2 mg EDTA per litre of distilled H_20). After 7 minutes at room temperature, the suspension was diluted with 15 ml RPMI to block further lysis. Following centrifugation, the pellet underwent two washes, each time being resuspended in 10 ml PBS, followed by centrifugation at 400 g for 8 minutes. Cells were mixed 1:1 with trypan blue (8 µl) and counted in a haemocytometer. Cells were resuspended in RPMI at a concentration of $1x10^6$ cells/ml and placed in a 96-well plate.

2.9.2 Peripheral Blood Mononuclear Cells

12-15 ml of peripheral blood were collected in a 50 ml Falcon tube and diluted 1:1 with RPMI/1% GPS/1% HEPES. This mixture was gently layered over 7 ml Ficoll-Paque in 25 ml universal tubes (17 ml max blood/universal tube). These were centrifuged for 30 minutes at 20°C, 400 g with no brake. The PBMC buffy layer was removed and transferred to 10ml RPMI/1% GPS/1% HEPES. Cells were then washed through three cycles of centrifugation (at 6 to 8 minutes, 400 g, 20^oC, brake 9) and resuspended in 10 ml RPMI. Cells were mixed 1:1 with trypan blue (8 µl) and counted in a haemocytometer. Cells were resuspended in RPMI at a concentration of $1x10^6$ cells/ml and placed in a 96-well plate.

2.9.3 Isolation, Storage and Thawing of Serum

For each subject a separate sample of peripheral blood was also collected in serum separating tubes and stored at 4^{o}C. This was centrifuged at 400 g for 8 minutes and the serum layer removed, placed in 500 µl aliquots in 1 ml cryovials and stored at -80^{o}C until ready for use. When required these serum samples were thawed at 37°C in a water bath while being gently rotated. All samples were analysed after a maximum of one freeze-thaw cycle.

2.10 Extraction of DNA for PTPN22 R620W Genotyping

DNA was extracted from whole blood samples using the QuickGene-810 system (Fujifilm, Japan) using a standardised protocol. The QuickGene-810 system (http://www.autogen.com/product-quickgene-810.htm) is a technique for extracting nucleic acids, based on the use of a porous polymer membrane which selectively traps nucleic acids. When ethanol is added to lysates of whole blood samples the polarity is reduced which promotes the adsorption of nucleic acids into the membrane. The membrane is washed with a low polarity solution (wash buffer) under low pressure to remove any contaminating components without desorbing the nucleic acids. Finally, the nucleic acids are eluted using a high polarity solution (elution buffer) under low pressure and a pure solution of nucleic acids is obtained.

EDB buffer (30 µl) was added to a 1.5 ml microcentrifuge tube, followed by whole blood (200 µl) and LDB buffer (250 µl) and vortexed for 15 seconds. Samples were incubated at 56°C for 2 minutes and >99% ethanol (250 µl) was added following this.

Samples were vortexed and loaded into the QuickGene-810 system, set on DNA whole blood mode. Following extraction, DNA samples were stored at 4°C until use.

2.11 PTPN22 R620W Genotyping

The Roche LightCycler 480 System (Roche Diagnostics Ltd. UK) was used to identify the single nucleotide polymorphism of PTPN22 (rs2476601) by real-time PCR and melting curve analysis (**Appendix 1**). This has previously been well-validated.[349]

Primers and probes included; primers: 5–GCCTCAATGAACTCCTCAAAC–3 (forward) and 5-CTGATAATGTTGCTTCAACGGA–3 (reverse), probes: the sensor (A) 5–CAGGTGTCCATACAGGAAGTG–3–FLU and the anchor 5–LCRED640–GGGGATTTCATCATCTATCCTTGGAGCAGTTG–PH.

Primers and probes were used at concentrations of 10 µM and 3 µM, respectively. The components for each PCR reaction (5.5 µl PCR grade water, 0.5 µl forward primer, 0.5 µl reverse primer, 0.3 µl anchor probe, 0.2 µl sensor probe and 2 µl genotyping master mix) were added to a 1.5 ml microcentrifuge tube and vortexed thoroughly. Into each well of a 96-well white qPCR plate was added 9 µl of reagent mix and 1 µl of the DNA extracted as described in **Chapter 2.10**.

2.12 Statistical Analysis

Statistical analysis was performed for all univariate analyses with GraphPad Prism version 5.0 (GraphPad Software, California 2008). Non-parametric continuous

comparisons were undertaken with the Mann Whitney U test for two groups, Kruskal-Wallis test (and Dunn's multiple comparison) for multiple groups. Correlation was undertaken with Spearman's rank correlation. Multivariable logistic regression analysis was with SPSS version 20 (IBM, Chicago, IL, 2012). The minimum level of confidence at which the results were to be judged significant was $p<0.05$.

3 DEVELOPMENT AND VALIDATION OF NOVEL IGF-1R AUTOANTIBODY ASSAYS IN GRAVES' DISEASE AND THYROID-ASSOCIATED OPHTHALMOPATHY

3.1 Introduction

As already discussed, there is a significant body of evidence for the role of IGF-1/IGF-1R and putative IGF-1R autoantibodies in the pathogenesis of TAO.

3.1.1 Summary of Current Evidence for a Role of IGF-1R in TAO

Early studies in this area established competition of [^{125}I]-IGF-1 with GD-IgG for binding to orbital fibroblast cell membranes.[261] It has since been demonstrated that IGF-1R is overexpressed on cultured retro-orbital fibroblasts from GD patients as well as on T and B lymphocytes from orbital tissue and peripheral blood, compared with healthy controls.[3,240] This elevated IGF-1R observed on T lymphocytes of patients with TAO is reduced following treatment with rituximab.[350]

In addition, IGF-1 and GD-IgG stimulate GAG and T cell chemoattractant (IL-16 and RANTES) production by orbital fibroblasts (blocked by the monoclonal anti-IGF-1R antibody, 1H7), and cotransfection with a dominant-negative IGF-1R plasmid attenuates such effects,[238,239,351] similar to that noted in cultured thyrocytes.[301] van Zeijl CJ et al (2011) found that TSH did not result in increased hyaluronan production by TAO orbital fibroblasts but that GD-IgG did, implying a non-TSH, non-cAMP signalling route, possibly representative of a mechanism related to IGF-1R activation and signalling.[201]

Recent data has established that CD34+ fibrocytes (cells for which an increasing evidence base exists linking autoimmune processes in the thyroid and the orbit in

TAO) also express IGF-1R.[123] Furthermore, twin studies indicate increased IGF-1R expression on lymphocytes in affected siblings, representative of an acquired rather than genetic parameter.[216] There is also data demonstrating location and functional interaction of TSH-R and IGF-1R.[187,258] Finally, Ezra et al (2012) have demonstrated that expression of genes related to IGF-1 binding and signalling (e.g. IGFBP-6, SGK-1 and SOCS3) are dysregulated in TAO orbital tissue, by microarray.[150] Indeed, on the basis of these findings, a clinical trial is currently taking place into the role of Teprotumumab, a humanised monoclonal IGF-1R antibody in the treatment of TAO (clinical trials identifier NCT01868997, EudraCT (European Union Drug Regulating Authorities Clinical Trials) number EU2014-000113-31).

Together these data, from a number of different groups, and over a number of years, suggest that, at least in a proportion of GD patients, GD-IgG may stimulate IGF-1R and contribute to the development of TAO. However, despite this weight of evidence for a role of IGF-1/IGF-1R in TAO pathogenesis, originating in 1986, even in 2013 no convenient assay had been published to be utilised specifically to measure IGF-1R-Ab in GD and TAO patients.

3.1.2 Existing Assays for the Measurement of IGF-1R Antibodies

Over the past decade a number of IGF-1R-Ab assays have been developed for other purposes but which, until recently, had never been translated to be used in studies of GD or TAO.

Chen et al (2003) developed an IGF-1 kinase receptor activation (KIRA) assay. This assay, based on a HEK-293 (Human Embryonic Kidney) cell line stably transfected with human IGF-1R, was developed with the purpose of measuring IGF-1 bioactivity in diseases related to atherosclerosis and cancer.[352] The assay functions on the basis of measuring autophosphorylation of the tyrosine residues of IGF-1R in response to stimulation with human serum *in vitro*, to determine the IGF-1R stimulating activity of that serum. The assay utilises a monoclonal capture antibody to IGF-1R (MAD1) and a biotinylated antiphosphotyrosine monoclonal antibody (BAM1676) as a detection antibody. The published intra-assay coefficient of variation was 5.6% and inter-assay coefficient of variation <15%.[352]

Yin et al (2011) optimised two enzyme-linked immunosorbent assays (ELISA) for detection and measurement of Dalotuzumab (MK 0646), a humanised anti-IGF-1R IgG1 antibody (blocking the binding of both IGF-1 and IGF-2 to IGF-1R) undergoing phase III clinical trials for use in cancer therapy, in human serum.[208,222] The purpose of the assay in this context was the investigation of the pharmacokinetic properties of Dalotuzumab. This group attempted to validate two ELISA, using an IGF-1R-mediated capture step and either a mouse anti-human IgG-Fc-specific antibody conjugated to horseradish peroxidase (HRP) or a biotinylated mouse anti-human IgG1-specific antibody. It was determined that only the ELISA utilising the anti-IgG1 antibody could be validated. The authors felt that their methods may be applied to detect other IGF-1R of interest. Indeed, the ELISA devised by Yin et al (2011) was used by Moshkelgosha et al (2013) to measure serum IGF-1R autoantibodies in a TAO animal model,[164,208] while that devised by Chen et al (2003) was used by Varewijck et al (2013), as discussed later.[352,353]

3.1.3 Principles of IGF-1R-Ab Immunoassays

The inspiration, basis and principle for the two distinct IGF-1R-Ab immunoassays I developed were previous ELISA established for the detection of TRAb (in GD) and Aquaporin-4-Ab (in neuro-inflammatory disorders), each of which have been shown to have good sensitivities and specificities.[354,355]

Principle of ELISA 1:[354] Presumed IGF-1R-Ab in the sera of GD+TAO+, GD+TAO- and HC subjects are allowed to interact with recombinant human IGF-1R (rhIGF-1R) coated onto ELISA plate wells (**Figure 3.1 A & B)**. After an incubation period, sera are discarded leaving IGF-1R-Ab bound to the plate-bound rhIGF-1R. Biotinylated Des(1-3)IGF-1 (an IGF-1 which lacks three N-terminal residues) is then added for further incubation, where it binds to plate-bound rhIGF-1R binding sites which have not been occupied, and therefore blocked, by serum IGF-1R-Ab already bound to rhIGF-1R. The use of Des(1–3)IGF-I (referred to as Biotin-IGF-1 throughout the rest of this chapter) is important as it binds IGF-IR with high affinity but does not bind IGFBP.[238] The amount of Biotin-IGF-1 bound to the plate can be measured by addition of streptavidin-horseradish peroxidase (sHRP), which itself binds to biotin and can be detected by the addition of 3,3',5,5'–tetramethylbenzidine (TMB), which turns blue on reaction with biotin (**Figure 3.1 C)**. This reaction is ceased by the addition of stop solution, causing the well contents to turn from blue to yellow. The absorbance, in terms of an optical density (OD) of the yellow reaction mixture, is then determined using an ELISA plate reader. A lower absorbance (lower OD) indicates the presence of increased IGF-1R-Ab in a sample as the IGF-1R-Ab inhibits binding of Biotin-IGF-1 to the ELISA plate coated with rhIGF-1R.

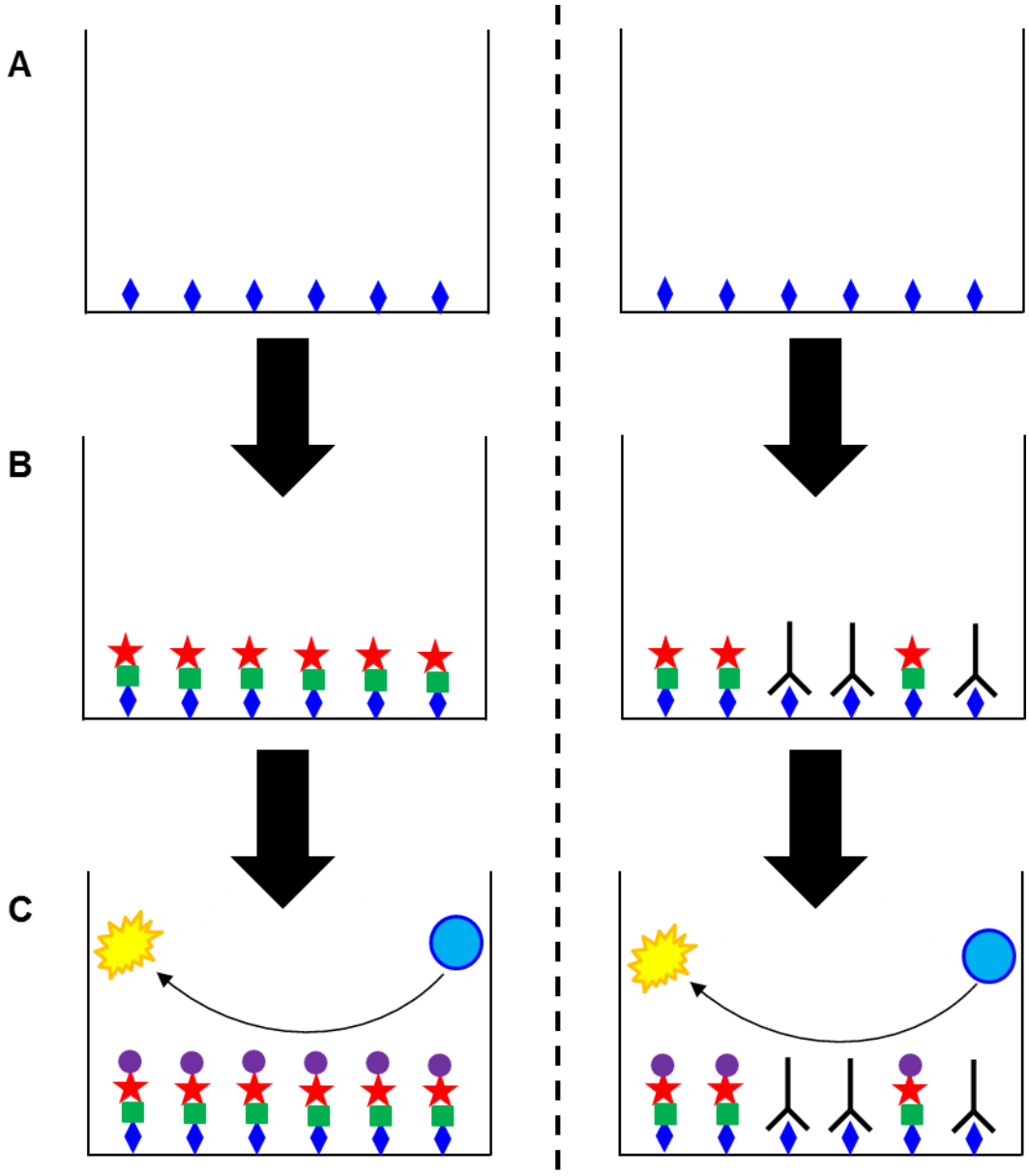

Figure 3.1: Diagrammatic representation of the principle of ELISA 1. Recombinant human IGF-1R (rhIGF-1R) (blue diamond) is coated onto ELISA plate wells (A). Biotinylated Des(1-3)IGF-1 (green square with red star) binds to rhIGF-1R, occupying the optimum proportion of binding sites (left panel, B). However, if IGF-1R-Ab (black figure) in human sera are allowed to interact with rhIGF-1R before Biotinylated Des(1-3)IGF-1 are introduced to the system, these occupy rhIGF-1R binding sites, meaning that Biotinylated Des(1-3)IGF-1 cannot do so (right panel, B). When strepavidin-HRP (purple circle) is then added, less is able to bind to Biotinylated Des(1-3)IGF-1 and there is subsequently a lesser ELISA signal determined from the substrate solution (blue circle converting to yellow circle) (C). The quantity of serum IGF-1R-Ab is therefore determined by the proportion of the maximum signal which is attenuated by their binding.

Principle of ELISA 2:[355] Presumed IGF-1R-Ab in the sera of GD+TAO+, GD+TAO- and HC subjects are allowed to interact with rhIGF-1R coated onto ELISA plate wells (**Figure 3.2 A & B**). After an incubation period, sera are discarded leaving IGF-1R-Ab bound to the plate-bound rhIGF-1R. A biotinylated IGF-1R (IGF-1R-Biotin) is added in a second incubation step. IGF-1R-Ab bound to rhIGF-1R coated on the plate will also interact with IGF-1R-Biotin due to the bivalent (or multivalent with soluble IgM) nature of antibodies (**Figure 3.2 B**). After further incubation, the well contents are discarded, leaving IGF-1R-Biotin bound to IGF-1R-Ab, which is in turn bound to plate-bound rhIGF-1R. The amount of IGF-1R-Biotin bound is then determined as in ELISA 1, with further steps involving sHRP, TMB, stop solution and measurement of absorbance using an ELISA plate reader (**Figure 3.2 C**). Higher absorbances (higher OD) indicate the presence of increased IGF-1R-Ab in samples of interest.

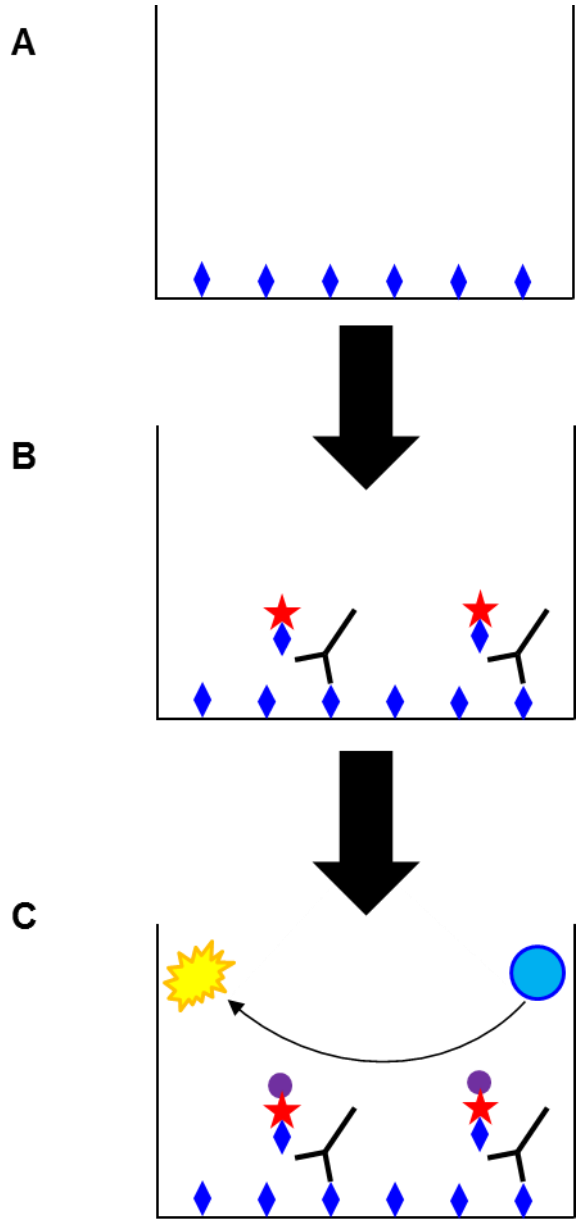

Figure 3.2: Diagrammatic representation of the principle of ELISA 2. Recombinant human IGF-1R (rhIGF-1R) (blue diamond) is coated onto ELISA plate wells (A). IGF-1R-Ab (black figure) in human sera are allowed to interact with rhIGF-1R. Due to the bivalent nature of immunoglobulins, a biotinylated rhIGF-1R (blue diamond with red star) may bind to the serum IGF-1R-Ab (B), When strepavidin-HRP (purple circle) is added, this binds rhIGF-1R plus IGF-1R-Ab plus biotinylated rhIGF-1R complex and there is a subsequently greater ELISA signal determined from the substrate solution (blue circle converting to yellow circle) (C). The quantity of serum IGF-1R-Ab is therefore determined by the optical density measured.

3.2 Aims and Objectives

In this chapter I aimed to establish and validate two novel ELISA-based assays for the measurement and quantification of IGF-1R-Abs, specifically in GD+TAO+ and GD+TAO- patients, with the aim of comparing these measurements with HC subjects. I also aimed to correlate IGF-1R-Ab with demographic factors, as well as clinical, genetic and immunological indices of GD and TAO, including thyroid function, TRAb and PTPN22 (R620W) GD susceptibility genotype.

3.3 Methods

The final ELISA 1 and ELISA 2 are presented in this section, with details of the optimisation, validation and subsequent use of each immunoassay in GD+TAO+, GD+TAO- and HC sera being fully described in **Chapter 3.4**.

3.3.1 Final Optimised IGF-1R-Ab ELISA 1

On the day prior to the ELISA, 100 µl of rhIGF-1R at 3000 ng/ml was used to coat each well of a 96-well ELISA plate (Nunc-Immuno Maxisor, Fisher Scientific), with the plate being sealed and incubated overnight at 4^{o}C.

On the day of the ELISA, each well was initially washed with 300 µl of wash buffer (PBS/Tween 20 0.05%) three times using a plate washer (Biochrom Asys Atlantis microplate washer). After the last wash, any remaining wash buffer was removed by inverting the plate and blotting it against clean paper towels. Wells were then blocked

with 300 µl of block buffer (PBS/Tween 20, 5%) and incubated at room temperature for one hour. Following this, further washes (as described above) were performed. 100 µl of human serum, either GD+TAO+, GD+TAO- or HC, diluted 1/100 in reagent diluent (PBS), were placed in the relevant wells in duplicate. The ELISA plate was then covered with an adhesive strip and incubated at 4^{o}C for 16 hours on a plate shaker (500 shakes/minute).

Following this, the three-wash step was repeated. 100 µl of Biotin-IGF-1 at 100 ng/ml was placed in each well, the plate again covered with an adhesive strip and incubated at room temperature for two hours. Following this, the three-wash step was repeated. 100 µl of sHRP was then added to each well at a dilution of 1/200, the plate again covered and incubated in the dark at room temperature for 20 minutes. A further three-wash step was then repeated. 100 µl of substrate solution (1:1 mixture of colour reagent A (H_2O_2) and colour reagent B (TMB)) was then placed in each well and incubated in the dark at room temperature for 20 minutes. Following this, 50 µl of stop solution (H_2SO_4) was added to each well and the plate gently tapped to ensure thorough mixing. The OD of each well was then determined using a microplate reader (Bio-tek Instruments EL808) set to read at 450 nm and 630 nm. Subtraction of the measured OD at 630 nm from that at 450 nm was then performed to correct for optical imperfections in the ELISA plate itself.

3.3.2 Final Optimised IGF-1R-Ab ELISA 2

On the day prior to the ELISA, 100 µl of rhIGF-1R at 1000 ng/ml was used to coat each well of a 96-well ELISA plate (Nunc-Immuno Maxisor, Fisher Scientific), with the

plate being sealed and incubated overnight at 4^{o}C. On the day of the ELISA, each well was initially washed with 300 µl of wash buffer (PBS/Tween 20 0.05%) three times using a plate washer (Biochrom Asys Atlantis microplate washer). After the last wash, any remaining wash buffer was removed by inverting the plate and blotting it against clean paper towels. Wells were then blocked with 300 µl of block buffer (PBS/Tween 20, 5%) and incubated at room temperature for one hour. Following this, further washes (as described above) were performed. 100 µl of human serum, either GD+TAO+, GD+TAO- or HC, diluted 1 in 10 in reagent diluent (PBS), were placed in the relevant wells in duplicate. The ELISA plate was then covered with an adhesive strip and incubated at 4^{o}C for 16 hours on a plate shaker. Following this, the three-wash step was repeated. 100 µl of IGF-1R-Biotin was then placed in each well, the plate again covered with an adhesive strip and incubated at room temperature for two hours. Following this, the three-wash step was repeated. 100 µl of sHRP was then added to each well at a dilution of 1/200, the plate again covered and incubated in the dark at room temperature for 20 minutes. A further three-wash step was then repeated. 100 µl of substrate solution (1:1 mixture of colour reagent A (H_2O_2) and colour reagent B (TMB) was then placed in each well and incubated in the dark at room temperature for 20 minutes. Following this, 50 µl of stop solution (H_2SO_4) was added to each well and the plate gently tapped to ensure thorough mixing. The OD of each well was then determined using a microplate reader (Bio-tek Instruments EL808) set to read at 450nm and 630nm. Subtraction of the measured OD at 630nm from that at 450nm was then performed to correct for optical imperfections in the ELISA plate itself.

3.3.3 Statistical Analysis

Statistical analysis was performed by GraphPad Prism version 5.0 (GraphPad Software, California 2008). D'Agostino-Pearson test determined that IGF-1R-Ab levels as measured by ELISA 1 and ELISA 2 were not normally distributed. Therefore, non-parametric comparisons between GD+TAO+, GD+TAO- and HC were undertaken with the Mann Whitney U test for two groups, Kruskal-Wallis test (and Dunn's multiple comparison) for multiple groups. Correlation was undertaken with Spearman's rank correlation. The minimum level of confidence at which the results were to be judged significant was $p<0.05$.

3.4 Results

3.5 ELISA 1

A human IGF-1R Duoset (R&D Systems, Abingdon, UK) was adapted to perform the function of an IGF-1R autoantibody ELISA. This IGF-1R Duoset comprises an IGF-1R monoclonal capture antibody which binds IGF-1R within a sample of interest (or rhIGF-1R or at varying concentrations, in order to obtain a standard curve). The IGF-1R or rhIGF-1R, in turn, is bound by a biotinylated polyclonal goat anti-human detection antibody which itself binds sHRP, leading to a blue colour change in a H_2O_2/TMB substrate solution and conversion to a yellow colour with a stop solution. Determination of the OD of this colour is undertaken using a microplate reader.

I instead bound rhIGF-1R directly to the ELISA plate and used the IGF-1R monoclonal capture antibody as an IGF-1R monoclonal antibody, the concentration of which could be adjusted to test the validity of the developing IGF-1R-Ab ELISA.

3.5.1 Determination of Optimum Concentrations of rhIGF-1R and Biotin-IGF-1

It was determined that not using IGF-1R capture antibody to bind rhIGF-1R to the ELISA plate was preferable as Biotin-IGF-1, even at 100 ng/ml and 1000 ng/ml, could not be detected when capture antibody was used (**Figure 3.3 A**). In addition, even without capture antibody, Biotin-IGF-1 at 1000 ng/ml resulted in too high a background signal, with OD of around 0.5 even without rhIGF-1R bound to the ELISA

plate (**Figure 3.3 B**). From this experiment it was determined to use no IGF-1R capture antibody prior to rhIGF-1R and to use Biotin-IGF-1 at 100 ng/ml.

It was noted that the signal gained from using rhIGF-1R at 1000 ng/ml and Biotin-IGF-1 at 100 ng/ml resulted in an optical density of only around 0.6. As the aim of the ELISA was to inhibit the maximum signal gained from optimum Biotin-IGF-1 binding to rhIGF-1R (by addition of IGF-1R-Ab presumably within sera), it was felt that a higher baseline optical density was required, with the aim being for a starting OD of around 1.

I therefore determined the optical density achieved with a higher range of rhIGF-1R from 1000 – 10,000 ng/ml, in 2000 ng/ml increments (with Biotin-IGF-1 standardised at 100 ng/ml) and found that there was a plateau of the OD at around 4000 ng/ml (**Figure 3.4 A**). The chosen OD of 1 was achieved at 3000 ng/ml of rhIGF-1R. Furthermore, the signal gained could be blocked by around 75% with 1 µg/ml IGF-1R monoclonal antibody, a percentage inhibition that itself plateaued at 3000 ng/ml of rhIGF-1R, before gradually decreasing (**Figure 3.4 B**) as rhIGF-1R continued to increase in concentration up to 10,000 ng/ml. For the balance of cost of reagents, attainment of a target baseline OD of 1 and the greatest sensitivity of detecting blocking by IGF-1R monoclonal antibody (and therefore, by extension, serum IGF-1R-Ab), an ELISA plate coating of 3000 ng/ml rhIGF-1R was chosen.

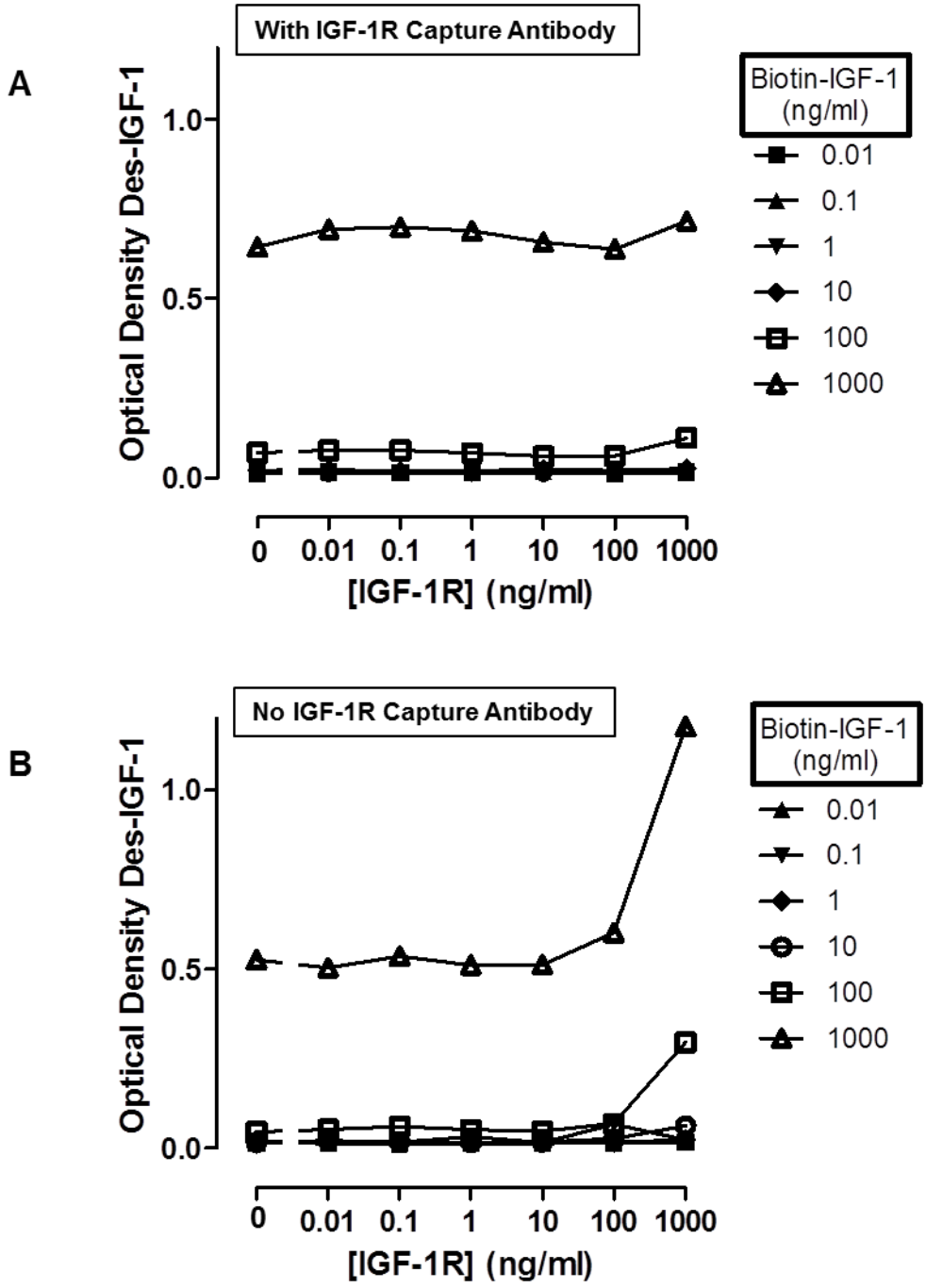

Figure 3.3: Optimisation of rhIGF-1R ELISA plate coating and Biotin-IGF-1 levels in ELISA 1. A range of concentrations of IGF-1R (0 – 1000 ng/ml) and Biotin-IGF-1 (0 – 1000 ng/ml) were used to establish the optimum relative levels of each, when the ELISA was undertaken with an IGF-1R capture antibody used to bind rhIGF-1R to the ELISA plate (A) and without such a capture antibody (B). Optical density determined from absorbance of each ELISA plate well at 450/630 nm. Each plot representative of two repeated experiments.

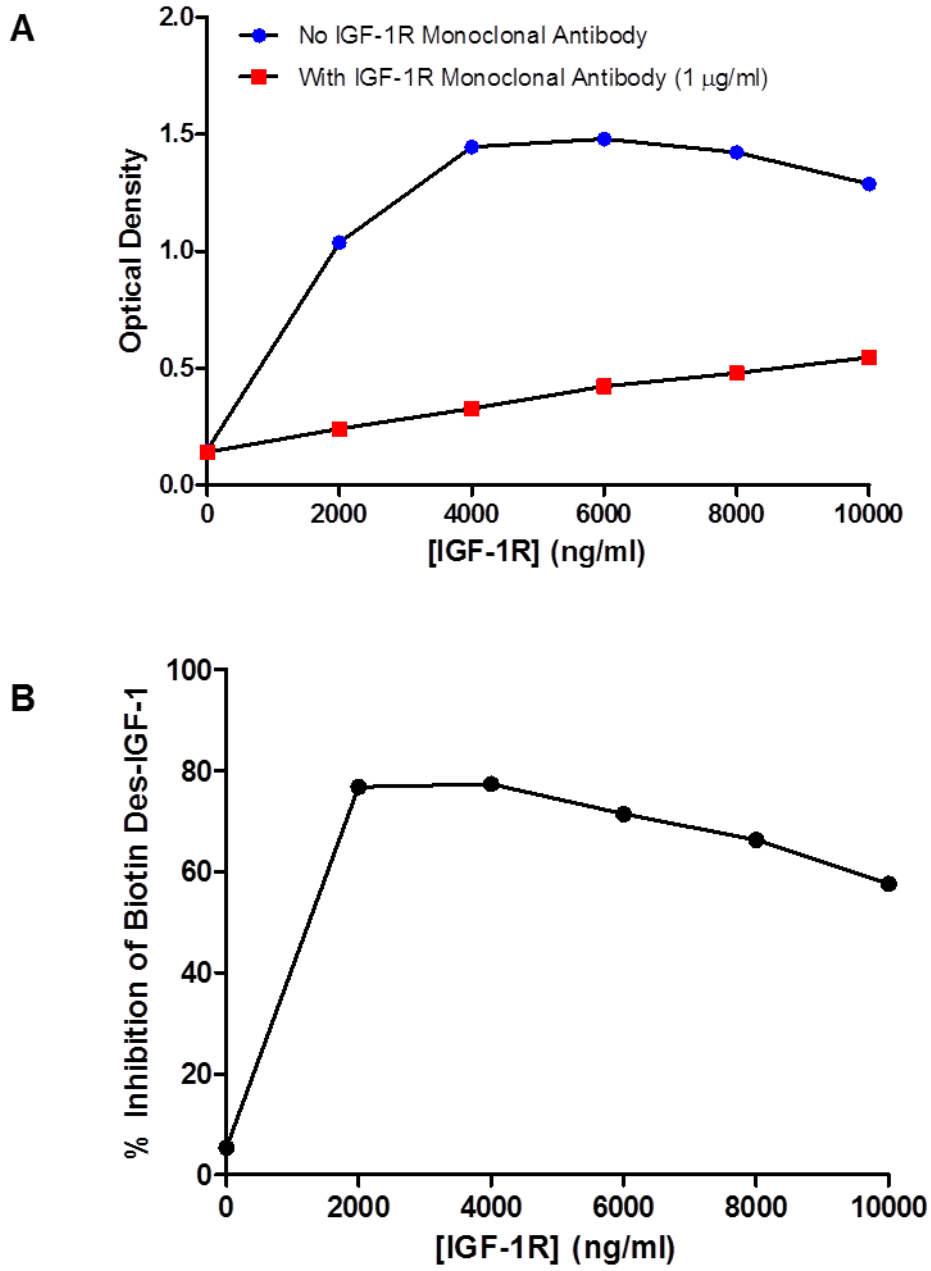

Figure 3.4: Optimisation of rhIGF-1R ELISA plate coating and detection of inhibition of Biotin-IGF-1 binding in ELISA 1. A range of rhIGF-1R concentrations from 0 – 10,000 ng/ml were investigated, with 1000 ng/ml increments and use of a standardised Biotin-IGF-1 concentration of 100 ng/ml. It was determined that the ELISA signal was optimal at around 3000 ng/ml. (A) IGF-1R monoclonal antibody, as expected, was found to inhibit Biotin-IGF-1 binding, with the greatest inhibition of the assay found at an rhIGF-1R ELISA plate coating of 3000 ng/ml. (B) Optical density determined from absorbance of each ELISA plate well at 450/630 nm. Each plot representative of two repeated experiments.

3.5.2 Determination of Optimum ELISA 1 Reagents and Conditions

A number of the conditions for ELISA 1 were further investigated (**Figure 3.5 A-C**). I compared the optical density gained with PBS or bicarbonate 0.05 M and found that PBS resulted in an OD closer to my preferred ELISA baseline signal of 1 and larger differences in the inhibition of this signal with increasing concentrations of IGF-1R monoclonal antibody, hence PBS was chosen to be used in all further assays (**Figure 3.5 A**).

I also analysed whether it would be advantageous to use a plate shaker during the incubation of IGF-1R monoclonal antibody or patient sera with the plate-bound rhIGF-1R. Again, greater differential inhibition from the baseline OD with shaking of the ELISA plate was observed (500 shakes per min) over a range of IGF-1R monoclonal antibody concentrations and continued to use this technique throughout all studies using patient sera (**Figure 3.5 B)**.

Finally, the optimum dilution of patient sera was evaluated, based on the percentage inhibition of the initial ELISA signal and the difference that could be observed between a pilot set of 12 patient samples (6 TAO, 6 HC). In summary, a serum dilution of 1 in 10 and that of 1 in 1000 resulted in there being no observable difference between patient samples – in the case of a 1 in 10 dilution the degree of non-specific binding was felt to be too high, while in the case of a 1 in 1000 dilution barely any diminution of signal between subjects could be observed (**Figure 3.5 C**). A serum dilution of 1 in 100 was therefore used.

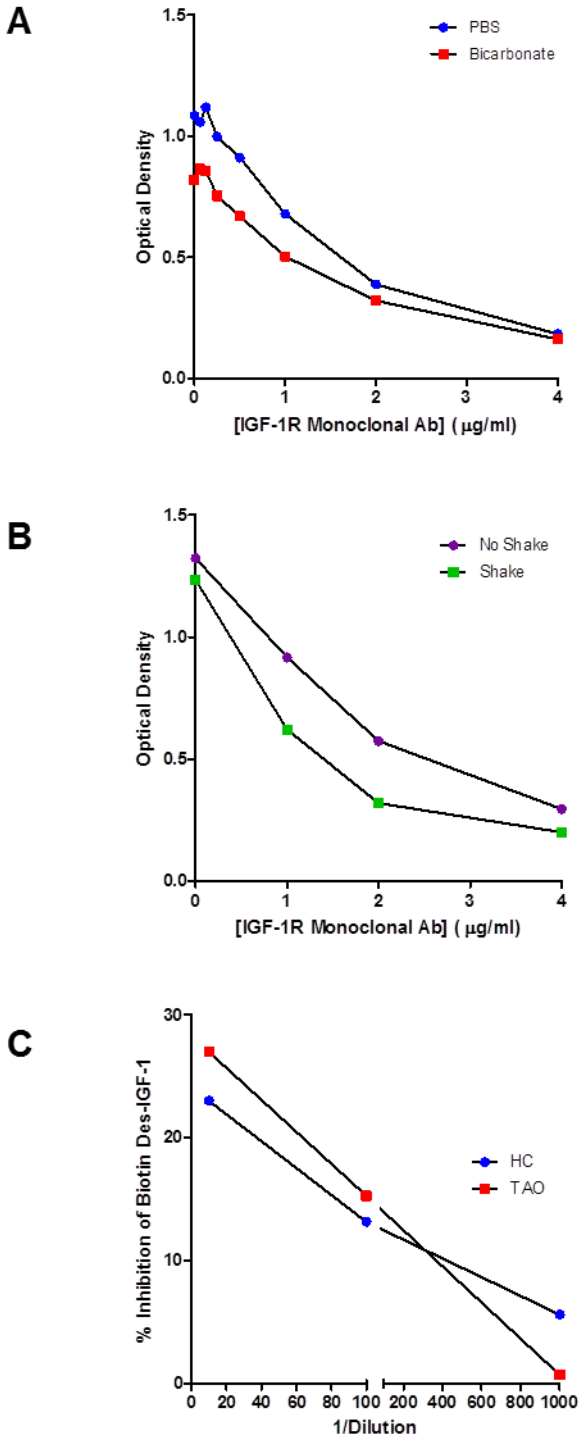

Figure 3.5: Optimisation of incubation conditions for ELISA 1. A number of the conditions for ELISA 1 were investigated, including whether PBS or bicarbonate 0.05 M would be the preferred diluent for IGF-1R monoclonal antibody (A), whether the ELISA plate should be shaken during the incubation of sera or IGF-1R monoclonal antibody with plate-bound rhIGF-1R (B) and what the optimum dilution of patient sera should be (C). On the basis of these studies, PBS was used as the IGF-1R monoclonal antibody and sera diluent, plates were shaken during incubation and a 1/100 dilution of sera was used for all subsequent analyses. Sera were pooled from 6 HC and 6 active TAO subjects in each experiment. Optical density determined from absorbance of each ELISA plate well at 450/630 nm. Each plot representative of two repeated experiments.

3.5.3 No Interference of Non-IGF-1R Monoclonal Antibody on ELISA 1

With rhIGF-1R at 3000 ng/ml, Biotin-IGF-1 at 100 ng/ml and 16 hour incubation of IGF-1R monoclonal antibody with plate-bound rhIGF-1R at 4^{o}C it was investigated whether recombinant IGF-1 (rIGF-1) (Peprotech, London) itself, or other non-IGF-1R commercial antibody, might interfere with the assay system, presumably by occupying rhIGF-1R binding sites, thereby preventing the binding of Biotin-IGF-1 and resulting in a lower OD which could erroneously be attributed to serum IGF-1R-Ab. This is clearly important given that IGF-1 itself, and other immunoglobulins, are present in human serum samples. Although the IGF-1R monoclonal antibody demonstrated blocking of Biotin-IGF-1 as normal, over a range of concentrations (0 – 2000 ng/ml), rIGF-1 at 0 – 1000 µg/ml was also seen to result in a reduction in the ELISA signal detected, with the original OD of 1.52 being reduced by almost 75% to 1.12 with only 0.01 µg/ml rIGF-1, suggesting that IGF-1 in serum samples may impact on the results of ELISA 1 (**Figure 3.6 A**). Furthermore, although this occurred at IGF-1 levels of 0.01 µg/ml, this was seen to plateau at concentrations of 0.1 µg/ml and above, which would be commensurate with normal, physiological levels of serum IGF-1 (0.01 to 1 µg/ml).[356] However, IL-6 monoclonal antibody, an IL-6 capture antibody obtained from an IL-6 ELISA kit (R&D Systems, Abingdon, UK) at 0 – 2000 ng/ml was not detected by ELISA 1 (**Figure 3.6 B**).

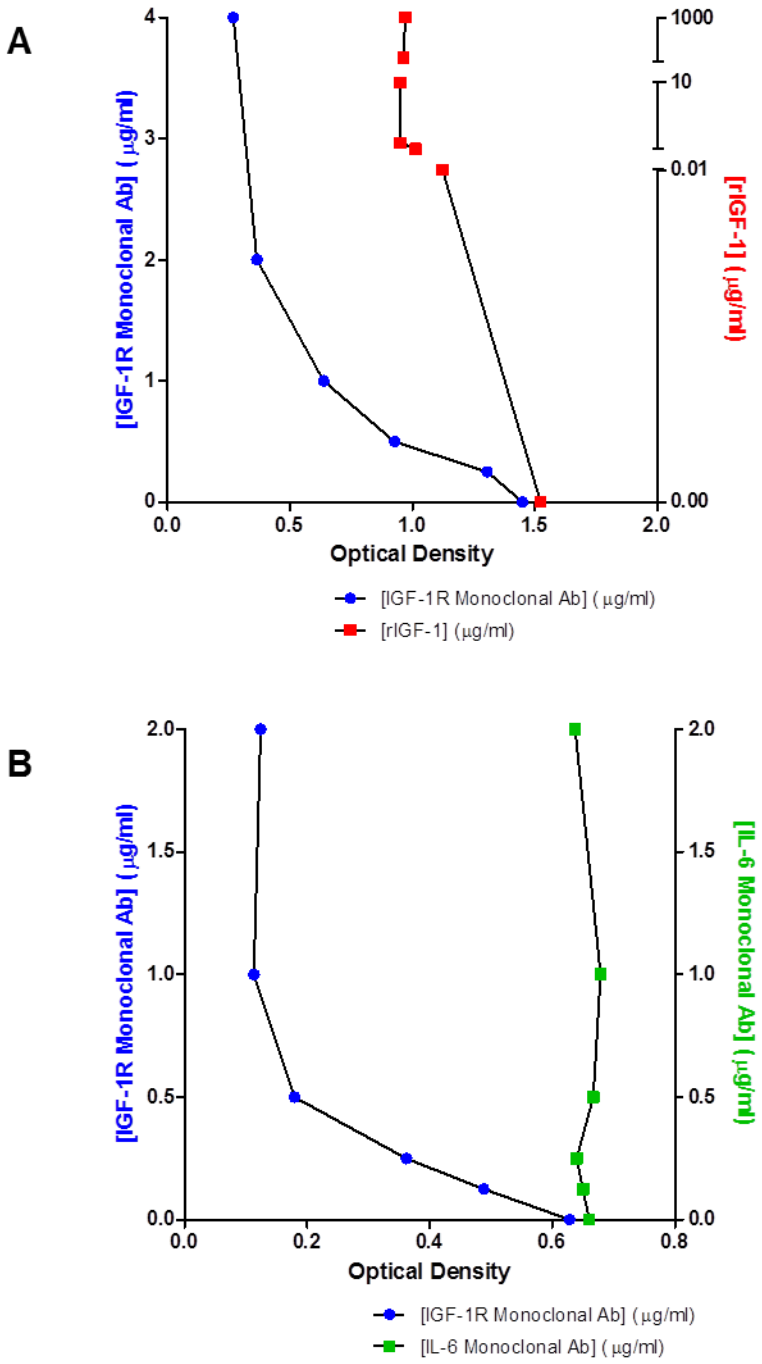

Figure 3.6: Effect of non-IGF-1R monoclonal antibody and rIGF-1 on ELISA 1. The effect of recombinant human IGF-1 (0 – 1000 µg/ml) (A) and IL-6 monoclonal antibody (0 – 2000 ng/ml) (B). ELISA 1 was undertaken with fully optimised conditions, with recombinant human IGF-1R (rhIGF-1R) at 3000 ng/ml, Biotin-IGF-1 at 100 ng/ml and 16 hour incubation of IGF-1R antibody at 4^{o}C. IGF-1R monoclonal antibody was utlised as previously (0 – 2000 ng/ml). Each plot representative of two repeated experiments.

3.6 ELISA 2

Similar to ELISA 1, the same existing IGF-1R Duoset (R&D Systems, Abingdon, UK) was modified to perform the function of an IGF-1R-Ab ELISA. In particular, the IGF-1R capture antibody was used as an IGF-1R monoclonal antibody in order to assess how varying concentrations of rhIGF-1R and IGF-1R-Biotin would function to detect putative IGF-1R-Ab in patient sera.

3.6.1 Biotinylation of Recombinant Human IGF-1R

rhIGF-1R (R&D Systems, Abingdon, UK) was biotinylated using a Lightning-Link-Biotin Type A biotinylation kit (Innova Biosciences, Cambridge) in accordance with instructions provided. Successful biotinylation of rhIGF-1R was confirmed with an IGF-1R-Biotin standard curve. (**Figure 3.7**)

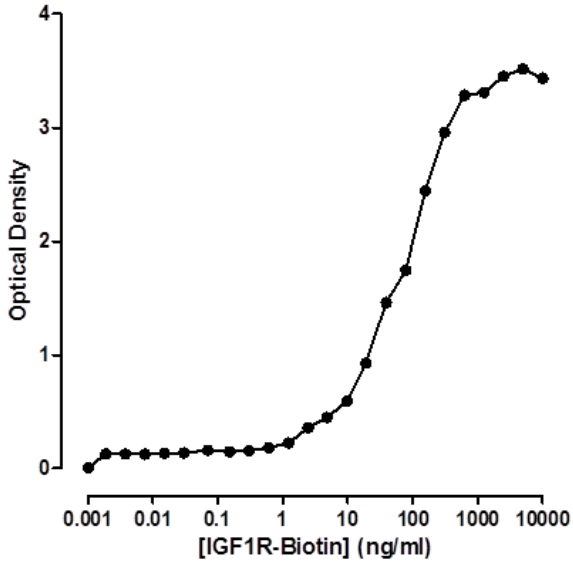

Figure 3.7: Confirmation of successful biotinylation of rhIGF-1R. Standard curve of IGF-1R-Biotin to plate-bound IGF-1R at concentration of 1000 ng/ml and incubation at 16 hours at 4^{o}C with IGF-1R monoclonal antibody at 100 ng/ml. Optical density determined from absorbance of each ELISA plate well at 450/630 nm. Plot representative of three repeated experiments.

3.6.2 Optimisation of rhIGF-1R and IGF-1R-Biotin Concentrations and Duration of IGF-1R Monoclonal Antibody Incubation

It was crucial to determine the most appropriate concentration of rhIGF-1r coating each ELISA plate well as there was concern that if the spacing between each IGF-1R molecule were too small (high rhIGF-1R concentration) then this may circumvent the main principle of the ELISA. That is, the rationale for the ELISA is that immunoglobulins are divalent, with the ability to bind two IGF-1R molecules – in this case the rhIGF-1R coating the ELISA plate and, in addition, serum IGF-1R monoclonal antibody. If each rhIGF-1R molecule were too close together then it is possible that IGF-1R-Ab would bind to two plate-bound rhIGF-1R and therefore not be able to bind IGF-1R monoclonal antibody in the test system, or IGF-1R-Ab in sera. Likewise, if the spacing between each IGF-1R molecule were too great (low rhIGF-1R concentration) there would be insufficient IGF-1R-Ab binding to generate a sufficient subsequent signal.

I therefore investigated a range of rhIGF-1R and IGF-1R-Biotin concentrations (0 – 1000 ng/ml for each), with varying concentrations of IGF-1R monoclonal antibody (0 - 1000 ng/ml). The ELISA was undertaken with only a one hour incubation of IGF-1R monoclonal antibody with rhIGF-1R and resulted in disappointing eventual OD of only around 0.32, even with the highest concentrations of rhIGF-1R, IGF-1R-Biotin and IGF-1R monoclonal antibody (**Figure 3.8**). I therefore increased the rhIGF-1R-IGF-1R monoclonal antibody incubation time to 16 hours and achieved more satisfactory OD, although again with rhIGF-1R and IGF-1R-Biotin concentrations each of 1000 ng/ml (**Figure 3.9**).

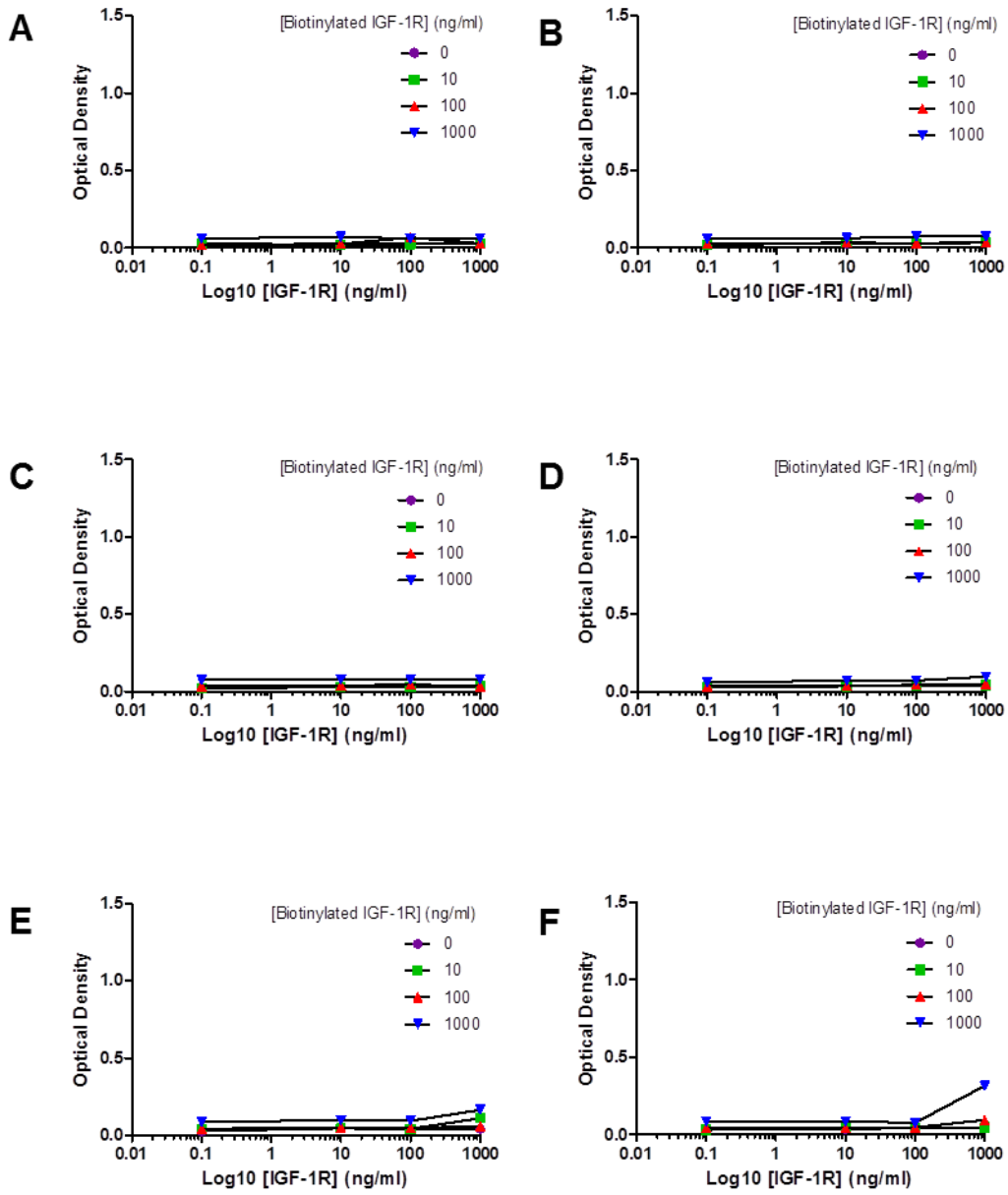

Figure 3.8: Optimisation of concentrations of rhIGF-1R and IGF-1R-Biotin in ELISA 2. A range of rhIGF-1R ELISA plate coating and IGF-1R-Biotin concentrations were used (0 – 1000 ng/ml for each) and varying concentrations of IGF-1R monoclonal antibody – 0 ng/ml (A), 0.1ng/ml (B), 1 ng/ml (C), 10 ng/ml (D), 100 ng/ml (E) and 1000 ng/ml (F). The ELISA was undertaken with only a one hour incubation of IGF-1R monoclonal antibody. In this system it can be seen that only 1000 ng/ml of IGF-1R monoclonal antibody could be detected with rhIGF-1R and IGF-1R-Biotin concentrations of 1000 ng/ml each (F). Each plot representative of two repeated experiments.

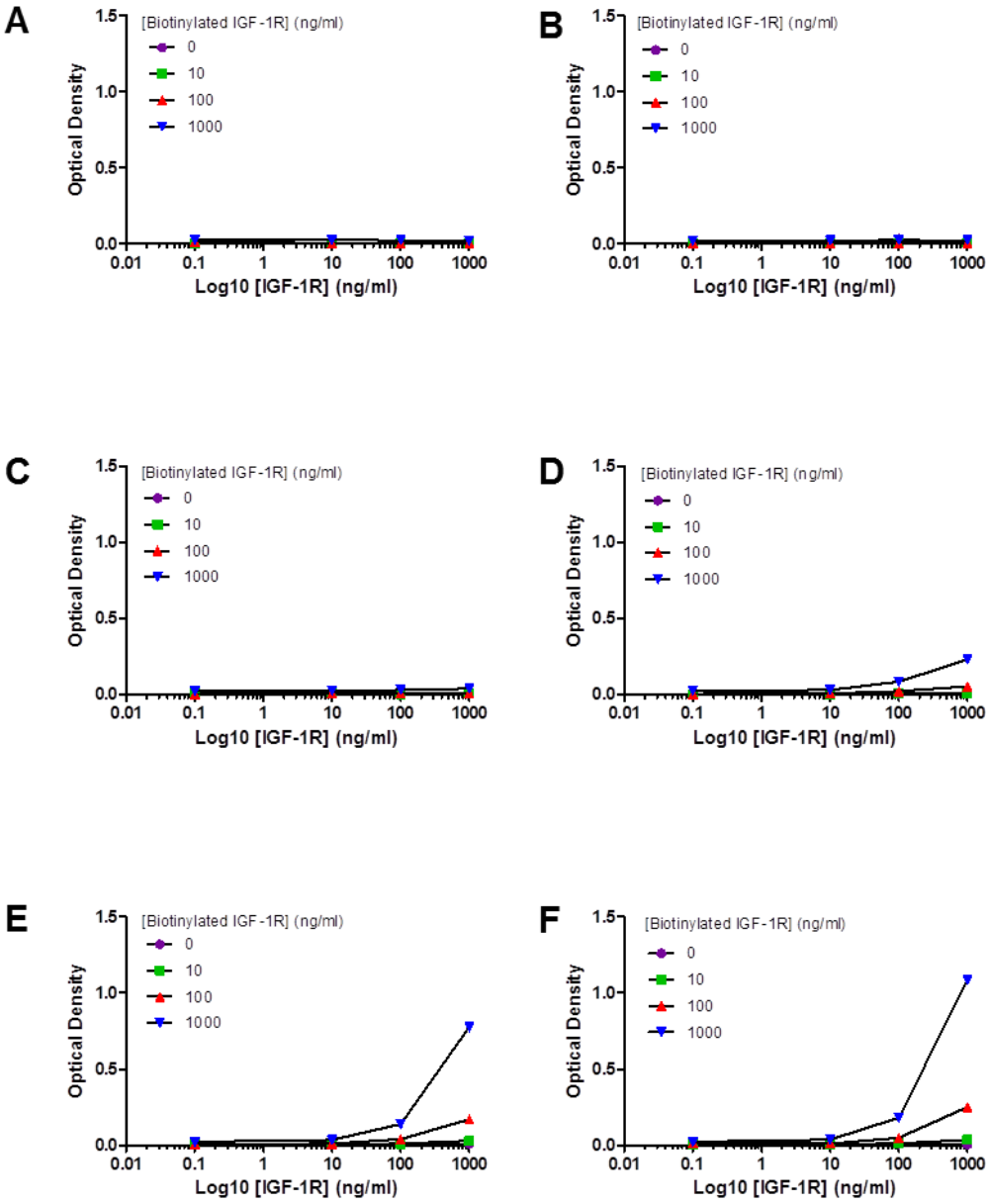

Figure 3.9: Optimisation of duration of incubation of IGF-1R monoclonal antibody with rhIGF-1R and IGF-1R-Biotin in ELISA 2. A range of rhIGF-1R ELISA plate coating and IGF-1R-Biotin concentrations were used (0 – 1000 ng/ml) and varying concentrations of IGF-1R monoclonal antibody – 0 ng/ml (A), 1 ng/ml (B), 10 ng/ml (C), 100 ng/ml (D), 1000 ng/ml (E) and 10,000 ng/ml (F). The ELISA was undertaken with 16 hour incubation of IGF-1R monoclonal antibody. In this system it can be seen that only 1000 ng/ml of IGF-1R monoclonal antibody could be detected with rhIGF-1R and IGF-1R-Biotin concentrations of 1000 ng/ml each (E & F). Each plot representative of two repeated experiments.

An attempt to evaluate if even higher concentrations of rhIGF-1R and IGF-1R-Biotin would result in higher eventual ODs, with a standardised concentration of IGF-1R monoclonal antibody (100 ng/ml), with 16 hour incubation, determined that a rhIGF-1R concentration of 1000 ng/ml was definitely the optimum, irrespective of the concentration of IGF-1R-Biotin used. Indeed, as rhIGF-1R concentration increased beyond 1000 ng/ml there was a deterioration in ODs achieved. Higher ODs were possible with increased IGF-1R-Biotin concentrations, unfortunately at the expense of higher background levels of OD even when no rhIGF-1R was coating each ELISA plate well. For example, the background OD level with IGF-1R-Biotin of 1000 ng/ml was 0.03, whereas at 5000 ng/ml it was 0.07 (**Figure 3.10**).

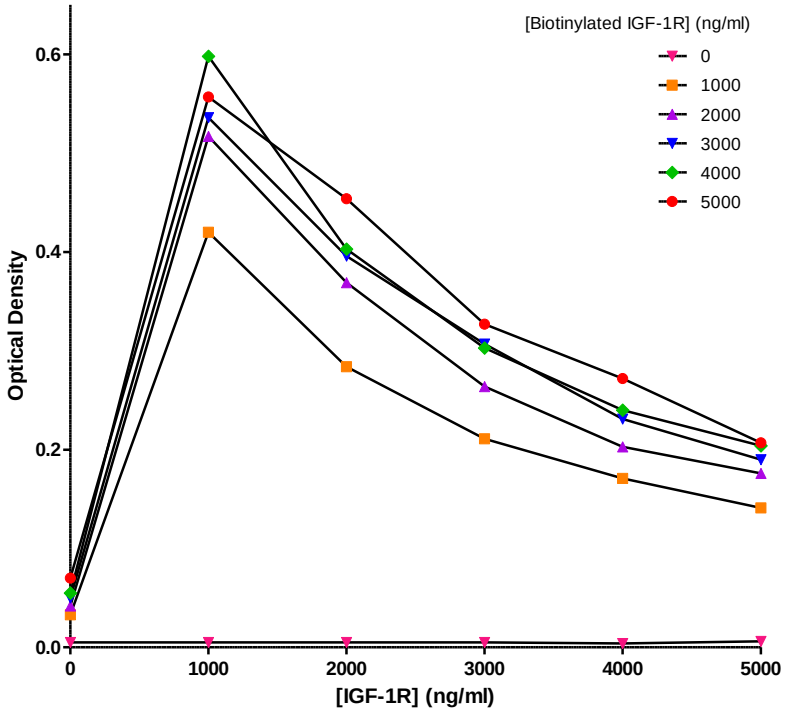

Figure 3.10: Evaluation of a range of rhIGF-1R and IGF-1R-Biotin concentrations in detecting IGF-1R monoclonal antibody in ELISA 2. With a standardised concentration of IGF-1R monoclonal antibody (100 ng/ml), with 16 hour incubation, it was determined that a rhIGF-1R concentration of 1000 ng/ml was the optimum, irrespective of the concentration of IGF-1R-Biotin used. Higher OD are achievable with higher concentrations of IGF-1R-Biotin, although at the expense of a higher background signal and expense of reagents. Each plot representative of two repeated experiments.

3.6.3 No Interference of Recombinant IGF-1 or Non-IGF-1R Monoclonal Antibody on ELISA 2

It was investigated whether rIGF-1 (Peprotech, London) itself might be detected by the assay system. Although IGF-1R monoclonal antibody was detected as normal, neither rIGF-1 at 0 – 100 μg/ml nor an IL-6 capture antibody obtained from an IL-6 ELISA kit (R&D Systems, Abingdon, UK), at 0 – 2000 ng/ml were detected by ELISA 2 (**Figure 3.11**). Importantly, normal levels of serum IGF-1 are 0.01 to 1 μg/ml,[356] so the levels of rIGF-1 used in this experiment were supra-physiological.

3.6.4 Optimum Dilution of Human Sera in ELISA 2

The optimum dilution of patient sera, based on the OD achieved and the difference in OD that could be detected between different subjects, was evaluated. In a pilot set of 12 patient samples, 6 TAO and 6 age- and sex matched HC, a serum dilution of 1/10 with PBS appeared to be the optimum, with dilutions of 1/100 and 1/1000 resulting in barely any detectable OD (**Figure 3.12**)

3.6.5 Consistent IGF-1R-Ab Measurements with Equivalent ELISA 2 Protocol

Using the sera of six of the most clinically active TAO patients in my cohort, alongside six age- and sex-matched HC for each of those patients, I undertook ELISA 2 with a 1/10 serum dilution with PBS and gained OD values for each in two separate experiments on two separate days, separated by a month. Gratifyingly, the OD values obtained were remarkably similar, attesting to the reproducibility and inter-experimental consistency of ELISA 2 (**Figure 3.13**).

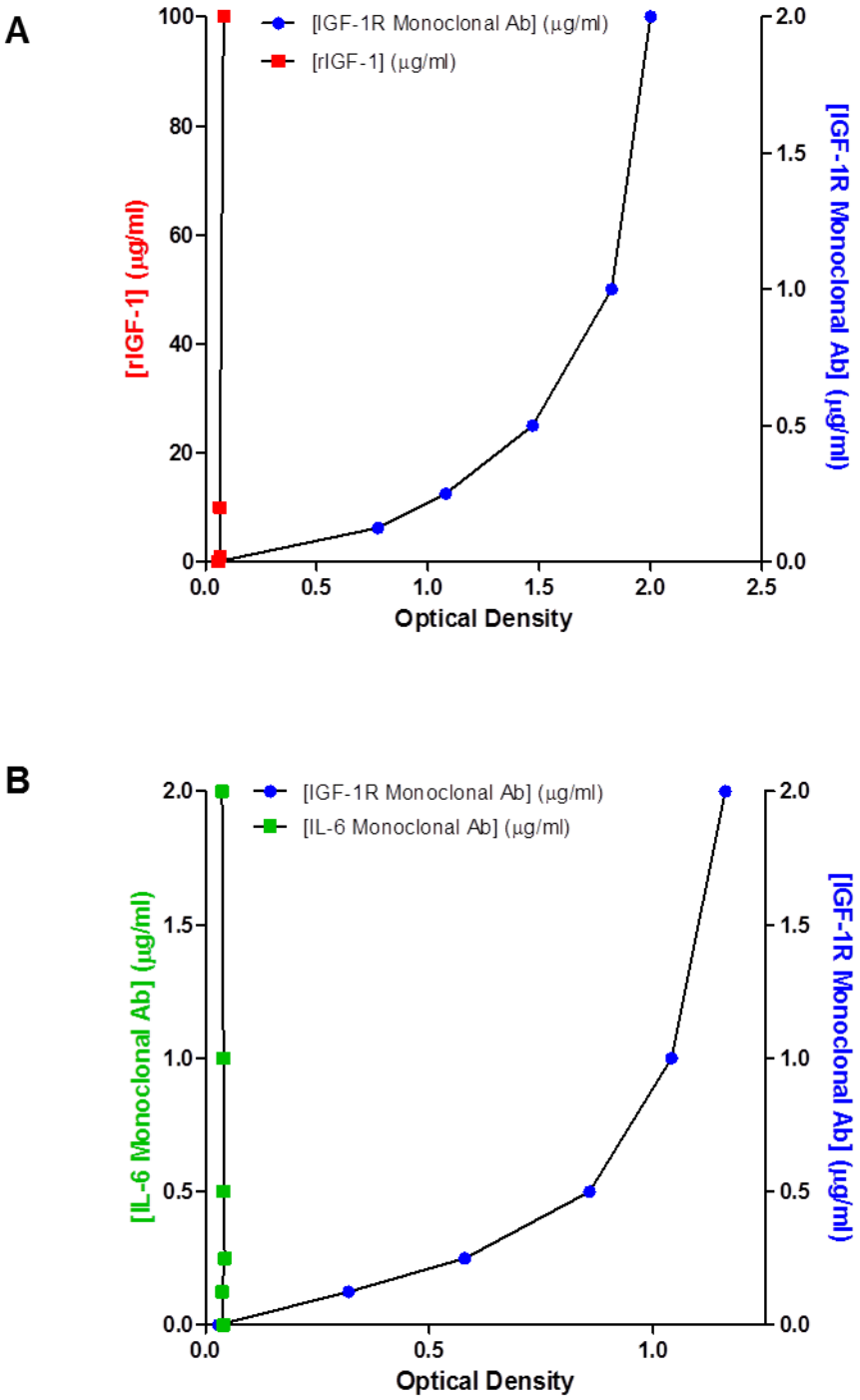

Figure 3.11: Effect of non-IGF-1R monoclonal antibody and rIGF-1 on ELISA 2. Although IGF-1R monoclonal antibody was detected as normal, over a range of concentrations (0 – 2000 ng/ml), neither recombinant human IGF-1 (rIGF-1) at 0 – 100 µg/ml (A) nor IL-6 monoclonal antibody at 0 – 2000 ng/ml (B) were detected by ELISA 2. ELISA 2 was undertaken with fully optimised conditions, with recombinant human IGF-1R (rhIGF-1R) at 1000 ng/ml, IGF-1R-Biotin at 1000 ng/ml and 16 hour incubation of serum with plate-bound rhIGF-1R at 4^{o}C. Each plot representative of two repeated experiments.

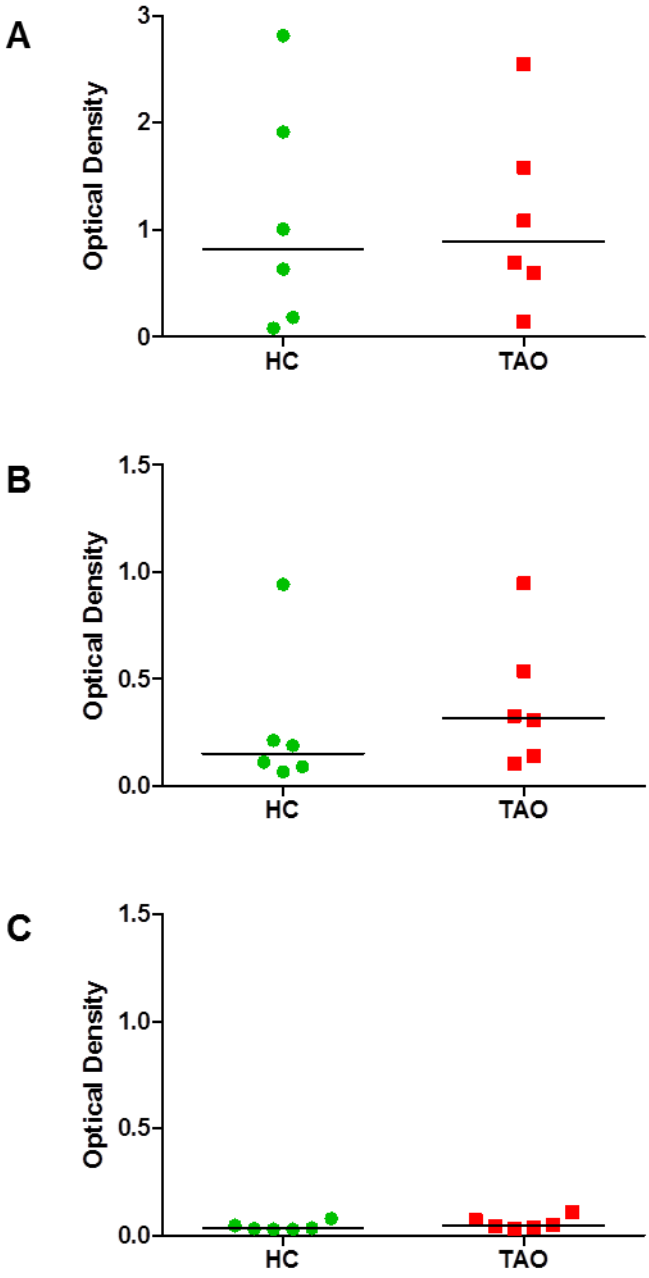

Figure 3.12: Investigation of the median effect of dilution of serum samples for GD+TAO+ and HC subjects. Sera of 6 GD+TAO+ and 6 age- and sex-matched HC were used in ELISA 2, either undiluted (A) or otherwise diluted 1 in 10 (B) or 1 in 100 (C) with PBS. rhIGF-1R 1000 ng/ml and IGF-1R-Biotin 1000 ng/ml. Incubation of undiluted or diluted serum samples for 16 hours with rhIGF-1R. On the basis of this study, a serum dilution of 1 in 10 was used in all further experiments related to participant sera. Data presented represent optical density determined from each individual serum sample, with horizontal line representing median value of all samples in that group. Results representative of two repeated experiments.

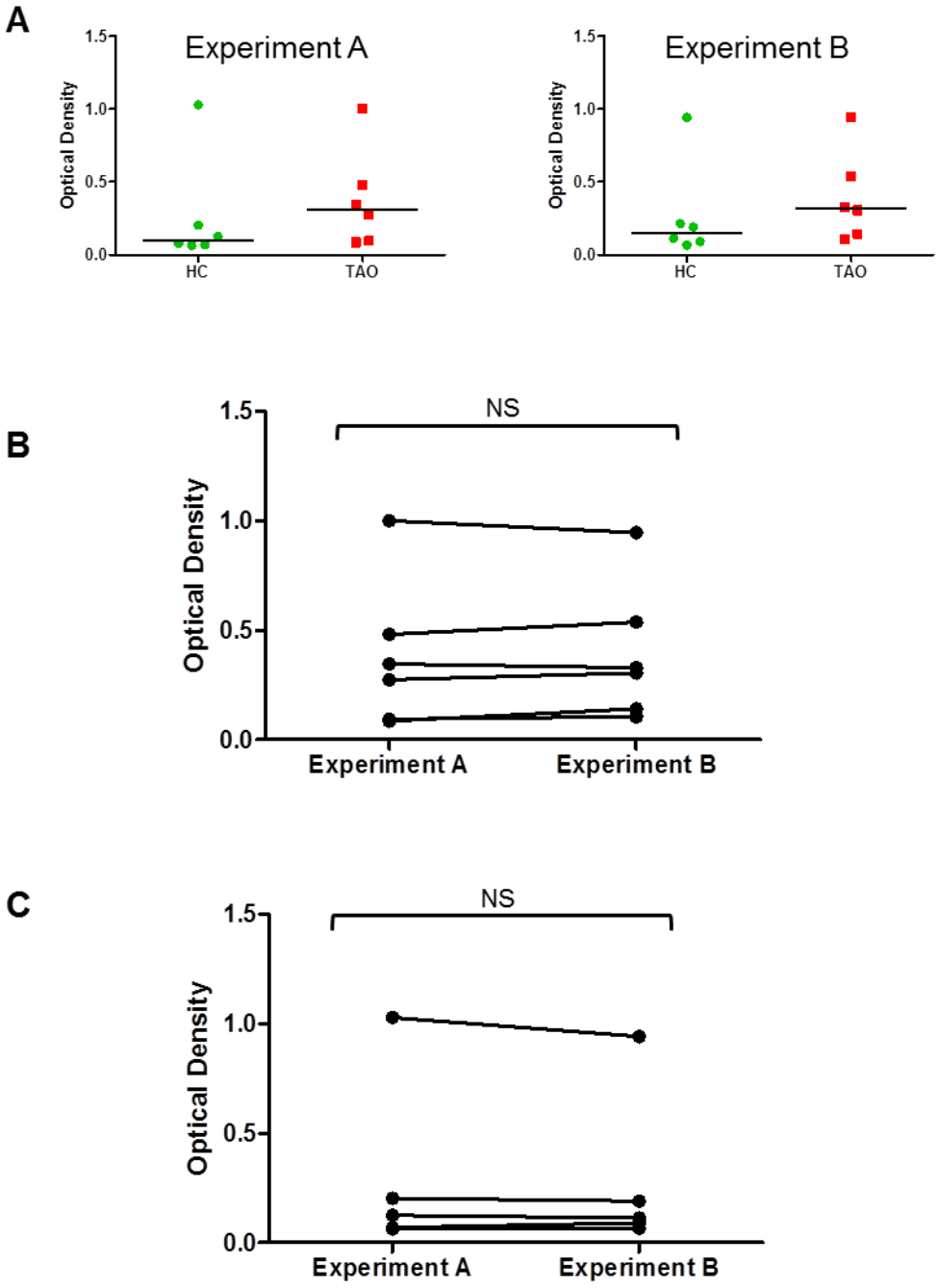

Figure 3.13: Consistency of optical density measurements between experiments for both GD+TAO+ and HC subjects with ELISA 2. IGF-1R-Ab were measured by ELISA 2 in the sera of six of the most clinically active GD+TAO+ patients in my cohort, alongside six age- and sex-matched HC for each of those patients. ELISA 2 was undertaken with serum diluted 1 in 10 in PBS and gained OD values for each subject in two separate experiments on two separate days a month apart (A). The OD values between the two separate experiments were compared for GD+TAO+ (B) and HC subjects (C). Non-parametric comparison of OD values for the separate experiments was undertaken with Wilcoxon matched pairs signed rank test. (Key: NS, Not significant). Plots representative of repeated experiment at different time points.

3.7 Use of ELISA 1 and ELISA 2 in GD+TAO+, GD+TAO- and HC Subjects

The following are results of the fully-optimised IGF-1R-Ab assays, based on inhibition of Biotin-IGF-1 binding to rhIGF-1R by IGF-1R-Ab (ELISA 1) or on binding of IGF-1R-Biotin to IGF-1R-Ab which, in turn, are bound to rhIGF-1R (ELISA 2).

3.7.1 Study Subjects

There were 110 GD+TAO+, 67 GD+TAO- subjects and 78 age- and sex-matched healthy controls (HC). Demographic and clinical parameters for these participants are summarised in **Table 3.1**.

Although there were no significant differences in terms of age, sex and cigarette smoking status, as well as thyroid status between the GD+TAO+ and GD+TAO- subjects, significant differences were observed in serum levels of TRAb between the three groups of interest, with 78% of GD+TAO+, 54% of GD+TAO- and 5% of HC being TRAb positive. The groups also differed in PTPN22 genotype, with 15% of GD+TAO+ patients being PTPN22 susceptibility SNP heterozygotes (GA) and 2% homozygotes (AA), as compared to 8% and 9% of GD+TAO- and HC, respectively, being heterozygotes and none being homozygotes (**Figure 3.14**). Furthermore, those patients with clinically active TAO (CAS ≥3) had significantly higher TRAb, with results approaching significance for cigarette smoking and dysthyroid status (**Figure 3.15**)

Table 3.1: Demographic features, clinical measures, thyroid function, TRAb status and PTPN22 (R620W) genotype for GD+TAO+, GD+TAO- and HC study groups.

	HC	GD+ TAO-	GD+ TAO+
Number	78	67	110
Median age in years (IQR)	44 (24)	46 (20)	51 (20)
Gender (M:F)	15 : 63	9 : 58	20 : 90
Smokers	51%	48%	57%
GD Duration >12 months	N/A	75%	90%
CAS≥3	N/A	N/A	18%
TAO Severity (Mild/Mod/Sev)	N/A	N/A	25 : 70 : 15
Thyroid Status (Hypo/Eu/Hyper)	N/A	5 : 41 : 21	11 : 85 : 14
TRAb Positive	5%	54%	78%
Thionamides	N/A	73%	53%

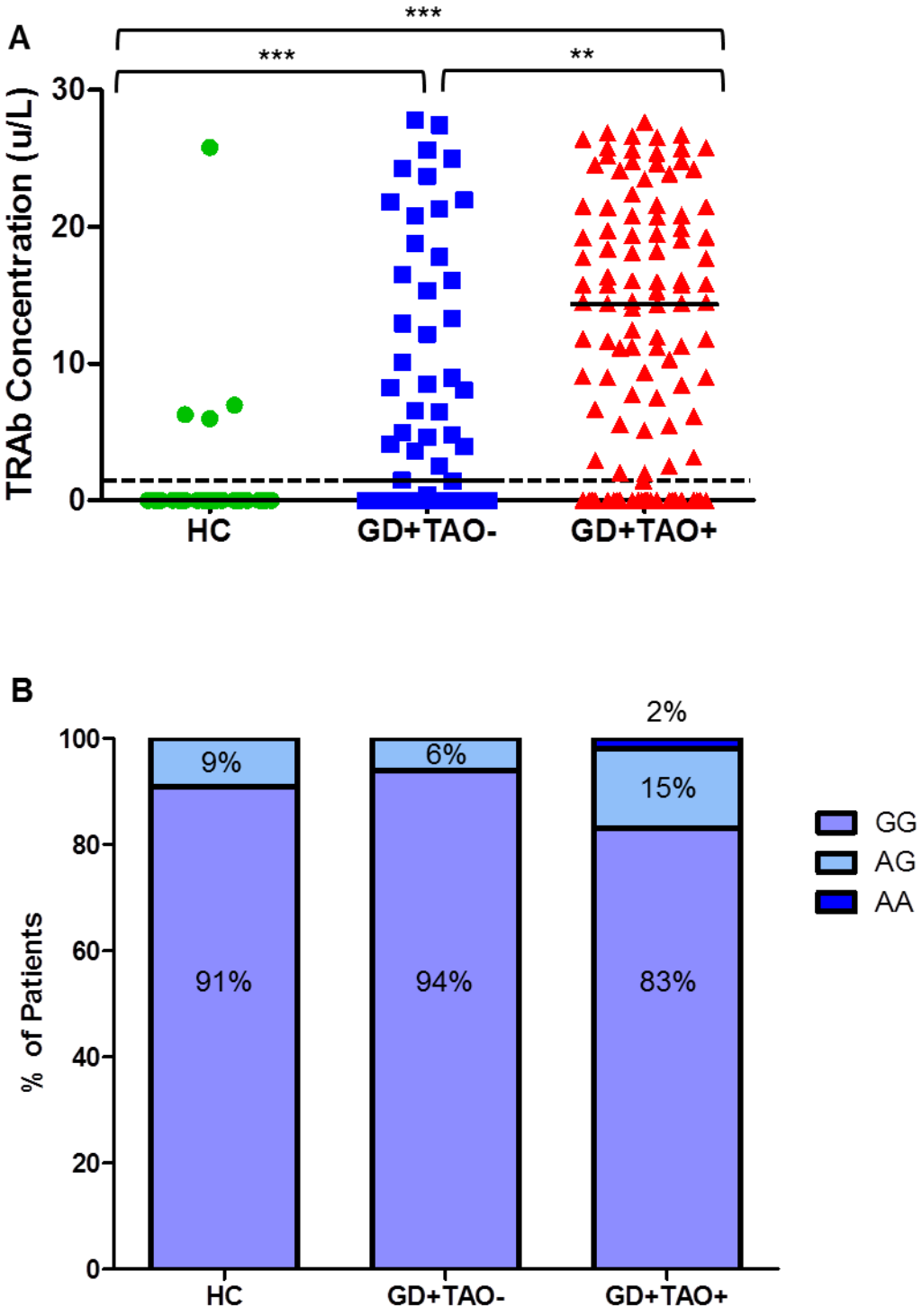

Figure 3.14: TRAb levels and PTPN22 (R620W) genotype in GD+TAO+, GD+TAO- and HC groups. Significant differences were observed in serum levels of TRAb between the 110 GD+TAO+, 67 GD+TAO- subjects and 78 age- and sex-matched healthy controls (HC). Dotted line indicates cut-off for definition of TRAb positivity (≥0.4 U/L) as defined by the assay data sheet (mean of duplicates). Non-parametric analysis was undertaken with Kruskal-Wallis (with Dunn's post-test). (NS: Not significant; **p<0.01; ***p<0.001) (A). PTPN22 (R620W) genotype of study groups based on real-time PCR and melting curve analysis (B).

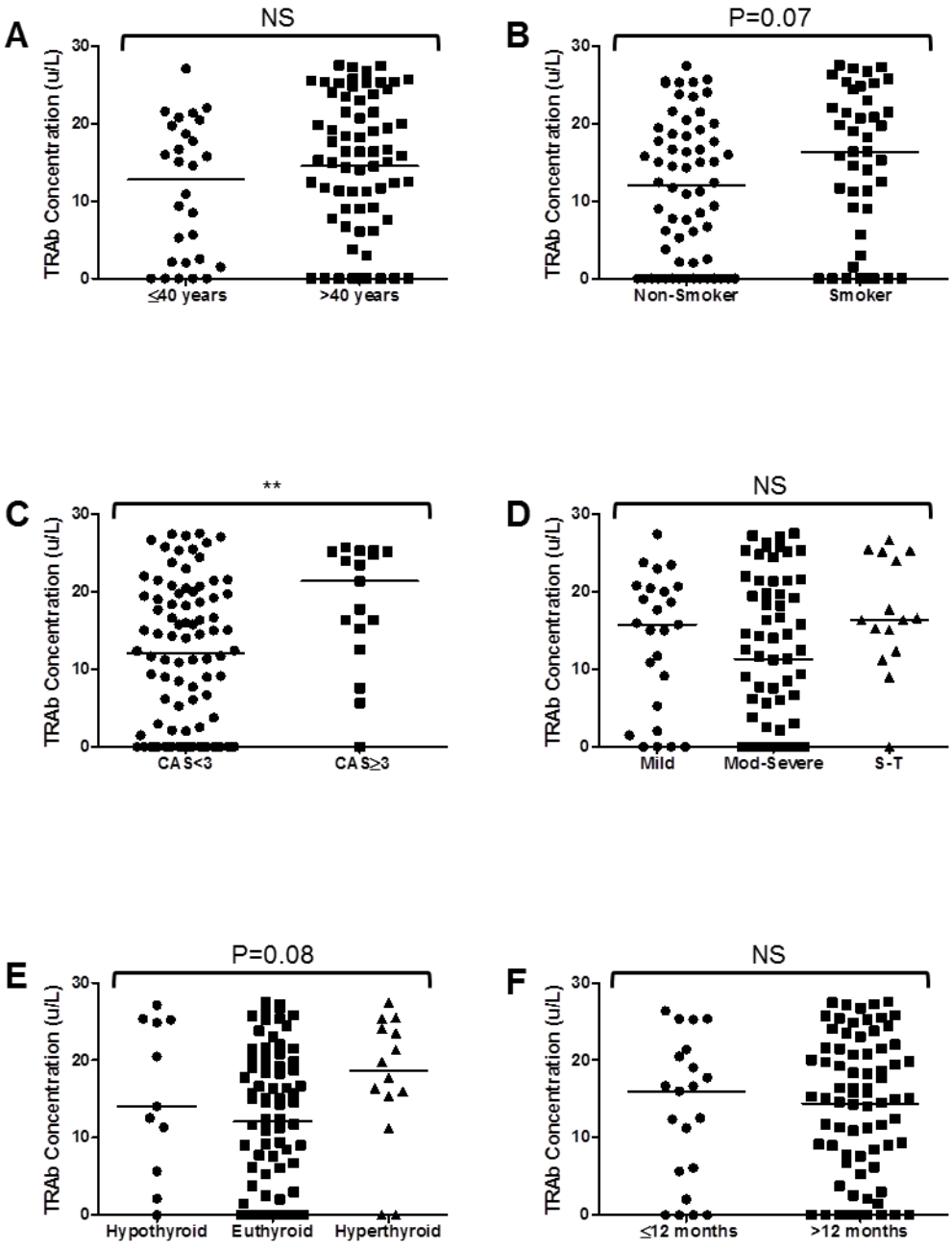

Figure 3.15: Relationship between TRAb levels and clinical, immunological and PTPN22 (R620W) genotype in GD+TAO+ subjects. No statistically significant differences were noted in age (A), cigarette smoking status (B), EUGOGO severity grade (D), thyroid function (E) or duration of GD (F). However, there was significant difference in TRAb with TAO clinical activity score (C). Non-parametric analysis was undertaken with Mann-Whitney U test (for two groups) or Kruskal-Wallis test (with Dunn's multiple comparison) for multiple groups. (NS, Not significant; **p<0.01).

3.7.2 IGF-1R-Ab are not elevated in GD+TAO+ or GD+TAO- subjects as compared to HC when measured by ELISA 1 or ELISA 2

Using both ELISA 1 (**Figure 3.16**) and ELISA 2 (**Figure 3.17**) no significant differences were noted in the median levels of serum IGF-1R-Ab measured between GD and HC controls and between GD+TAO+ and GD+TAO- patients. With respect to ELISA 1, the median percentage inhibition of Biotin-IGF-1 binding in the GD+TAO+ (13%, IQR 10.5) , GD+TAO- (14%, IQR 9.6) and HC (14%, IQR 11.7) group were not significantly different. Similarly, if it is assumed that the levels of IGF-1R-Ab in serum are normally distributed and one uses means, the proportion of subjects defined as IGF-1R-Ab positive, irrespective of whether this is stated to be 1, 2 or 3 standard deviations above the mean IGF-R-Ab of the HC population, are also no different. For example, if we set a cut-off at 2 standard deviations above the HC mean IGF-1R-Ab, then the proportion of “IGF-1R-Ab positive” subjects in the GD+TAO+, GD+TAO- and HC group are 4.7%, 6.3% and 4.2%, respectively (using ELISA 2).

3.7.3 No correlation between IGF-1R-Ab as measured by ELISA 1 and ELISA 2 and clinical, immunological or genetic features of GD and TAO

Those GD+TAO+ patients with active TAO (CAS ≥3) were shown to have significantly higher TRAb levels than those with inactive TAO (CAS<3). Such TRAb results also approached statistical significance for those GD+TAO+ patients who were cigarette smokers (as compared to non-smokers) and for those who were either hypothyroid or hyperthyroid (as compared to euthyroid) (**Figure 3.15**). No significant association was found in terms of any demographic, clinical or immunological parameter, nor in terms of PTPN22 (R620W) genotype, and IGF-1R-Ab levels, as

measured by either ELISA 1 or ELISA 2 (**Figure 3.18 and 3.19**). There were no changes in the findings when inactive TAO patients of over 18 months duration were removed from analysis ('burnt out' cases) (**Appendix 2 and 3**). These univariate analyses were confirmed by multivariable logistic regression (**Appendix 4 and 5**).

3.7.4 No correlation between IGF-1R-Ab, TRAb and TPO-Ab but significant correlation between IGF-1R-Ab as measured by ELISA 1 and ELISA 2

As demonstrated in **Figures 3.20 and 3.21**, there was no correlation between IGF-1R-Ab, as measured by either ELISA 1 or ELISA 2, with either TRAb or TPO-Ab in the GD+TAO+ patients. The lack of correlation between TRAb and TPO-Ab may be explained by the TPO-Ab having been measured at the time when the patient was initially diagnosed with GD, sometimes a significant number of months in the past and certainly prior to the taking of peripheral blood and separation of serum for storage. This may have meant that with time and treatment there was an alteration in the autoantibody constituents of the serum of each of the patients analysed, with a proportion of patients who were previously TPO-Ab positive now being TRAb negative. The TPO-Ab for each subject were also determined independently by the UHB clinical immunology laboratory whereas TRAb were measured with a TRAb ELISA kit (ElisaRSRTM TRAb 3rd Generation, Cardiff, UK). However, it is encouraging to note that IGF-1R-Ab levels as measured by ELISA 1 and ELISA 2 did show significant correlation, with Spearman's r of 0.31 ($p=0.0001$). This suggests that the two ELISA are at least measuring the same constituent of the serum.

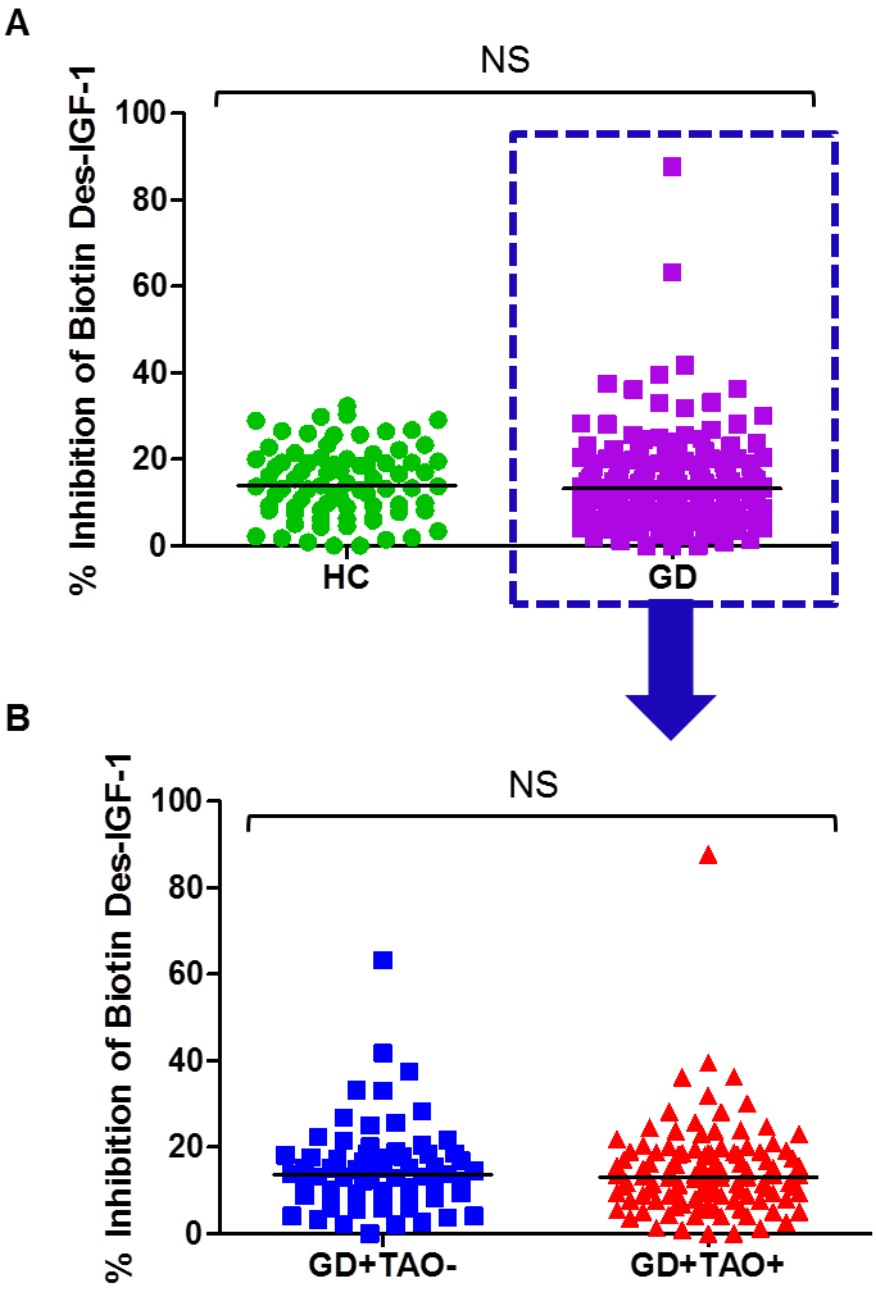

Figure 3.16: Comparison of IGF-1R-Ab levels as measured by ELISA 1 in the study populations. No significant difference was observed in serum levels of IGF-1R-Ab between 177 GD patients and 78 age- and sex-matched healthy controls (A), nor between the 110 GD+TAO+ and 67 GD+TAO- subjects (B), using ELISA 1 (mean of duplicates). Non-parametric analysis was undertaken with Mann-Whitney U test. (NS, Not significant).

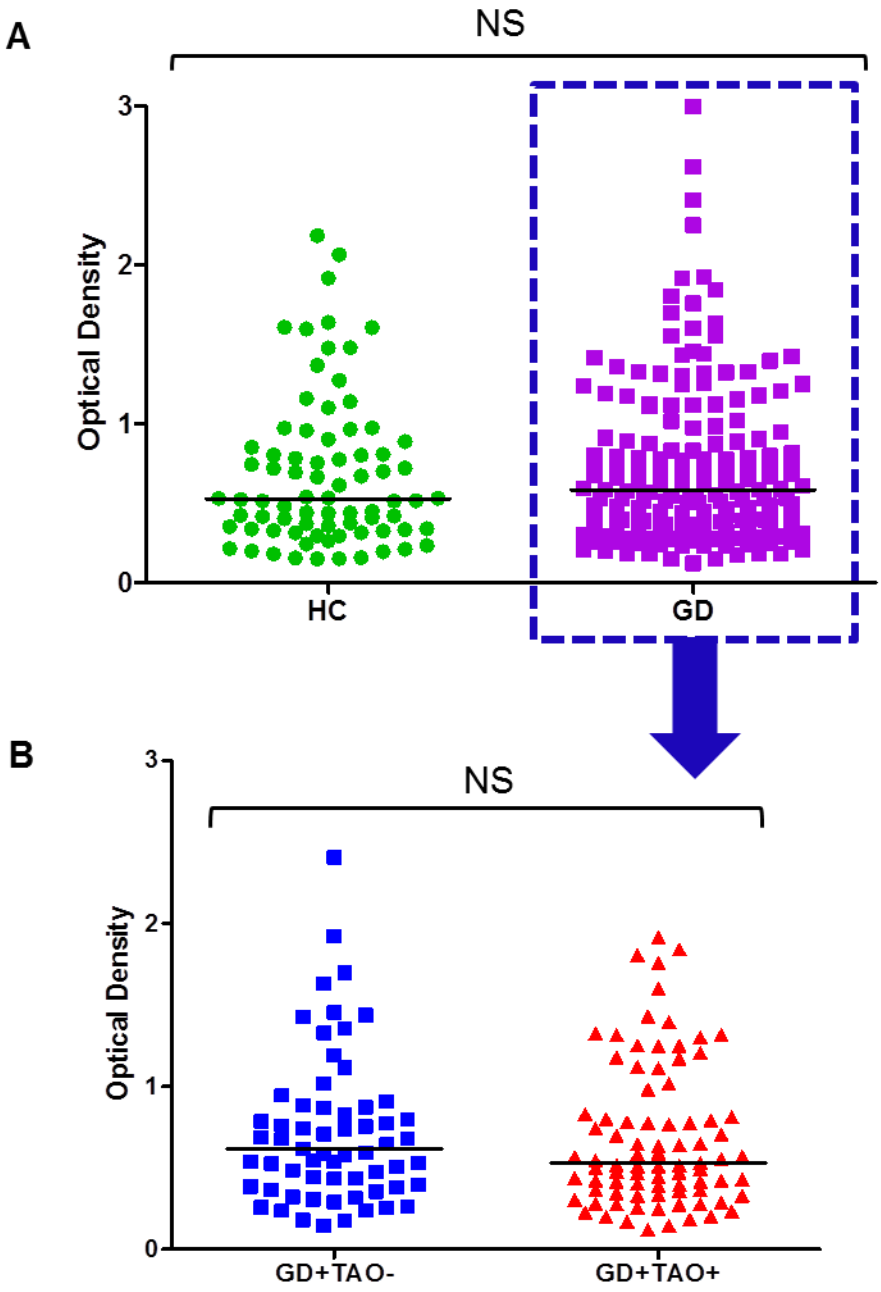

Figure 3.17: Comparison of IGF-1R-Ab levels as measured by ELISA 2 in the study populations. No significant differences were observed in serum levels of IGF-1R-Ab between 177 GD (combined GD+TAO+ and GD+TAO-) patients and 78 age- and sex-matched healthy controls (A), nor between the 110 GD+TAO+ and 67 GD+TAO- subjects, using ELISA 2 (B) (mean of duplicates). Non-parametric analysis was undertaken with Mann-Whitney U test. (NS, Not significant).

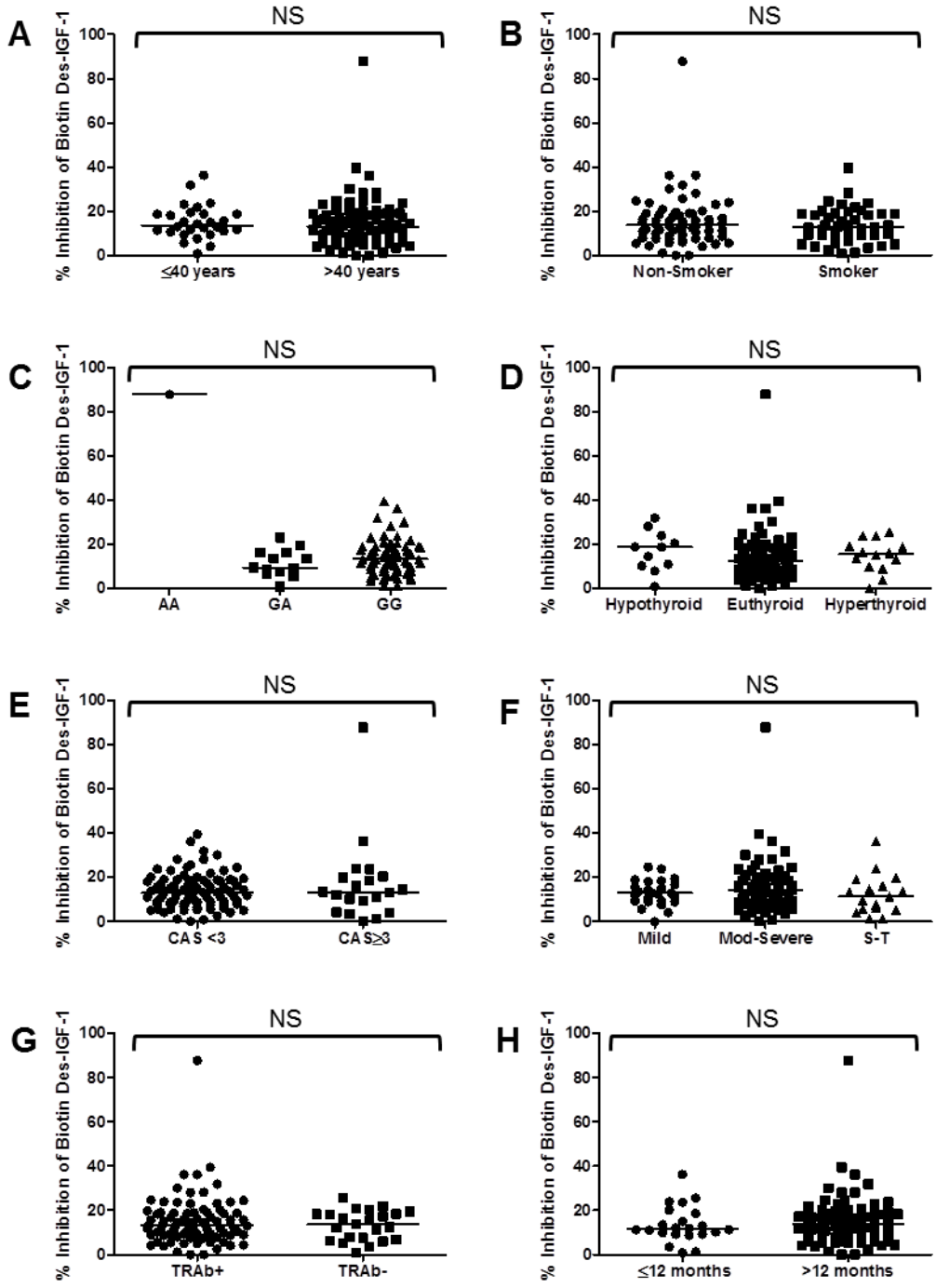

Figure 3.18: Relationship between IGF-1R-Ab as measured by ELISA 1 and clinical, immunological and PTPN22 (R620W) genotype in GD+TAO+ subjects. No statistically significant differences were noted in age (A), cigarette smoking status (B), PTPN22 genotype (C), thyroid status (D), TAO clinical activity score (E), EUGOGO severity grade (F), TRAb status (G) or duration of GD (H). Non-parametric analysis was undertaken with Mann-Whitney U test (for two groups) or Kruskal-Wallis test (with Dunn's multiple comparison) for multiple groups. (NS, Not significant).

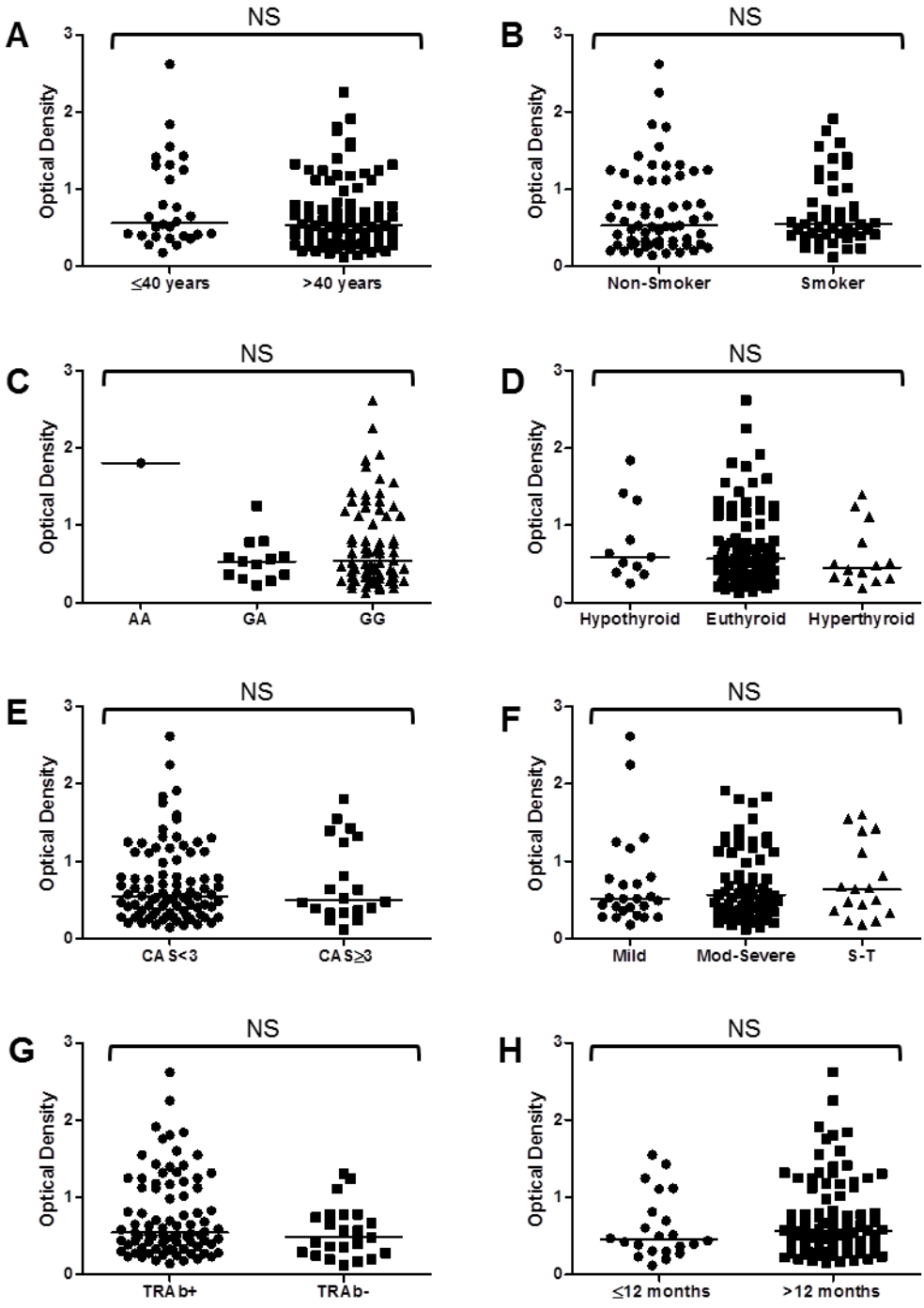

Figure 3.19: Relationship between IGF-1R-Ab as measured by ELISA 2 and clinical, immunological and PTPN22 (R620W) genotype in GD+TAO+ subjects. No statistically significant differences were noted in age (A), cigarette smoking status (B), PTPN22 genotype (C), thyroid status (D), TAO clinical activity score (E), EUGOGO severity grade (F), TRAb status (G) or duration of GD (H). Non-parametric analysis was undertaken with Mann-Whitney U test (for two groups) or Kruskal-Wallis test (with Dunn's multiple comparison) for multiple groups. (NS, Not significant).

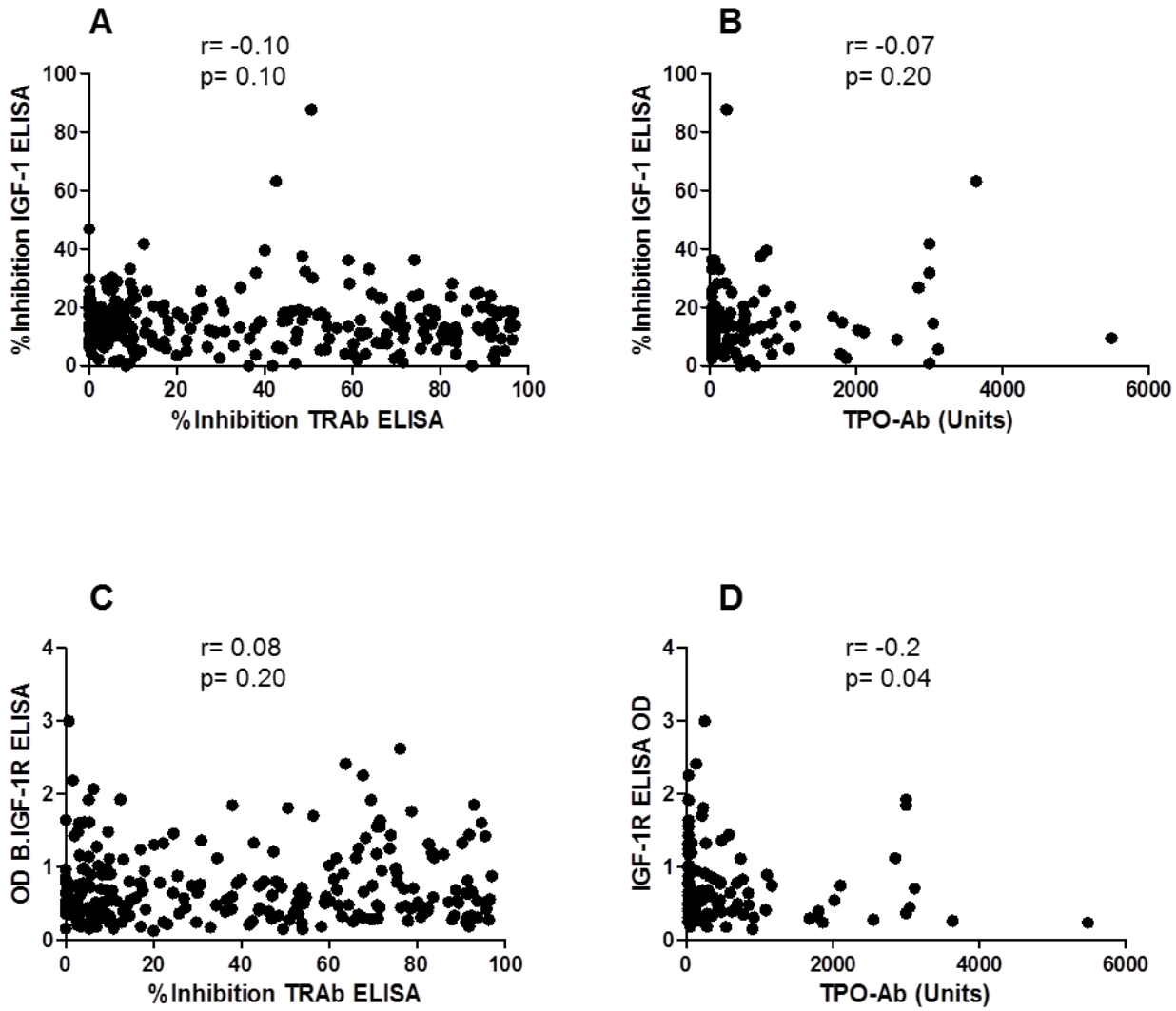

Figure 3.20: Correlation between measured levels of serum IGF-1R-Ab and TRAb or TPO-Ab with ELISA 1 and ELISA 2. No correlation between serum IGF-1R-Ab and either TRAb or TPO-Ab with ELISA 1 (A & B) for GD+TAO+ and GD+TAO- subjects. For ELISA 2 (C & D) there was a small but statistically significant negative correlation between IGF-1R-Ab and TPO-Ab (D). Note: fewer subjects had undergone measurement of TPO-Ab than TRAb. Non-parametric analysis was undertaken with Spearman's rank correlation.

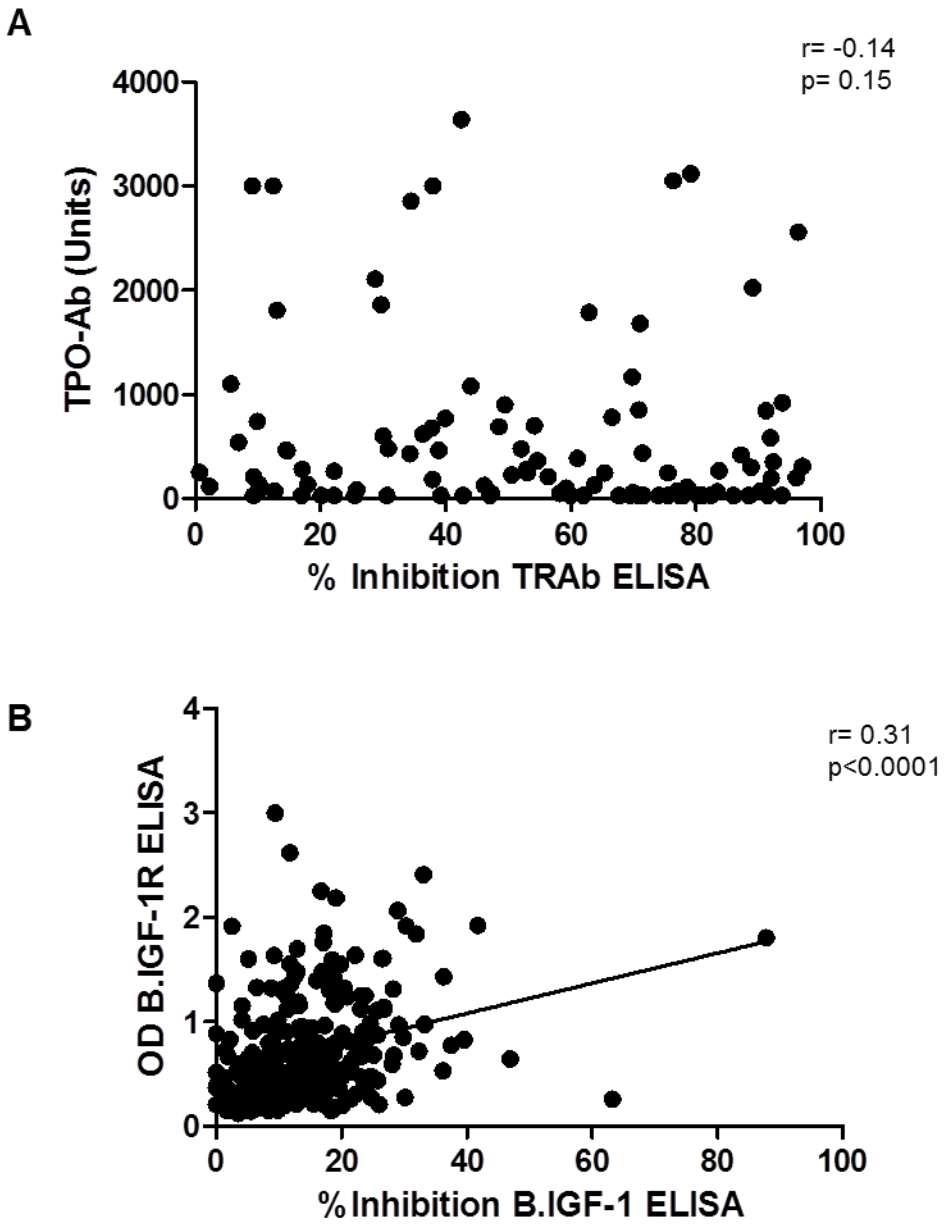

Figure 3.21: Correlation between measured levels of TRAb and TPO-Ab and between IGF-1R-Ab as measured with ELISA 1 and ELISA 2. No correlation between serum TRAb and TPO-Ab (A). However, serum IGF-1R-Ab, as measured with ELISA 1 and ELISA 2 did demonstrate significant correlation in GD+TAO+ and GD+TAO- subjects (B). Non-parametric analysis was undertaken with Spearman's rank correlation.

3.8 Discussion

Despite extensive validation, evidence for good inter-assay agreement and consistency of measures in a large population of age- and sex-matched GD+TAO+, GD+TAO- and HC, I found no difference in IGF-1R-Ab with either of the assays. There was also no correlation of IGF-1R-Ab with TAO clinical activity or severity. This is contrary to previous findings examining the effect of putative GD-IgG on orbital fibroblasts, mediated by presumed IGF-1R-Ab.[238,239,261] However, since developing the ELISA, two other groups have published their own IGF-1R-Ab assays which may be valid for therapeutic and pathogenic IGF-1R-Ab detection and which, to some extent, concur with my findings.

3.8.1 Published IGF-1R-Ab Detection Assays in TAO Patients

Minich et al (2013) utilised a luminescent immunoprecipitation assay, generating an IGF-1R-luciferase fusion protein which was stably transfected into HEK-293 cells.[232] These cells were then subject to immunoprecipitation studies in 108 TAO and 92 HC subject sera. All samples were gained within 12 months of the first symptoms of TAO. Crucially, the cut-off point for IGF-1R-Ab positivity was chosen as signals located more than 3 standard deviations from the mean signals of healthy controls. In this study 10% of TAO and 11% of HC were positive for IGF-1R-Ab, a finding that was independent of serum IGF-1 levels. In addition, purified IgG were equivalent to the original serum samples. In TAO patients for whom there were greater than three consecutive samples over an average period of 2 years, IGF1-R-Ab were consistently elevated. However, no stimulatory effects on IGF-1R

autophosphorylation were seen with TAO sera. In addition, serum IGF-1R-Ab+ samples reduced IGF-1-mediated activation of HepG2 (hepatocellular carcinoma) cells and MCF-7 (breast cancer) cell viability. This was proposed to confirm that IGF-1R-Ab in this study were IGF-1R antagonists. In contrast to TSAb, no subjects with stimulatory IGF-1R-Abs were identified. Importantly, as with my data, there were no associations between IGF-1R-Ab levels and severity or activity of TAO, or of TRAb levels. This group therefore concluded that there was no evidence from their study to support a role for IGF-1R-Ab in TAO pathogenesis.[232]

Varewijck et al (2013) undertook a prospective study of 70 consecutive TAO patients (26 euthyroid on antithyroid therapy, 39 subclinical hyperthyroidism, 5 still hyperthyroid), with a mean CAS of 1.6 (range 0-5), median time after diagnosis of GD of 3 years and median time after TAO diagnosis of 1 year.[353] They used an IGF-1 kinase receptor activation assay, based on the measurement of autophosphorylation of tyrosine residues of IGF-1R in response to stimulation with human serum *in vitro*, in order to determine serum IGF-1R activating capacity. Again, this involved a HEK-293 cell line stably transfected with the human IGF-1R gene and IGF-1R-Ab activity was compared with TBII.[353] Compared to healthy controls, the IGF-1R stimulating activity of TAO subject sera was low-normal and total serum IGF-1 was normal. However, a significant inverse relationship between total IGF-1 and CAS was noted. In contrast to the results of my assays there was positive correlation between TBII and CAS. Moreover, there was positive correlation between IGF-1R stimulating activity and age in patients with TBII above the mean +1SD, although no such relationship for those with lower levels of TBII. Overall, IgG depletion (by protein G magnetic beads) did not change IGF-1R stimulating activity. However, in 10 of 20

patients the IGF-1R stimulating activity decreased after IgG depletion, an effect mainly seen in those with higher IGF-1R stimulating activity. Varewijck et al therefore concluded that it was possible that GD-IgG might contribute to IGF-1R activation in this GD subset.[353]

3.8.2 Criticisms of Current IGF-1R-Ab Detection Assays

The evidence presented by my assays and the studies of Minich et al and Varewijck et al are unexpected in that they may be argued to conflict with the body of evidence available for the involvement of IGF-1R in TAO pathogenesis. However, a number of criticisms have been made regarding some aspects of the experimental design of each of the studies.[357]

Smith (2013) highlighted that a number of confounding factors may have been present, particularly in reflecting the true complexity of the IGF-1 and IGF-1R pathway. For example, levels of IGF-1, IGF-2 and IGFBP were not measured or taken into account in interpreting some of the results, particularly as cultured cell lines may produce some of these factors.[357] Given the relative binding affinities of IGF-1, IGF-1 and insulin, if IGFs or IGFBP were higher or lower in any of the groups then these could have resulted in under- or overestimation of the true levels of IGF-1R-Ab.[357] Certainly there is alteration of the IGF-1 system in RA, with low or normal IGF-1 but increased or normal IGFBP as compared with controls.[358,359] However, normal levels of IGF-1, IGF-2 and IGFBP have been documented in TAO patients.[356] In addition, as TAO activity correlates with TRAb levels (although not necessarily TPO-Ab),[46,159] patients with active TAO and high TRAb should have high titres of

other autoantibodies. If there were multiple other autoantibodies in the sera of GD+TAO+ or GD+TAO- subjects these may have interfered with IGF-1R-Ab interactions with rhIGF-1R.[357]

Neither of the published assays, nor my own, used human orbital fibroblasts as the target for the putative serum antibodies. Studies examining the effect of IGF-1 and GD-IgG have utilised cultured human fibroblasts, aiming to more directly replicate *in vivo* conditions. It is conceivable, therefore, that antibody-induced receptor activation may be tissue-specific and that the particular "unique attributes" of GD orbital fibroblasts may facilitate representative cellular responses mediated by GD-IgG. Hence, using such an "artificial" *in vitro* target as a cultured cell line transfected with a particular receptor (as in the published IGF-1R-Ab assays) or a recombinant receptor protein (as in my IGF-1R-Ab assays) may not be sufficiently "physiological" to permit true findings to be revealed.[125,357]

For instance, in the case of ELISA 1, there is the assumption that serum IGF-1R-Ab block the binding of Biotin-IGF-1 to IGF-1R. This may not necessarily be the case if, for example, IGF-1R-Ab bind to separate epitopes on IGF-1R. Furthermore, if rhIGF-1R is of an inappropriate configuration or incorrectly glycosylated for true IGF-1R-Ab then an accurate representation of IGF-1R-Ab levels may not be obtained. If any of these assay systems is an imperfect means of measuring IGF-1R-Ab levels and activity it follows that each may therefore not be valid to correlate with any clinical or immunological measure. I did attempt to optimise an ELISA based on that of Yin et al (2011), with presumed binding of IGF-1R-Ab to plate-bound rhIGF-1R and using a

secondary biotin-conjugated donkey anti-human IgG Fc-γ specific antibody and a goat anti-human IgG to bind IGF-1R-Ab, but without success.

It has also been stated that a definition of IGF-1R-Ab positivity of 3 standard deviations above the mean of the healthy controls, as in the study of Minich et al, is an arbitrary cut-off. This, combined with the possibility of not detecting low affinity IGF-1R-Ab with the assay techniques chosen, as is the case with those autoantibodies in SLE and glomerulonephritis. I utilised the Duoset IGF-1R capture antibody as a positive control in my studies. However, this may not replicate the true situation as this capture antibody will have been specifically raised to the recombinant IGF-1R protein used to bind putative IGF-1R-Ab in patient serum. One would assume that the interaction between these two molecules would be of particular high affinity, likely not in the physiological range of any putative IGF-1R-Ab interacting with IGF-1R on, for example, orbital fibroblasts. It was certainly the case, in other studies, that some pathogenic antibodies were of low affinity, low enough perhaps not to be detected by an immunoassay.[360,361] It would therefore have been instructive to have utilised an alternative IGF-1R monoclonal antibody, such as 1H7, which could have further validated ELISA 1 and 2.

Finally, the previous evidence of IGF-1R and TSH-R colocalisation has not been taken into account.[187,258] Indeed, there are further examples of interactions between IGF-1R and other receptors. Carapancea et al (2007) found co-expression of IGF-1R and platelet derived growth factor receptor (PDGFR) in two high-grade glioma cell lines. Targeting both receptors increased cell death in both cell lines, greater than

inhibition of either receptor alone.[362] Other studies have found similar cross-talk between IGF-1R and epidermal growth factor receptor (EGFR).[256,363]

3.8.3 Rationalisation of IGF-1R-Ab Detection Assay Findings

To add credence to the findings of my assays, recently validated animal models also found that IGF-1R may not have such a direct link with TAO. Moshkelgosha et al (2013) found that all BALB/c mice gained high levels of TSH-R antibodies, predominantly with stimulatory function after TSH-R plasmid immunisation. The majority also had IGF-1R antibodies.[164] However, Zhao et al (2011) determined that, although those mice injected with TSH-R A-subunit plasmid developed high levels of both TSH-R antibodies and IGF-1R antibodies, those injected with an IGF-1Rα subunit plasmid developed IGF-1R antibodies but no changes in phenotype.[343] Moreover, simultaneous challenge by double antigen immunisation with the two plasmids (TSH-R and IGF-1R) at distant anatomical sites reduced the incidence of hyperthyroidism, potentially as a consequence of antigenic competition.[164,343]

If serum IGF-1R-Ab are not specifically present in GD or TAO patients at levels above those in HC subjects, this raises the question as to the reasons for the multiple existing sources of experimental data which appear to validate the role of autoantibodies to IGF-1R in TAO. There is certainly evidence for a role of IGF-1/IGF-1R in autoimmunity. In a number of animal models, levels of IGF-1 are associated with altered disease outcomes.[356,364,365] With respect to TAO, sources have postulated that IGF-1 may be produced locally in the orbit as a result of prior inflammatory processes. It has also been proposed that IGF-1 may be secreted in an

autocrine or paracrine manner by orbital tissues, with subsequent increased IGF-1R expression on orbital fibroblasts, adipocytes and lymphocytes.[232] Another explanation is of epitope spreading and a step-wise generation of increasing numbers and diversity of autoantigens, progressively resulting in more disease manifestations.[357]

Even if this hypothesis of local up-regulation of IGF-1/IGF-1R signalling in active TAO patients were to be accepted, the type of autoantibodies produced may not be in keeping with their necessary potentiation of autoimmune activity. That is, although it has been demonstrated that IGF-1R expression is increased on TAO orbital fibroblasts and infiltrating lymphocytes,[238,240] if the local IGF-1R-Abs involved in TAO were of the same nature as those found in TAO serum in the studies of Varewijck et al, then they would have an inhibitory rather than stimulatory effect on IGF-1R-related signalling. They would therefore be expected to reduce, rather than increase, the usual trophic effects of IGF-1.[353] It has been hypothesised that those Igs that influence the TSH-R could be those activating IGF-1R. However, others have stated that because of differences in their molecular structure it is more likely that there are two distinct autoantibodies – one to TSH-R and another to IGF-1R.[357]

There is also always the possibility, as in the case of rheumatoid factor in RA, that at least a proportion of IGF-1R-Ab may be IgM rather than IgG in nature.[366] For example, in patients with autoimmune diseases (e.g. SLE, RA, MS primary biliary cirrhosis), the monomeric form of IgM is found at greater levels, possibly related to exposure to infectious agents (e.g. Epstein-Barr virus, Human Herpes Virus-6, *Mycobacteria*, *Chlamydia Pneumoniae*, *Escherichia Coli*). It is uncertain whether this elevation of IgM is a cause or consequence of the autoimmunity in these diseases.[367]

Although IGF-1R-Ab were quantified in the relevant patient sera, the relative activity of these antibodies was not determined. In particular, whether the antibodies were stimulatory, inhibitory or neutral in nature. Although there were no quantifiable differences in IGF-1R-binding antibodies between GD+TAO+, GD+TAO- and HC groups, it could be argued that there may be differing proportions of stimulatory or inhibitory antibodies, with a preference for stimulatory IGF-1R-Ab in the GD+ groups. However, Varewijck et al found that in TAO serum the IGF-1R-Ab they detected had a universally inhibitory, rather than stimulatory effect. Again this is in contrast with previous studies which found stimulatory effects of GD-IgG.

3.8.4 Recent Developments in TSH-R Antibody Assays

As previously detailed, there are a number of TRAb assays in existence that have been investigated in GD and TAO patients.[159,160,162] Recently a number of newer TRAb assays have been evaluated for their ability to predict the severity (as defined by NO SPECS rather than the EUGOGO severity scale) of TAO course in untreated, newly-diagnosed (duration of ocular symptoms <6 months) TAO subjects. In particular, it has been proposed that these assays are able to discriminate between TSAb and TBAb. Jang et al (2013) determined, with two separate assays (a third-generation TBII assay and a thyroid-stimulating immunoglobulin (TSI) bioassay), those patients with higher TRAb at initial measurement were at greater risk of more severe TAO at one year.[368] This is clinically relevant as those patients with higher TRAb may warrant closer follow-up and more aggressive treatment to reduce risks of disease progression. This study also demonstrated that a single TRAb measurement may provide adequate information to predict TAO course.

The same group, in a separate study, found a positive correlation between TRAb with three assays (two of the same assays as in their previous study as well as a separate TBII assay) and TAO clinical activity as defined by CAS. On multivariate regression analysis the results of these assays were also significantly correlated with specific TAO features such as proptosis (for two of the assays) and proptosis, soft tissue involvement and extraocular muscle involvement for one of the assays, based on the use of Mc4-CHO cells.[369] However, there was no such association between TRAb and DON with any of the assays. In a larger group of TAO patients, in whom TSI and TBII were measured simultaneously, Jang et al (2014) found that TAO was more active and severe in those with greater TSI as compared to greater TBII.[370]

3.8.5 Future Directions for the Development of IGF-1R-Ab Assays in TAO

Although no differences in IGF-1R-Ab between GD+TAO+, GD+TAO- and HC, or between GD+TAO+ patients of different activity and severity were found, my assays may still be of utility. In particular, with the possible future use of commercial IGF-1R monoclonal antibodies as treatments, in TAO and in other diseases, one may desire to measure the serum levels of these therapeutic antibodies and correlate this with any possible treatment effect as an outcome measure in clinical trials. With a successful IGF-1R-Ab assay now developed it may be possible to convert this to a Luminex platform, binding the IGF-1R moiety to a relevant Luminex bead alongside other such autoantigens in GD and TAO such as TPO, TG and TSH-R, permitting the measurement of each of these in sera in one assay.

There was no correlation between IGF-1R-Ab levels as measured with my assay and TRAb as measured with an existing commercial ELISA. However, I did not measure the actual functional activity of these TRAb and could therefore not distinguish between TRAb of stimulatory, inhibitory or neutral function. Studies by Tsui et al (2008) and Kumar et al (2012) conclude that TSH-R and IGF-1R signalling are closely linked in the TAO orbit.[187,258] Whether this represents a true physical association is uncertain. It may also be that there is indirect modulation due to common downstream signalling cascades. If this were to be the case then this may explain why IGF-1R-Ab were not necessarily measured in any of the assays devised for use in TAO patients.[187,257]

It may also have been instructive to have used another cohort of patients in which the IGF-1 axis is deranged, or in which IGF-1 may have a role in pathogenesis, such as RA. These would have acted as a separate disease control cohort to validate my findings in GD and TAO.[371] Indeed, an interesting previous observation is that there may be a common pathway in GD and RA in that the stimulatory activity of GD-IgG may and RA-IgG not be specific to GD and RA, respectively. For example, Pritchard et al (2004) demonstrated stimulation of TAO orbital fibroblasts by IgG from RA patients and stimulation of RA synovial fibroblasts by IgG from GD patients, further showing that this was likely mediated by IGF-1R.[372]

My assay would appear to be more user-friendly than some of those already reported. Varewiijck et al required 48 hours of culture of HEK-293 cells, followed by stimulation for 15 minutes at 37^{o}C with increasing amounts of human rIGF-1 (0.06-1.0 nmol/L) or serum samples. Serum samples were diluted 1 in 10, in keeping with

my assays. Varewijck et al used wells coated with monoclonal Ab to IGF-1R (MAD1) capture antibody and mainly examined TBII rather than stimulatory TRAb. The assays I devised and validated were not as labour-intense and do not require cell culture facilities or expertise.

It may be that the subjects recruited do not possess IGF-1R-Ab. It may be, for example, that IGF-1R-Ab are only present in high titre in those with early-onset GD, those with hyperthyroid GD or those prior to CBZ or PTU treatment. It may be necessary, therefore to gain sera from other, alternative subjects with these particular clinical characteristics. Against this assertion, a large number of sera from carefully assessed GD and TAO patients, representing all of those adhering to inclusion and exclusion criteria in two large tertiary referral centres over a two-year period. It would have been difficult to have recruited more subjects.

3.9 Conclusion

No difference in IGF-1R-Ab levels could be determined using two distinct, well-validated assays in GD+TAO+, GD+TAO- and HC subjects. Furthermore, there was no association between IGF-1R-Ab and clinical activity or severity of TAO, dysthyroid status, duration of GD, PTPN22 (R620W) GD susceptibility polymorphism or cigarette smoking. Despite the available evidence for IGF-1R autoimmunity in TAO my study is largely in agreement with those of Minich et al (2013) and Varewijck et al (2013) in that IGF-1R-Ab cannot be readily detected in sera of GD+TAO+ and GD+TAO- patients.

4 T LYMPHOCYTE PHENOTYPE IN GRAVES' DISEASE AND THYROID-ASSOCIATED OPHTHALMOPATHY

4.1 Introduction

4.1.1 T Lymphocytes in TAO

Although the main pathogenic events in TAO appear to be localised to the orbital tissues, it is felt likely that any underlying immunologic abnormalities may be represented, and therefore detectable, in the peripheral blood.[277,280] It has been proposed that TAO is, at least partly, a T lymphocyte-mediated disorder, given that infiltration of both CD8+ and CD4+ T helper cells into the orbital tissues of TAO patients has previously been observed.[135,281,282,373] Some studies have found that the majority of orbital tissue T cell clones make Th1 cytokines, namely IFN-γ, IL-2 and TNF-α, rather than Th2 cytokines such as IL-4, IL-5 or IL-10.[283,285] However, other studies have shown predominantly Th2 cytokine mRNA.[203] Although the Th1/Th2 paradigm is now outdated, early studies demonstrated both cell-mediated (Th1) and humoral (Th2) responses, with Th1 predominating in early disease and Th2 later.[281,288] However, the antigen specificity of these T cells has not yet been fully established. Hence, at present, T cells are thought to be recruited to the orbital tissues through an apparently non-antigen-specific mechanism. The importance of T lymphocytes in the initiation and progression of the ophthalmic manifestations of GD has been emphasised by a number of authors, while alterations in the homeostasis of T cell phenotype in TAO and other systemic autoimmune diseases have also previously been described.

TAO subjects have also been shown to have increased CD3+IGF-1R+ T cells, particularly of the CD45RO+ phenotype.[240] However, further investigation of relative

T cell IGF-1R expression in subjects with TAO as compared to HC, and the possible functional and immunological consequences of this require further elucidation. In addition, studies into T cell profiles, including alterations in memory status and T helper phenotype in peripheral blood, and how these vary with factors such as duration of AITD, presence of thyroid dysfunction, TRAb status, cigarette smoking and clinical activity scoring in TAO are also necessary.

4.1.2 Significance of T Lymphocyte Memory Phenotype in Health and Disease

As discussed in **Chapter 1.21**, according to a T lymphocyte differentiation model, peripheral CD4+ and CD8+ T lymphocytes can each be divided into four functionally distinct memory populations based on their expression of isoforms of the protein tyrosine phosphatase receptor, CD45, and the lymphocyte homing marker CCR7, with naïve (CD45RO- (or CD45RA+) CCR7+), CM (CD45RO+ (or CD45RA-) CCR7+), EM (CD45RO+ (or CD45RA-) CCR7-) and EMRA (CD45RO- (or CD45RA+) CCR7-) as defined by flow cytometry.

The CD4+ and CD8+ T cell memory compartments are of a fixed ‘size’, hence if one of the memory subtypes is increased in proportion then one or more of the other proportions must be reduced. This balance of the T cell memory populations is critical in maintaining adequate peripheral tolerance but also effective immune function, particularly as each population has differing proliferative, homing and effector characteristics.[374,375] Memory T cell homeostasis is incompletely understood,[376] but antigen-specific activation and differentiation of naive lymphocytes generates short-lived EM and longer-lived CM T cells.[374] CM T cells have more

limited effector function but home to secondary lymphoid organs, while EM T cells, although having a lesser proliferative capacity, are directed to peripheral tissues and are capable of secreting effector cytokines such as IFN-γ and TNF-α, producing perforin and having cytotoxic effects.[273,377,378] CM T cells may rapidly proliferate and gain EM status when stimulated with antigen. EMRA cells have the greatest levels of perforin and granzyme, and are the most differentiated.

4.1.3 CD4+ and CD8+ T Cell Subsets in Peripheral Blood in GD and TAO

As described in **Chapter 1.22**, several groups have found a deviation in the distribution of CD4+ and CD8+ T cell memory subsets in the peripheral blood of patients with GD and TAO.[277,280,379] In particular, it has been proposed that levels of thyroid hormones may affect T cell subsets.[380] Alteration in the distribution of these T cell populations has also been proposed to justify the role of T cells in GD autoimmunity.[381]

Vaidya et al (2005) examined the peripheral blood T cell phenotype of euthyroid patients with “moderately severe active TAO” and compared them with HC by flow cytometry. Although CD3+ T cells were equivalent between TAO and controls, there were increased CD4+ T cells, and a subsequently higher CD4+/CD8+ ratio, in TAO as compared to HC. In addition, patients with TAO had a higher proportion of naïve (CD4+CD45RA+) T cells and lower memory (CD4+CD45RO+) T cells, although no differences in CD8+ cells.[277] Another study found increased proportions of CD4+CD62L+, CD4+ICAM-1+, CD8+CD62L+ and CD8+ICAM-1+ peripheral blood T lymphocytes in TAO as compared to HC. Only the proportion of CD8+CD54+ T cells

were higher in TAO than GD patients and CD4+/CD8+ ratio was equivalent between TAO, GD and HC groups.[382]

In contradiction with the findings of Vaidya et al, other groups have determined increased CD4+CD28- and CD8+CD28- T cells in TAO as compared with HC. CD28- cells were predominantly CD45RO+, suggesting that they were activated or memory T cells. Furthermore, GD-derived T cells produced more intracellular IFN-γ than those from healthy controls, and the CD4+CD28- and CD8+CD28- T cells in TAO patients produced more intracellular IFN-γ than those from GD patients without TAO. These findings correlated positively with serum TRAb, suggesting an important role of IFN-γ-producing CD28- T cells in the pathogenesis of GD and TAO.[383]

Xia et al (2006) found that peripheral blood Th1 (as defined by IFN-γ positivity) were greater than Th2 (as defined by IL-4 positivity) T cells in 20 TAO subjects as compared to 20 each of GD and HC subjects. The Th1/Th2 ratio in TAO patients was therefore also higher than in the other groups. The proportion of CD4+ T cells was also higher in TAO and GD subjects than HC but CD8+ T cells were lower in TAO and GD patients than HC, with a resulting increased CD4+/CD8+ ratio. There was also a positive correlation between an increasing percentage of Th1 cells (and the Th1/Th2 ratio) with CAS, although not with TRAb titres. The conclusion was that Th1 cells predominate in TAO, representing a shift in T cell subsets from GD to TAO.[384]

Correlation between T cell subtypes and immunological measures have also been determined. Bossowski et al (2003) found an increased CD4+/CD8+ ratio, CD4+ and CD4+CD45RO+ cells with a decrease in CD8+ cells and CD4+CD45RA+ cells in

untreated GD patients as compared with HC. There was a positive correlation between serum fT4 and CD4+CD45RO+ cells and between TRAb and CD4+ cells but negative correlation between TRAb, TPO-Ab and TG-Ab and CD8+ cells.[381] The elevation in CD4+ T cells, particularly in those with active TAO, has been proposed to mediate the autoantibody responses important in TAO.[280]

However, although T cells have been defined as being either naïve or memory subsets by CD45RA and CD45RO, the markers CCR7 or CD62L have not been widely used to subclassify these further. Therefore, despite numerous previous studies, the CM and EM phenotype of CD4+ and CD8+ T cells in the peripheral blood of GD and TAO patients are not precisely delineated. The difficulties related to this have been expounded upon by Matteuci et al (2011). This group explained that CD4+ or CD8+ cells found to be CD45RA+ might by naïve cells, but could also be EMRA cells. Likewise, CD4+ or CD8+ cells found to be CD45RA- might be memory cells, but without further subdivision into EM or CM cells, which physiologically are of markedly differing function.[385] Determination of these phenotypes may therefore provide important insights into T cell homeostasis in GD and TAO.

4.2 Aims and Objectives

The aim of this chapter was to definitively characterise CD4+ and CD8+ T cell memory populations in GD+TAO+, GD+TAO- patients and age- and sex-matched HC, in particular investigating peripheral blood percentages of CD4+ T helper subtypes such as Treg and Tfh cells. Furthermore, we wished to determine the range of cytokines secreted by these cells and to evaluate their activation status. In each

case we aimed to explore any associations of perturbations in T cell homeostasis with clinical and immunological measures.

4.3 Methods

4.4 Cell Sorting of CD4+ and CD8+ Memory T Cell Populations

60 ml of peripheral venous blood was collected from HC, and PBMC isolated as previously described (**Section 2.9.2**). at the same time of day. Compensation between two colours used in the staining was achieved by staining 5 x 10^5 cells with individual fluorochrome-conjugated antibodies. The cells for the population sort were stained with an antibody mix of either anti-CD4 PECy7 or anti-CD8β PECy5, along with anti-CD45RO PETR and anti-CCR7 AlexaFluor 488 (FITC channel) in a volume of 500 µl. The cells were stained for 20 minutes on ice, after which they were washed and filtered through a 30 µm filter (Miltenyi Biotech) and placed into 5 ml round-bottom polypropylene tubes (Falcon 352063). The cells were sorted on the Mo-Flo fluorescence-activated cell sorter (Dako Cytomation), after being gated on forward and side scatter profiles to include only live lymphocytes, and on cell surface marker combinations to select memory populations of interest. These populations included only CD4+ or only CD8β+ cells and were based on expression of CD45RO (or CD45RA) and CCR7 as previously discussed (**Figure 4.1**). This experimental protocol is summarised in **Appendix 6**.

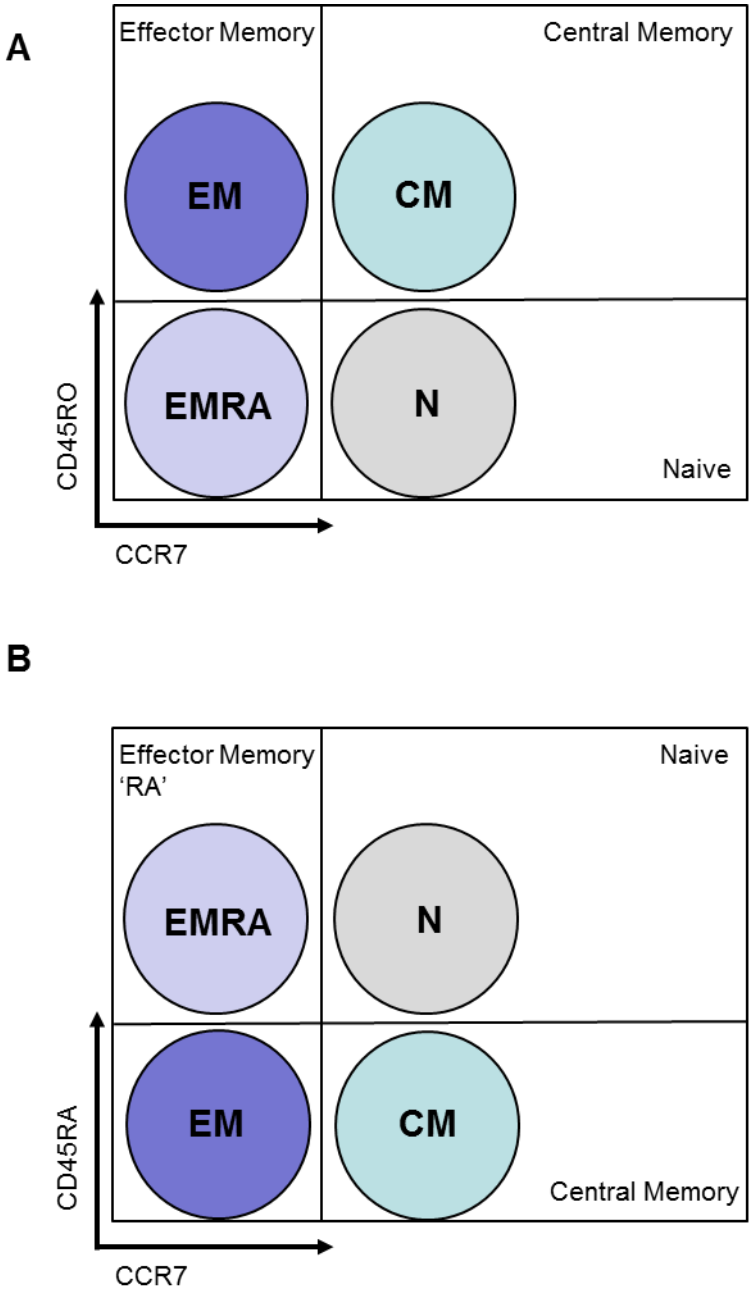

Figure 4.1: Identification of T cell memory subsets by flow cytometry. Following identification of lymphocytes from their forward and side scatter characteristics, CD4+ and CD8+ T cell memory status may be defined based on their expression of CD45RO and CCR7 (A) or CD45RA and CCR7 (B), with division into by CD45RO- (CD45RA+) CCR7+ (Naive), CD45RO+ (CD45RA-) CCR7+ (Central Memory, CM), CD45RO+ (CD45RA-) CCR7- (Effector Memory, EM) and CD45RO- (CD45RA+) CCR7- (Effector Memory RA, EMRA).

4.4.1 Carboxyfluorescein Diacetate Succinimidyl Ester (CFSE) CD4+ Memory T Cell Proliferation Assay

The sorted CD4+ T cell memory populations were labelled with carboxyfluorescein diacetate succinimidyl ester (CFSE, Invitrogen). CFSE is a fluorescent cell staining dye used to monitor lymphocyte proliferation due to the progressive halving of CFSE fluorescence within daughter cells following each cell division. The cells were transferred to a universal tube and washed twice with 10 ml sterile PBS, before being resuspended in PBS at 50 µl/10^6 cells. 2.5 µl of 10M CFSE was added to 5 ml of sterile PBS to give a 2 µM solution. This was added at a 1:1 ratio to the cell suspension to give a final CFSE concentration of 2.5 µM, and incubated for 10 minutes at room temperature with periodic shaking. At 10 minutes an equal volume of RPMI/10%HIFCS was added. After a further minute the cells were washed with PBS once and then with RPMI/10%HIFCS twice. The cells were resuspended in RPMI/10%HIFCS at 2x10^5/ml.

CFSE-labelled PBMC were placed in a 96-well plate at 2x10^5 per well in 100 µl RPMI/10% HIFCS. Cells were stimulated with 50 µl of human T cell activator anti-CD3/CD28 beads (Caltag/Invitrogen, Paisley, UK) at a bead-to-cell ratio of 1:32 and five ten-fold serial dilutions of 50 µl recombinant human IGF-1 (rhIGF-1) from 0.0001 µg/ml to 1.0 µg/ml in the appropriate wells (as well as “blank” wells containing only RPMI/10% HIFCS but no rhIGF-1). These incubated at 37^{o}C in 5% CO_2 for 4 days. Additional wells containing unstimulated PBMC for compensation purposes were allocated.

After four days, cells were centrifuged for 4 minutes at 400 g at 4°C, the supernatant removed and the 96-well plate gently vortexed. Cells were stained with anti-CD4 PE Cy7 surface marker antibody (made up in 50 µl at appropriate dilution) and incubated on ice in the dark for 20 minutes. 100 µl of PBS/2% BSA was added to each anti-CD4 PE Cy7-labelled well prior to further centrifugation and removal of supernatant. Cells were then resuspended in 100 µl of PBS/2% BSA and pipetted into FACS tubes containing 195 µl of PBS/2% BSA as well as 5 µl of counting beads. For dead cell exclusion, 30 µl Sytox blue dye, a nucleic acid stain that penetrates the compromised plasma membranes of dead cells but does not cross normal cell membranes, was added at a concentration of 1/800 to the FACS tubes and incubated for 5 to 10 minutes prior to flow cytometry. The above experimental protocol is summarised in **Appendix 7**.

4.4.2 Phosflow Protocol: Investigation of PI3K and MAPK Signalling in Recombinant IGF-1-Stimulated CD4+ and CD8+ T Cells

PBMC were isolated (as previous described) and resuspended at $1x10^6$ cells in 100 µl RPMI/10% HIFCS per well of a 96-well plate. Additional wells for compensation purposes were composed of 20 µl of positive and negative compensation beads. PBMC were allowed to rest for 3 hours at 37^oC, 5% CO_2. After this period, cells were treated with appropriate stimuli, depending on the experiment. For experiments related to phospho-Akt and phospho-ERK1/2 following cell stimulation by IGF-1, either 2.5 µl of recombinant IGF-1 at concentrations from 0.0001 to 10 µg/ml, 2.5 µl of "blank" (RPMI/10%HIFCS) or PMA at 750 ng/ml as a positive control were used. For experiments related to phospho-Stat5 following cell

stimulation by IL-2, either 2.5 µl of IL-2 at 100 U/ml, 2.5 µl of "blank" (RPMI/10%HIFCS) or PMA at 750 ng/ml as a positive control were used. In each circumstance, cells were incubated in stimulating conditions at 37^{o}C for 20 minutes.

Following this, cells were fixed by adding 100 µl of pre-warmed BD cytofix buffer, mixing gently and incubating at 37^{o}C for 10 minutes. Cells were centrifuged for 8 minutes at 600 g at 4°C, the supernatant removed and the 96-well plate gently vortexed Cells were then permeabilised by adding 50 µl of chilled BD Perm Buffer III, mixed gently and incubated on ice for 30 minutes. Cells were washed twice, each time by adding 150 µl of BD stain buffer, centrifuging at 600 g for 8 minutes and discarding the supernatant. Cells were stained with surface marker antibodies and Phosflow antibodies (made up in 50 µl) and incubated at room temperature wrapped in foil for 20 minutes. Following this, 150 µl of BD stain buffer was added to each well prior to further centrifugation at 600g for 8 minutes and removal of supernatant. Cells were resuspended in 100 µl of BD stain buffer and placed into FACS tubes containing 200 µl of BD stain buffer before being run on the flow cytometer. This experimental protocol is summarised in **Appendix 8**.

4.5 Antibody Staining for Flow Cytometry

4.5.1 Antibody Staining of Cell Surface Markers

Depending on the cells being examined (lysed whole blood or PBMC) between 50-100 µl of cells were placed in to 96-well plates (with a typical count per well of 1x10^{6} cells). Additional wells for compensation purposes were composed of 20 µl of

positive and negative compensation beads. Cells were centrifuged for 4 minutes at 400 g at 4°C, the supernatant removed and the 96-well plate gently vortexed. Cells were stained with surface marker antibodies (made up in 50 µl at appropriate dilutions) and incubated on ice in the dark for 20 minutes. 100 µl of PBS/2% BSA was added to each well prior to further centrifugation and removal of supernatant. For dead cell exclusion, 30 µl Sytox blue dye was added at a concentration of 1/800 to the FACS tubes and incubated for 5 to 10 minutes prior to flow cytometry. CD4+ and CD8+ T cell memory populations were determined as detailed (**Figure 4.2** and **4.3**).

4.5.2 Intracellular Cytokine Staining

Where possible $1x10^6$ cells were resuspended in 50 µl of RPMI/10% HIFCS into a 96-well plate. To stimulate the cells to produce cytokine, a stimulation solution containing PMA and Ionomycin (both at a concentration of 500 ng/ml) was added to cells for stimulation while RPMI/10% HIFCS was added to any non-stimulated wells. To prevent cytokine release, 2 µg/ml of Brefeldin A was added to all the wells, including those cells not for stimulation. The wells were made up to 200 µl with RPMI/10% HIFCS or stimulation solution and left in the incubator at 37ºC, 5% CO_2, for 3 hours.

Following this the plate was centrifuged for 4 minutes at 4ºC and 400 g and the supernatant discarded. Surface antibodies were made up to 50 µl in PBS/2%BSA. The plate was left on ice in the dark for 15 minutes. The wells were washed with 100 µl of PBS/2%BSA and centrifuged for 4 minutes at 4ºC and at 400 g. The cells were then fixed and permeabilised. The supernatant was removed by flicking the plate and

the cells were re-suspended in 50µl of Reaction Buffer A (Caltag/Invitrogen, Paisley, UK). The plate was left at room temperature and kept in the dark for 15 minutes. The wells were washed with 100µl of PBS/2%BSA and centrifuged. The antibodies for intracellular staining were made up to 50 µl using Reaction Buffer B (Caltag/Invitrogen, Paisley, UK) added to the wells, and left for 15 minutes in the dark at room temperature. The wells were then washed with 100 µl of PBS/2%BSA and centrifuged. Once the cells had been re-suspended in 300 µl of PBS/2% BSA they were then analysed on the flow cytometer. Compensation beads were used to bind a single antibody for fluorescence compensation purposes (as previously described).

4.5.3 Surface and Intracellular Staining Analysis

Flow cytometry was undertaken with a Dako-Cyan ADP High Performance flow cytometer (Dako, Colorado). Multi-colour cytometry compensation was performed using anti-mouse Ig κ negative control compensation beads, individually stained with each flurorochrome conjugated-antibody. This circumvents spectral overlap by adjusting for false positives from other flurorochromes. Analysis was undertaken with Summit 4.3 for Windows (Dako, Colorado 2007). The number of events analysed per sample was between 10,000 and 500,000.

Calibration was checked on a daily basis with Flowcheck Fluorospheres (Beckman Coulter Inc). Isotype controls were used to determine the level of background non-specific binding. The level of median fluorescence intensity (MFI) was used to distinguish between high and low levels of expression, with ΔMFI being calculated by: MFI [Test Antibody] – MFI [Isotype Control].

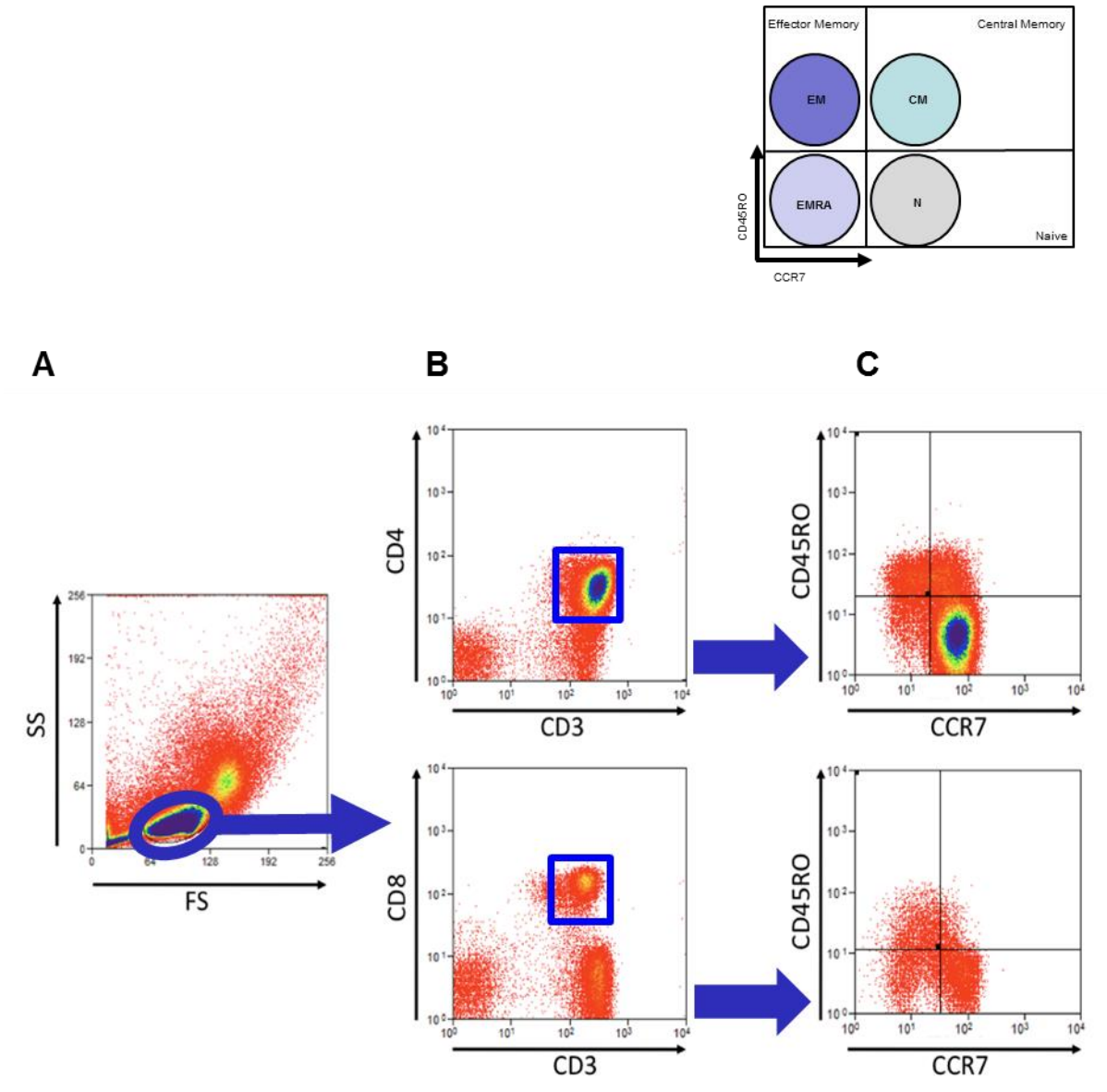

Figure 4.2: Gating strategy for determining CD4+ and CD8+ memory T cell populations in PBMCs of GD+ TAO+, GD+ TAO- and HC subjects. For T cells the lymphocyte gate of the forward and side scatter profile (Panel A) was utilised, with subsequent separation into CD4+ and CD8+ populations (Panel B). Memory populations were then differentiated by CD45RO- CCR7+ (Naive), CD45RO+ CCR7+ (Central Memory, CM), CD45RO+ CCR7- (Effector Memory, EM) and CD45RO- CCR7- (Effector Memory RA, EMRA) (Panel C).

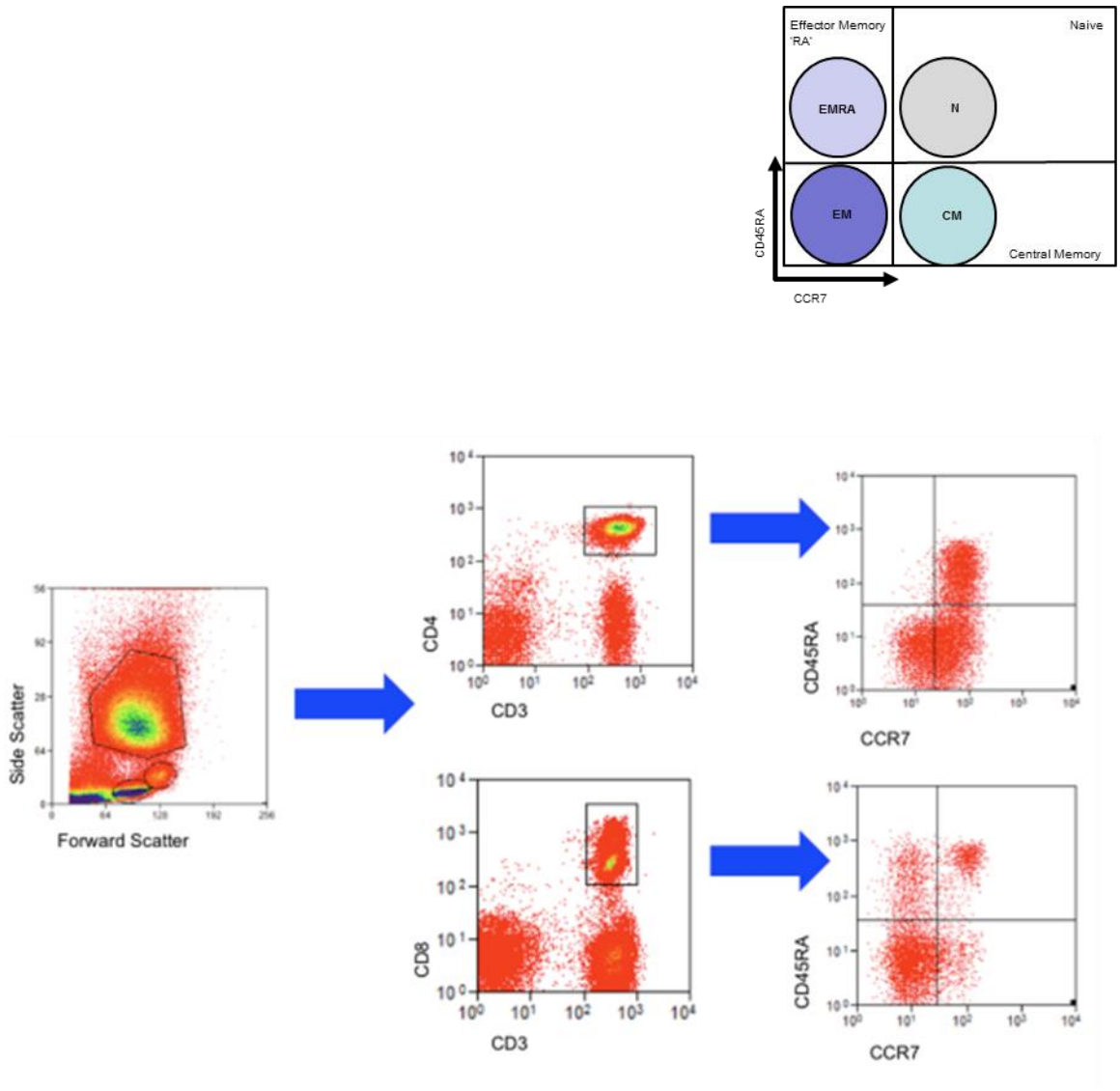

Figure 4.3: Gating strategy for determining CD4+ and CD8+ memory T cell populations in lysed whole blood of GD+ TAO+, GD+ TAO- and HC subjects. For T cells the lymphocyte gate of the forward and side scatter profile (Panel A) was utilised, with subsequent separation into CD4+ and CD8+ populations (Panel B). Memory populations were then differentiated by CD45RA and CCR7 into Naïve (CD45RA+ CCR7+), CM (CD45RA- CCR7+), EM CD45RA- CCR7- (Panel C) and for CD8+ also an EMRA (CD45RA+ CCR7-) population (Panel C).

4.6 Results

4.6.1 Study Subjects

63 GD (37 GD+TAO+, 26 GD+TAO-) subjects and 27 age- and sex-matched HC were identified. Demographic and clinical indices are summarised in **Table 4.1**. Of the GD+TAO+ subjects, 9 were defined as having clinically active TAO (CAS ≥3).

Table 4.1: Demographic features, clinical measures, thyroid function, TRAb status and PTPN22 (R620W) genotype for T cell study groups It should be noted that not all of the subjects in each group were used for each experimental component undertaken, for example in studies on regulatory T cells there were 24 GD+TAO+, 21 GD+TAO- and 27 HC. However, subjects within each group were always age- and sex-matched for each experiment.

	HC	GD+ TAO-	GD+ TAO+
Number	27	26	37
Median age in years (IQR)	45 (28)	43 (16)	51 (20)
Gender (M:F)	6 : 19	6 : 20	10 : 27
Smokers	52%	54%	57%
GD Duration >12 months	N/A	81%	92%
CAS≥3	N/A	N/A	24%
TAO Severity (Mild/Mod/Sev)	N/A	N/A	9 : 19 : 9
Thyroid Status (Hypo/Eu/Hyper)	N/A	8 : 16 : 2	7 : 27 : 3
TRAb Positive	5%	54%	57%
Thionamides	N/A	71%	57%

4.6.2 Peripheral Blood CD4+ and CD8+ T Cell Memory Populations in GD+TAO+, GD+TAO- and HC

Median CD4/CD8 ratios (with IQR) were 4.1 (3.4), 3.8 (2.0) and 3.1 (2.2) in the GD+TAO+, GD+TAO- and HC groups, respectively, with no statistically significant differences (using Kruskal-Wallis test and Dunn's multiple comparisons). The proportion of naive CD4+ T cells were significantly increased in GD+TAO+ and GD+TAO- patients, while EM CD4+ T cells were significantly decreased, compared with HC (**Figure 4.4**, summarised in **Table 4.2**). There were no significant differences between the groups in terms of CM and EMRA CD4+ T cells. There were no significant differences between GD+TAO+ and GD+TAO- subjects in any of the CD4+ T cell memory phenotypes.

Table 4.2: Median percentages (with interquartile range) for each of the CD4+ T cell memory populations in each of the three participant cohorts. Non-parametric analysis was undertaken by Kruskal-Wallis test (with Dunn's post-test).

CD4+	HC	GD+TAO-	GD+TAO+	P
Naive	58% (27)	66% (27)	66% (19)	**0.01**
CM	19% (14)	20% (20)	15% (8)	0.05
EM	16% (14)	8% (6)	10% (8.5)	**<0.0001**
EMRA	6% (3.5)	4% (4)	5% (6)	0.27

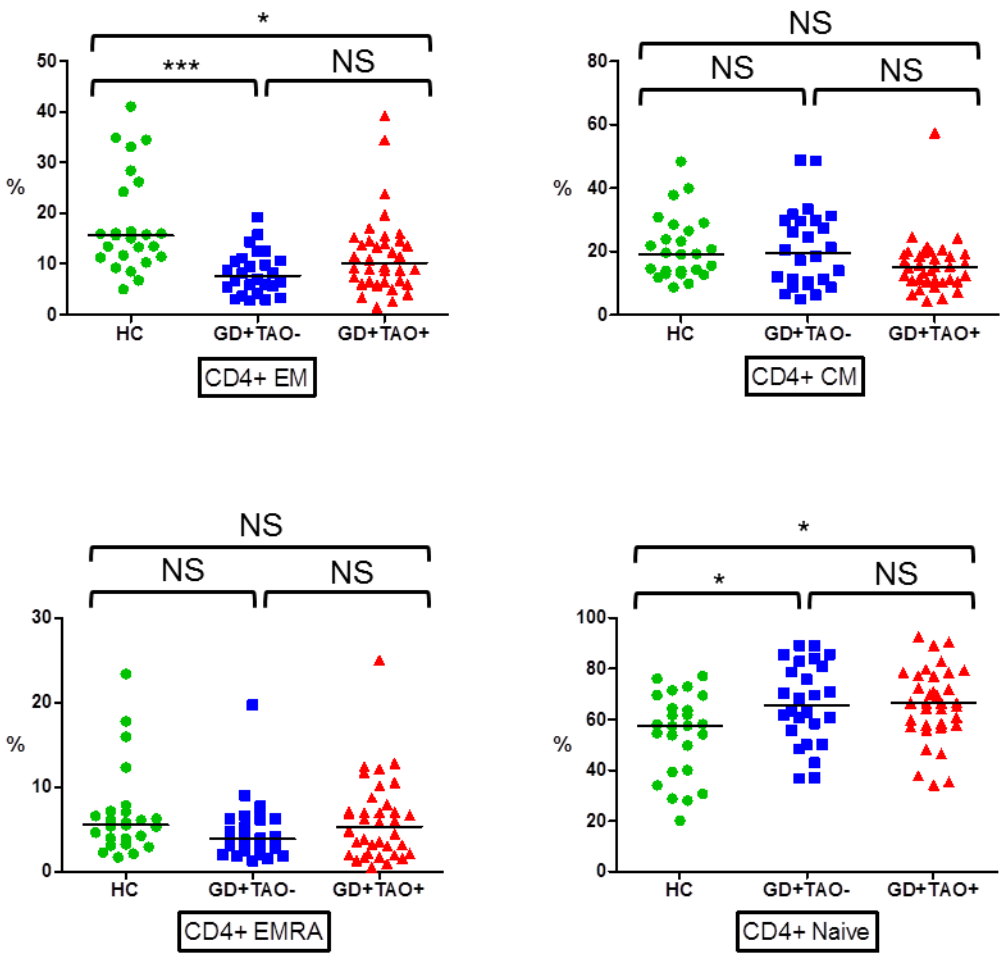

Figure 4.4: Increased naïve CD4+ T cells and decreased EM populations, in GD+TAO+ and GD+TAO- patients compared with HC. Proportions of CD45RO- CCR7+ (Naïve), CD45RO+ CCR7+ (Central Memory, CM), CD45RO+ CCR7- (Effector Memory, EM) and CD45RO- CCR7- (Effector Memory RA, EMRA) CD4+ T cells were defined. The proportion of naive CD4+ T cells were increased in GD+TAO+ and GD+TAO- patients compared with HC, while EM CD4+ T cells were also increased in GD+TAO+ and GD+TAO- subjects. There were no significant differences between GD+TAO+ and GD+TAO- subjects. Non-parametric analysis was undertaken with Kruskal-Wallis test (with Dunn's multiple comparison). (Key: NS: Not significant; *p=0.01 to 0.05; **p=0.001 to 0.01; *** p<0.001).

Similarly, naïve CD8+ T cells were significantly increased in GD+TAO+ and GD+TAO- patients, while EMRA CD8+ T cells were significantly reduced, compared with HC. For EM CD8+ T cells, there was a significant decrease, as compared to HC, only in the GD+TAO+ group. There were no significant differences between GD+TAO+ and GD+TAO- subjects in any of the CD8+ T cell memory phenotypes (**Figure 4.5**, summarised in **Table 4.3**).

Table 4.3: Median percentages (with interquartile range) for each of the CD8+ T cell memory populations in each of the three participant cohorts. Non-parametric analysis was undertaken by Kruskal-Wallis test (with Dunn's post-test).

CD8+	HC	GD+TAO-	GD+TAO+	P
Naive	48% (37)	64% (31)	70% (35)	**0.004**
CM	3% (3.5)	3% (4)	3% (6)	0.9
EM	18% (14)	15% (12)	10% (11.5)	**0.02**
EMRA	26% (34)	16% (15)	15% (17)	**0.009**

When the CD4+ and CD8+ T cell memory populations, which were determined to be significantly altered in GD patients (compared with HC), were analysed further in a combined group of GD+TAO+ and GD+TAO- subjects, there were no associations between proportions of the abnormal CD4+ and CD8+ memory populations and a range of clinical measures, including TAO clinical activity and severity. Indeed, the only factor determined to have significant association with the skewed populations was age (**Table 4.4**).

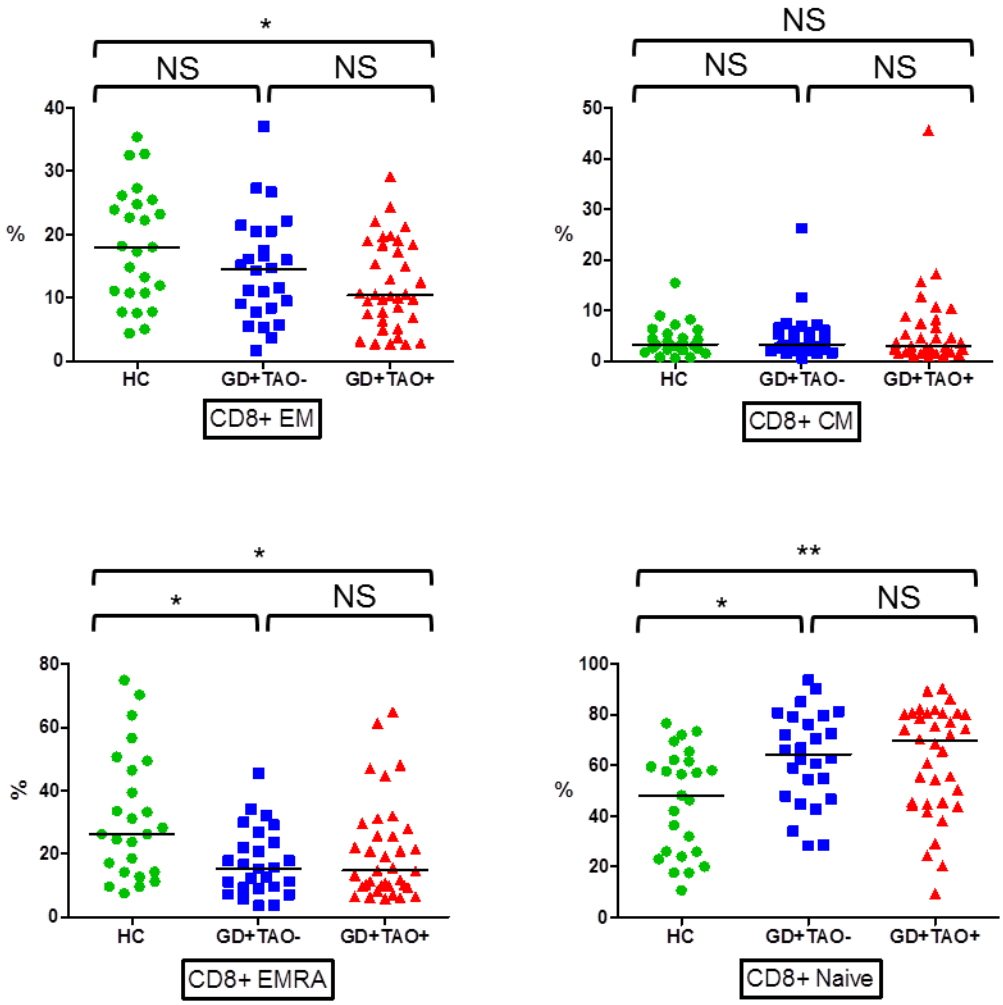

Figure 4.5: Increased naïve CD8+ T cells and decreased EM populations, in GD+TAO+ patients, with decreased EMRA in GD+TAO+ and GD+TAO- patients compared with HC. Proportions of CD45RO- CCR7+ (Naïve), CD45RO+ CCR7+ (Central Memory, CM), CD45RO+ CCR7- (Effector Memory, EM) and CD45RO- CCR7- (Effector Memory RA, EMRA) CD8+ T cells were defined. The proportion of naive CD8+ T cells were increased and EMRA CD8+ T cells were decreased in GD+TAO+ and GD+TAO- patients compared with HC. EM CD8+ T cells were significantly reduced in only GD+TAO+ subjects compared to HC. There were no significant differences between GD+TAO+ and GD+TAO- subjects. Non-parametric analysis was undertaken with Kruskal-Wallis test (with Dunn's multiple comparison). (Key: NS: Not significant; *p=0.01 to 0.05; **p=0.001 to 0.01).

Table 4.4: Summary of factors assessed for contribution to elevations of CD4+ and CD8+ Naïve T cell populations and reduction in CD4+ and CD8+ EM (and CD8+ EMRA) populations in GD (GD+TAO+ and GD+TAO- combined) and HC subjects. Non-parametric analysis was undertaken either by Mann-Whitney test (for two groups) Kruskal-Wallis test (with Dunn's post-test) (for more than two groups).

	CD4+ Naive	CD4+ EM	CD8+ Naive	CD8+ EM	CD8+ EMRA
Age	* **≤40 years:** 71% (30) **>40 years:** 63% (33)	** **≤40 years:** 6.5% (4.5) **>40 years:** 11% (8.4)	*** **≤40 years:** 80% (16) **>40 years:** 56% (29)	* **≤40 years:** 8.4% (8.5) **>40 years:** 15% (9.4)	** **≤40 years:** 10% (8.9) **>40 years:** 21% (18)
CAS	NS	NS	NS	NS	NS
TAO Severity	NS	NS	NS	NS	NS
Smoking	NS	NS	NS	NS	NS
GD Duration	NS	NS	NS	NS	NS
Thyroid Status	NS	NS	NS	NS	NS
TRAb Status	NS	NS	NS	NS	NS
PTPN22 Genotype	NS	NS	NS	NS	NS

4.6.3 Analysis of cytokine production from peripheral blood T cells in GD+ TAO+, GD+ TAO- and HC

We also determined the cytokines produced by PMA- and ionomycin-stimulated CD4+ and CD8+ T cells in the three study groups. IFN-γ (representative of Th1 cells), IL-5 (representative of Th2 cells), IL-17 (representative of IL-17-producing Th17 CD4+ T cells) and IL-21 (representative of Tfh cells) were chosen for analysis, with percentage cytokine secretion determined as shown in **Figure 4.6**.

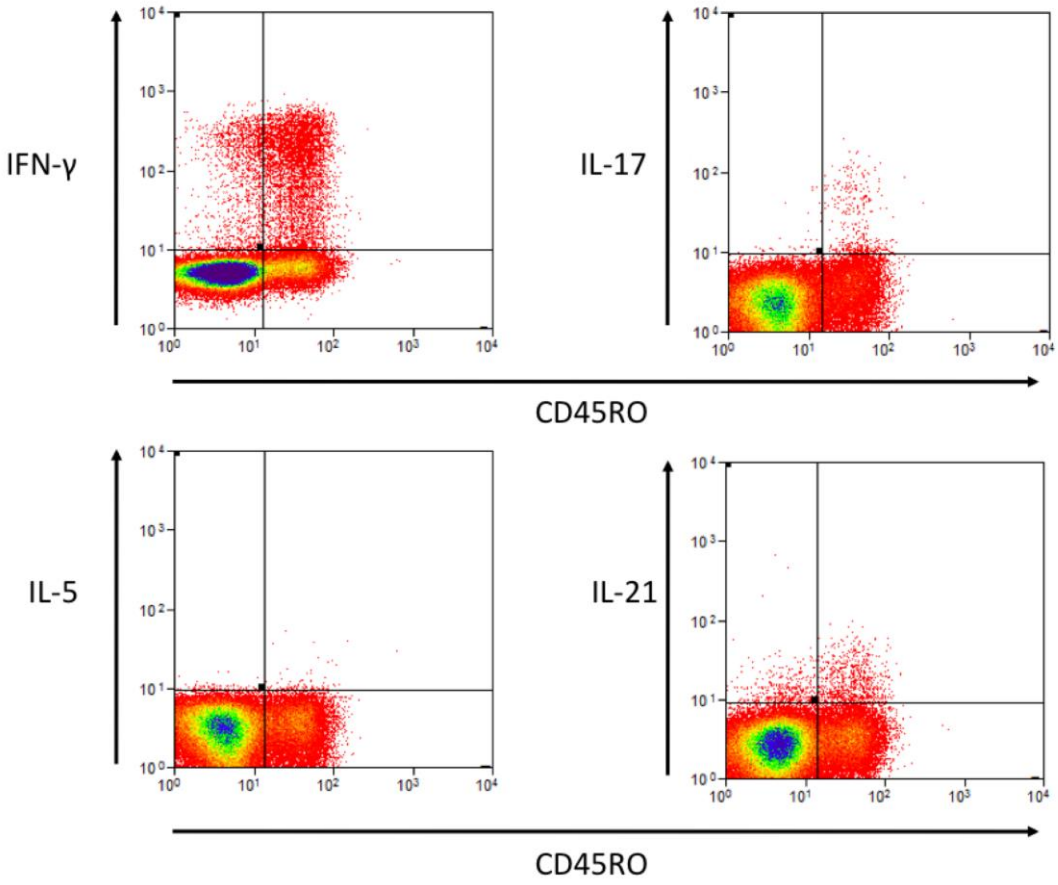

Figure 4.6: Gating strategy for determining cytokine secretion by CD4+ and CD8+ CD45RO+ and CD45RO- T cell populations in PBMCs of GD+ TAO+, GD+ TAO- and HC subjects. PMA- and ionomycin-stimulated cytokine secretion of CD4+ and CD8+ T cells. For T cells the lymphocyte gate of the forward and side scatter profile, as previously described, was utilised. There was subsequent separation into CD45RO+ and CD45RO- populations for IFN-γ, IL-17, IL-5 and IL-21.

Interestingly, CD4+CD45RO+ T cells from GD+TAO+ produced significantly less IFN-γ than HC, while GD+TAO- produced less IL-17 (**Figure 4.7**, summarised in **Table 4.5**). There were no significant differences in IL-5 or IL-21 produced by CD4+ T cells of any of the groups. In CD8+CD45RO+ T cells, the only abnormality noted was that both GD+TAO+ and GD+TAO- subjects produced less PMA- and ionomycin-stimulated IFN-γ than HC (**Figure 4.8**, summarised in **Table 4.6**).

Table 4.5: Median percentages (with interquartile range) of a range of intracellular cytokines detected for PMA- and ionomycin-stimulated CD4+ T cells in each of the three participant cohorts. Non-parametric analysis was undertaken by Kruskal-Wallis test (with Dunn's post-test).

CD4+	HC	GD+TAO-	GD+TAO+	P
IFN-γ	9.6% (6.8)	5.3% (6.8)	4.8% (4.2)	**0.006**
IL17	0.6% (0.6)	0.3% (0.4)	0.4% (0.4)	**0.003**
IL-5	0.3% (0.4)	0.2% (0.3)	0.3% (0.4)	0.4
IL-21	0.3% (0.4)	0.3% (0.3)	0.4% (0.7)	0.12

Table 4.6: Median percentages (with interquartile range) of a range of intracellular cytokines detected for PMA- and ionomycin-stimulated CD4+ T cells in each of the three participant cohorts. Non-parametric analysis was undertaken by Kruskal-Wallis test (with Dunn's post-test).

CD8+	HC	GD+TAO-	GD+TAO+	P
IFN-γ	11% (11)	9.6% (9)	6.3% (8)	**0.01**
IL17	0.1% (0.4)	0.3% (0.2)	0.2% (0.3)	0.4
IL-5	0.2% (0.4)	0.3% (0.5)	0.5% (0.5)	0.09
IL-21	0.1% (0.2)	0.1% (0.3)	0.2% (0.2)	0.7

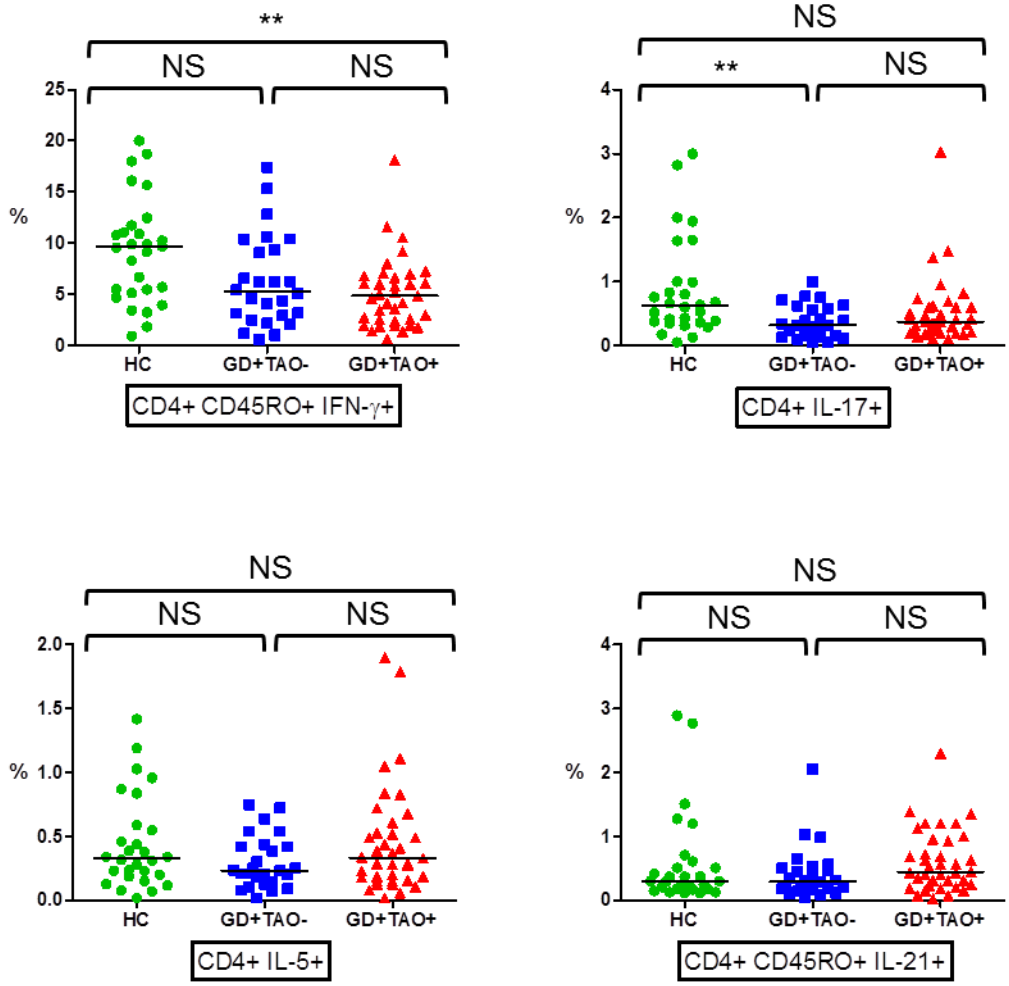

Figure 4.7: Reduced cytokine production by CD4+ T cells in GD+TAO+ and GD+ TAO- compared with HC subjects. Reduced PMA-ionomycin-stimulated IFN-γ production by CD4+ T cells from GD+TAO+, and reduced IL-17 production by GD+TAO+, as compared with HC. Non-parametric analysis was undertaken with Kruskal-Wallis test (with Dunn's multiple comparison). (Key: NS: Not significant; **p=0.001 to 0.01).

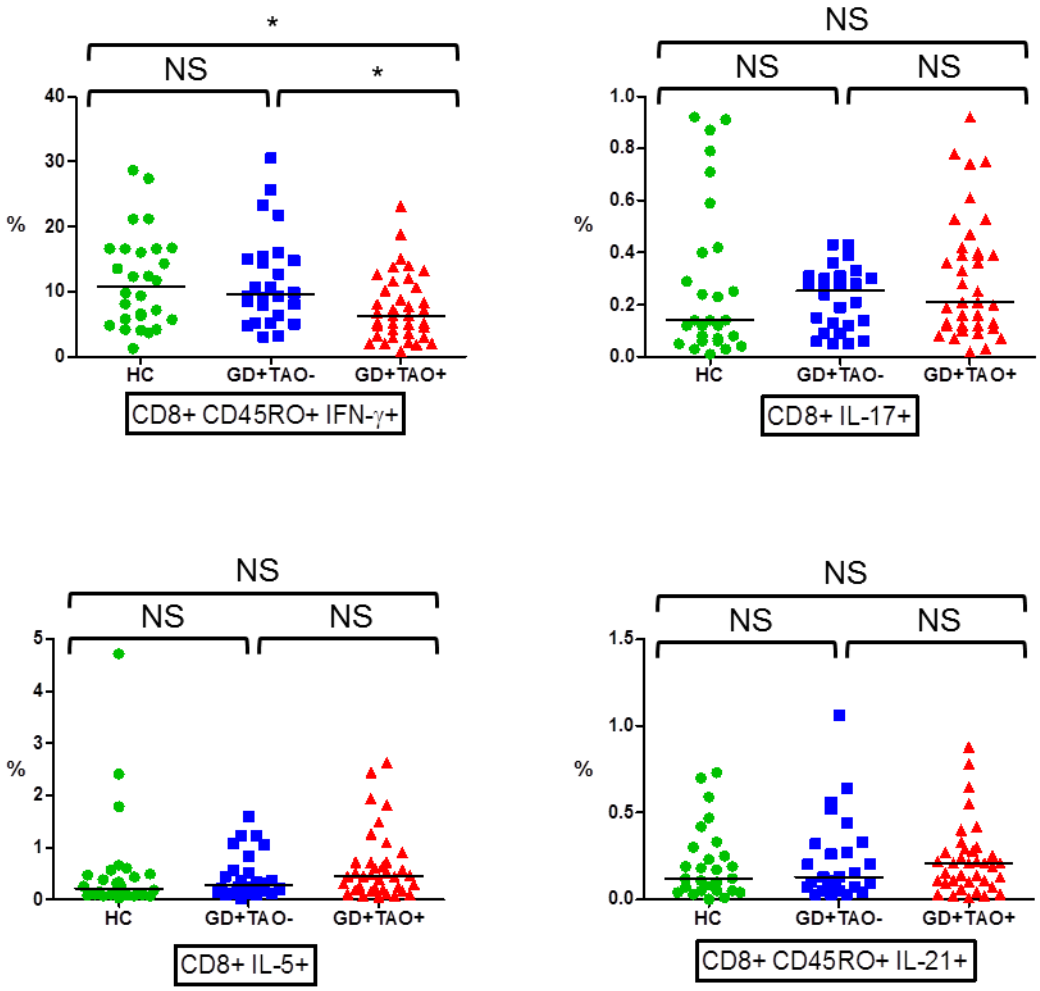

Figure 4.8: Reduced cytokine production by CD8+ T cells in GD+TAO+ and GD+ TAO- compared with HC subjects. Reduced PMA-ionomycin-stimulated IFN-γ production by CD8+ T cells from GD+TAO+ and GD+TAO- subjects as compared with HC. Non-parametric analysis was undertaken with Kruskal-Wallis test (with Dunn's multiple comparison). (Key: NS: Not significant; *p=0.01 to 0.05).

Again, when IFN-γ production by CD4+ and CD8+ T cells in GD (GD+TAO+ and GD+TAO- combined) were analysed further there were no associations with a range of clinical measures, including TAO clinical activity and severity. Once again, the only factor determined to have significant association with the IFN-γ production by CD8+, although not CD4+, T cells was age (**Table 4.7**).

Table 4.7: Summary of factors assessed for contribution to CD4+ and CD8+ T cell cytokine production in GD (GD+TAO+ and GD+TAO- combined) and HC subjects. Non-parametric analysis was undertaken either by Mann-Whitney test (for two groups) Kruskal-Wallis test (with Dunn's post-test) (for more than two groups).

	CD4+ IFN-γ	CD8+ IFN-γ
Age	NS	** **≤40 years:** 8.2% (5.5) **>40 years:** 15% (14)
CAS	NS	NS
TAO Severity	NS	NS
Smoking	NS	NS
GD Duration	NS	NS
Thyroid Status	NS	NS
TRAb Status	NS	NS
PTPN22 Genotype	NS	NS

4.6.4 CD4+CD25^{High}CD127^{Low} Treg in GD+ TAO+, GD+ TAO- and HC

CD4+CD25^{High}CD127^{Low} regulatory T cells were characterised in accordance with **Figure 4.9**. The proportion of CD25^{High}CD127^{Low} cells as a proportion of total CD4+ cells was determined for each of the study groups. There was no statistically significant difference in the percentage of these cells in GD+TAO+ and GD+TAO- cohorts, as compared with HC. Median percentage of CD4+CD25^{High}CD127^{Low} T cells (IQR) in GD+TAO+, GD+TAO- and HC subjects were 7.2% (3.5), 6.1% (4.8) and 6.8% (3.5), respectively (**Figure 4.10**).

4.6.5 CD4+CXCR5+ T Follicular Helper Cells and IL-21 in GD+ TAO+, GD+ TAO- and HC Subjects

Although there had been no increase in IL-21-producing CD4+ T cells on PMA and ionomycin stimulation (**Figure 4.7**, **Table 4.5**), we evaluated the peripheral blood percentage of CD4+CXCR5+ T follicular helper cells in the three study groups. Median percentage of CD4+CXCR5+ T cells (IQR) in GD+TAO+, GD+TAO- and HC subjects were 11% (4), 11% (3.4) and 12% (4), respectively (**Figure 4.11**). There were no significant differences between the groups. Similarly, evaluating serum IL-21 levels between GD and HC subjects determined no differences, and there was no association between serum IL-21 levels and any GD or TAO clinical factors (**Figures 4.12 and 4.13**).

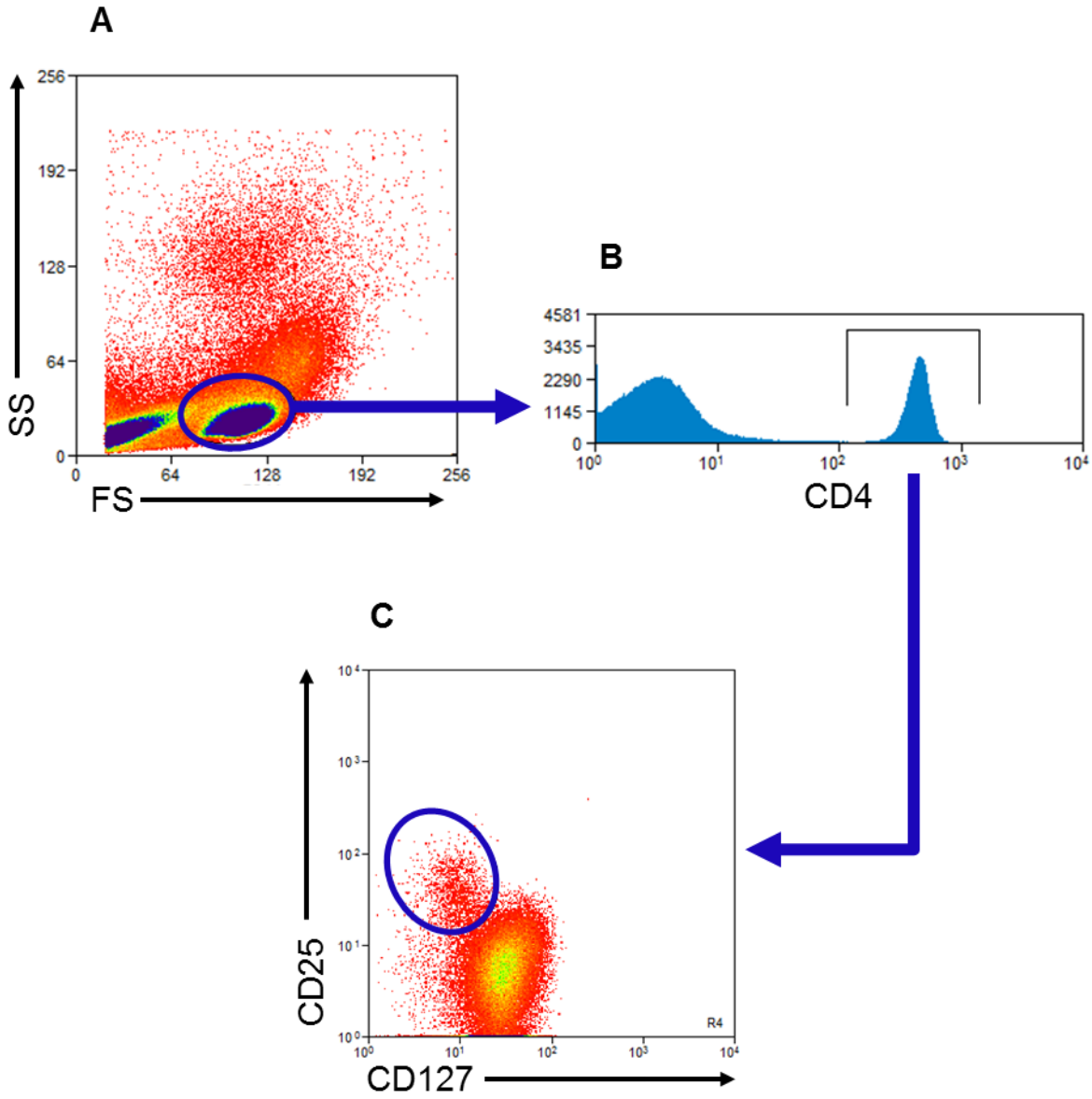

Figure 4.9: Gating strategy used to determine CD4+ CD25^{High} CD127^{Low} T cells, representative of regulatory T cells (Treg), in PBMCs of GD+TAO+, GD+TAO- and healthy subjects. The lymphocyte gate of the forward scatter (FS) and side scatter (SS) profile (A) was utilised, with subsequent gating on the CD4+ population (B). CD25^{High} CD127^{Low} T cells were then gated on as indicated (C).

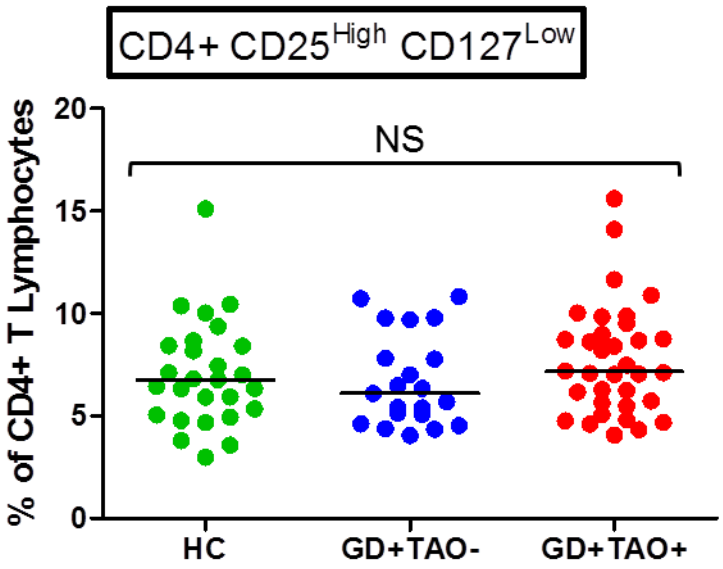

Figure 4.10: No significant difference in CD4+CD25^{High}CD127^{Low} regulatory T cells as a proportion of total CD4+ T cells in PBMCs of 34 GD+TAO+, 21 GD+TAO- and 27 age- and sex-matched healthy control (HC) subjects. Median percentage of CD4+ CD25^{High} CD127^{Low} T cells indicated for each of the study groups of interest. Non-parametric analysis was undertaken with Kruskal-Wallis test (with Dunn's post hoc test) (NS, Not significant).

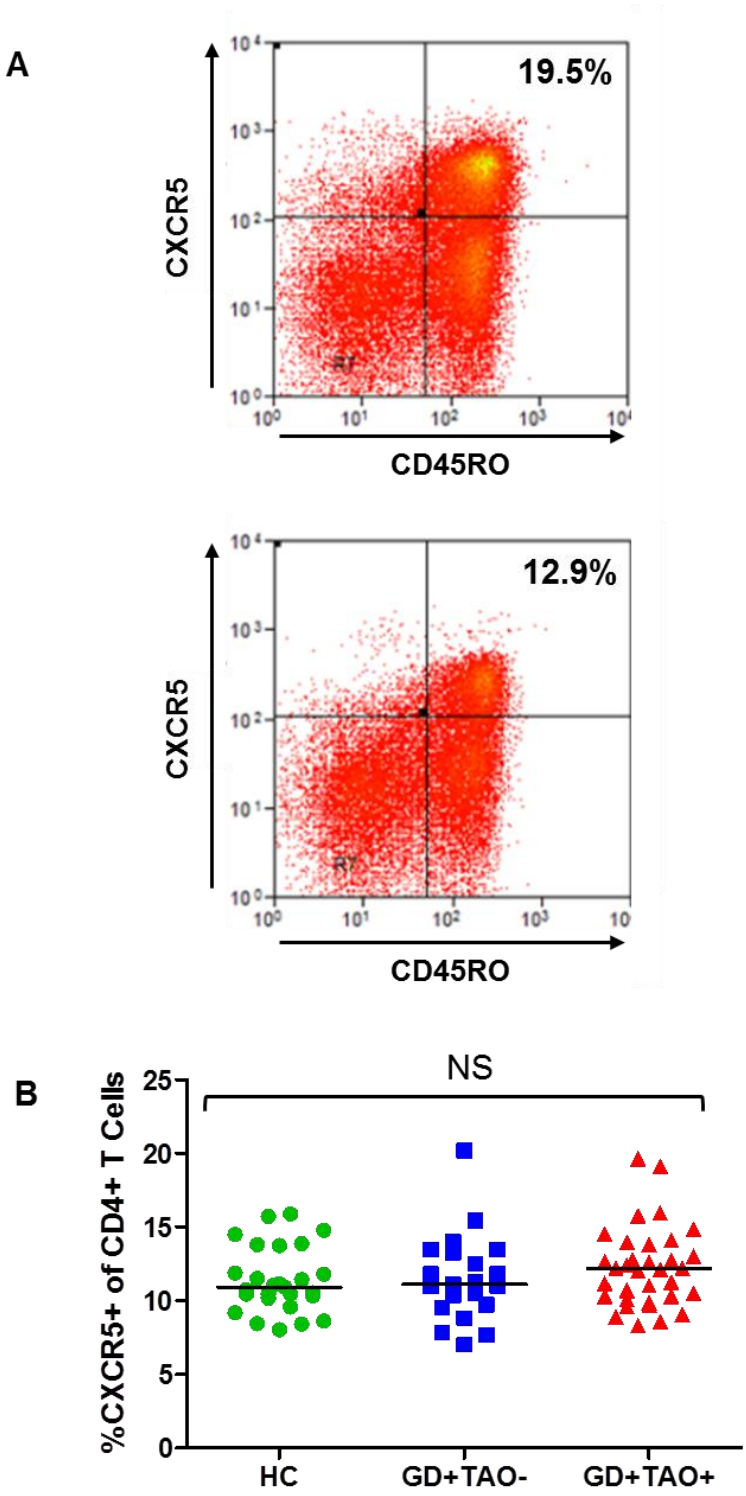

Figure 4.11: Representative flow cytometry plots for CD4+ CXCR5+ T follicular helper cells. Proportion of CXCR5+ CD4+ T lymphocytes determined from T cell gate on forward and side scatter profiles and CD3+CD4+ T cells (A). Proportion of CXCR5+ cells of CD4+ T cells in GD+TAO+, GD+TAO- and HC subjects. 34 GD+TAO+, 21 GD+TAO- and 27 HC subjects (B).

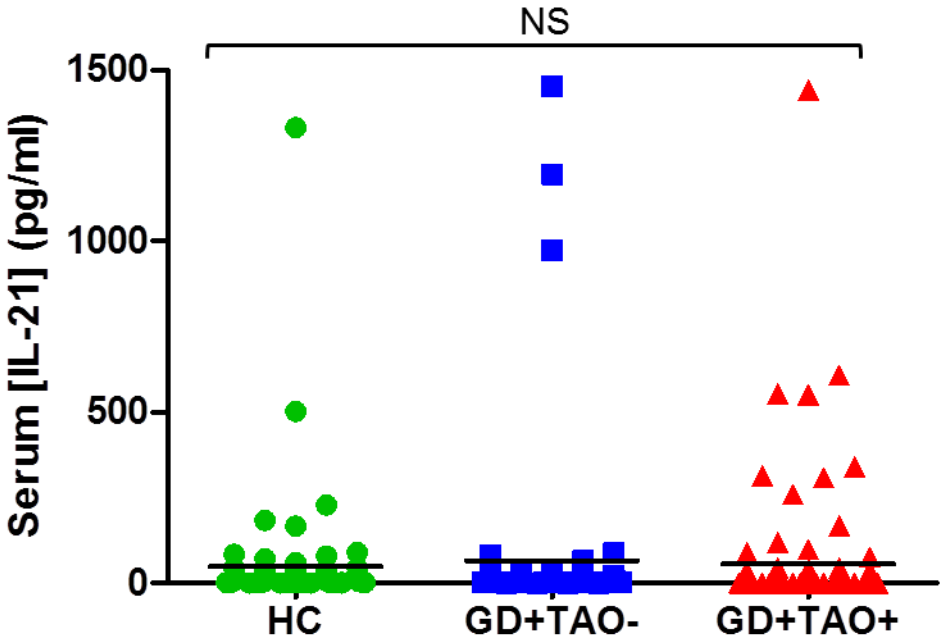

Figure 4.12: Serum IL-21 levels in GD+TAO+, GD+TAO- and HC subjects. IL-21 levels determined by ELISA for 85 GD+TAO+, 63 GD+TAO- and 72 HC subjects using commercial IL-21 ELISA. Median IL-21 levels in these groups were 48pg/ml, 66 pg/ml and 55 pg/ml, respectively.

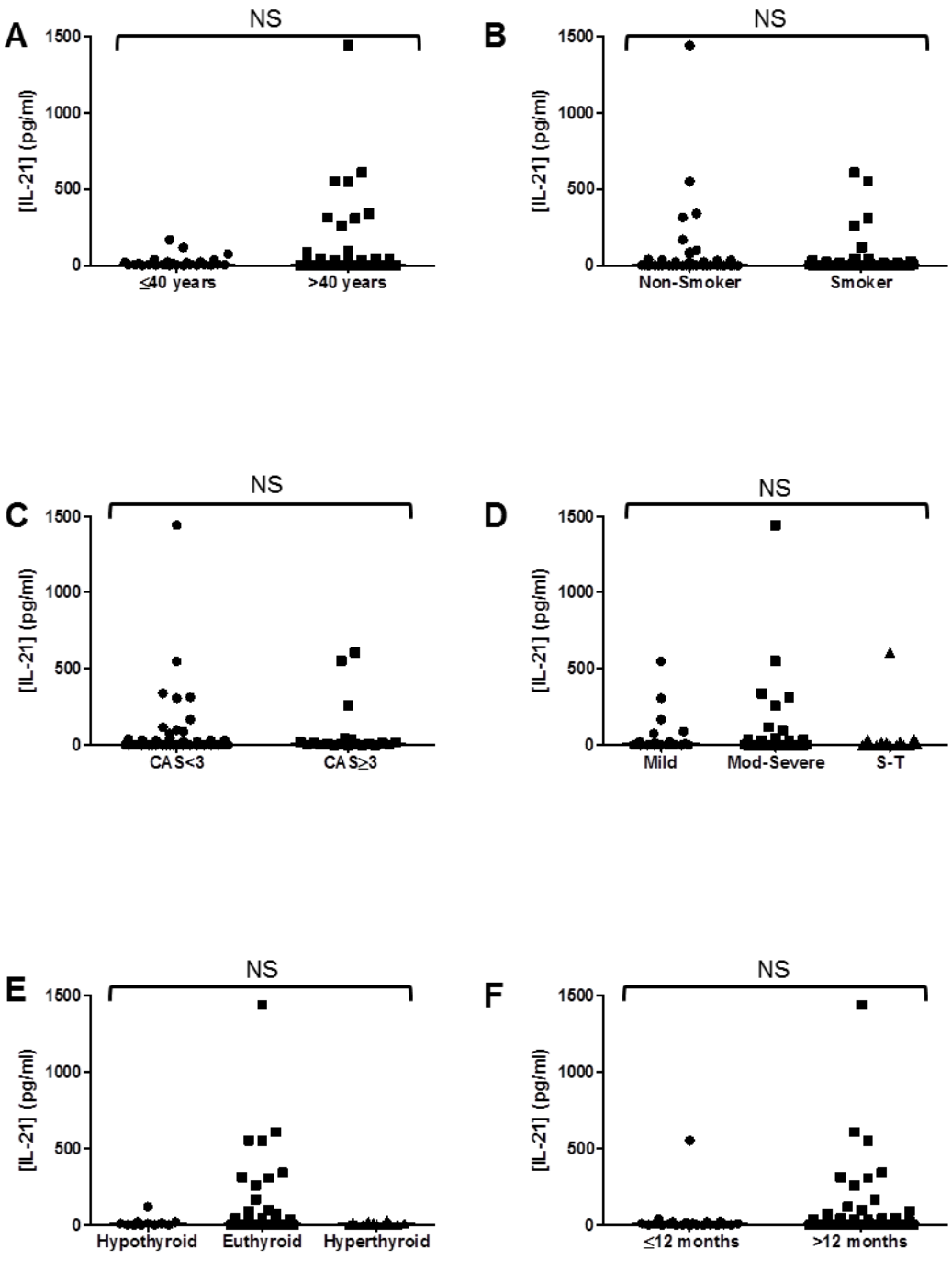

Figure 4.13: Relationship between IL-21 levels and clinical, immunological and genetic factors in GD+TAO+ subjects. No statistically significant differences were noted in age (A), cigarette smoking status (B), TAO clinical activity score (C), EUGOGO severity grade (D), thyroid status (E) or duration of GD (F). Non-parametric analysis was undertaken with Mann-Whitney U test (for two groups) or Kruskal-Wallis test (with Dunn's multiple comparison) for multiple groups. (NS, Not significant).

4.6.6 Early and Late T Cell Activation Marker Expression in GD+ TAO+, GD+ TAO- and HC Subjects

Early (CD69) and late (CD71, CD154) T cell activation marker expression by CD4+ and CD8+ T cells were measured in all three cohorts of interest (**Figure 4.14**). **Figures 4.15 A & B** show that there was no statistically significant difference in the expression of any of these markers in either CD4+ or CD8+ T cells between GD+TAO+, GD+TAO- and HC subjects. There was also no correlation between expression of early and late T cell activation markers by CD4+ and CD8+ T cells and TAO clinical activity or severity.

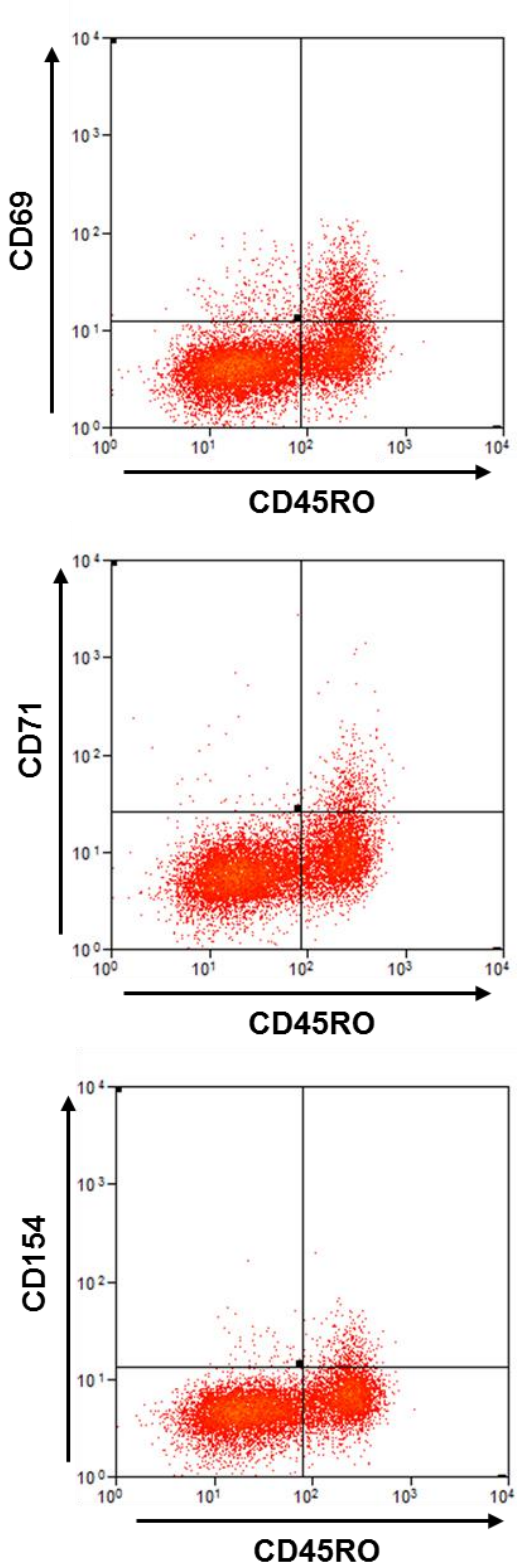

Figure 4.14: Representative flow cytometry plots for CD4+ and CD8+ T lymphocyte activation status. CD3+CD4+ and CD3+CD8+ T cells divided into naïve (CD45RO-) and memory (CD45RO+) and investigated for early (CD69) and late (CD71, CD154) activation markers in PBMCs.

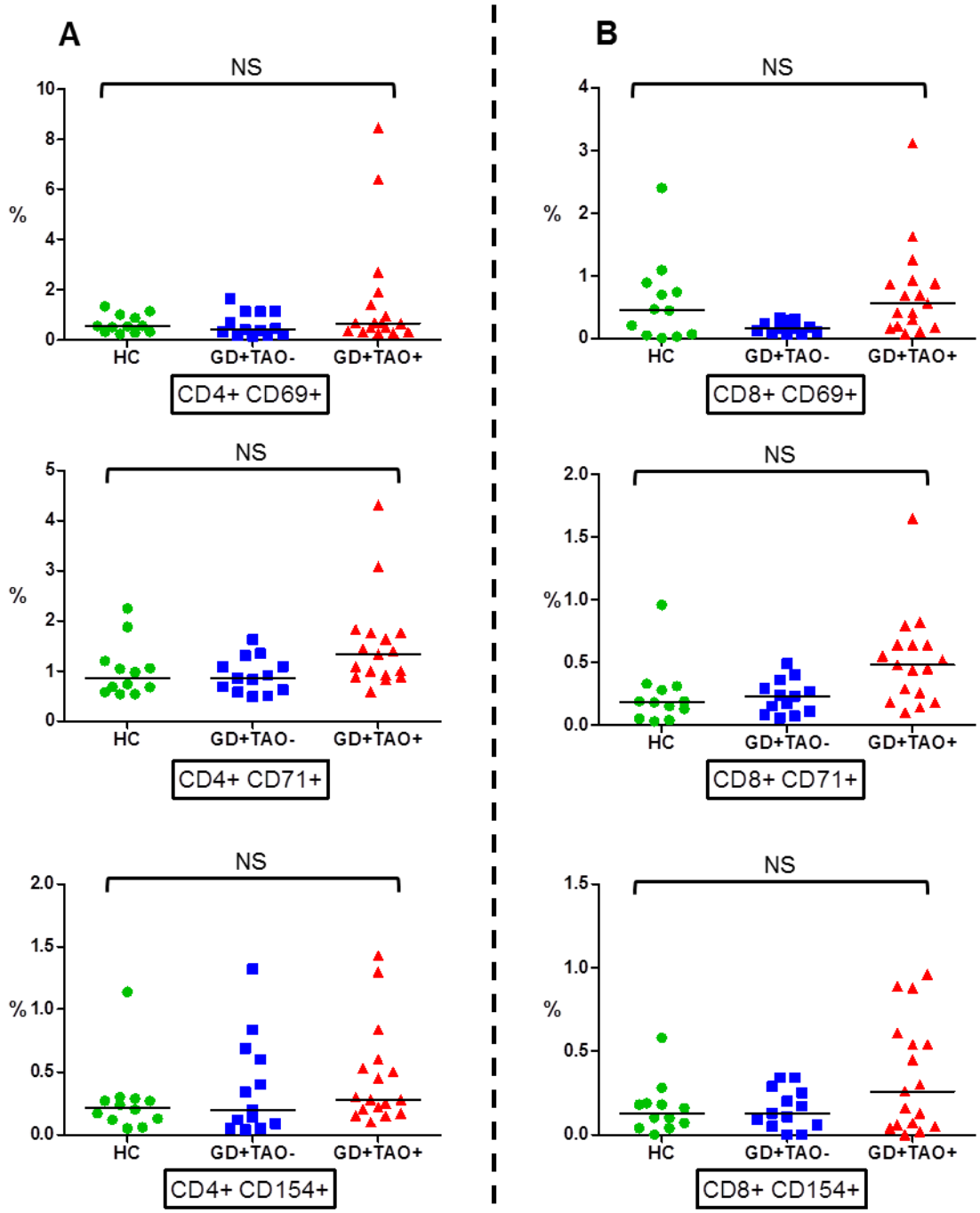

Figure 4.15: Early and late activation markers on CD4+ (A) and CD8+ (B) T cells in GD+TAO+, GD+TAO- and HC. Non-parametric analysis was undertaken with Kruskal-Wallis test (with Dunn's multiple comparison). (Key: NS: Not significant).

4.6.7 IGF-1R Expression on CD4+ and CD8+ T Cell Memory Populations by GD+ TAO+, GD+ TAO- and HC Subjects

CD4+ and CD8+ T cell memory subtypes for measurement of IGF-1R expression were defined as described and illustrated in **Figure 4.3**. **Figures 4.16 A & B** demonstrate IGF-1R fluorescence patterns distinct from those of an isotype control in each of the naïve and memory populations in both CD4+ and CD8+ cells. To reiterate, ΔMFI was defined as: MFI [Test Antibody] – MFI [Isotype Control]. IGF-1R expression was higher on CD4+ than CD8+ T cell memory populations.

There were no statistically significant differences in IGF-1R expression in any of the CD4+ or CD8+ memory populations in GD+TAO+ or GD+TAO- subjects as compared with HC (**Figures 4.17** and **4.18**, summarised in **Tables 4.8** and **4.9**). There were no associations between levels of IGF-1R expression on CD4+ and CD8+ memory populations and TAO clinical activity.

Validation of the experimental techniques with two thyroid cancer cell lines (K1 and TPC1), determined that it was possible to detect IGF-1R expression on these cell types with the IGF-1R monoclonal antibody and isotype control used in all experiments (**Appendix 9**)

Table 4.8: Summary of ΔMFI for IGF-1R expression on CD4+ T cell memory populations. Non-parametric analysis was undertaken with Kruskal-Wallis test (with Dunn's post-test).

CD4+	HC	GD+TAO-	GD+TAO+	P
Naive	8.5 (5.2)	7.2 (6.2)	11 (5.5)	0.09
CM	3.9 (1.6)	1.6 (3.0)	3.2 (3.3)	0.15
EM	2.2 (1.4)	2.5 (2.2)	3.3 (3.1)	0.27

Table 4.9: Summary of ΔMFI for IGF-1R expression on CD8+ T cell memory populations. Non-parametric analysis was undertaken with Kruskal-Wallis test (with Dunn's post-test).

CD8+	HC	GD+TAO-	GD+TAO+	P
Naive	6.0 (2.0)	4.1 (6.1)	6.4 (2.9)	0.13
CM	2.4 (1.5)	2.7 (4.0)	3.5 (4.3)	0.25
EM	2.1 (1.8)	2.5 (2.2)	3.3 (3.1)	0.50
EMRA	2.0 (1.7)	2.3 (2.8)	3.0 (3.9)	0.3

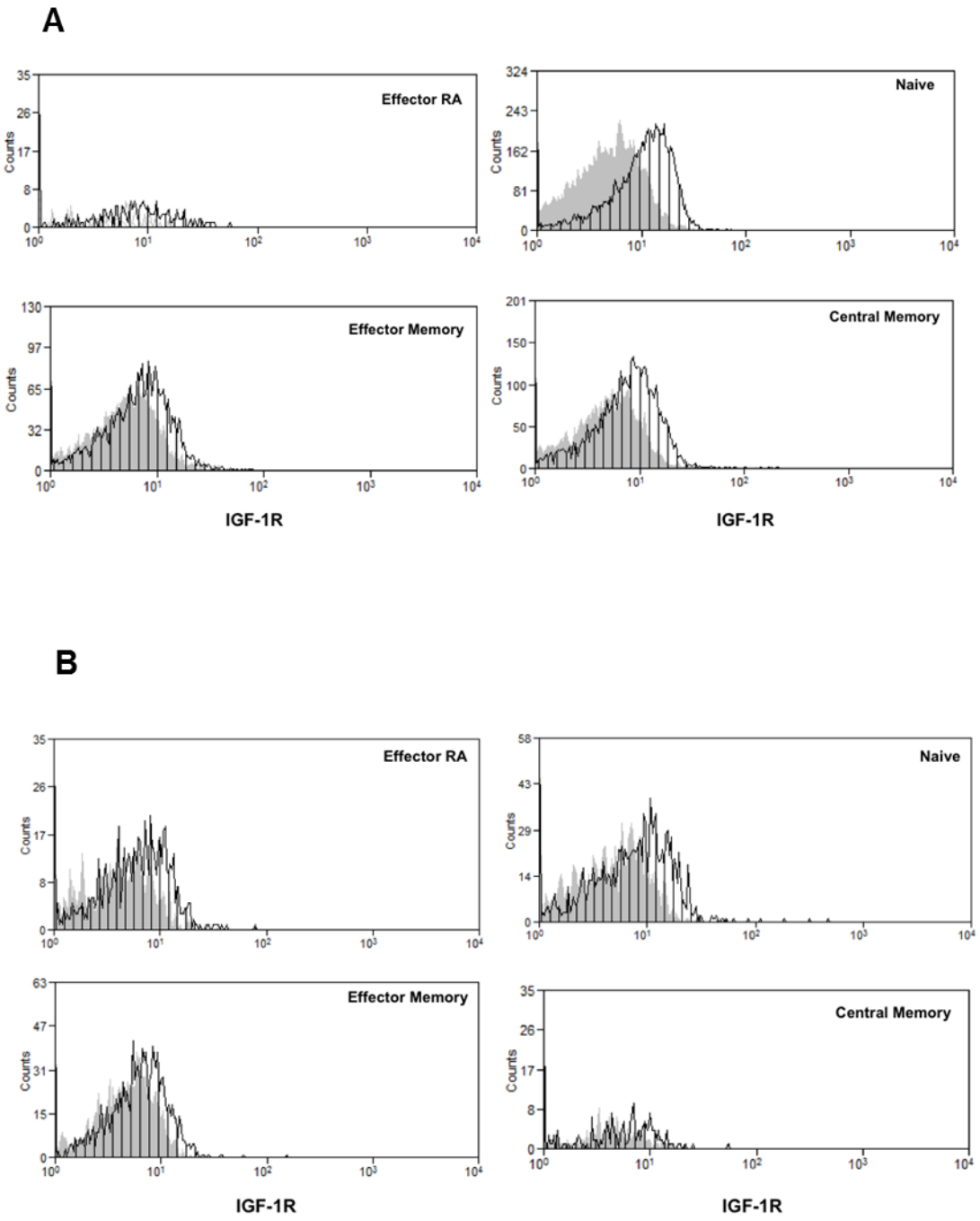

Figure 4.16: Representative plots for IGF-1R expression on different naïve and memory T cell populations of CD4+ (A) and CD8+ (B) T cells (black, hatched curves) from lysed whole blood of TAO and HC subjects compared with isotype control (solid grey curves). Example shown is for HC subject. For each population ΔMFI was calculated as MFI [IGF-1R] – MFI [Isotype Control].

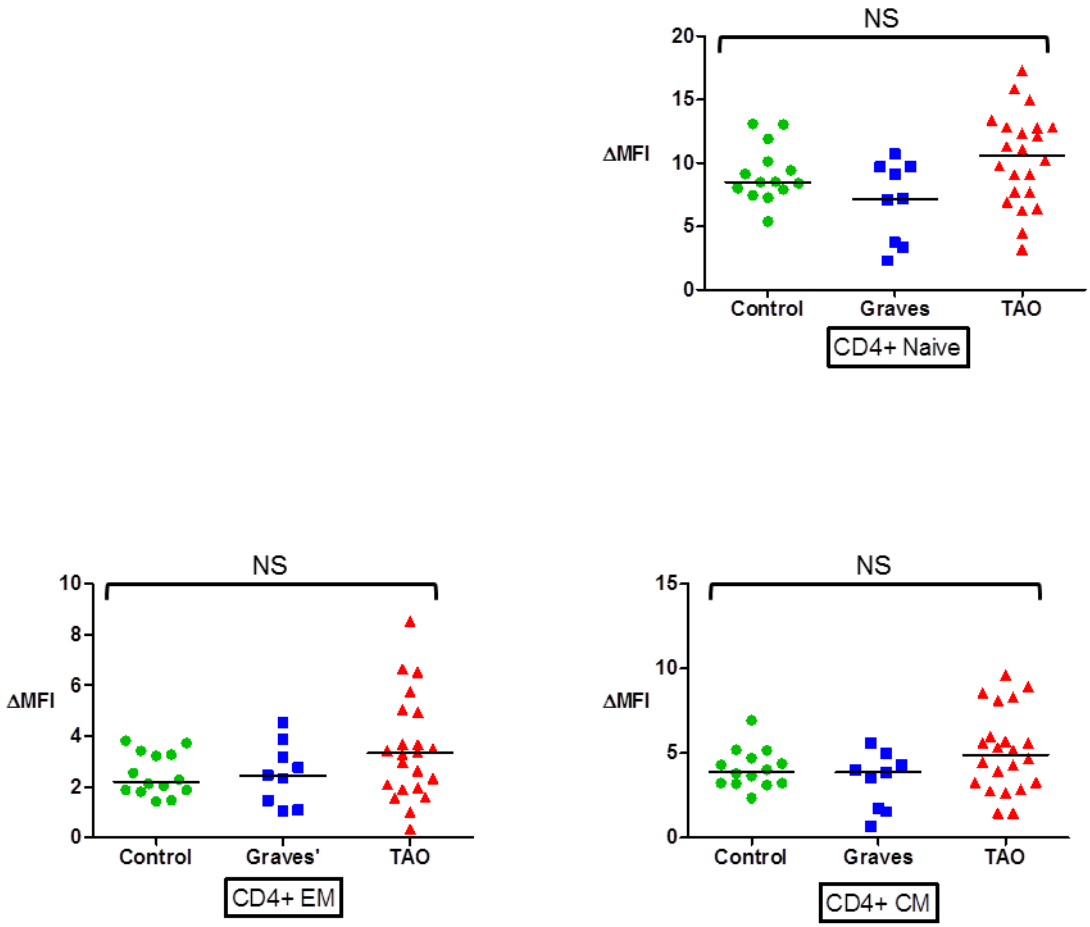

Figure 4.17: No difference in IGF-1R ΔMFI for CD4+ T cell memory populations in lysed whole blood of GD+TAO+, GD+TAO- as compared with HC subjects, comparing naïve, CM and EM CD4+ cells. No data for CD4+ EMRA cells is presented as this population was too small to permit analysis. Non-parametric analysis was undertaken with Kruskal-Wallis test (with Dunn's multiple comparison). (Key: NS: Not significant).

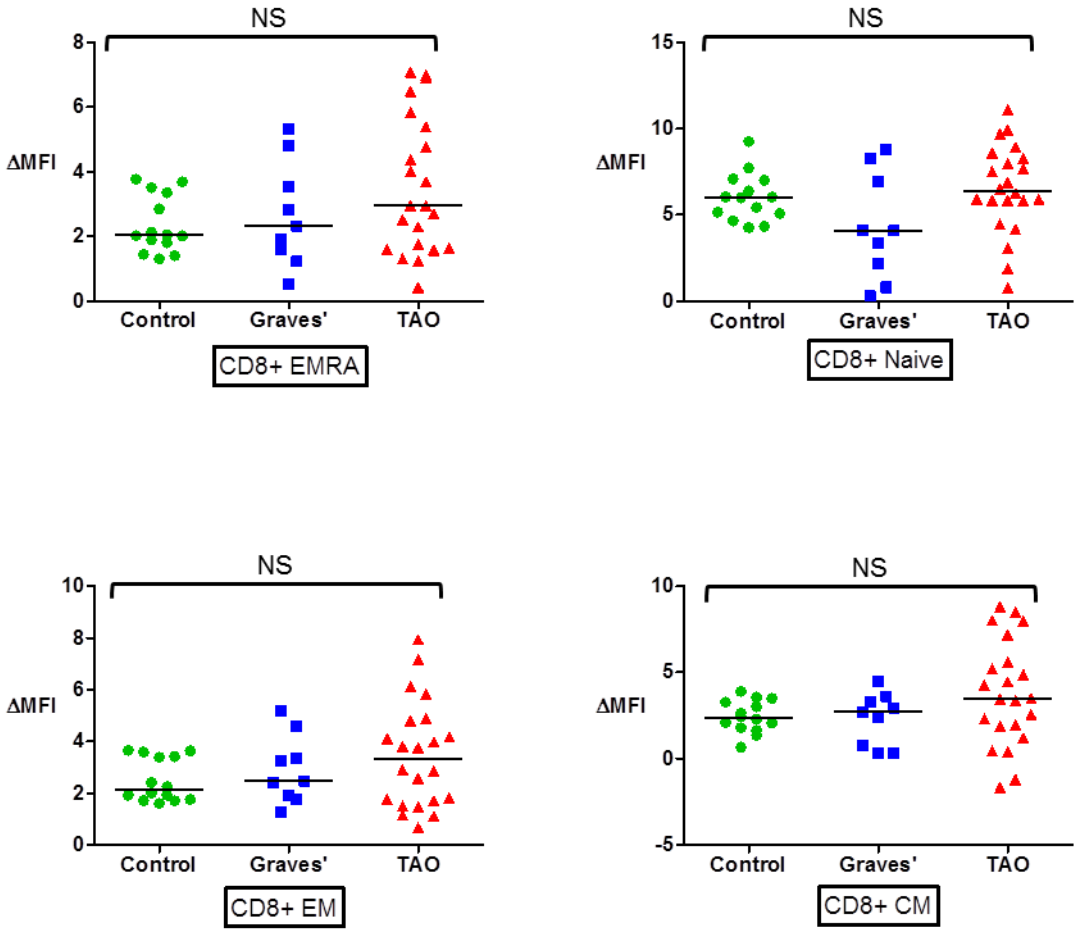

Figure 4.18: No difference in IGF-1R ΔMFI for CD8+ T cell memory populations in lysed whole blood of GD+TAO+, GD+TAO- as compared with HC subjects, comparing naïve, CM, EM and EMRA CD8+ cells. Non-parametric analysis was undertaken with Kruskal-Wallis test (with Dunn's multiple comparison). (Key: NS: Not significant).

4.6.8 Effect of Recombinant IGF-1 on T Cell IGF-1R Signalling Pathways and IGF-1R-Mediated Proliferation

4.6.9 IGF-1-Stimulated Phospho-Akt and Phospho-ERK1/2 from T Cells

A minimal effect of rhIGF-1 was noted for Phospho-Akt and no effect was noted for Phospho-ERK1/2 (**Figures 4.19** and **4.20**) in stimulating IGF-1R in PBMC from HC. To validate this we performed analogous experiments and noted no effect when GD+TAO+, GD+TAO- or HC sera were used, either in PBMC or in a thyroid cancer cell line (K1 and TPC1) with established expression of TSH-R and IGF-1R.[386] It is interesting to observe that, at least for Phospho-Akt, the level of expression progressively increased with IGF-1 concentration to a maximum at 0.1 μg/ml and then diminished at the 1.0 μg/ml and 10 μg/ml IGF-1 concentrations.

4.6.10 IGF-1-Stimulated T Cell Proliferation

When CD4+ T cells were sorted into their constituent memory populations (naïve, CM and EM), utilising the anti-CD3/CD28 bead-to-cell ratio of 1:32 for all wells, and maintaining the range of IGF-1 concentrations, we noted no definite increase in the proliferation of any of the CD4+ T cell memory populations, as measured by CFSE proliferation (explained in **Section 4.4.1**) and corrected for by the number of counting beads, over the range of concentrations of IGF-1 utilised (**Figures 4.21 & 4.22**).

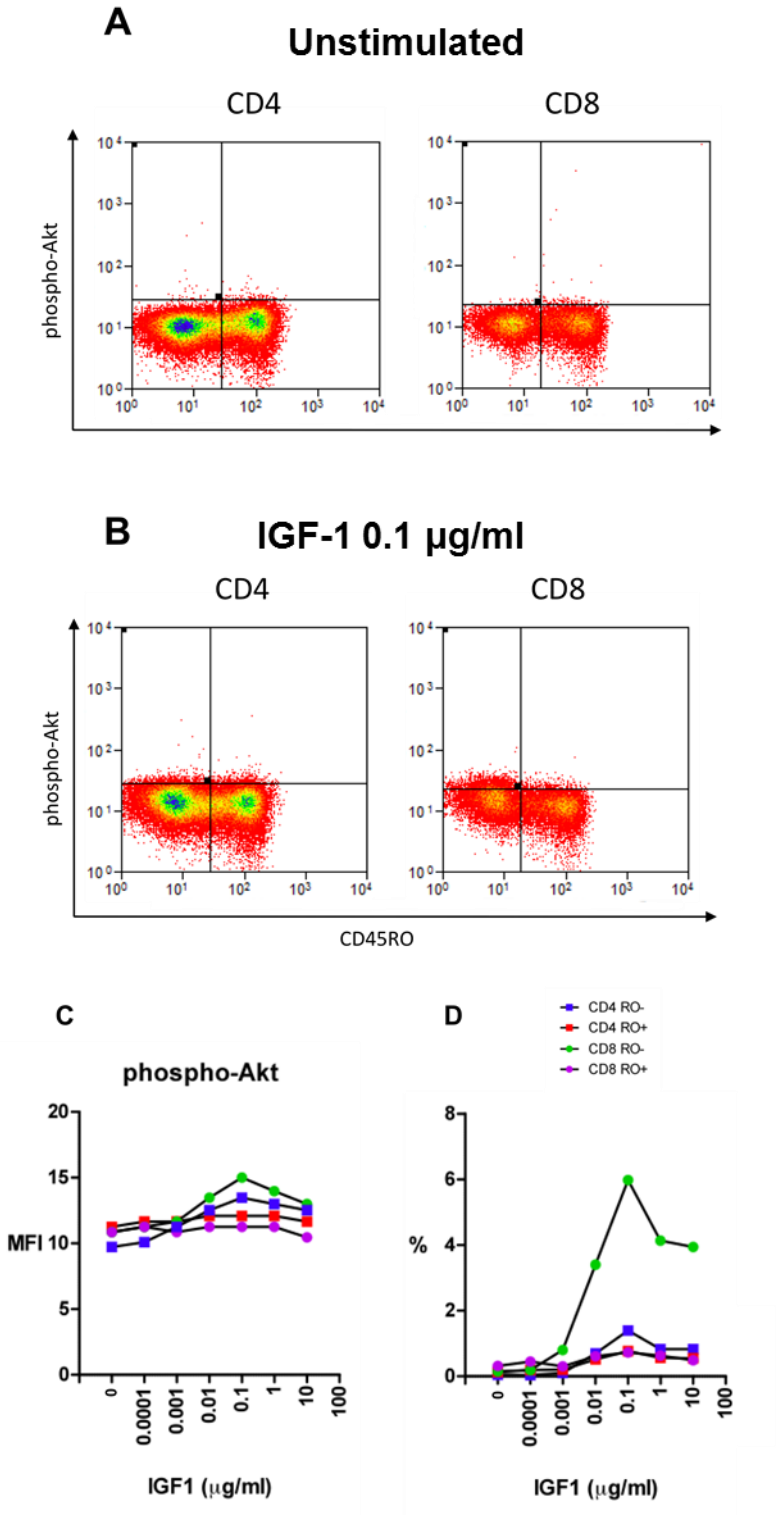

Figure 4.19: Increased Phospho-Akt expression, predominantly in peripheral blood CD8+ CD45RO- T cells, with optimal stimulating concentration of recombinant IGF-1 of 0.1µg/ml (Healthy Control). CD4+ and CD8+ T cells were identified as previously described and either left unstimulated (Panel A) or stimulated by a range of IGF-1 concentrations (Panel B). Phospho-Akt expression was defined by Phospho-Akt MFI (Panel C) or by percentage of Phospho-Akt positive cells (Panel D). Representative figure of n=3.

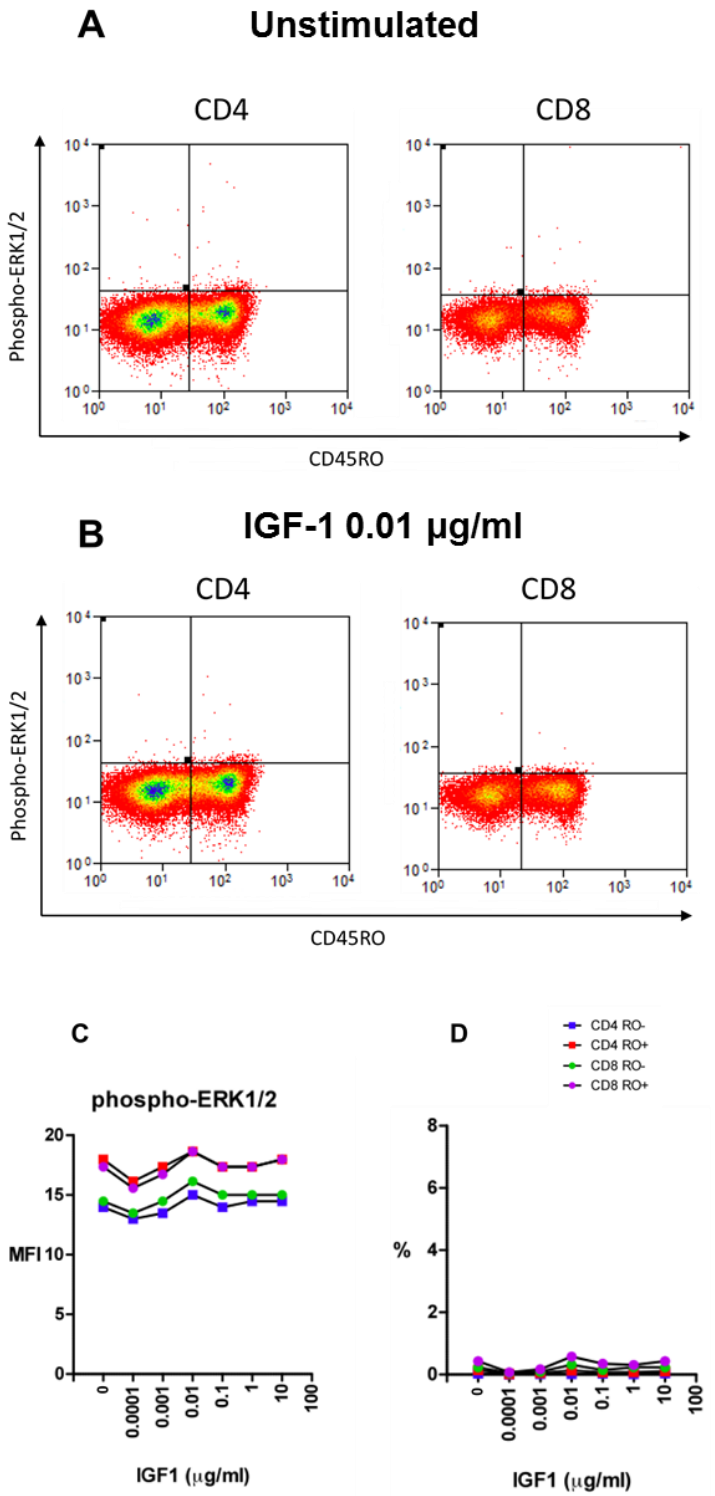

Figure 4.20: No change in Phospho-ERK1/2 expression by peripheral blood CD4+ or CD8+ T cells when stimulated with a range of concentrations of recombinant human IGF-1 (Healthy Control). CD4+ and CD8+ T cells were identified as previously described and either left unstimulated (Panel A) or stimulated by a range of IGF-1 concentrations (Panel B). Phospho-ERK1/2 expression was then defined by Phospho-ERK1/2 MFI (Panel C) or by percentage of Phospho-ERK1/2 positive cells (Panel D). Representative figure of n=3.

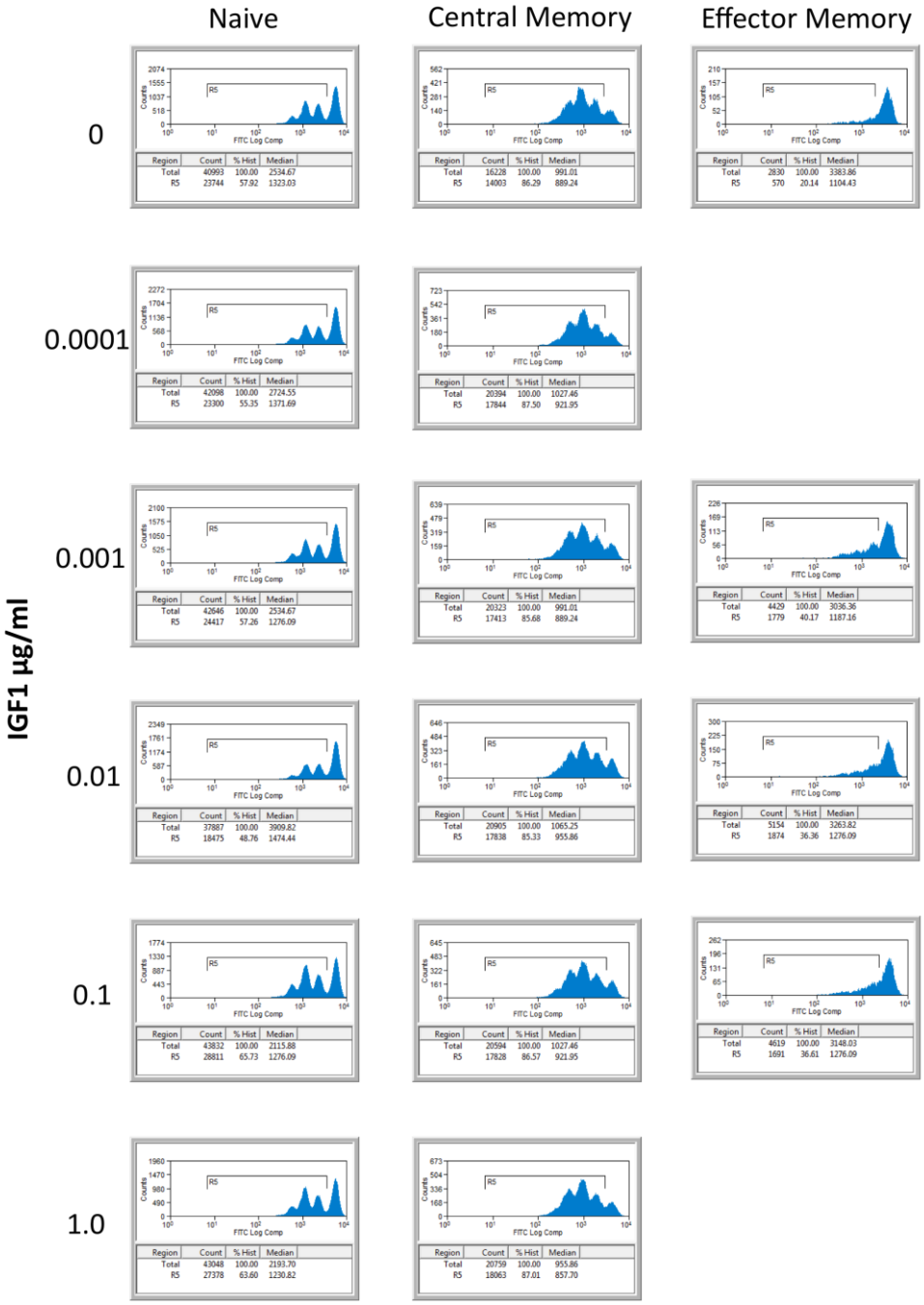

Figure 4.21: CFSE proliferation plots for CD4+ T cells sorted into their memory populations. In all cases, the purity of the sorted T cell memory populations was >97%. Cells were cultured for 4 days in the presence of CD3/CD28 beads at a bead-to-cell ratio of 1:32 and a range of rIGF-1 concentrations (0 – 1 µg/ml).

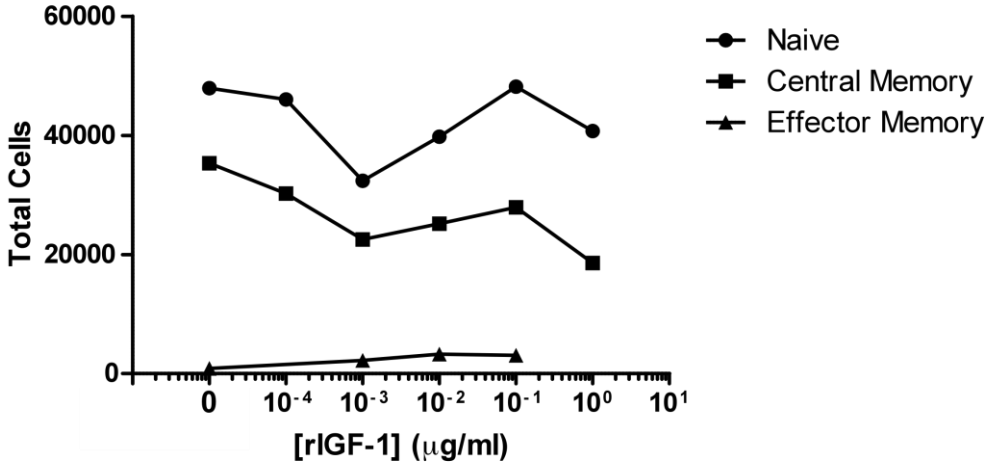

Figure 4.22: No observed effect of recombinant IGF-1 in differentially mediating the proliferation of CD4+ memory T cell populations in the presence of CD3/CD28 beads at a bead-to-cell ratio of 1:32 and a range of rIGF-1 concentrations (0 – 1 µg/ml) after a 4 day culture. Figure 4.22 represents the outcome of the experiment represented Figure 4.21, with the total number of cells determined by an adjustment for the number of counting beads in each sample. Representative results of two separate experiments.

4.7 Discussion

Some of the previous studies in GD and TAO, which have aimed to evaluate T lymphocyte memory status, have not divided T cells into their four memory phenotypes. My study is novel in that previous work has largely distinguished CD4+ and CD8+ T cells as memory or naïve on the basis of CD45RA or CD45RO alone. This is an oversimplification. We went a step further, utilising CCR7 to separate T cells into naive, EM, CM and EMRA populations. We also further differentiated GD patients into GD+TAO+ and GD+TAO- groups. Finally, we correlated T cell memory phenotype with a range of disease parameters.

4.7.1 Theories on Perturbation of T Cell Memory Populations in Disease States

This study determined that, while the peripheral blood CD4+/CD8+ ratio was unchanged, CD4+ and CD8+ T lymphocyte memory profiles, as defined by CD45RO and CCR7, are skewed in patients with GD and TAO. This observation was noted both from intracellular cytokine staining studies in PBMC and from IGF-1R expression data performed on lysed whole blood of a distinct cohort of GD+TAO+ and GD+TAO- patients and HC, at different times. Specifically, we observed a reduction in EM CD4+ and CD8+ T cells and a concomitant elevation of naïve T cells in GD+TAO+ and GD+TAO- subjects. Separate components of the results are complementary in that the reduced proportions of EM T lymphocytes are appropriately reflected in reduced stimulated cytokine production by GD+TAO+ and GD+TAO- subjects as compared to HC, even though no change in activation markers (CD69, CD71 and CD154) for either CD4+ or CD8+ T cells was observed. Whether

there are any changes in the *in vivo* functioning of the CD4+ and CD8+ T cell populations was not determined by this study.

It is interesting that this perturbation in T cell memory subtype proportions is "shared" between GD and TAO, with no increased derangement in those patients with differing thyroid status, cigarette smoking, longer duration or more active orbital inflammatory disease. The mechanism for the aberration of T cell phenotype is uncertain. If one accepts the model of T memory cell differentiation proposed by Sallusto et al (1999),[273] my findings suggest that there is a delay in the differentiation of CD4+ and CD8+ naive T cells to more mature memory status. This may also reflect a compensatory mechanism whereby new T cells are being produced to replace EM cells migrating to, and being sequestered in, sites of inflammation such as the thyroid or orbit.

This alteration in peripheral blood T cell homeostasis in GD and TAO is in keeping with other autoimmune and inflammatory diseases, where a range of different changes in CD4 and CD8 T cell memory phenotypes have been observed. An equilibrium of both CD4+ and CD8+ memory T cells is constantly taking place, with consumption of T cells matched by influx of new T cells from the thymus. This is especially so in inflammatory and autoimmune conditions because of higher-than-usual requirements for lymphocyte turnover. In particular, EM T cells are consumed in inflammatory processes, with antigenic responses resulting in activation-induced apoptosis, although there may also be an effect of thionamide or immunosuppressant drugs.[377] Again, this could be what we are observing in TAO – an increased turnover

of EM cells with a compensatory increase in CD4+ and CD8+ T cells of the naïve phenotype.

Alternatively, this may be representative of the effects of putative IGF-1R-Ab on T cells. These data demonstrate differential expression of IGF-1R on CD4+ and CD8+ T cells, with highest levels on naive cells and progressive reduction in expression from CM to EM to EMRA. Given the well-documented role of the IGF-1/IGF-1R axis in promoting T cell proliferation and reducing T cell apoptosis,[240] it may be attractive to propose that the data demonstrating a progressive reduction in IGF-1R expression as T cells differentiate from naïve to CM to EM may explain why there is an alteration in GD+ TAO+ and GD+ TAO- subjects. It could be that IGF-1 or IGF-1R-Ab are acting differentially on T cell memory subsets, preferentially expanding the naive T cell pool over other subsets, through increased proliferation or preferential survival, or both. However, one must consider that, as has been suggested, the differentiation of memory T cells may not be linear at all.[387,388] In addition, as described in **Chapter 3**, and by other authors, putative serum IGF-1R-Ab have not been found to be elevated in GD+TAO+ or GD+TAO- subjects as compared to HC,[232,353] and serum IGF-1 levels are also equivalent in these groups.[356]

To investigate further whether patient medications were a significant influence we could have included another group of subjects without autoimmune thyroid disease but who were still hyperthyroid and required similar medications. For example, those with hyperthyroidism due to toxic multinodular goitre or amiodarone-induced thyrotoxicosis. These patients are also on CBZ or PTU, but do not have the underlying autoimmunity of those with GD or TAO.

4.7.2 T Cell Memory Subsets in Systemic Autoimmune Disease

While this study recognised no change in CD4+/CD8+ ratio between study groups, this is in contrast to other research groups in TAO.[277,384,389] A wide array of previous similar studies in other autoimmune and inflammatory human diseases have also noted alterations in T cell memory populations, although these are often contradictory. There have been various hypotheses as to why such dysregulation occurs, with theories ranging from deranged T cell homeostasis, altered T cell activation and thymic involution.[390-392]

Reduced CD4+CD45RA+, but not CD8+CD45RA+, T cells have been found in peripheral blood in MS.[393] Increased CD4+CD45RO+ cells have been noted in peripheral blood in primary biliary cirrhosis.[394] Increased CD45RA and CCR7 expression on CD8+ T cells have been noted in recent-onset type 1 diabetic children.[395] Additionally, in RA it has been found that EM (CD45RA-CD62L-) CD8+ T cells were significantly decreased, whereas CM (CD45RA-CD62L+) CD8+ T cells were increased, as compared with controls. There were no such differences in naïve and EMRA CD8+ T cells. The CM CD4+ T cell subpopulation was increased in RA patients, whereas the naive and EM phenotype of CD4+ T cells did not differ. In the same study, patients with SLE displayed no change in the distribution of naïve or memory CD4+ or CD8+ T cells.[377]

In RA, increased proportions of CD45RO+ peripheral blood T cells were observed in RA patients with higher IgM rheumatoid factor titres,[366] in keeping with other studies in SLE and MS which found reduced CD4+CD45RA+ T cells.[396,397] Studies in juvenile

systemic sclerosis and type 1 diabetes mellitus found increased EMRA CD4+ cells, while naive and CM cells were reduced.[385,398] Likewise, there was an accumulation of these terminally differentiated memory T cells in SLE,[399] and an increase in the ratio of CD8+ EMRA cells in RA, which previous groups had labelled “false naïve” CD4+ and CD8+ cells, correlating with duration of disease.[374,400] This latter point was proposed to be representative of the effect of chronic antigen stimulation of T cell memory phenotypes.[374] In contrast with the findings of Fekete et al (2007), other studies have found a reduction in EMRA CD8+ T cells and increase in CM CD8+ cells in RA. There was also an increase in CM CD4+ T cells in RA patients as compared with controls. There was no such difference in any CD4+ or CD8+ T cell memory population in SLE.[377]

In type I diabetes mellitus, another T cell mediated organ-specific autoimmune disease, Matteucci et al (2011) found that intermediate and long-term glycaemic control affected T cell memory profile, noting negative correlation with CM and naive cells, and positive correlation with EMRA cells.[385] In contrast, proportions of CD45RA+CD4+ cells, and tendency to CD45RA+CD8+ cells T cells were lower in paediatric type I diabetes mellitus patients, and decreased further with increased age.[401] In sarcoidosis a subgroup with good prognosis disease had reduced expression of Th1 cytokines and also FoxP3+ cells in bronchoalveolar lavage (BAL) fluid, the inflammatory site in sarcoidosis.[276]

Wikén et al (2011) established that the most common T cell subset in BAL were EM cells (CD45RO+CD27-) followed by CM cells (CD45RO+CD27+), with the opposite being found in peripheral blood.[276] As already stated, this could be the same situation

in GD and TAO. That is, the EM cells are reduced in peripheral blood as they have been preferentially trafficked to the primary site of inflammation, the orbital tissues. This may be an erroneous view, given that EM T cells were reduced in both GD and TAO in my studies. However, this may once again be representative of the previous finding of orbital manifestations (representative of TAO) being seen on orbital imaging even in GD patients without clinical signs of TAO.[25]

4.7.3 T Lymphocyte Memory Phenotype and Ageing

It was crucial to ensure that the three groups of study subjects were appropriately age-matched. It is known that the proportion of memory T lymphocytes (although not necessarily with any alteration in the ratio of CM to EM cells) increases with age, at the expense of naïve cells.[374,402] This has been demonstrated in both CD4+ and CD8+ populations, despite no change in total numbers of both types of T cell with increasing age,[403] even though other studies have recognised thymic involution in the elderly.[404] Paradoxically, ageing is associated with increased IFN-γ production.[405] With respect to CD8+ T cells this is felt to be due to accumulation of EMRA cells.[406]

Generally, there is an increase in the differentiation state of T cells with age. Hong et al (2004) demonstrated that elderly subjects (>65 years) had a decreased frequency of naïve and increased frequency of EM and EMRA CD8+ T cells compared to young (≤40 years). Interestingly, the frequency of CM cells was equivalent.[407] However, in these groups, the proportion of naïve CD8+ T cells was 9.5% in the elderly and 46.4% in the young, while EM CD8+ T cells was 28.2% in the elderly and 51.3% in the young, much different to the findings my groups. Understandably and predictably

there was a strong correlation between the proportions of naïve and EM CD8+ cells, with the implication being that there are homeostatic mechanisms in place to balance the total T cell pool.[407] Groups have hypothesised that an increase in EM cells with age is a compensatory mechanism for a decrease in naïve T cells. Another hypothesis is that prolonged or repeated exposure to antigen with age results in a loss of naïve cells, but this would be opposite to my findings in TAO patients. Certain cytokines such as IL-7 and IL-15 are known to influence T cell memory status. If one of these cytokines were affected in GD or TAO then that may result in skewing of T cell phenotype.[408]

4.7.4 IGF-1R Expression on T Cell Memory Subtypes

We have demonstrated no significant difference in IGF-1R expression on any of the peripheral blood CD4+ or CD8+ T cell memory subsets, as measured by flow cytometry, between GD+TAO+, GD+TAO- and HC. This data is in contradiction with that of Douglas et al (2007) who documented that T cells from peripheral blood and orbital tissue in patients with GD are skewed toward the CD3+IGF-1R+ phenotype, particularly in the CD45RO+ memory T cell population, with CD45RA+IGF-1R+ naïve T cells appearing similar between GD and controls.[240]

My data demonstrates generally low expression of IGF-1R on all T cell memory subsets, both CD4+ and CD8+, but with a higher expression on CD4+. In both CD4+ and CD8+ cells, this level of expression gradually reduces as T cells progress from naïve to CM and then to EM. These largely divergent findings may be as a result of my method of defining positivity of IGF-1R expression. Douglas et al (2007)

determined IGF-1R expression on the basis of the percentage of T cells that were IGF-1R+, whereas we examined IGF-1R expression by the comparison between MFI for IGF-1R and an isotype control. Douglas et al (2007) also noted a difference in IGF-1R expression between CD4+ memory and CD8+ memory cells. One may imagine that if serum IGF-1 levels were altered in GD or TAO, or if there were stimulating IGF-1R-Ab, then this could explain an up- or down-regulation of IGF-1R expression on immune cells. Certainly, serum IGF-1 levels have been found to be consistently elevated in hyperthyroid GD.[409] However, other studies have shown that serum levels of total and free IGF-1 and IGFBP are equivalent to controls in euthyroid GD, even with active TAO.[356]

Nearly all immunological cells express IGF-1R.[235] IGF-1R is expressed on monocytes, natural killer cells and CD4+ T cells, with lesser levels on CD8+ cells and the lowest level of expression on B cells. Somewhat in contrast, Stuart et al (1991) found that IGF-1R expression was highest on monocytes and B cells but with only low levels on T cells.[410] Intravenous administration of IGF-1 stimulates T cell development from thymocytes, with CD4-CD8- cells having 3-4 times more IGF-1R per cell compared with CD4-CD8+, CD4+CD8- and CD4+CD8+ cells.[223] Furthermore IGF-1R is involved in the transition of T cells from the G_0- to G_1-phase of the cell cycle. Indeed, T cells cannot enter S-phase of the cell cycle when IGF-1R expression is inhibited by anti-sense RNA.[411] IGF-1 has been shown to result in three-fold increase in T cell proliferation in a dose-dependent fashion, plateauing around 10 ng/ml, as measured by [^{3}H]TdR incorporation.[412] This effect was abrogated by the monoclonal IGF-1R antibody αIR3. IGF-1 also promotes B cell development in the bone marrow.[413]

Kooijman et al (1995) analysed the expression of IGF-1R on human peripheral T lymphocytes of differing activation and maturation status, in healthy individuals. In this study 87% of CD4+CD45RA+ and 66% of the CD8+CD45RA+ cells were IGF-1R+, while 37% of the CD4+CD45RO+ and 38% of the CD8+CD45RO+ cells were IGF-1R+, as defined by binding of αIR3. In addition, activated CD4+ and CD8+ T cells had lower levels of IGF-1R expression than non-activated T cells. From this it was postulated that the reduced IGF-1R positivity of activated T lymphocytes meant that T cell activation correlates with IGF-1R downregulation, or otherwise that the IGF-1R- cells were those which were preferentially activated.

This is in keeping with the observation that T cells internalise IGF-1R following activation with IGF-1,[262] but in contrast to findings of other groups who determined that IGF-1R, IGF-2R and insulin receptor are all expressed on PHA-activated T cells. This IGF-1R expression was noted to be greatest around the time of maximum T lymphocyte proliferation, but expression was maintained throughout an 8–11 day T cell culture.[236] If reduced IGF-1R positivity of activated T lymphocytes correlates with IGF-1R downregulation (or otherwise that IGF-1R- cells were those preferentially activated) this would be in keeping with recent studies that have suggested that IGF-1R-Ab in GD and TAO are inhibitory rather than stimulatory.[232]

Laurberg et al (2012) verified an increase in IGF-1R density on CD4+ cells in steroid- and disease modifying anti-rheumatic drug (DMARD)-naïve RA patients as compared to controls, irrespective of whether the RA patients were treated with combinations of methotrexate and cyclosporin or methotrexate and placebo. However, there was no

such difference in the proportions of IGF-1R+ cells.[371] As compared with controls, elevations in IGF-1R MFI have been noted in other pathologies such as Crohn's disease, in the bowel lamina propria and submucosa.[414] This, combined with the findings in RA and GD suggests that there is an increase in IGF-1R expression on T lymphocytes under inflammatory conditions. Against this assertion is the observation that the IGF-1R positivity did not change in patients with RA before and during immunosuppressive treatment.[371]

McCoy et al (2014) studied 8 patients with moderate-to-severe TAO treated with rituximab.[350] It was determined that TAO clinical indices improved for these individuals and that reduced IGF-1R+CD3+ and IGF-1R+CD4+ and IGF-1R+CD8+ T cells were noted 4-6 weeks after treatment. In two patients the levels of the IGF-1R+ T cells returned to pre-treatment levels after 16 weeks. From this, it was postulated that T cell IGF-1R expression may be a biomarker for the clinical response to rituximab in TAO, although it was uncertain whether this was because of increased turnover of IGF-1R+T cells or whether IGF-1R expression was reduced on T cells. In similar findings, Cohen et al (2005) demonstrated that CP-751,871 (another high-affinity IGF-1R monoclonal antibody) was able to inhibit IGF-1 ligand binding to IGF-1R and to down-regulate IGF-1R *in vitro* and *in vivo* in a human tumour xenograft model. CP-751,871 was also seen to induce down-regulation of IGF-1R on *ex vivo* human PBMC, including CD3+CD4+ and CD3+CD8+ T lymphocytes and CD19+ B lymphocytes from healthy volunteers.[212] Such down-regulation of cell surface receptors with antibody binding has been observed with other receptors such as HER2,[415] as well as IGF-1R.[416,417]

4.7.5 T Cell Activation Markers in GD and TAO

We found no difference in early and late T cell activation markers between the study groups. Expression of CD69 is associated with activation and proliferation of lymphocytes and has previously been shown to be present at sites of inflammation (e.g. rheumatoid joints).[418-420] Indeed, CD69 is among the earliest markers upregulated following T cell activation,[419] and is also rapidly down-regulated.[418] Likewise, CD25 (IL-2Rα) expression is up-regulated as a result of T cell activation, with a consequent increase in response to IL-2.[418] Douglas et al (2006) found the fraction of T cells expressing CD69 and CD25 in TAO patient peripheral blood (already rendered euthyroid by either radioiodine or surgical thyroidectomy) to be higher than controls, although there was no correlation between disease activity and the expression of these markers.[127] There was also no difference in HLA-DR expression by T cells in TAO subjects as compared with controls.[127]

Likewise, Gessl et al (1998) examined the expression of T cell activation markers HLA-DR and CD69 on naïve (CD45RA+) and memory (CD45RA-) CD4+ and CD8+ T cells in peripheral blood of those with untreated, hyperthyroid GD. Compared to healthy subjects, these GD patients did not have increased HLA-DR expression on memory CD4+ or CD8+ cells but did have increased HLA-DR on naive CD8+ T cells. In addition, those GD patients who had been rendered euthyroid on MMZ had greater HLA-DR expression on total and memory CD4+ and CD8+ T cells than those with hyperthyroid GD. However, proportions of total CD4+ and CD8+ cells expressing CD69 were increased in the hyperthyroid GD patients, but normalised following thyrostatic treatment. This group therefore suggested an association of HLA-DR with

ongoing autoimmunity and that CD69 expression may related to thyroid hormone concentration.[421]

CD154 (CD40 ligand) is expressed by activated T cells, and is known to interact with CD40 on B and T cells, having a particular role in B cell activation and differentiation, but also inhibiting T cell apoptosis. CD154 is thought to be increased in human autoimmune disease (e.g. SLE) and, in mouse models, anti-CD154 antibodies have been shown to inhibit thyroiditis, lupus nephritis and experimental allergic encephalomyelitis. Watanabe et al (2004) studied peripheral blood T cell expression of CD154 by subjects with GD and control subjects, finding that intensities of CD154 expression on CD4+ T cells from euthyroid GD subjects were reduced as compared with controls, although not varying between subjects with different GD severity. This group therefore hypothesised that a reduction in CD154 may result in a negative effect on T cell autoreactivity, promoting autoimmunity.[422]

Previous studies in RA have noted an increase in CD8+ terminally differentiated effector memory/central memory T cell ratio in RA patients compared with controls, correlating with disease duration. However, there was no difference in CD4+ or CD8+ T cell memory subsets between RA and controls. This group suggested that this represented the effect of persisting antigen-driven immune responses.[374]

4.7.6 Regulatory T Lymphocytes in TAO

We also determined no difference in the proportion of CD4+ T cells with a Treg phenotype ($CD25^{High}CD127^{Low}$) in GD+TAO+, GD+TAO- and HC groups, although

some may argue that this requires further validation with measurement of the proportion of FoxP3+ cells and also investigation into the actual regulatory functioning of these cells. Derangements in the balance between effector and regulatory T cells are a principal feature in autoimmune disease pathogenesis.[423] This is important in TAO as manifestations of this disease are felt to represent a balance between pro- and anti-inflammatory cytokines.[424]

Previous studies have established that Treg may contribute to the development of such diseases as type I DM, MS, RA and inflammatory bowel disease.[389,425,426] Treg have also been found to be reduced,[425,427] or unchanged,[428,429] in peripheral blood in MS patients as compared to HC. Two studies have analysed Treg in GD, with no difference being detected compared with HC in terms of Treg frequencies.[430,431] However, one of these studies found that there was a reduction in anti-inflammatory IL-10 production by GD Tregs as compared with HC.[431] Further to these two studies, Kahaly et al (2011) examined Treg in TAO and found that, although TAO and HC Treg (CD4+CD25+FoxP3+) frequencies were equivalent, both TAO and HC Treg frequency and activity was increased with rabbit polyclonal anti-T lymphocyte globulin, greater than those for GD Treg.[389]

4.7.7 IL-21 and T Follicular Helper Cells in GD and TAO

Given the previous literature regarding a possible role for IL-21 in AITD related to Alemtuzumab treatment of MS patients,[345] we evaluated PBMC for Tfh. Secretion of Il-21 has been proposed to be a major role of Tfh.[347] Tfh, as previously discussed, have been postulated to be a T helper subtype involved in the regulation of B cell

immunity, particularly in promoting migration to germinal centres through the chemokine receptor, CXCR5. In addition to CXCR5, other surface molecules such as ICOS (inducible costimulator) or PD-1 (programmed death-1) are felt to be involved in Tfh functioning. Indeed, in other studies evaluating SLE and systemic sclerosis patients, CD4+ T cells were defined as being Tfh on the basis of CXCR5 and ICOS positivity and CD4+CXCR5+ T cells did not correlate with autoantibody levels.[432]

Although not evaluating TAO patients, Zhu et al (2012) found higher percentages of CD4+CXCR5+ICOS^{High} T cells in patients with GD and Hashimoto's thyroiditis as compared to controls, but CD4+CXCR5+ T cells were equivalent in these groups.[433] Median percentages of CD4+CXCR5+ T cells are not directly presented in their data, but their figures suggest proportions of around 15-20% for each group, commensurate with my data. In this study, CD4+ cells from GD and HT patients expressed greater IL-21 when stimulated by PHA than control subjects. There was also a positive correlation between CD4+CXCR5+ICOS^{High} cells and serum autoantibodies (TRAb, TPO-Ab, TG-Ab). However, overall, there was no change in the proportion of CD4+CXCR5+ICOS^{High} T cells following treatment of GD with MMZ and PTU (for 6 months).[433] It may, therefore, be that the definition of Tfh as being CD4+CXCR5+ was insufficient. Certainly Zhu et al (2012) advocated use of ICOS or PD-1 in addition to CXCR5 as, for instance, Th17 cells may also express CXCR5.[434]

Furthermore, Jia et al (2011) found elevated serum levels of IL-21 in 40 GD patients, at significantly greater levels than 42 TAO patients and 24 HC, with IL-21 levels being 95.0 pg/mL in TAO patients and 87.2 pg/mL in HC.[435] Data for GD patients were not directly presented, but appeared to be around 120 pg/mL. Again, each of

these measurements is greater than that measured in this study. This group also found that IL-21 gene single nucleotide polymorphisms, rs907715 and rs13143866 are associated with GD and TAO, respectively, with the conclusion being that IL-21 is associated with GD and TAO.

4.8 Conclusion

In summary, skewing of memory T cell populations as seen in this study may represent dysregulated lymphocyte homeostasis, with preferential generation or survival of naïve T cells, increased sequestration of effector memory T cells in inflamed tissues or an effect of thionamide or immunosuppressant drugs. Further understanding of the mechanisms involved in this shift in T cell differentiation and memory phenotype may provide further information to elucidate the pathogenesis of TAO in patients with GD.[377]

5 METABOLOMIC ANALYSIS OF SERUM IN GRAVES' DISEASE AND THYROID-ASSOCIATED OPHTHALMOPATHY

5.1 Introduction

5.1.1 Current Challenges in the Diagnosis and Management of TAO

It has already been established that TAO is a heterogeneous condition encompassing a spectrum of manifestations, from mild to very severe, and may be of such significance to result in visual impairment and debilitating facial disfigurement.[1] This heterogeneity makes stratifying those GD patients at risk of developing TAO, and those TAO patients at risk of the most active and severe disease, exceptionally difficult. Early diagnosis remains important as the cosmetic and functional manifestations of TAO are irreversible, often requiring a range of surgical procedures for rehabilitation, in the form of combinations of orbital decompression, squint and eyelid surgery to return an individual to a functionally and aesthetically acceptable situation.

At present there are an array of difficulties in predicting TAO onset and eventual severity, for which the current tools of clinical activity and severity scoring advocated by EUGOGO are suboptimal. For instance, although it is said that 30-50% of patients with GD will go on to develop TAO, it is currently not possible to determine exactly which GD patients will be affected, nor which will be in the minority (3-5%) who develop severe, sight-threatening manifestations. If it were possible to differentiate these patients at an early, even pre-symptomatic, stage it may permit the targeting of more intensive medical and ophthalmic monitoring to those at greatest risk, as well as the focusing of specific interventions such as smoking cessation or early immunosuppression.

The diagnosis of TAO can itself be extremely challenging, particularly as GD has ocular manifestations (e.g. lid lag and lid retraction) that do not necessarily signify orbital inflammatory disease but are instead representative of thyrotoxicosis and consequent sympathetic nervous system overactivity. The ability to differentiate these patients on the basis of an objective measure would be extremely beneficial.

Finally, it is currently often difficult to discern if patients with TAO have persisting active, inflammatory disease or “burnt-out” disease with signs of venous congestion, as both are characterised by conjunctival injection and chemosis. This is important as it is crucial to identify the correct time to undertake rehabilitative surgery for TAO. In the absence of sight-threatening TAO, the usual strategy is to wait until the active phase of disease has ended before performing orbital decompression, squint or eyelid surgery. However, if this surgery is undertaken too early then a patient may go on to require further interventions or repeat procedures that should not have been necessary.

In light of the difficulties associated with correct classification of TAO, discriminatory biomarkers would be extremely useful. A biomarker is defined as a “characteristic that is objectively measured and evaluated as an indicator of normal biologic processes, pathogenic processes, or pharmacologic responses to a therapeutic intervention”.[436] As already described, previous studies have extensively investigated the epidemiology, inflammatory mechanisms, genetics and lifestyle risk factors of both GD and TAO in large cohorts of patients. The pathogenesis of TAO is complex, with interaction between a number of genetic polymorphisms (e.g. PTPN22, CTLA-

4),[89,437] candidate molecules (e.g. TSH-R, IGF-1R)[357] and patient-specific factors such as cigarette smoking.[29] These multiple influences mean that analysing the influence of a single putative biomarker that predicts TAO onset and prognosticates the course and severity of the ensuing orbital disease, while controlling for so many other variables, is extremely difficult.

5.1.2 Metabolomics: a role in GD and TAO diagnosis?

Metabolomics is the systematic analysis of the metabolite profile of a body fluid or tissue.[438] It is a powerful technique, capable of reproducibly identifying and quantifying multiple metabolites in a biofluid (e.g. serum, cerebrospinal fluid, urine). Metabolomics is based on the concept that the metabolic properties of tissues are altered by disease processes in such a way that distinct pathologies may be reflected in unique metabolite patterns - each condition having a unique metabolomic "fingerprint".[438]

Metabolites are the final downstream products of the interaction between genetic and environmental factors in disease development. Metabolomics therefore provides a 'snap-shot' of metabolic processes at a specific point in time, facilitating the integration of multiple interacting disease-modifying factors and generating a global overview of the summative effect of genetics and environment. This is of particular relevance in GD and TAO as a number of studies have previously demonstrated metabolic changes in these conditions, with increases in oxidative metabolites in plasma and tissues.[141] In addition, TAO orbital fibroblasts display an altered redox metabolite balance when cultured.[439] These specifically altered metabolites may in

turn reflect more widespread metabolic changes at the tissue, organ or system level. If this is the case, the investigation of the global metabolite fingerprint could provide a novel means of characterising these patients.

5.1.3 Role of Metabolomics in Autoimmune and Inflammatory Diseases

Metabolomics has previously been successfully applied in the diagnosis and classification of a number of medical conditions. For example, metabolomic analysis of bronchoalveolar (BAL) fluid has been shown to distinguish cystic fibrosis patients with higher versus lower levels of inflammation.[440] Analysis of serum in coronary heart disease was able to discriminate different degrees of coronary artery stenosis.[441] Metabolomic analysis of faecal extracts has been determined to differentiate patients with Crohn's disease from those with ulcerative colitis,[442] whilst analysis of plasma discriminates those with RA (of different degrees of disease activity) from healthy controls. Importantly, these differences resolve following treatment.[443] *Ex-vivo* metabolomic analysis of brain tumour biopsies has been shown to differentiate malignant from normal tissue, and urinary metabolite profiles can identify patients with renal cell carcinoma from controls.[444,445]

Metabolomic analysis of cerebrospinal fluid has also been undertaken in a number of neurological conditions. In MS, metabolomics had a sensitivity and specificity of 80% and 53%, respectively, for predicting diagnosis.[446] Similarly, in idiopathic intracranial hypertension, metabolomics had a sensitivity of 71% and specificity of 70%. Likewise, CSF from patients with bacterial or fungal meningitis could be separated from viral meningitis and healthy controls.[446,447] With reference specifically to ocular

disease, metabolomics has shown potential to distinguish different forms of inflammatory uveitis.[448] A distinctive metabolic profile for proliferative diabetic retinopathy has also been identified.[449] As yet, none of the published studies seems to have achieved a sensitivity or specificity suitable for diagnostic purposes, but each provide evidence that metabolomic analysis may support differential diagnosis or prognosis.

5.1.4 Metabolomic Techniques and the Principles of Nuclear Magnetic Resonance (NMR)

A range of techniques have been applied for metabolomic analysis. Most metabolomic studies make use of untargeted approaches where the resulting metabolite content is not presumed or predicted. These methods include gas or liquid chromatography, mass spectrometry and nuclear magnetic resonance (NMR). While these are each different approaches, the end target in all methods is identification and quantification of the tested sample. In contrast, targeted techniques such as chemometric assays or metabolite arrays, allow direct quantification of known metabolites in a given sample. These are often useful for confirming and validating the findings of untargeted methods.

This study was performed using NMR due to the availability of local facilities (Henry Wellcome Building for NMR, University of Birmingham) and relative simplicity of sample preparation. NMR functions on the principle that atomic nuclei have spin properties, aligning themselves if placed in a magnetic field. If these aligned nuclei are provided with a radiofrequency pulse they absorb energy and resonate. Each of

the nuclei will resonate at a different frequency, based on their atomic mass and structure (**Figure 5.1**). The resulting frequency spectra reflect the functional groups of the original molecule and can therefore be used to identify the constituent metabolites in a sample, while peak heights reflect concentration.

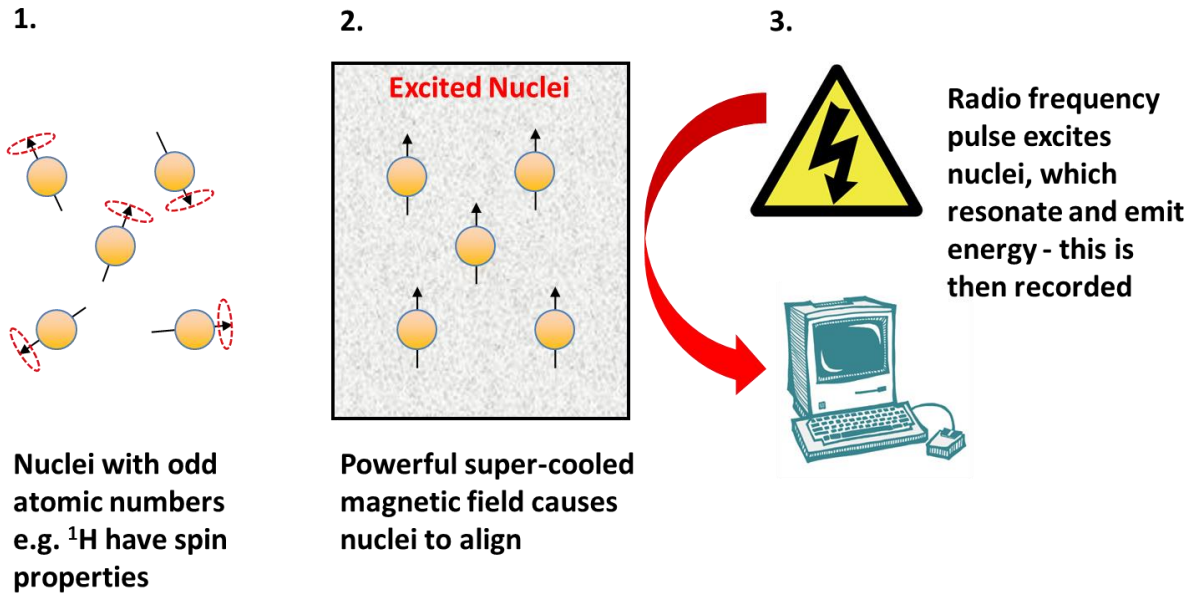

Figure 5.1: Schematic diagram of the principles of ^{1}H-nuclear magnetic resonance (^{1}H-NMR) spectroscopy.

5.2 Aims and Objectives

Metabolomics has not previously been utilised in GD or TAO, but would appear to be a potentially useful approach given the complex interaction between intrinsic and extrinsic factors in these diseases. In this chapter we assessed the value of ^{1}H-NMR-based metabolomic profiling as a novel means of differentiating a large cohort of GD+TAO+, GD+TAO- and age- and sex-matched HC, examining exactly which metabolites are altered in each situation and their relative sensitivity and specificity for establishing accurate diagnoses alongside established clinical criteria.

Furthermore, we aimed to correlate metabolomic profiles according to disease duration, clinical activity, thyroid hormone and autoantibody status and cigarette smoking status.

In this study we hypothesise that (1) there is a characteristic metabolomic pattern in GD+TAO+ serum that differentiates them from GD+TAO- and HC subjects and (2) metabolite patterns distinguish TAO patients of different clinical activity and severity.

5.3 Methods

5.3.1 ^{1}H-NMR Spectroscopy

After thawing, serum samples (1 ml) were centrifuged at 15,000 g for 5 minutes. 200 µl of serum was removed from each sample and passed through a 3 kDa filter (Pall Nanosep, VWR, Lutterworth) which had previously been washed six times with warmed, distilled water. The serum filtrate was buffered with phosphate buffer (100 mM) and brought to concentrations of 10% D_2O (deuterium oxide) and 0.5 mM TMSP (trimethylsilyl-2,2,3,3-tetradeuteropropionic acid) internal standard. Each sample was then centrifuged and loaded into a standard 1.7 mm NMR tube (Bruker Rheinstetten, Germany) for spectroscopy.

One-dimensional (1D) 1H-NMR spectra were acquired at 300 °K using a standard spin-echo pulse sequence, with excitation sculpting (a method of removing signal derived from water without losing signal from other metabolites associated with water protons) to suppress any residual water, on a DRX 600 MHz NMR spectrometer

(Bruker BioSpin, Rheinstetten, Germany) with a cryoprobe. Two-dimensional (2D) J-Resolved (JRES) NMR spectra were obtained as previously described.[450] Samples were processed and data calibrated with respect to the TMSP signal. Spectra were read into Prometab (version 2) software within MatLab (version 7.0, MathWorks, Cambridge, UK) and truncated to a range of 0.2–10.0 parts per million. Spectra were segmented into 0.005 ppm (2.5 Hz) chemical shift "bins," and the spectral areas within each bin were integrated. Spectra were corrected for baseline offset, normalised to a total spectral area of unity and a generalised log (glog) transformation applied to increase weighting of smaller peaks. A data matrix was compiled, with rows representing single samples and chemical shifts in columns.

5.3.2 Statistical Analysis of Metabolomic Data

NMR spectra were excluded from analysis if they displayed poor data quality, such as distorted baselines or unusually broad peak widths. However, outlying metabolite profiles with satisfactory spectra were assumed to be due to biological variation or disease diversity and were therefore maintained in the analysis.

Data bins from groups of spectra were mean-centered and assessed using principal component analysis (PCA) and partial least-squares discriminant analysis (PLS-DA) using PLS_Toolbox (version 3.5, Eigenvector, Washington, USA). PLS-DA is a supervised analysis technique which builds a model to evaluate separation between groups based on known factors. The PLS-DA model was cross-validated using Venetian blinds, a method which re-assigns randomly selected blocks of data to the PLS-DA model to determine accuracy of the model in correctly assigning class

membership. Identification of relevant metabolite peaks in the spectra, that permitted discrimination of groups of interest, was carried out using Chenomx NMR Suite (version 4.0, Chenomx, Alberta, Canada), an NMR analysis program which provides a library of a range of metabolites which may be found in biofluids, in conjunction with the Human Metabolome Database (www.hmdb.ca/). The peak heights of metabolites of interest were compared in the study groups using Mann-Whitney test (for two groups) and Kruskal-Wallis test (with Dunn's post-test) (for more than two groups).

5.3.3 Multivariate Analysis by Genetic Algorithm

GALGO, a genetic algorithm available in the statistical environment R, was also applied to the data as a method of multivariate variable selection. GALGO combines genetic algorithm-driven multidimensional searches and statistical classification methods to find combinations of variables that can distinguish between sample classes using a nearest centroid classification approach.

The results of GALGO analyses are presented as PCA plots, where the x- and y-axes represent first and second principal components providing the greatest variation between samples and the next largest unrelated variation, respectively. GALGO analysis was cross-validated using K-fold cross-validation, where the original sample is randomly partitioned into subsamples and each observation is used for both training and validation.

All metabolomic processing and analysis was undertaken in conjunction with Dr. Stephen Young and Mr. Martin Fitzpatrick of the Rheumatology Research Group,

Centre for Translational Inflammation Research, School of Immunity and Infection, University of Birmingham Medical School.

5.4 Results

5.4.1 Study Subjects

The subject sera used in this study are the same as those used in the IGF-1R-Ab immunoassay studies of **Chapter 3**. Of 110 GD+TAO+ subjects, 20 were determined to be clinically active (CAS ≥3) and 90 inactive (CAS <3). Sixty-seven GD+TAO- subjects and 78 age- and sex-matched HC were also recruited. There were no statistically significant differences in median age, ratio of males to females or the percentage of smokers between the three groups (see **Table 3.1**).

5.4.2 Differentiation of Study Subjects by Metabolomic Profiles

No definite differentiation was obtained on any of the unsupervised, PCA analyses. PLS-DA demonstrated good separation of GD (combined GD+TAO+ and GD+TAO-) subjects from HC individuals along latent variable 1 (LV1) (**Figure 5.2 A**), with the discrimating metabolite peaks on a weightings plot being those for isopropanol (1.17 and 4.03), higher in GD subjects (**Figure 5.2 B**). Furthermore, it was possible to separate the two groups of GD patients on PLS-DA, those with and without TAO, on a PLS-DA plot (**Figure 5.3 A**), again on the basis of two isopropanol peaks (1.17 and 4.03) as well as a lactate peak (1.34) (**Figure 5.3 B**). In this case, these peaks were positive in the GD+TAO+ group as compared with GD+TAO-. Taking this further,

GD+TAO+ subjects could be discriminated with PLS-DA on the basis of their metabolomic profile into those with active (CAS≥3) and inactive (CAS<3) TAO (**Figure 5.4 A**). There were a range of metabolite peaks principally contributing to this, with positive peaks toward the active TAO group for lactate (1.33) and pyruvate (2.38) alongside reduced peaks toward the inactive TAO group for isopropanol (1.17 and 4.02) and methylguanidine (2.83) in the active TAO group (**Figure 5.4 B**).

The means by which these differentiating peaks (in **Figure 5.4 B**) were identified from comparison of the metabolomic spectra and use of Chenomx NMR Suite and the Human Metabolome Database is illustrated (**Figure 5.5 A-D**). Interestingly, PLS-DA analyses were also able to separate GD (GD+TAO+ and GD+TAO- combined) patients on the basis of their positive of negative TRAb status (**Figure 5.6 A & B**), their thyroid status (hyper-, hypo- or euthyroidism) (**Figure 5.7 A & B**) and PTPN22 (R620W) genotype (**Figure 5.8 A & B**). In each case, the peaks distinguishing between groups were a combination of lactate, ethanol and isopropanol.

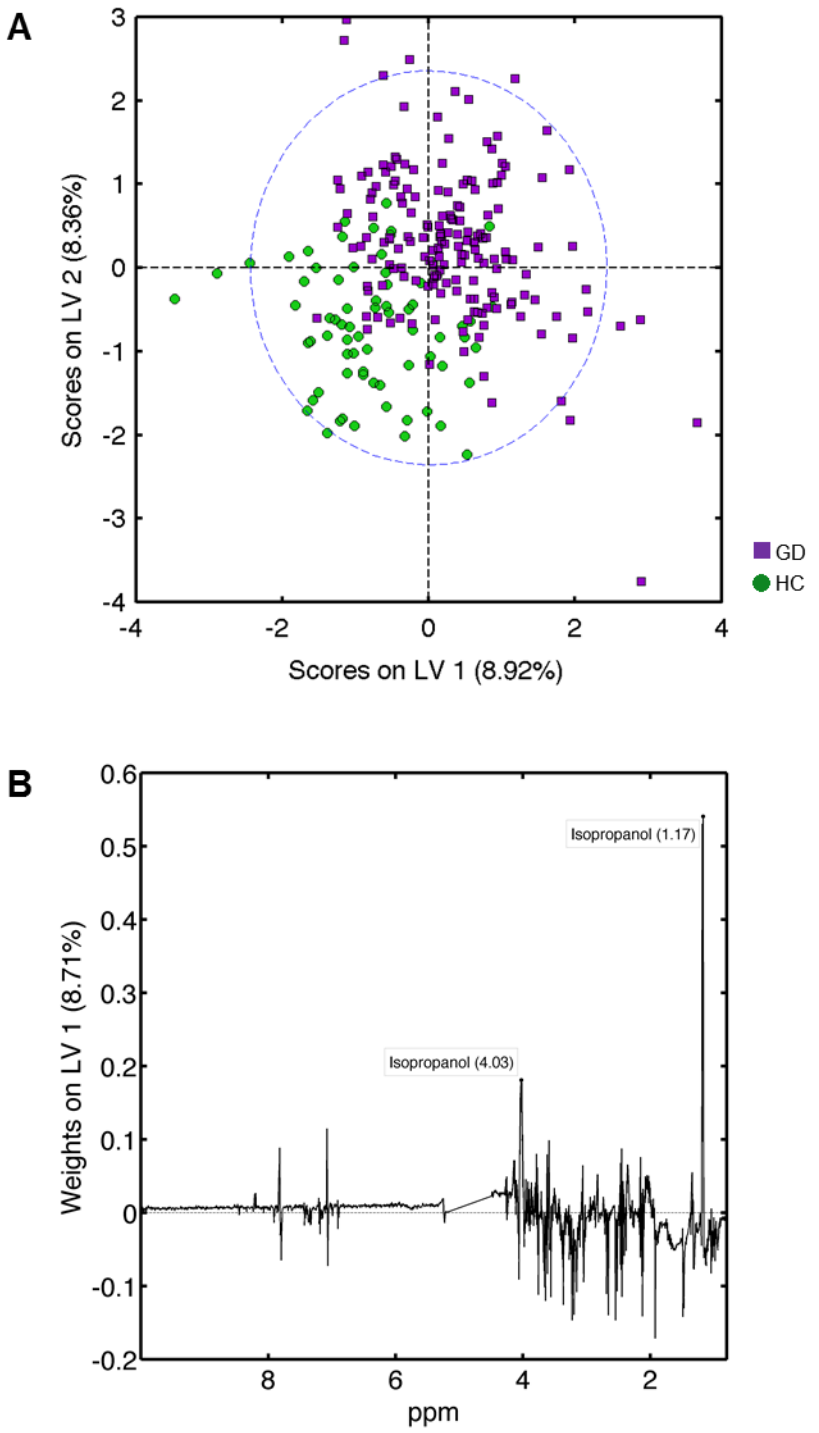

Figure 5.2: Partial least squares discriminant analysis (PLS-DA) of serum NMR spectra from GD and HC subjects. PLS-DA model on 2 latent variables (LV) constructed to determine if GD (combined GD+TAO+ and GD+TAO-) and HC groups could be separated on the basis of their metabolomic spectra (A); a weightings plot permitted assessment of the contribution of specific metabolites to the discrimination between GD and HC subjects. The metabolites which provide the greatest degree of discrimination between GD and HC are indicated. Positive peaks correspond to metabolites at higher concentration in GD relative to HC, and vice versa for the negative peaks (B).

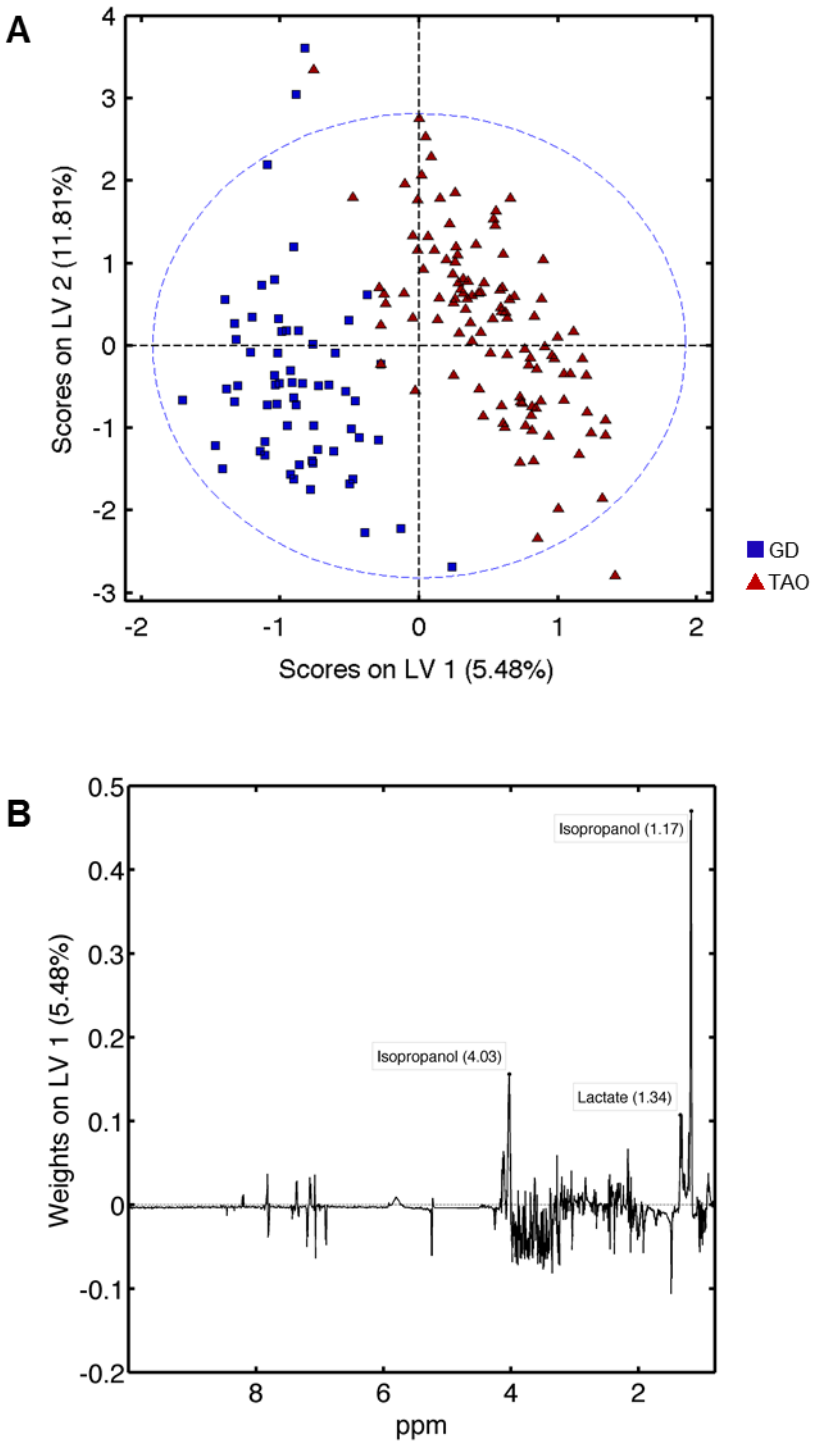

Figure 5.3: Partial least squares discriminant analysis (PLS-DA) of serum NMR spectra from GD and TAO subjects. PLS-DA model on 2 latent variables (LV) constructed to determine if GD (GD+TAO-) and TAO (GD+TAO+) groups could be separated on the basis of their metabolomic spectra (A); a weightings plot permitted assessment of the contribution of specific metabolites to the discrimination between GD and TAO subjects. The metabolites which provide the greatest degree of discrimination between GD and TAO are indicated. Positive peaks correspond to metabolites at higher concentration in TAO relative to GD, and vice versa for the negative peaks (B).

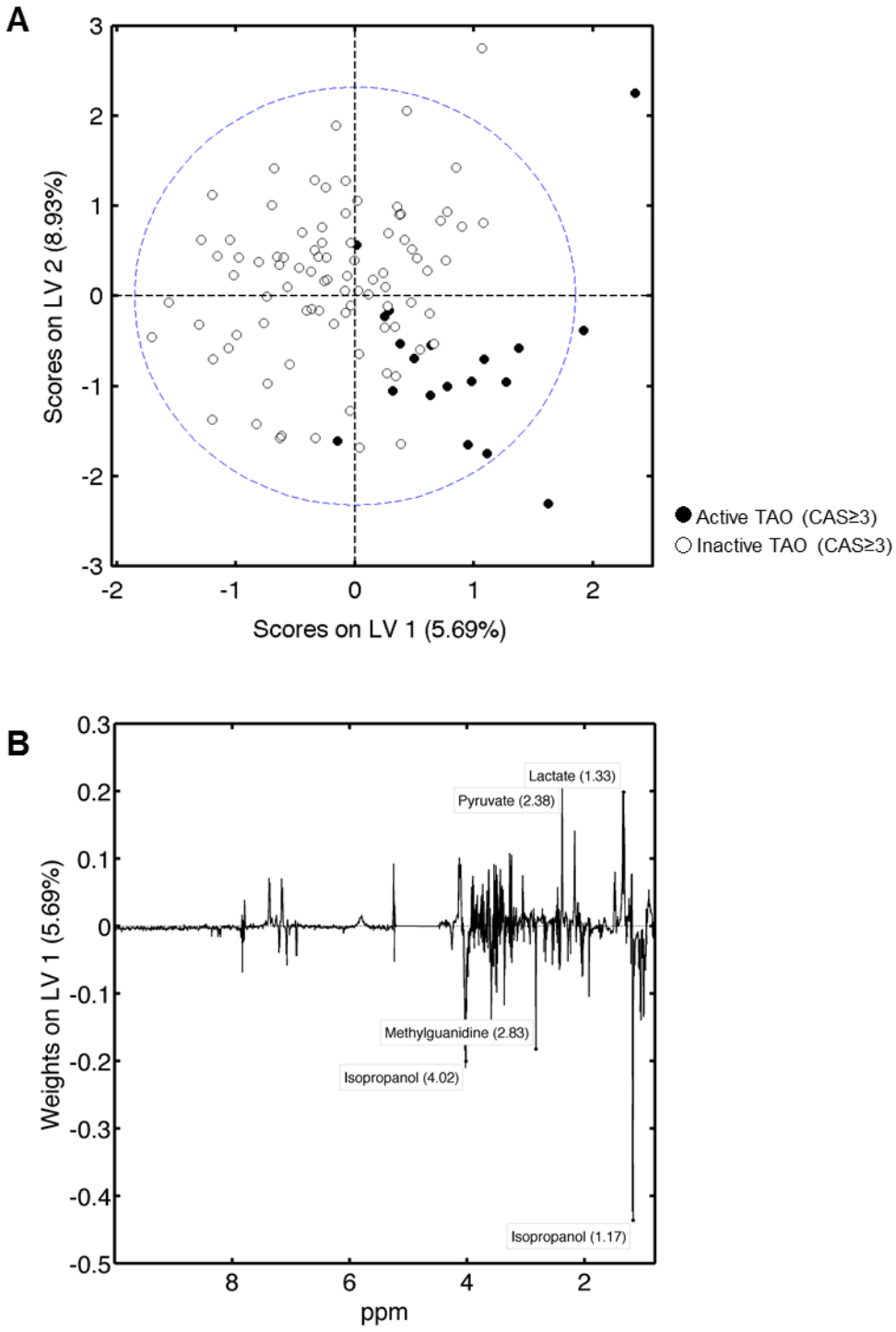

Figure 5.4: Partial least squares discriminant analysis (PLS-DA) of serum NMR spectra from active and inactive TAO subjects. PLS-DA model on 2 latent variables (LV) constructed to determine if active GD+TAO+ and inactive GD+TAO+ groups could be separated on the basis of their metabolomic spectra (A); a weightings plot permitted assessment of the contribution of specific metabolites to the discrimination between active and inactive TAO subjects. The metabolites which provide the greatest degree of discrimination between the two groups are indicated. Positive peaks correspond to metabolites at higher concentration in active TAO relative to inactive TAO, and vice versa for the negative peaks (B).

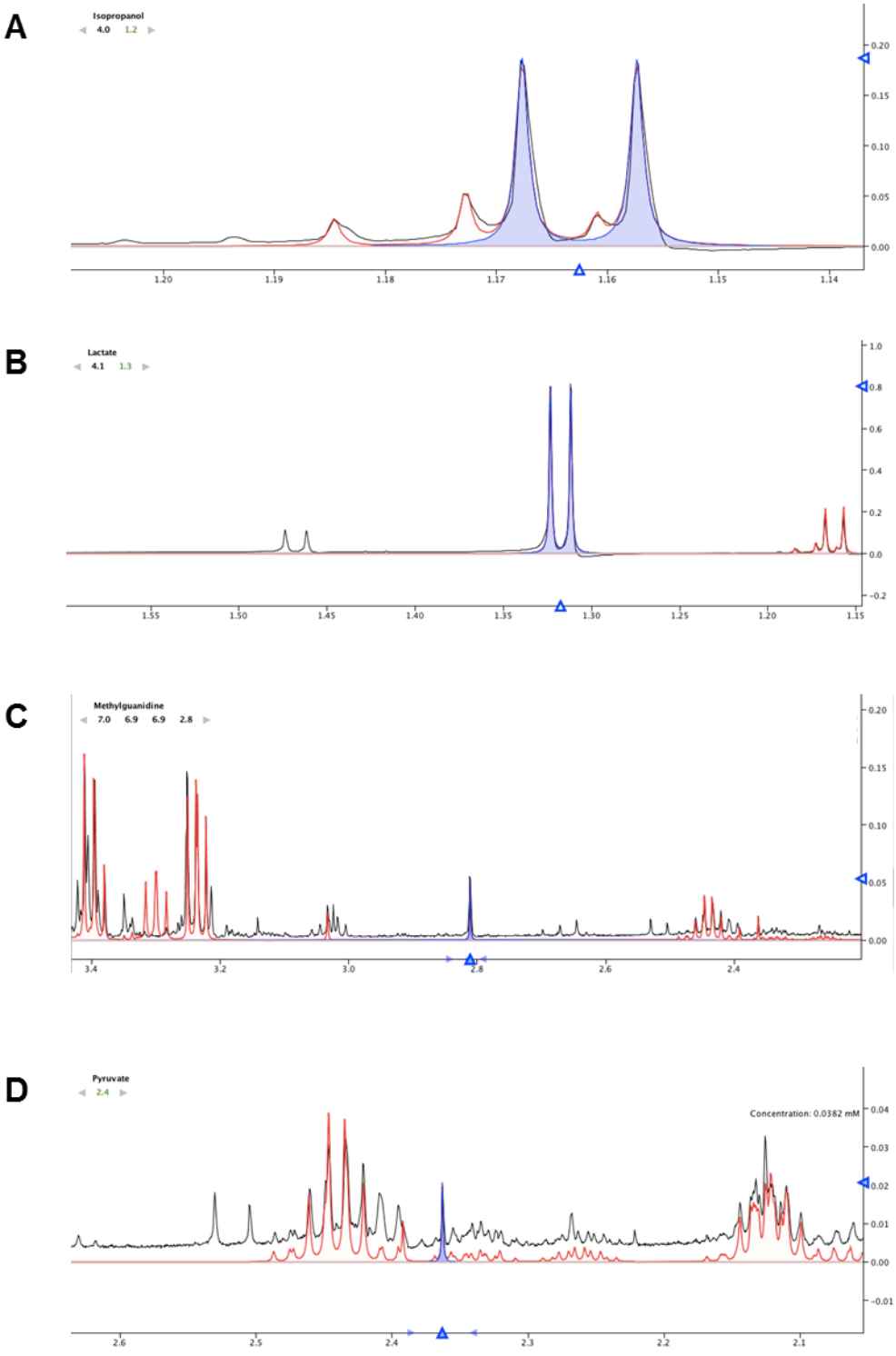

Figure 5.5: Identification of relevant metabolite peaks contributing to active or inactive TAO using Chenomx NMR suite in combination with the Human Metabolome Database. Relevant peaks noted from weightings plot of **Figure 5.4 B** analysed and determined to be isopropanol (A), lactate (B), methylguanidine (C) and pyruvate (D). Black lines determine the metabolomic spectra of the group of interest, blue peaks those identifying particular metabolites within Chenomx NMR suite and red peaks other metabolites permitting localisation of metabolites of interest within the spectra.

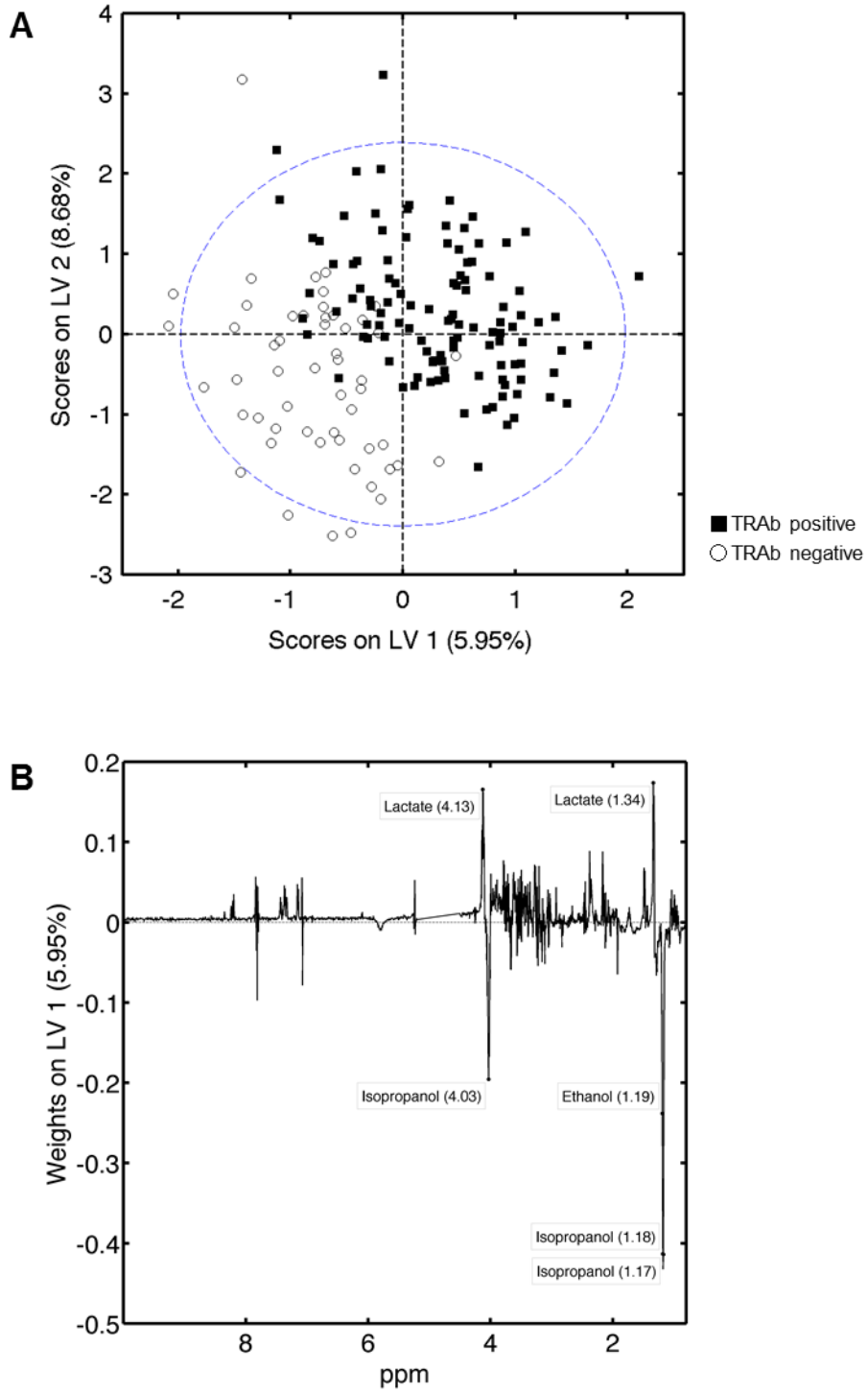

Figure 5.6: Partial least squares discriminant analysis (PLS-DA) of serum NMR spectra from GD patients based on their TRAb status. PLS-DA model on 2 latent variables (LV) constructed to determine if GD (combination of GD+TAO+ and GD+TAO-) subjects could be separated on the basis of their metabolomic spectra (A); a weightings plot permitted assessment of the contribution of specific metabolites to the discrimination between the different TRAb status. The metabolites which provide the greatest degree of discrimination between the three groups are indicated. Positive peaks correspond to metabolites at higher concentration in TRAb+ relative to TRAb-, and vice versa for the negative peaks (B).

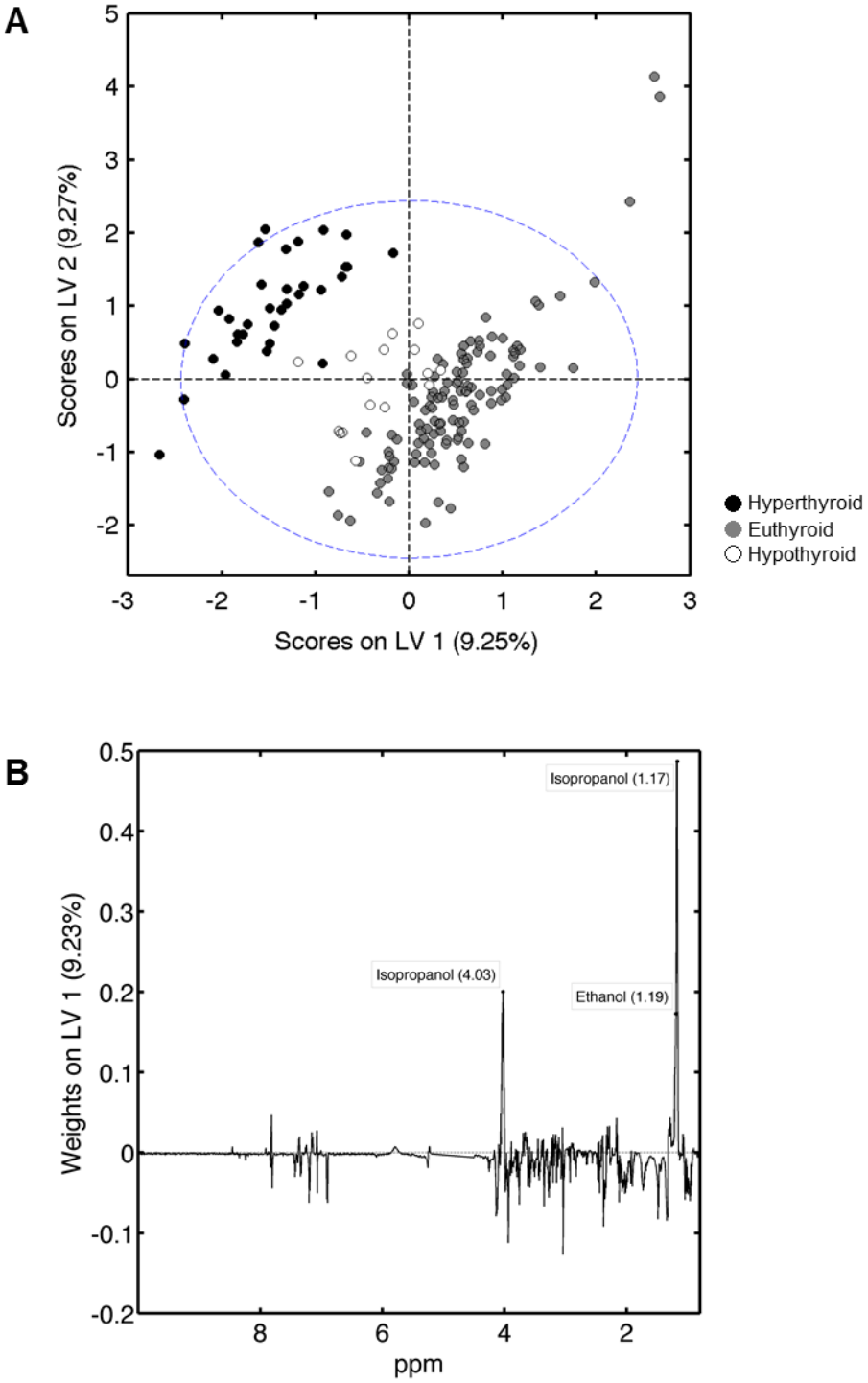

Figure 5.7: Partial least squares discriminant analysis (PLS-DA) of serum NMR spectra from GD patients based on their thyroid function. PLS-DA model on 2 latent variables (LV) constructed to determine if GD (combination of GD+TAO+ and GD+TAO-) subjects could be separated on the basis of their thyroid function (hypo-, hyper- or euthyroid) by their metabolomic spectra (A); a weightings plot permitted assessment of the contribution of specific metabolites to the discrimination between the different thyroid functions. The metabolites which provide the greatest degree of discrimination between the three groups are indicated. Positive peaks correspond to metabolites at higher concentration in euthyroid and hypothyroid relative to hyperthyroid, and vice versa for the negative peaks (B).

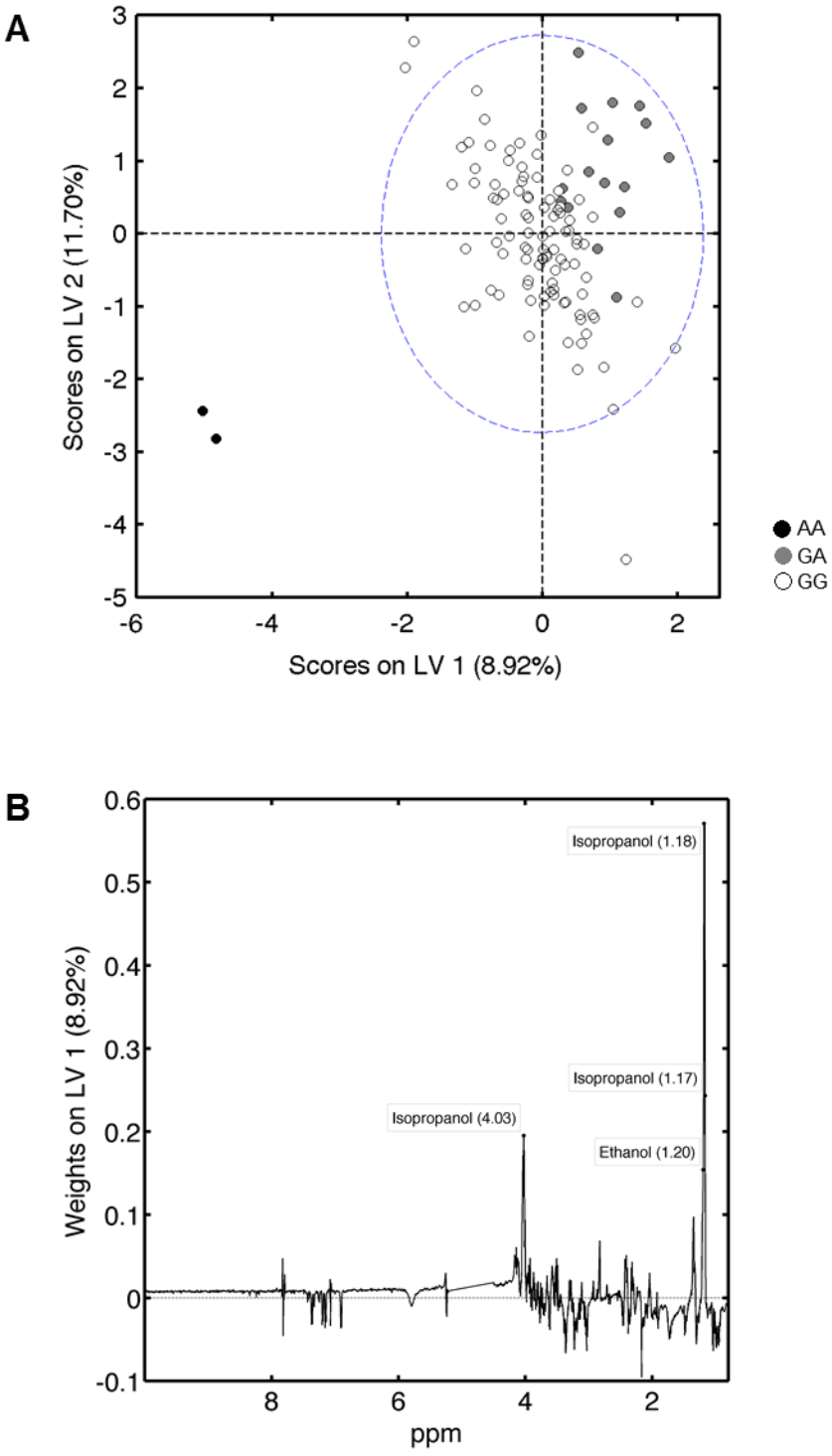

Figure 5.8: Partial least squares discriminant analysis (PLS-DA) of serum NMR spectra from GD patients based on their PTPN22 (R620W) genotype. PLS-DA model on 2 latent variables (LV) constructed to determine if GD (combination of GD+TAO+ and GD+TAO-) subjects could be separated on the basis of their metabolomic spectra (A); a weightings plot permitted assessment of the contribution of specific metabolites to the discrimination between the different PTPN22 (R620W) genotypes. The metabolites which provide the greatest degree of discrimination between the three groups are indicated. Positive peaks correspond to metabolites at higher concentration in those to the right of the axis, LV1, and vice versa for the negative peaks. (B)

5.4.3 Sensitivity and specificity of analysis models for discriminating groups

The sensitivity and specificity of the PLS-DA models for differentiating the groups of interest, as well as their sensitivity and specificity as cross-validated by Venetian blinds (explained in **Section 5.3.2**), are displayed in **Table 5.2**.

Table 5.2: Uncorrected and cross-validated sensitivities and specificities for each of the PLS-DA analyses undertaken in GD+TAO+, GD+TAO- and HC and demonstrated in **Figures 5.2 – 5.8**.

Groups Analysed	Sensitivity	Specificity	Sensitivity (CV)	Specificity (CV)
GD HC	78%	85%	47%	66%
GD TAO	97%	96%	63%	64%
Active TAO Inactive TAO	85%	85%	73%	30%
TRAb+GD TRAb- GD	91%	92%	51%	62%
Hypothyroid Euthyroid Hyperthyroid	99%	94%	66%	63%
PTPN22 GG GA AA	91%	89%	38%	19%

5.4.4 Comparison of metabolites discriminating groups of interest

On assessing the spectral peak areas on weightings plots (proportional to metabolite concentration) of the primary metabolites responsible for differentiation of groups of interest in univariate analysis, it was determined that, overall, only isopropanol (1.17) was significantly elevated in GD+TAO+ subjects, as compared with GD+TAO- and HC groups overall (**Figure 5.9**). However, on analysis of active (CAS≥3) and inactive (CAS<3) TAO subjects only pyruvate (2.38) was found to be significantly elevated in the active group (**Figure 5.10**).

GALGO analysis determined that many of the same peaks were of importance in multivariable analysis as those that were identified from PLS-DA models. In particular, lactate (1.34 and 1.35) and isopropanol (4.06) were peaks that were common between PLS-DA and GALGO (**Figure 5.11**)

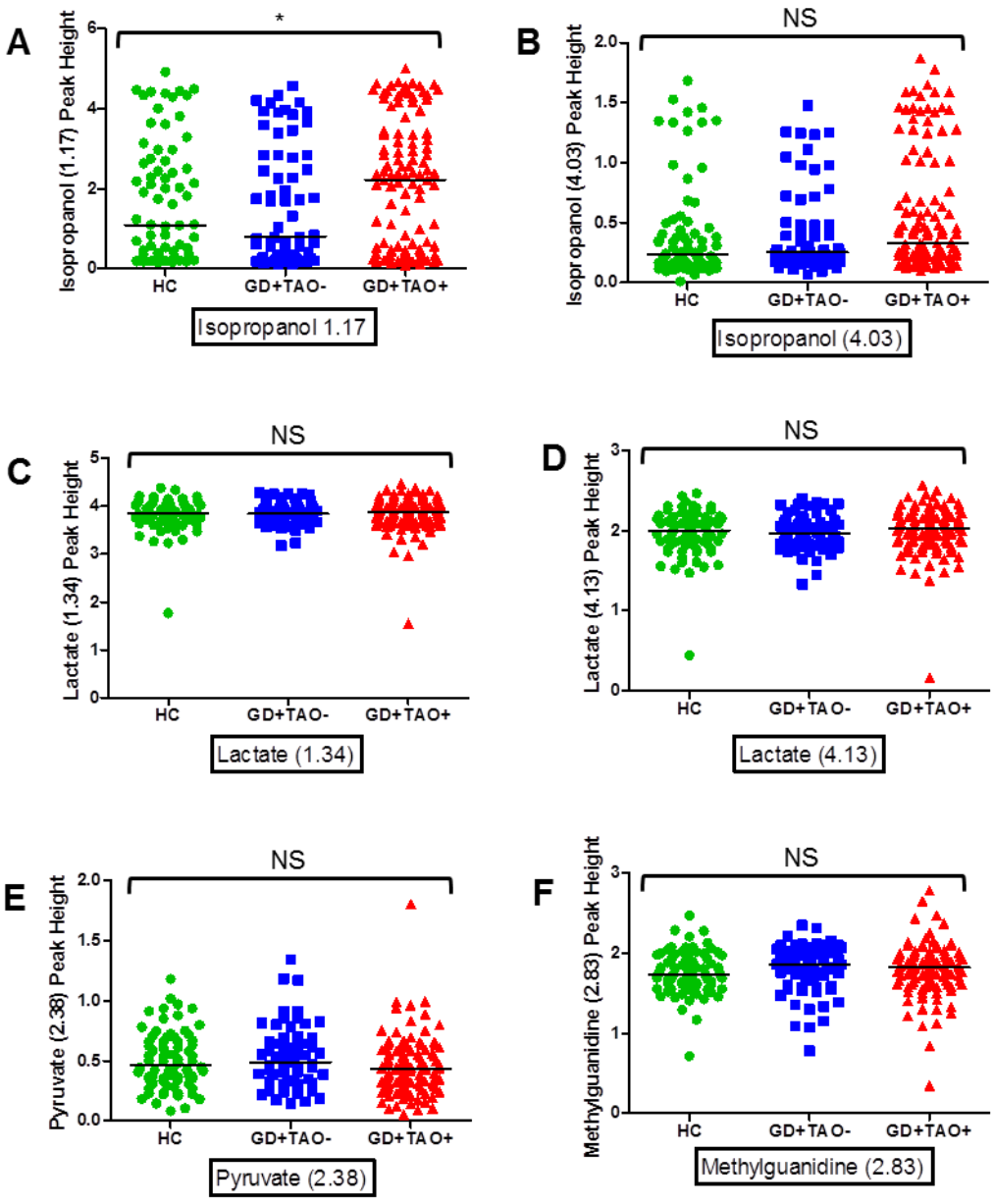

Figure 5.9: Concentration of discriminating metabolites identified from PLS-DA models in GD+TAO+, GD+TAO- and HC groups. Peak heights (proportional to the concentration of each metabolite) for the principal metabolites determined to differentiate groups of interest from PLS-DA weightings plots. Metabolites shown, (A) Isopropanol (1.17), (B) Isopropanol (4.03), (C) Lactate (1.34), (D) Lactate (4.13), (E) Pyruvate (2.38) and (F) Methylguanidine (2.83). Analysis of Isopropanol (1.17) between GD+TAO+ and GD+TAO- also demonstrated significant elevation in GD+TAO+ (P=0.03, data not shown) Non-parametric analysis was undertaken with Mann-Whitney test (for two groups) or Kruskal-Wallis test (with Dunn's multiple comparison) (more than two groups). (Key: NS: Not significant; *p=0.01 to 0.05).

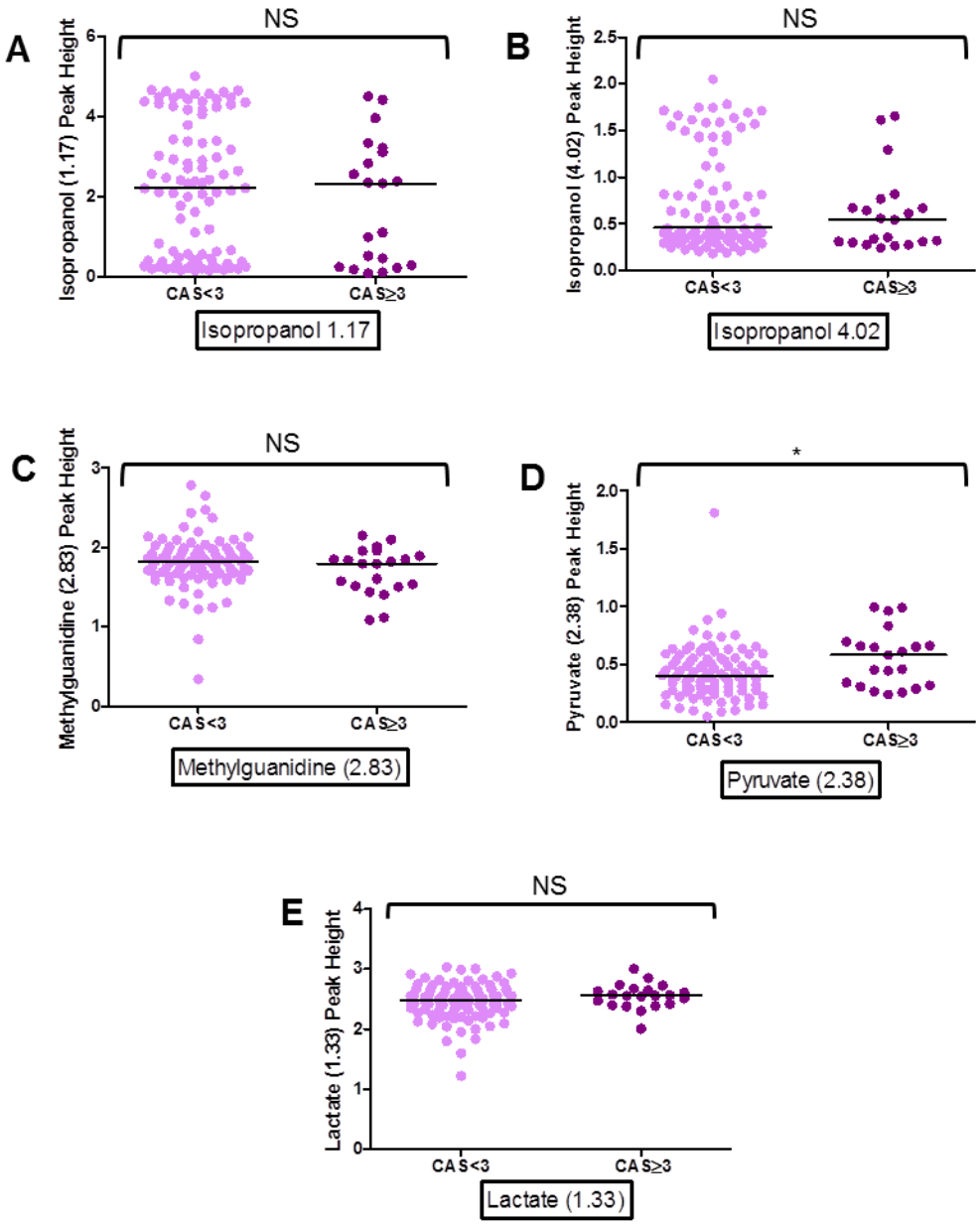

Figure 5.10: Concentration of discriminating metabolites identified from PLS-DA models in active and inactive TAO. Peak heights (proportional to the concentration of each metabolite) for the principal metabolites determined to separate active (CAS≥3) and inactive (CAS<3) TAO subjects from PLS-DA weightings plots. Metabolites shown, (A) Isopropanol (1.17), (B) Isopropanol (4.02), (C) Methylguanidine (2.83), (D) Pyruvate (2.38) and (E) Lactate (1.33) Non-parametric analysis was undertaken with Mann-Whitney U test. (Key: NS: Not significant; *p=0.01 to 0.05).

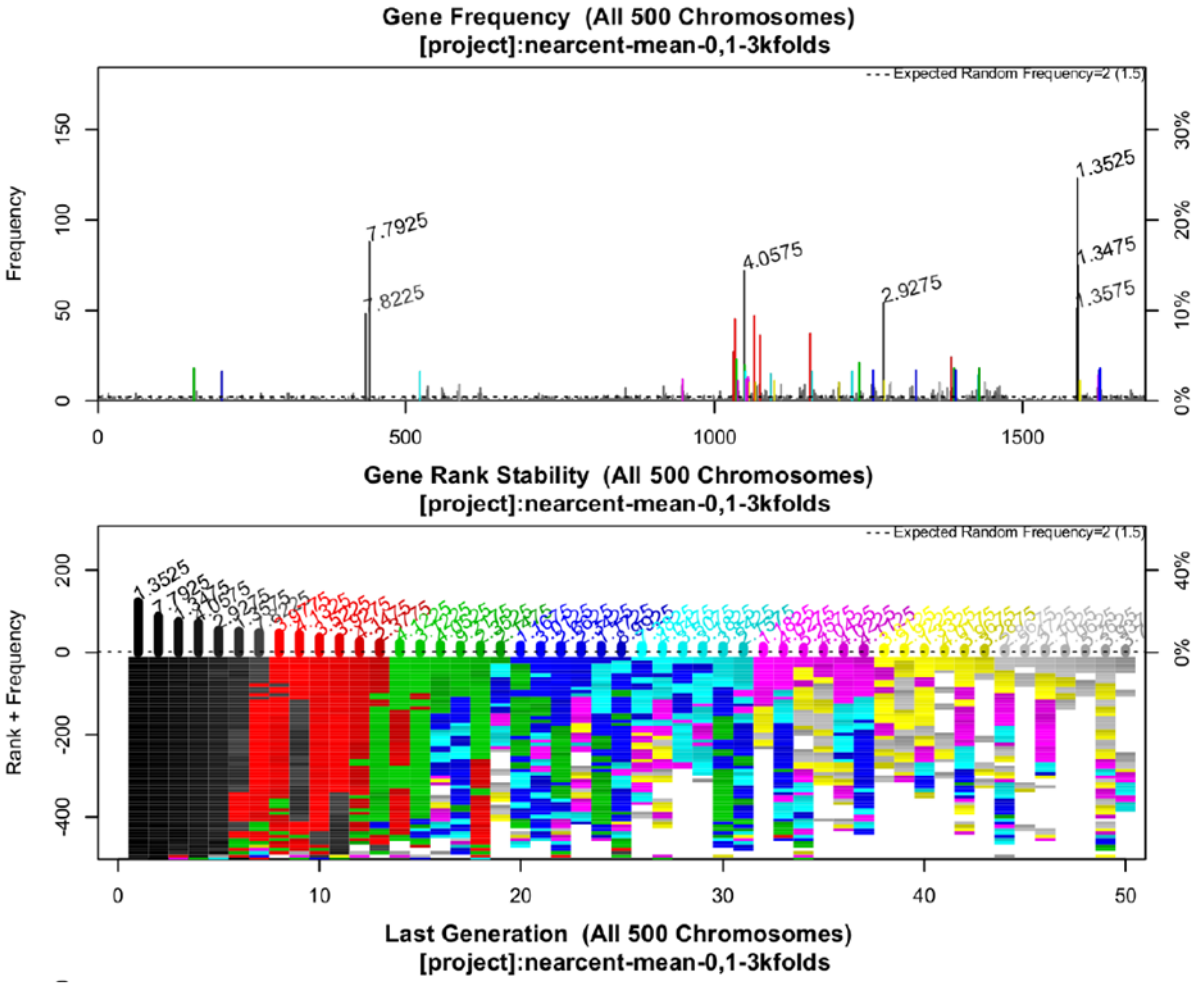

Figure 5.11: Multivariable selection of NMR spectra of serum from GD+TAO+, GD+TAO- and HC with GALGO. Analysis of the study groups following selection of NMR spectral bins which best discriminated between the conditions. 500 solutions were found in 500 search cycles matched with the corresponding spectra, with forward selection procedure using the 157 most frequent bins.

5.5 Discussion

This is the first study to evaluate the use of metabolomics in GD and TAO. In this large cohort of GD+TAO- and GD+TAO+ subjects, alongside age- and sex-matched HC, we demonstrate the potential of metabolomics to differentiate GD+TAO- and GD+TAO+ patients and also GD+TAO+ patients of differing levels of clinical activity. In addition, GD subjects could be separated on the basis of their thyroid autoantibody status, thyroid function and PTPN22 (R620W) genotype.

5.5.1 Metabolites identified as putative biomarkers in GD and TAO

The range of metabolites principally found to be responsible on PLS-DA analysis were not extensive. Although cross-validated sensitivities and specificities for the separation of groups were generally poor as compared with some other studies in the literature, the concentrations of two of the differentiating metabolites identified from the PLS-DA models, namely isopropanol (1.17) and pyruvate (2.38), were found to be significantly elevated in GD+TAO+ (as compared with GD+TAO- and HC) and active GD+TAO (as compared with inactive GD+TAO+) subjects, respectively. It is acknowledged that substantial validation is still required, particularly with separate patient cohorts. However, this study highlights a possible future role for these metabolites as biomarkers in GD and TAO.

Biomarkers have the potential to facilitate diagnosis, predict prognosis, monitor disease progression and impart information on disease causality, matters that are crucial for clinicians caring for those with GD and TAO. Importantly, a clinically useful

biomarker must be minimally invasive, cheap, sensitive, reproducible and rapid. Each of these pre-requisites are met by ^{1}H-NMR spectroscopy as it is an automated, high-throughput technique with each metabolite spectrum acquired within half an hour. The technique is also reproducible, and sensitive to the nanogram range.[451] NMR requires only small sample volumes and is non-destructive, meaning that samples can be reprocessed. The technique can also be quantitative if, as in the case of this study, a reference sample is used. As human metabolome databases become more complete this technology may be translated into clinical tests in an even wider range of conditions, including GD and TAO.

There are, however, a number of potential challenges associated with ^{1}H-NMR. For example, spectral peak congestion may occur when the resonances of multiple metabolites overlap. This may mean that low concentration metabolites are obscured if they coincide with more prominent metabolites. This may impede metabolite recognition, limit accuracy of metabolite identification and impair pattern recognition multivariate analyses. For example, the isopropanol peaks identified as permitting differentiation in my analyses are very close in the metabolomic spectrum to those for 3-hydroxybutyrate. It is also critical that sample collection and storage is consistent in order to minimise degradation of metabolites. Lenz et al (2003) investigated whether there may be day-to-day variation in metabolomic profiles due to lifestyle and dietary differences. Reassuringly, the blood and urine spectra of healthy controls showed little variability on different study days.[452] Likewise, variability of 163 serum metabolites in 100 healthy individuals over a four-month period demonstrated good reproducibility, suggesting that for the majority of metabolites a single measurement may be sufficient, at least for healthy subjects.[453]

5.5.2 Isopropanol

Isopropanol (isopropyl alcohol; 2-propanol; C_3H_7OH) is a constituent of normal serum, with typical mean concentration of 83.3 ± 132.8 µM as determined by NMR.[454] The uppermost limit of isopropanol in my studies was 300 µM. The Human Metabolome Database states that small amounts of isopropanol are produced by human gut bacteria. This may be significant given that large studies, such as INDIGO (Investigation of Novel biomarkers and Definition of the role of the microbiome In Graves' Orbitopathy), are being undertaken to investigate changes in the gut microbiota in patients with GD and TAO. No specific published literature could be found to corroborate the statement about isopropanol production in the gut made by the Human Metabolome Database, but a number of studies have examined the role of other volatile organic compounds (VOC), carbon-based chemicals that may be emitted from faeces and breath and may also be detected in blood, as biomarkers in a range of diseases. Unfortunately, the analysis of these metabolites is difficult due to their abundance and complexity. However other VOC, such as hexanal, 1-octen-3-ol and octane have been presented as possible biomarkers of liver cancer and 3-methylbutanal is elevated in chronic hepatic encephalopathy.[455]

Isopropanol is best known as a solvent, tissue preservative and disinfectant. In particular it is a primary constituent of sanitising alcohol hand gel and alcohol wipes used in the pre-preparation of skin prior to venepuncture for peripheral blood. This is obviously of concern as the biofluid used for analysis in this study was serum derived from peripheral blood. Initially, this raised the possibility of the isopropanol simply being a contaminant in samples.

Denery et al (2011) undertook a study of differing blood-taking methods prior to the use of such samples in metabolomics analysis. This group highlighted that future large-scale metabolomics analysis may be carried out on biofluids, particularly blood, which have been 'banked' and for which there is inadequate knowledge of collection and storage protocols.[456] In their study blood was taken either through capillary puncture with a sterile lancet, or formal venepuncture. However, in each case a 70% isopropyl alcohol wipe was used to clean the area prior to sampling, and allowed to air-dry. In addition, the first spot of blood released following lancet puncture was wiped away with clean gauze.

Reassuringly, analysis with liquid chromatography-mass spectrometry determined only slight differences between the various preparation methods. Despite this, 23 significant differences were noted in metabolite compounds between samples collected either by capillary or venous routes from the same subjects, with the majority being ascribed to the materials used to pre-treat the skin. Obviously, the concerning factor was that some of these differences were in molecules of identical mass and molecular formula to human metabolites, meaning that they could be mistakenly attributed to actual differences in metabolite profiles. However, only the capillary sampling method resulted in the aberrant finding of metabolites related to 70% isopropyl alcohol wipes. Indeed, the authors commented that the same wipes were used for pre-treating the venepuncture site as the capillary sampling site, and argued that the larger volume of blood collected, possibly in addition to the lesser contact time with the skin, during venepuncture meant that any metabolites associated with the wipe were limited.[456]

Certainly this was the case with my sampling methods. Every peripheral blood sampling, and each serum sample preparation, was undertaken by myself using a 21 gauge needle and blood taken from the antecubital fossa. Despite being a multi-site study there were no discrepancies in blood-taking protocol between different clinical areas. In addition, the blood samples were taken and processed non-consecutively, that is, the GD+TAO+ samples were interspersed with GD+TAO- or HC subjects. Indeed, it was often the case that the taking of a GD+TAO+ blood sample was followed within minutes by the taking of a GD+TAO- or HC sample (a healthy friend or relative attending hospital with a GD+TAO+ of GD+TAO- patient and recruited as a HC). In addition, it is the personal preference of the researcher who took all of the blood samples in this study not to use a 70% isopropyl alcohol wipe prior to venepuncture, in keeping with published evidence.[457] Further, gloves were always used for venepuncture, meaning that there would be no isopropyl alcohol gel on the hands of the phlebotomist in contact with the recruited subject. Serum sample preparation for NMR spectroscopy was unchanged from a range of experiments undertaken by the same group and no solvent was used in any part of the processing. Finally, despite isopropanol being found as being significant in these metabolomic analyses, no related products contained in alcohol wipes or hand gel, such as acetone, were detected.

5.5.3 Methylguanidine

Methylguanidine ($C_2H_7N_3$) is a metabolite related to protein catabolism, and may also be produced in putrefaction. It is synthesised from creatinine, associated with the

synthesis of H_2O_2, and is considered a uraemic toxin.[458] The pathogenesis of diseases such as chronic renal failure involve reduced urine production, decreased excretion of urea and methylguanidine and accumulation of these substances in plasma and tissues of patients.[459] Indeed, methylguanidine was one of six urinary metabolites found to have have good discriminatory ability in an NMR-based metabolomics study of canine transitional cell bladder cancer.[458]

Conversely, methylguanidine may be increased as a compensatory mechanism, protecting against cytotoxic effects of ROS, inhibiting pro-inflammatory nitric oxide synthase and scavenging O^{2-} and metabolites such as peroxynitrites, produced in inflammatory conditions. There is evidence that methylguanidine may have an anti-inflammatory role in that it decreases the degree of tissue damage in an endotoxic shock mouse model, again likely due to inhibition of nitric oxide synthesis and TNF-α secretion.[460,461]

5.5.4 Lactate and Pyruvate

Pyruvate (pyruvic acid, $C_3H_4O_3$) can be made from glucose through glycolysis, converted back to glucose via gluconeogenesis, or to fatty acids through acetyl coenzyme A. Pyruvate supplies energy to cells through the Krebs cycle (also known as the tricarboxylic acid cycle (TCA) or citric acid cycle) in aerobic conditions or is converted to lactate (lactic acid, $C_3H_6O_3$) under anaerobic conditions (**Figure 5.12**). An imbalance in each of these metabolites may therefore indicate that there is a contribution of oxidative stress in GD and TAO subjects.

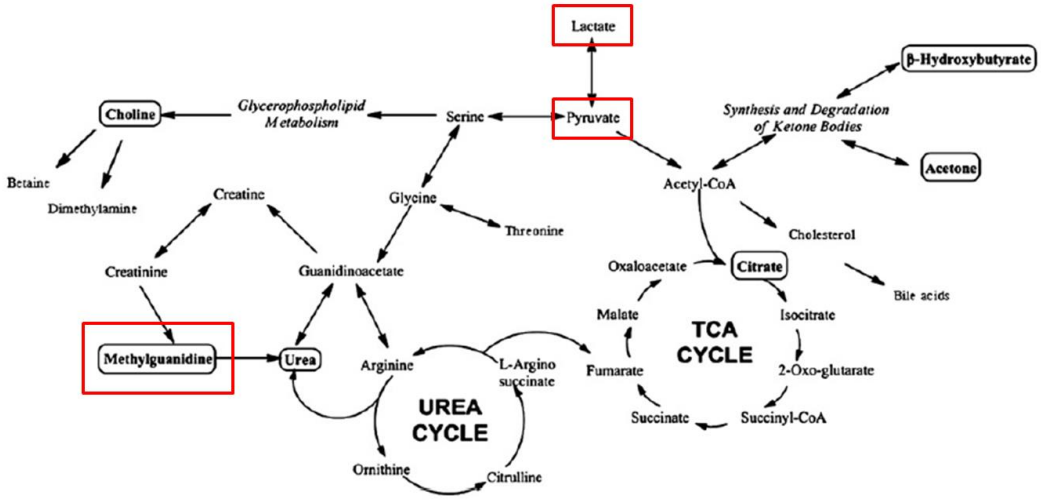

Figure 5.12: Simplified diagram of common metabolic pathways showing some of the relevant discriminating metabolites in GD subjects, indicated in red (taken from Zhang et al 2008).[458]

5.5.5 Established Metabolic Abnormalities in GD and TAO

These metabolomic findings are in keeping with previous studies which have demonstrated derangement of the metabolic status of GD and TAO patients. Changes related to ROS metabolism, have been identified in hyperthyroid GD patient thyroid tissue and plasma, with increased byproducts of lipid peroxidation, increased SOD activity and reduced anti-oxidant enzymes such as GPx compared to controls.[141,462] Serum oxidative stress markers, present during the hyperthyroid phase of GD, normalise following attainment of the euthyroid state, effects that have been proposed to be independent of anti-thyroid treatment.[143]

Furthermore, when groups of untreated autoimmune, hyperthyroid GD (without TAO) and non-autoimmune hyperthyroid toxic multinodular goitre patients were compared, there were equivalent increases in peripheral blood oxidative stress markers. When euthyroidism was established in each of these groups with MMZ there was

normalisation of all oxidative parameters in both groups, suggesting that the observed oxidative stress was due to hyperthyroidism rather than autoimmunity.[463] When hyperthyroid GD patients with and without TAO were compared, oxidative stress markers were again elevated in both groups. However, attainment of the euthyroid state with MMZ resulted in normalisation of oxidative stress markers only in those without orbital inflammation, not in those with ocular manifestations, suggesting that orbital inflammation itself contributes to peripheral blood measures of oxidative stress.[146] In patients with euthyroid but active TAO, oxidative stress markers were again elevated. These normalised with corticosteroid treatment but recurred when corticosteroids were ceased.[145]

These findings are in keeping with my metabolomic data demonstrating differentiation of GD+TAO+ subjects from GD+TAO-. All of the GD patients had current or previous hyperthyroidism, and the consequent hypercatabolic state associated with this, but were heterogeneous in their dysthyroid status at the time of blood sampling. It would appear that the most significant contribution to the metabolic difference between the groups was the orbital inflammation experienced by the GD+TAO+ patients. Of course, the great hope was that the metabolomic PLS-DA model would have separated GD+TAO+ and HC patients into two very separate groups, with the GD+TAO- distributed between these – those GD+TAO- subjects who would go on to develop TAO being closer in metabolomic profile to the GD+TAO+ group, whilst those GD+TAO- who would never develop TAO being closer to the HC. However, this was not observed to be the case.

A number of *in vitro* studies have suggested that increased O^{2-} production has a pathogenic role in TAO. Fibroblasts from severe TAO, but not control subjects, have been shown to proliferate in response to superoxide radicals in a dose-dependent manner.[113] In addition, TAO orbital fibroblasts have been shown to have increased O^{2-} and SOD activity as compared to control orbital fibroblasts.[464] Cultured TAO orbital fibroblasts also display an altered redox metabolite balance, with elevated oxidative stress markers, reduced antioxidant molecules (e.g. glutathione), reduced enzymes involved in protection from oxidative stress (e.g. GPx) and hypersensitivity to a H_2O_2 oxidative stress model, compared to age-matched normal controls.[439,465] It is therefore relevant that some of the metabolites found to permit metabolomic differentiation of GD+TAO+ subjects from GD+TAO- and HC were those associated with oxidative stress and hypoxic metabolism. For example, increased lactate (produced when glucose is broken down and oxidised to pyruvate) was one of the metabolites associated with the GD+TAO+ group. This also provides a metabolic link between IGF-1 and TAO as Fu et al (1991) previously demonstrated a role for IGF-1 in priming neutrophils for superoxide anion secretion.[466]

Previous studies have advocated the use of antioxidants as treatments for GD and TAO. Indeed, Seven et al (1998) found that treatment with vitamin C (ascorbate) supplementation decreased oxidative stress in groups of hyperthyroid subjects treated with PTU as well as controls.[467] However, no clinical trial of vitamin C supplementation in GD or TAO patients has yet been undertaken. Nevertheless, as already discussed, a successful trial of the use of the antioxidant trace element selenium in reducing disease activity has been undertaken in patients with mild TAO.[49]

The inflammatory state within the TAO orbit has been hypothesised to be related to infiltration of CD4+ and CD8+ T lymphocytes, plasma cells and macrophages. It is interesting, therefore, to note the differentiation of GD+TAO+ and GD+TAO- subjects by PTPN22 R620W genotype (even though the numbers in the study population carrying the allelic variant conferring GD susceptibility were low). The PTPN22 variant is associated with increased risk for the development of multiple autoimmune diseases.[468] A specific association with TAO has not been noted, however this PTPN22 SNP is associated with a change in lymphocyte memory populations as well as the cytokine profile observed following activation of T lymphocytes. Overall, these alterations have a tendency to increase autoimmunity, preserving autoreactive lymphocytes or impeding mechanisms that regulate autoreactivity.[468]

5.5.6 Conclusion

With increasing utilisation of diverse immunosuppressant (e.g. azathioprine) and monoclonal antibody (e.g. rituximab) therapies in TAO, and the advent of "personalised medicine" - the tailoring of healthcare based on knowledge of the genetic or metabolic characteristics of an individual - it is crucial to have robust, impartial methods for determining responses to treatment. The clinical methods we utilise at present are imperfect and require greater objectivity. Similarly, in developing future novel treatments from clinical trials we require more concrete outcome measures to determine the efficacy of particular candidate treatments. In summary, this study, combining clinical phenotyping of a large cohort of GD and TAO subjects with PTPN22 (R620W) genotyping, thyroid function, TRAb and metabolomic data,

demonstrates the translational potential of metabolomics as a diagnostic tool for TAO in those with GD and identifies a number of biologically plausible metabolites which may permit discrimination of such groups.

6 GENERAL DISCUSSION

6.1 Introduction

The pathogenesis of TAO is poorly understood. This thesis has explored a range of immunological parameters, namely serum IGF-1R-Ab, peripheral T lymphocyte phenotype and serum metabolite profiles, with potential to function as biomarkers in GD and TAO. There is a large body of existing evidence in TAO for a role of the IGF-1/IGF-1R axis, alterations in peripheral blood T cell memory status and T helper phenotype, as well as for aberrations in metabolism either as a cause or consequence of TAO pathogenesis, and this thesis has both supported and challenged some of these assertions in equal measure.

6.2 Summary of experimental findings

This thesis has demonstrated that:

1. It is possible to reliably and repeatably measure monoclonal IGF-1R antibody with two novel immunoassays, based on the principles of existing assays used in the quantification of other autoantibodies;

2. These immunoassays can be utilised in human sera, with subsequent measurement of putative serum IGF-1R-Ab;

3. There is no significant difference in levels of measured IGF-1R-Ab between GD+TAO+, GD+TAO- and age- and sex-matched HC individuals and no correlation

between IGF-1R-Ab and any clinical parameter, particularly TAO clinical activity and severity scores, in keeping with recent studies utilising cell-based IGF-1R-Ab assays;

4. T cell memory phenotype (both CD4+ and CD8+) is skewed in GD and TAO, with elevated proportions of naïve (CD45RO-CCR7+) and reduction of effector memory (CD45RO+CCR7-) T cells, with additional evidence of reduction in effector memory RA (CD45RO-CCR7-) CD8+ T cells, as compared to HC;

5. The altered memory phenotype in GD and TAO is matched by a reduction in IFN-γ production by CD4+ and CD8+ T cells following PMA and ionomycin stimulation, without any change in the (early or late) activation state of T lymphocytes;

6. There is no apparent variation between GD+TAO+, GD+TAO- and HC in proportions of CD4+CD25^{High}CD127^{Low} regulatory T cells or CD4+CXCR5+ T follicular helper cells. In addition serum IL-21 levels, proposed to contribute to TAO pathogenesis from studies of MS patients undergoing immune reconstitution following Alemtuzumab therapy, were also unchanged;

7. Metabolomic analysis of sera was able to differentiate GD+TAO+, GD+TAO- and HC patients, with additional separation of GD+TAO+ subjects on the basis of their clinical activity scores. Other parameters on which it was possible to distinguish patient groups included thyroid function, TRAb status and PTPN22 (R620W) GD susceptibility genotype.

8. Candidate metabolite markers found to discriminate groups of interest on metabolomic analysis included lactate, isopropanol, methylguanidine and pyruvate, although measuring the actual concentrations of metabolites, only isopropanol (GD+TAO versus GD+TAO-) and pyruvate (active GD+TAO+ versus inactive GD+TAO+) demonstrated significant differences.

6.3 Is there over- or under-estimation of rates of TAO in GD?

In the context of immunological measures we have determined no difference between GD+TAO+ and GD+TAO- patients, for example in T cell memory phenotype or in IGF-1R-Ab immunoassays. It was hoped that a differentiation between the groups may have been possible based on one of these parameters, with subsequent potential to use these as biomarkers. However, in retrospect, the clinical separation of GD patients into TAO+ and TAO- groups may be difficult given that TAO can be demonstrated by orbital imaging in the majority of patients with GD.[25] Indeed, many previous studies in GD have not necessarily distinguished those with ophthalmic manifestations of GD from those without.

It may also be that there is an overestimation of the rate of TAO in GD patients. Anecdotally, the oft-quoted rate of the presence of clinically manifest TAO in GD patients appears to be unrealistically high. The accepted literature attests that 30-50% of GD patients will go on to develop TAO, with 85% of these doing so within 18 months of their diagnosis with AITD.[22] From my cohort of GD patients (without clinically apparent orbitopathy at recruitment) only one subject has apparently developed TAO, with a current minimum follow-up of over 18 months.

Reviewing the published literature in this area, TAO is felt to be clinically relevant in 25% of unselected GD patients if eyelid signs are excluded and 40% if eyelid signs are included.[469] It is interesting to note that many of the articles stating a 30-50% rate of TAO in GD patients either do not make reference to the original source of this data, instead quoting a review paper (which itself may have referenced yet another review) and not providing an adequate original reference. The earliest reference that could be found from an extensive retrospective review of the TAO literature was by Teng et al in 1977. However, this article was actually concerned with the follow-up of a cohort of euthyroid TAO patients over a number of years, in order to determine their eventual thyroid function, rather than a group of GD patients followed up to determine the proportion developing TAO.[470] It may therefore be that the rate of conversion to TAO in GD patients is less than that often cited. This is important in the future planning of services for GD and TAO, in providing a rationale for future large-scale studies in this area and in power calculations for future clinical trials.

6.4 A context for the role of the IGF-1/IGF-1R axis in TAO

If it is not the case that serum IGF-1R-Ab bind to IGF-1R on orbital fibroblasts, initiating production of T cell chemoattractants and hyaluronic acid and inducing proliferation and differentiation toward orbital preadipocytes or myofibroblasts, then what other models of TAO pathogenesis may be proposed? Is there an interaction between IGF-1R and TSH-R following TRAb binding to TSH-R? Does IGF-1R potentiate TSH-R-mediated signalling? Is there a shared antigenic epitope between TSH-R and IGF-1R?

From the results of the various reported IGF-1R-Ab assays it has been suggested that IGF-1 itself may act in an autocrine/paracrine manner within orbital tissues. If autocrine/paracrine orbital IGF-1 production were elevated in TAO then orbital fibroblasts would be well-equipped to bind IGF-1, given their higher levels of IGF-1R expression and exaggerated inflammatory responses. Certainly, there is evidence for autocrine/paracrine functioning of IGF-1 in other tissues. When hepatic IGF-1 secretion is abolished in a mouse model, with a 75% reduction in serum IGF-1, normal postnatal growth still takes place. This has been presumed to be because of autocrine/paracrine production of IGF-1.[471,472] There is also evidence that cells of the immune system can produce IGF-1 and IGFBP,[473,474] and levels of IGF-1 can be modulated by cytokines.[475] In addition, IGF-1 induces T cells to produce differing T helper cytokines,[225] and activation of the T lymphocyte receptor complex alters IGF-1R expression.[236] Whether locally-produced IGF-1R-Ab or autocrine/paracrine IGF-1 contributes to the pathology in TAO has not yet been explored.

6.5 Comparison between TAO and RA as a model for future investigations in peripheral T cell memory phenotype

It is possible to draw similarities with TAO and other autoimmune diseases, particularly RA. It has been proposed, for example, that RA may develop in a non-linear fashion. This condition is known to be related to a number of genetic polymorphisms and environmental risk factors.[476] Prior to development of the full manifestations of synovitis in the primary site of inflammation, the synovial joint, (analogous to orbital inflammatory disease in TAO) there is a period of systemic

autoimmunity with rheumatoid factor and anti–citrullinated protein antibodies (akin to the TRAb, TPO-Ab and TG-Ab which may be present in GD).[477] Indeed, the presence of these antibodies may predict future RA development.[478] Likewise, RA is a T cell-mediated autoimmune condition likely related to an antigen-specific response, much as TAO is presumed to be.[281,479] Inflammatory activity in TAO damages surrounding structures such as EOMs, blood vessels and the optic nerve, just as in RA the surrounding tendons, ligaments and bone may be damaged. Furthermore, despite definite joint-related disease there are also peripheral blood T lymphocyte phenotypic changes.[374]

Following from the data on T cell phenotype and ageing, and given the age-matched status of the healthy controls, the increased naïve cells and reduced EM, with reduced IFN-γ production seen in the GD and TAO patients appears to be concordant with an apparent reversal of immunological ageing. In RA it has been postulated that there is “premature immunosenescence”, with loss of expression of CD28 and oligoclonal T cell proliferation, possibly due to a defect in generating new T lymphocytes.[480]

In GD and TAO patients it may be possible to undertake a similar strategy to Koetz et al (2000), who measured TCR rearrangement excision circles (TREC) as a measure of the output of newly generated T cells from the thymus in RA patients. If new, naive T cells are truly increased there would be an increase in TREC-containing cells. In addition, if there is a true increase in naïve cells this would result in an adaptation by the ‘system’ to maintain homeostasis by reducing the proportion of memory T cells, as we observed. Another strategy would therefore be to measure telomere length to

assess the degree of T cell turnover and proliferation. For example in RA it was found that TREC were reduced, suggesting reduced thymic activity, and telomere length was shortened as compared to age-matched controls.[480] One would hypothesise that the opposite would be seen in TAO, with increased thymic emigration responsible for increased naïve T cells. Again, this could link to a role of IGF-1R, which has been recognised to facilitate thymocyte development and, by extension, naïve T cell production by the thymus.[223]

6.6 Autoantibody profiling in GD and TAO

Questions remain about the nature of the autoantigens in GD. GD is regarded as a true autoimmune disease due to its organ-specific impact on the thyroid gland, alongside a range of extra-thyroidal manifestations restricted to the orbit, pre-tibial skin and acra of the finger. Further evidence is the recently published recapitulation of thyroid autoimmunity and orbital inflammation in an animal model of TAO by immunisation with TSH-R plasmid.[164] Lastly, there are generally good, although unpredictable, responses to immunosuppressive treatments.

Rather than continuing to investigate only a limited selection of autoantigens, there may be a role for wider profiling of the serum autoantibody repertoire in GD and TAO. It is possible, for example, that autoimmune diseases, including AITD, are initiated by a number of autoantigens rather than a single target. In addition, it remains uncertain whether autoantibodies are the precipitants of autoimmune disease or whether they are a secondary effect related to inflammatory tissue damage. In this regard, protein microarrays consisting of a range of protein fragments, possible antigens, against

which to test serum immunoglobulins may provide a high-throughput means of generating novel future biomarkers. Libraries of such proteins exist, such as the Human Protein Atlas project. Certainly, such a strategy has recently been used in a range of autoimmune and inflammatory diseases, including MS, SLE, ankylosing spondylitis and autoimmune hepatitis.[481-483]

For example, Ayoglu et al (2013) tested 90 plasma samples, of only 10 µl volume, from MS patients for 11,520 protein fragments of 80-100 residues, representing 7644 unique proteins. Following this, 51 differentially regulated antigens were found from verification in 376 further MS patients.[481] Importantly the antigen library did not necessarily consist of proteins known to be associated with MS. Rather, the potential epitopes were produced and selected in an unbiased manner, aiming to be based on unique sequences from protein-encoding genes from different regions of low similarity. This inherently untargeted approach is felt to be the strength of the technique in identifying novel disease targets. The authors acknowledged that the limitation of the methodology is that it may not take account of epitopes which have the ability to alter their conformation. However, it is attractive to consider the possibility of utilising the serum samples already biobanked in GD and TAO patients in such a technique.

6.7 Alternative strategies for metabolic analysis in GD and TAO

The candidate metabolic biomarkers identified in my study to differentiate GD and TAO patients (isopropanol) and active and inactive TAO patients (pyruvate) require validation with a new cohort of GD, TAO and HC subject samples. In addition, a

wider variety of different biofluids and tissues should be gained including urine and, given the possible role for the gut microbiome in producing isopropanol, faeces.

There is an expanding role for metabo-genomics in the assessment of disease, combining examination of genotype with genome-wide association studies (GWAS) and metabolic markers to learn more about the consequences of specific polymorphisms on the downstream effects of both genetics and environment.[484] Clearly, no particular susceptibility genes have been noted for TAO, but those for GD (e.g. PTPN22, CTLA-4) could certainly be evaluated

Longitudinal sampling of individual subjects should be given priority. Serum and urine could be taken from the initial time of presentation with GD and repeated sampling undertaken throughout all stages of disease - commencement of anti-thyroid drug treatment, radioiodine treatment, subsequent development of TAO and following the active, stable and quiescent phases of disease. In so doing one may hope to predict the likelihood of onset of TAO in patients initially presenting with GD alone and also to prognosticate responses to existing and future therapies. Certainly, there are indications that this may be possible in such diseases as RA.[485] Furthermore, longitudinal sampling would: 1) permit a time-course of the variations in the important metabolite peaks occurring during the course of GD and TAO; 2) permit identification of any “switch” in metabolic pathways which predominate at different stages in disease; 3) eliminate any variations in dietary, medication and lifestyle factors that are inherent in different subjects within the same study group. The difficulty of such a study is that samples would need to be taken from a large number of GD patients in order for there to be a sufficient number of eventual subjects to follow through to the

full course of their TAO, particularly given previous comments in this chapter about the possibly erroneous published rates of conversion from GD to TAO.

It may be possible to examine the metabolomic profile of orbital fibroblast supernatant as a means of dissecting the metabolic responses to different insults. In particular, culturing orbital fibroblasts from TAO patients with different oxidative stress stimuli such as cigarette smoke extract, hypoxic conditions or H_2O_2, or otherwise antioxidative molecules such as ascorbic acid. Furthermore, culturing orbital fibroblasts with GD-IgG and assessing the metabolomic outcomes may be a strategy for assessing the downstream activities of genes associated with a switch in orbital fibroblast phenotype. In this way it may be possible to differentiate metabolites, and hence metabolic pathways, that are switched on or off in an *in vitro* model of TAO.

6.8 *In vivo* imaging of TAO orbital inflammation

Taking metabolite evaluation further, there is precedent for extending NMR analysis of biofluids to non-invasive, *in vivo* imaging of diseased anatomical sites and prognosticating disease states based on such imaging. For example ^{1}H-NMR spectroscopy (MRS), the magnetic resonance imaging of a diseased structure, and evaluating the metabolite profile within, has been shown to have a role in the assessment of paediatric brain tumours.[486,487] In this technique a small area of interest is examined with NMR and bioinformatic techniques being used to measure the metabolite profile of that structure.

Recent studies have assessed the role of MRS within low-grade paediatric brain tumours. Significant differences were found between brain tumour histological subtypes, with discriminatory metabolites such as choline and myoinositol being determined.[486] In addition, a prospective study imaging paediatric brain tumour patients, with median follow-up of 35 months, determined that MRS biomarkers such as glutamine and N-acetyl aspartate predicted improved brain tumour survival.[487] It is reasonable to assume that this may be extended to imaging of the orbital structures such as orbital adipose tissue and EOMs in TAO, taking GD patients at presentation with clinical manifestations of TAO, performing MRS and following these patients up over time to determine metabolites associated with subsequently more active or severe disease, or disease that responded poorly to immunosuppressive treatment.

Magnetic resonance imaging (MRI) is a routine part of TAO patient assessment, so extending this investigation to include MRS should not be prohibitively expensive, or uncomfortable for patients. MRI T2 relaxation times have been shown by a number of authors to correlate with TAO clinical activity.[488] However, this still does not address the fundamental question for patients with GD, namely whether they will develop TAO at all. Another *in vivo* imaging technique may be of utility in GD and TAO in this regard. Digital infrared thermal imaging (thermography), measuring the temperature of a structure as a surrogate for inflammatory processes occurring, has been established in two studies to discriminate active from inactive TAO and to correlate with cessation of inflammatory activity following high-dose corticosteroid therapy.[489,490] The natural extension of this cheap, quick, non-invasive technique is to prospectively and longitudinally image GD patients from their presentation with AITD and throughout any eventual development of TAO. It would be hypothesised that any

developing orbital inflammatory process could be detected in a patient classified to only have GD and necessary steps taken to treat TAO early.

Escalating intervention, in terms of medical and surgical therapies, is based on the clinical identification of inflammatory activity. Selectively targeting interventions such as smoking cessation, selenium (or other anti-oxidants) and possible future development of immuno-modulatory drugs to those patients at greatest risk of progression will be both more cost effective of benefit to patients.

6.9 Conclusion

A number of biomarkers for a range of diseases already exist, so to aim for such indicators is not necessarily an unachievable ambition in GD and TAO. For example, BRCA genes to determine risks of breast cancer,[491] blood pressure as a risk factor for stroke, levels of certain forms of cholesterol in coronary and vascular disease and C-reactive protein in inflammation. Furthermore, anti-citrullinated antibodies can be detected in the blood before the first symptoms of RA appear.[477]

One may argue that it is currently futile to explore biomarkers permitting the early diagnosis and prognosis of TAO as, at present, no pre-emptive treatment strategies are available to obviate TAO. It is acknowledged that no large-scale, randomised trials currently exist on, for example, the role of smoking cessation in GD in preventing TAO. Neither is their evidence for the early treatment with immunosuppressive therapies (whether corticosteroid, disease-modifying agents or biologic therapies) in preventing TAO development. However, one may use the

alternative argument that if such therapies are created in future, therapies that can prevent TAO onset in GD patients, then to target these therapies will require a biomarker to determine exactly which patients should be treated.

The key to the optimal future management of TAO is in the identification of GD patients most likely to be afflicted by the extra-thyroidal manifestations of orbital inflammatory disease at the earliest possible, even pre-clinical, stage. Further, the earliest recognition of those TAO patients pre-determined to have the most active and severe disease will provide the best possibility to intervene and avoid the debilitating and possibly sight-threatening consequences of this disease.

7 APPENDICES

7.1 Appendix 1

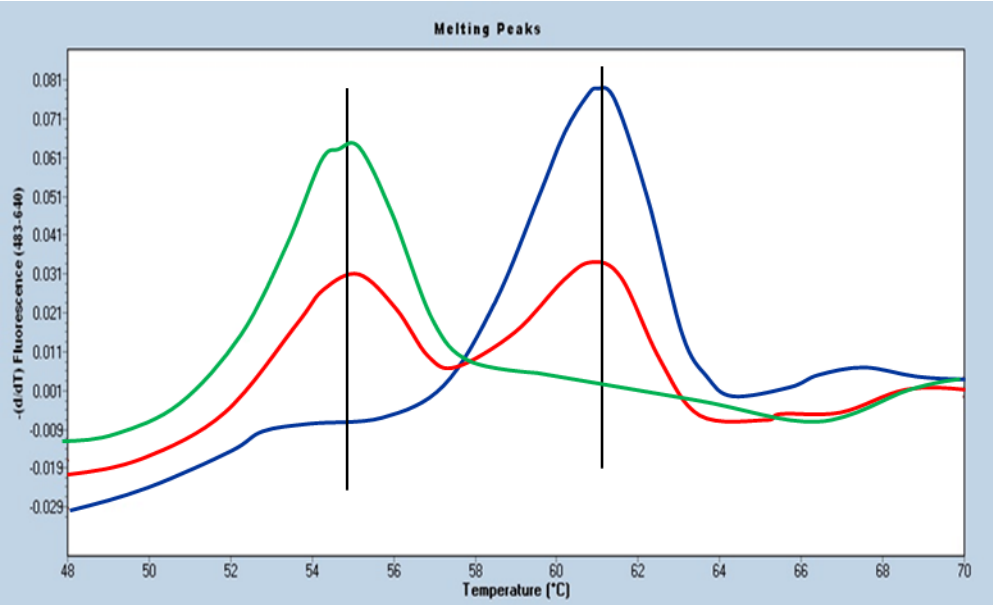

Wild type 1 peak
55°C ± 2.5

Heterozygous 2 peaks
55°C ± 2.5 and 61°C ± 2.5

Homozygous 1 peak
61°C ± 2.5

Appendix 1: Representative example of the output and interpretation of melting curve analysis for determination of PTPN22 (R620W) genotype from whole blood samples of GD+TAO+, GD+TAO- and HC subjects. Subjects were divided into GG (wild type), GA (heterozygotes) and AA (homozygous for R620W single nucleotide polymorphism). Complete protocol is detailed in **Chapter 2.10** and **2.11**.

7.2 Appendix 2

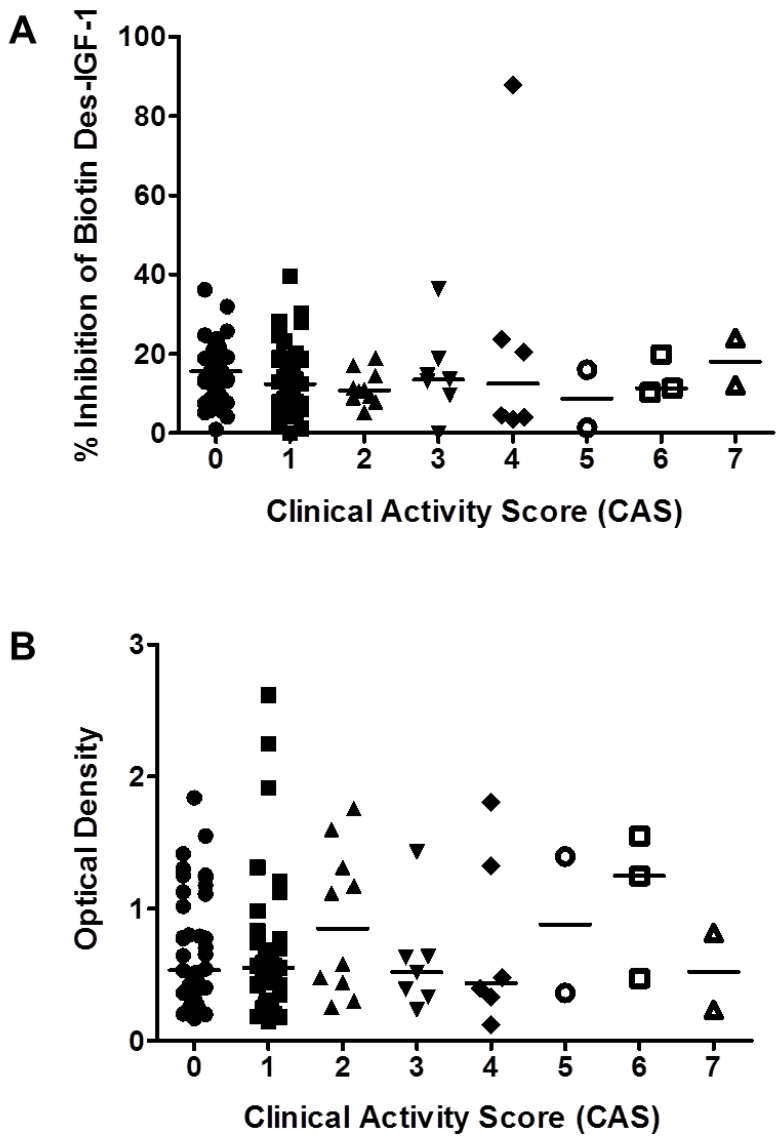

Appendix 2: Results of IGF-1R-Ab ELISA 1 (A) and ELISA 2 (B) for GD+TAO+ subjects demonstrating the full spectrum of clinical activity scores (CAS). Horizontal lines represent median results for each CAS group. There were no significant differences between any of the patient groups with either ELISA 1 or ELISA 2. Non-parametric analysis was undertaken with Kruskal-Wallis (with Dunn's post-test). (NS: Not significant).

7.3 Appendix 3

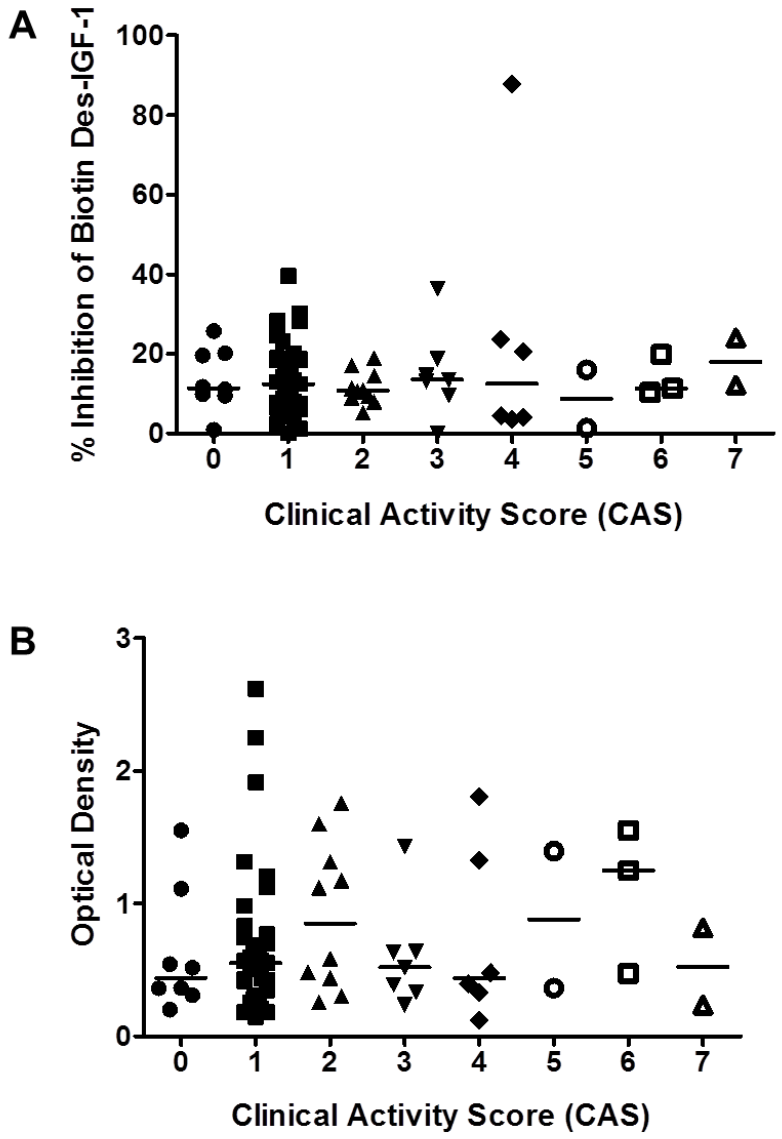

Appendix 3: Results of IGF-1R-Ab ELISA 1 (A) and ELISA 2 (B) for GD+TAO+ subjects demonstrating the full spectrum of clinical activity scores (CAS). In this analysis any patients with CAS of 0 and with TAO for >18 months (and therefore presumed to be 'burnt out' cases) were removed from the analysis. Horizontal lines represent median results for each CAS group. There were no significant differences between any of the patient groups with either ELISA 1 or ELISA 2. Non-parametric analysis was undertaken with Kruskal-Wallis (with Dunn's post-test). (NS: Not significant).

7.4 Appendix 4

Variable	Odds Ratio
Age	
≤40 years	1.0
>40 years	0.49 (0.1 – 2.9) p=0.4
Sex	
Female	1.0
Male	2.4 (0.4 – 14.5) p=0.3
Smoker	
No	1.0
Yes	1.2 (0.3 – 4.1) p=0.8
Duration of GD	
≤12 months	1.0
>12 months	1.5 (0.4 – 5.9) p=0.5
Thyroid Status	
Euthyroid	1.0
Hypothyroid	0.7 (0.1 – 4.8) p=0.7
Hyperthyroid	1.7 (0.2 – 16.1) p=0.7
CAS	
<3	1.0
≥3	0.7 (0.2 – 2.9)p=0.6

Appendix 4: Multivariable logistic regression analysis to assess the independent association of the results of IGF-1R-Ab ELISA 1 with GD+TAO+ subject age, sex, cigarette smoking status, duration of GD, thyroid status (euthyroid, hypothyroid, hyperthyroid) and clinical activity score (CAS). There was no independent association of IGF-1R-Ab as assessed by either assay with any of the variables examined, validating the univariate analyses determined in **Chapter 3.7.4**. For ELISA 1 the comparison was for those patients with percentage inhibition of Biotin Des-IGF-1 of <20% or ≥20%.

7.5 Appendix 5

Variable	Odds Ratio
Age	
≤40 years	1.0
>40 years	0.9 (0.2 – 4.0) p=0.9
Sex	
Female	1.0
Male	4.1 (0.7 – 22.8) p=0.1
Smoker	
No	1.0
Yes	1.7 (0.5 – 5.4) p=0.4
Duration of GD	
≤12 months	1.0
>12 months	1.1 (0.3 – 3.9) p=0.9
Thyroid Status	
Euthyroid	1.0
Hypothyroid	1.4 (0.2 – 9.7) p=0.7
Hyperthyroid	0.3 (0.02 – 4.6) p=0.4
CAS	
<3	1.0
≥3	0.5 (0.1 – 2.0) p=0.3

Appendix 5: Multivariable logistic regression analysis to assess the independent association of the results of IGF-1R-Ab ELISA 2 with GD+TAO+ subject age, sex, cigarette smoking status, duration of GD, thyroid status (euthyroid, hypothyroid, hyperthyroid) and clinical activity score (CAS). There was no independent association of IGF-1R-Ab as assessed by either assay with any of the variables examined, validating the univariate analyses determined in **Chapter 3.7.4**. For ELISA 2 the comparison was for those patients with Optical Density of <1 and ≥1.

7.6 Appendix 6

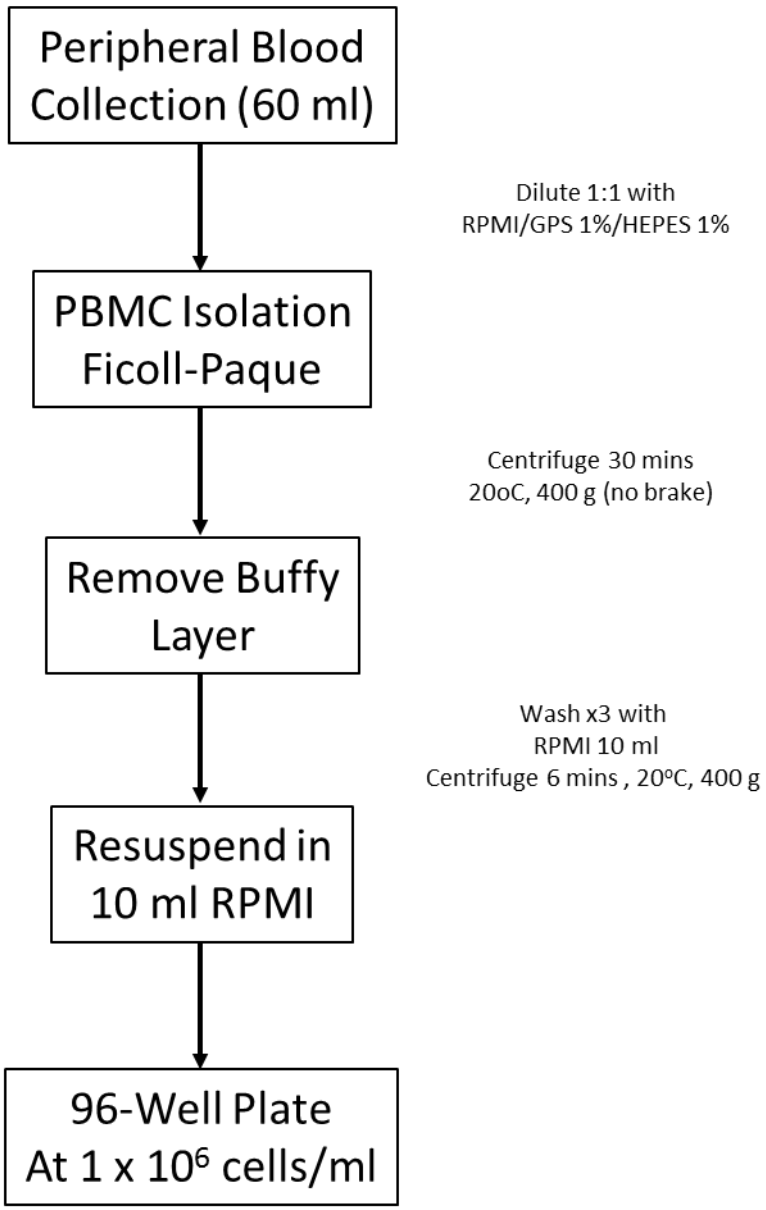

Appendix 6: Summary of the protocol for preparation of peripheral blood mononuclear cells (PBMC) from whole blood samples. Complete protocol is detailed in (**Chapter 2.9.2**).

7.7 Appendix 7

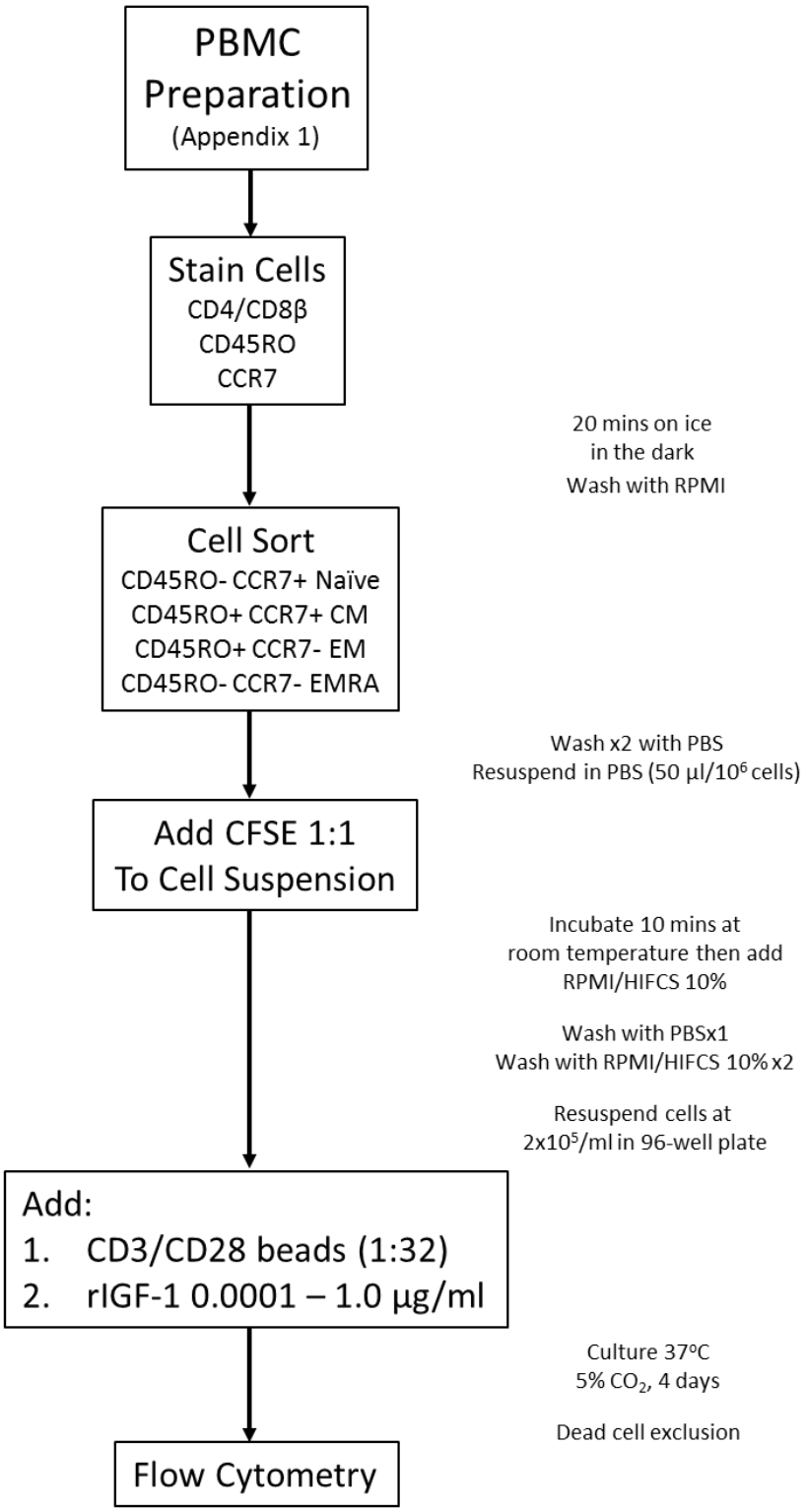

Appendix 7: Summary of the protocol for preparation of peripheral blood mononuclear cells (PBMC) from whole blood samples for cell sorting and carboxyfluorescein diacetate succinimidyl ester (CFSE) proliferation studies. Complete protocol is detailed in **Chapter 4.4.1**.

7.8 Appendix 8

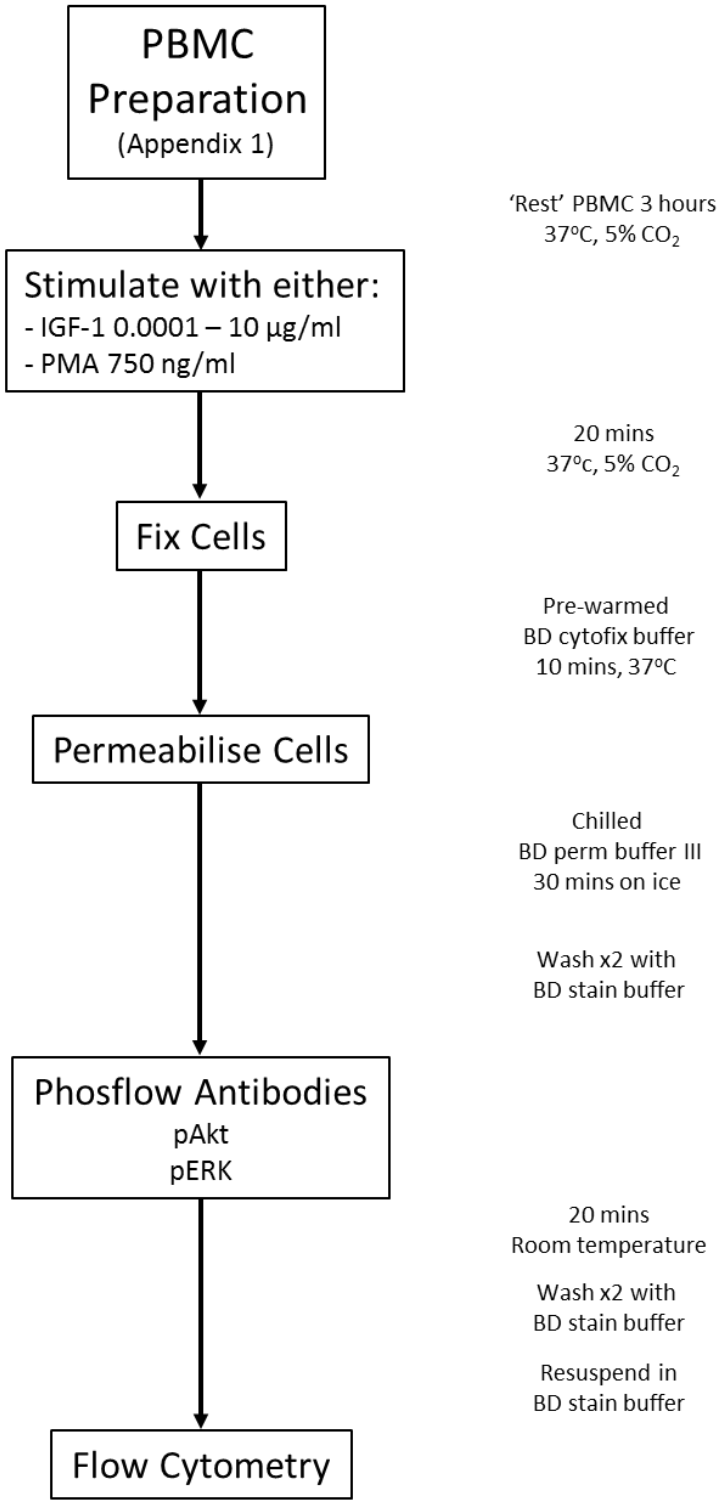

Appendix 8: Summary of the protocol for preparation of peripheral blood mononuclear cells (PBMC) from whole blood samples for Phosflow analysis. Complete protocol is detailed in **Chapter 4.4.2**.

7.9 Appendix 9

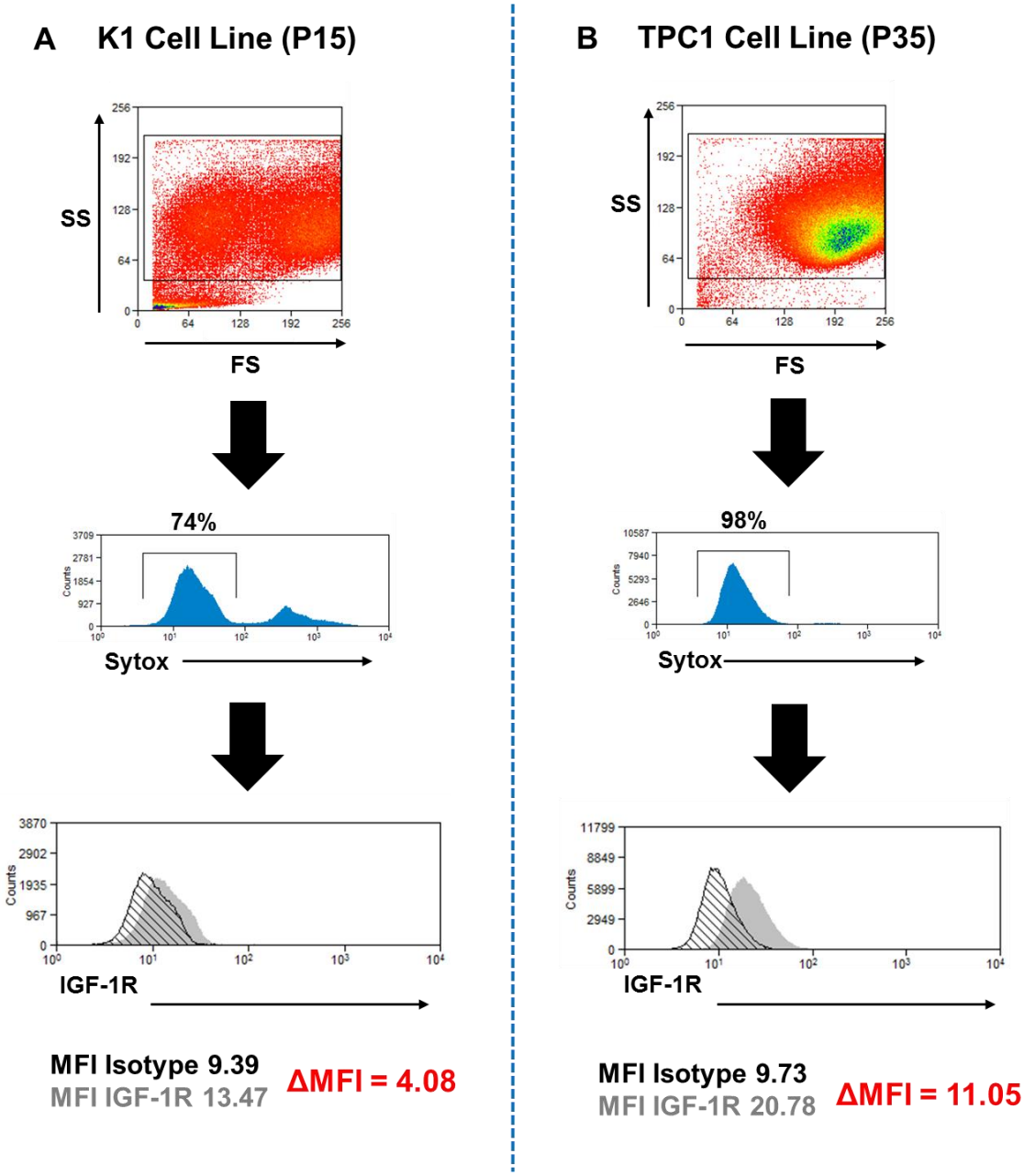

Appendix 9: Representative plots for IGF-1R expression on different two thyroid cancer cell lines, K1 (A) and TPC1 (B), kindly provided by the University of Birmingham Translational Thyroid Research Group. These experiments were performed as positive controls for IGF-1R surface staining studies of CD4+ and CD8+ memory T lymphocyte populations of CD4+ (A) and CD8+ (B) For each population ΔMFI was calculated as MFI [IGF-1R] – MFI [Isotype Control]. Complete protocol for IGF-1R surface staining is detailed in **Chapter 4.5.1** and the T lymphocyte IGF-1R ΔMFI in **Chapter 4.6.7**.

8 REFERENCES

1. Prabhakar BS, Bahn RS, Smith TJ. Current perspective on the pathogenesis of Graves' disease and ophthalmopathy. Endocr Rev 2003;24:802-35.

2. Bartalena L, Baldeschi L, Dickinson A, et al. Consensus statement of the European Group on Graves' orbitopathy (EUGOGO) on management of GO. Eur J Endocrinol 2008;158:273-85.

3. Douglas RS, Naik V, Hwang CJ, et al. B cells from patients with Graves' disease aberrantly express the IGF-1 receptor: implications for disease pathogenesis. J Immunol 2008;181:5768-74.

4. Khoo DH, Eng PH, Ho SC, et al. Graves' ophthalmopathy in the absence of elevated free thyroxine and triiodothyronine levels: prevalence, natural history, and thyrotropin receptor antibody levels. Thyroid 2000;10:1093-100.

5. Morshed SA, Latif R, Davies TF. Delineating the autoimmune mechanisms in Graves' disease. Immunol Res 2012;54:191-203.

6. Chen CR, Pichurin P, Nagayama Y, Latrofa F, Rapoport B, McLachlan SM. The thyrotropin receptor autoantigen in Graves disease is the culprit as well as the victim. J Clin Invest 2003;111:1897-904.

7. Akamizu T. Monoclonal antibodies to thyroid specific autoantigens. Autoimmunity 2003;36:361-6.

8. Khalilzadeh O, Noshad S, Rashidi A, Amirzargar A. Graves' ophthalmopathy: a review of immunogenetics. Curr Genomics 2011;12:564-75.

9. Naik VM, Naik MN, Goldberg RA, Smith TJ, Douglas RS. Immunopathogenesis of thyroid eye disease: emerging paradigms. Surv Ophthalmol 2010;55:215-26.

10. Tao TW, Cheng PJ, Pham H, Leu SL, Kriss JP. Monoclonal antithyroglobulin antibodies derived from immunizations of mice with human eye muscle and thyroid membranes. J Clin Endocrinol Metab 1986;63:577-82.

11. Effraimidis G, Wiersinga WM. Mechanisms in endocrinology: autoimmune thyroid disease: old and new players. Eur J Endocrinol 2014;170:241-52.

12. Yoshihara A, Yoshimura Noh J, Nakachi A, et al. Severe thyroid-associated orbitopathy in Hashimoto's thyroiditis. Report of 2 cases. Endocr J 2011;58:343-8.

13. Bartley GB, Fatourechi V, Kadrmas EF, et al. Clinical features of Graves' ophthalmopathy in an incidence cohort. Am J Ophthalmol 1996;121:284-90.

14. Bartley GB, Fatourechi V, Kadrmas EF, et al. Long-term follow-up of Graves ophthalmopathy in an incidence cohort. Ophthalmology 1996;103:958-62.

15. Bartley GB, Fatourechi V, Kadrmas EF, et al. Chronology of Graves' ophthalmopathy in an incidence cohort. Am J Ophthalmol 1996;121:426-34.

16. Bartalena L, Tanda ML. Clinical practice. Graves' ophthalmopathy. N Engl J Med 2009;360:994-1001.

17. Rootman J. Inflammatory diseases of the orbit. Highlights. J Francais D'Ophtalmologie 2001;24:155-61.

18. Grove AS, Jr. Evaluation of exophthalmos. N Engl J Med 1975;292:1005-13.

19. Lawton NF. Exclusion of dysthyroid eye disease as a cause of unilateral proptosis. T Ophthal Soc UK 1979;99:226-8.

20. Weetman AP. Graves' disease. N Engl J Med 2000;343:1236-48.

21. Noth D, Gebauer M, Muller B, Burgi U, Diem P. Graves' ophthalmopathy: natural history and treatment outcomes. Swiss Med Wkly 2001;131:603-9.

22. Bahn RS. Graves' ophthalmopathy. N Engl J Med 2010;362:726-38.

23. Brent GA. Clinical practice. Graves' disease. N Engl J Med 2008;358:2594-605.

24. Bartley GB. The epidemiologic characteristics and clinical course of ophthalmopathy associated with autoimmune thyroid disease in Olmsted County, Minnesota. T Am Ophthal Soc 1994;92:477-588.

25. Villadolid MC, Yokoyama N, Izumi M, et al. Untreated Graves' disease patients without clinical ophthalmopathy demonstrate a high frequency of extraocular muscle (EOM) enlargement by magnetic resonance. J Clin Endocrinol Metab 1995;80:2830-3.

26. Cawood T, Moriarty P, O'Shea D. Recent developments in thyroid eye disease. BMJ 2004;329:385-90.

27. Tunbridge WM, Vanderpump MP. Population screening for autoimmune thyroid disease. Endocrin Metab Clin 2000;29:239-53, v.

28. Putta-Manohar S, Perros P. Epidemiology of Graves' orbitopathy. Pediatr End Rev 2010;7 Suppl 2:182-5.

29. Manji N, Carr-Smith JD, Boelaert K, et al. Influences of age, gender, smoking, and family history on autoimmune thyroid disease phenotype. J Clin Endocrinol Metab 2006;91:4873-80.

30. Tellez M, Cooper J, Edmonds C. Graves' ophthalmopathy in relation to cigarette smoking and ethnic origin. Clin Endocrinol 1992;36:291-4.

31. Lim SL, Lim AK, Mumtaz M, Hussein E, Wan Bebakar WM, Khir AS. Prevalence, risk factors, and clinical features of thyroid-associated ophthalmopathy in multiethnic Malaysian patients with Graves' disease. Thyroid 2008;18:1297-301.

32. Edmunds MR, Huntbach JA, Durrani OM. Are ethnicity, social grade, and social deprivation associated with severity of thyroid-associated ophthalmopathy? Ophthal Plast Recons 2014;30:241-5.

33. Bartalena L, Marcocci C, Tanda ML, et al. Cigarette smoking and treatment outcomes in Graves ophthalmopathy. Ann Intern Med 1998;129:632-5.

34. Pfeilschifter J, Ziegler R. Smoking and endocrine ophthalmopathy: impact of smoking severity and current vs lifetime cigarette consumption. Clin Endocrinol 1996;45:477-81.

35. Prummel MF, Wiersinga WM. Smoking and risk of Graves' disease. JAMA 1993;269:479-82.

36. Regensburg NI, Wiersinga WM, Berendschot TT, Potgieser P, Mourits MP. Do subtypes of graves' orbitopathy exist? Ophthalmology 2011;118:191-6.

37. Daumerie C, Duprez T, Boschi A. Long-term multidisciplinary follow-up of unilateral thyroid-associated orbitopathy. Eur J Int Med 2008;19:531-6.

38. Eckstein AK, Losch C, Glowacka D, et al. Euthyroid and primarily hypothyroid patients develop milder and significantly more asymmetrical Graves ophthalmopathy. Br J Ophthalmol 2009;93:1052-6.

39. Selva D, Chen C, King G. Late reactivation of thyroid orbitopathy. Clin Exp Ophthalmol 2004;32:46-50.

40. Perros P, Crombie AL, Kendall-Taylor P. Natural history of thyroid associated ophthalmopathy. Clin Endocrinol 1995;42:45-50.

41. Eckstein AK, Lax H, Losch C, et al. Patients with severe Graves' ophthalmopathy have a higher risk of relapsing hyperthyroidism and are unlikely to remain in remission. Clin Endocrinol 2007;67:607-12.

42. Armengol MP, Juan M, Lucas-Martin A, et al. Thyroid autoimmune disease: demonstration of thyroid antigen-specific B cells and recombination-activating gene expression in chemokine-containing active intrathyroidal germinal centers. Am J Path 2001;159:861-73.

43. Douglas RS, Tsirbas A, Gordon M, et al. Development of criteria for evaluating clinical response in thyroid eye disease using a modified Delphi technique. Arch Ophthalmol 2009;127:1155-60.

44. Frueh BR. Why the NOSPECS classification of Graves' eye disease should be abandoned, with suggestions for the characterization of this disease. Thyroid 1992;2:85-8.

45. Mourits MP, Koornneef L, Wiersinga WM, Prummel MF, Berghout A, van der Gaag R. Clinical criteria for the assessment of disease activity in Graves' ophthalmopathy: a novel approach. Br J Ophthalmol 1989;73:639-44.

46. Gerding MN, van der Meer JW, Broenink M, Bakker O, Wiersinga WM, Prummel MF. Association of thyrotrophin receptor antibodies with the clinical features of Graves' ophthalmopathy. Clin Endocrinol 2000;52:267-71.

47. Dolman PJ, Rootman J. VISA Classification for Graves orbitopathy. Ophthal Plast Recons 2006;22:319-24.

48. Mourits MP, Prummel MF, Wiersinga WM, Koornneef L. Clinical activity score as a guide in the management of patients with Graves' ophthalmopathy. Clin Endocrinol 1997;47:9-14.

49. Marcocci C, Kahaly GJ, Krassas GE, et al. Selenium and the course of mild Graves' orbitopathy. N Engl J Med 2011;364:1920-31.

50. Duntas LH. Selenium and inflammation: underlying anti-inflammatory mechanisms. Horm Metab Res 2009;41:443-7.

51. Bartalena L, Krassas GE, Wiersinga W, et al. Efficacy and safety of three different cumulative doses of intravenous methylprednisolone for moderate to severe and active Graves' orbitopathy. J Clin Endocrinol Metab 2012;97:4454-63.

52. Marcocci C, Bartalena L, Tanda ML, et al. Comparison of the effectiveness and tolerability of intravenous or oral glucocorticoids associated with orbital radiotherapy in the management of severe Graves' ophthalmopathy: results of a prospective, single-blind, randomized study. J Clin Endocrinol Metab 2001;86:3562-7.

53. Kahaly GJ, Pitz S, Hommel G, Dittmar M. Randomized, single blind trial of intravenous versus oral steroid monotherapy in Graves' orbitopathy. J Clin Endocrinol Metab 2005;90:5234-40.

54. Rajendram R, Lee RW, Potts MJ, et al. Protocol for the combined immunosuppression & radiotherapy in thyroid eye disease (CIRTED) trial: a multi-centre, double-masked, factorial randomised controlled trial. Trials 2008;9:6.

55. Kahaly G, Schrezenmeir J, Krause U, et al. Ciclosporin and prednisone v. prednisone in treatment of Graves' ophthalmopathy: a controlled, randomized and prospective study. Eur J Clin Invest 1986;16:415-22.

56. Sanyal P, Bing-You RG, Braverman LE. Use of methotrexate to treat isolated Graves ophthalmopathy developing years after thyroidectomy and iodine 131 treatment of papillary thyroid cancer. Endocr Pract 2008;14:422-5.

57. Bartalena L, Marcocci C, Tanda ML, et al. Orbital radiotherapy for Graves' ophthalmopathy. Thyroid 2002;12:245-50.

58. Mourits MP, van Kempen-Harteveld ML, Garcia MB, Koppeschaar HP, Tick L, Terwee CB. Radiotherapy for Graves' orbitopathy: randomised placebo-controlled study. Lancet 2000;355:1505-9.

59. Durrani OM, Reuser TQ, Murray PI. Infliximab: a novel treatment for sight-threatening thyroid associated ophthalmopathy. Orbit 2005;24:117-9.

60. Paridaens D, van den Bosch WA, van der Loos TL, Krenning EP, van Hagen PM. The effect of etanercept on Graves' ophthalmopathy: a pilot study. Eye 2005;19:1286-9.

61. Hegedus L, Smith TJ, Douglas RS, Nielsen CH. Targeted biological therapies for Graves' disease and thyroid-associated ophthalmopathy. Focus on B-cell depletion with Rituximab. Clin Endocrinol 2011;74:1-8.

62. El Fassi D, Clemmensen O, Nielsen CH, Silkiss RZ, Hegedus L. Evidence of intrathyroidal B-lymphocyte depletion after rituximab therapy in a patient with Graves' disease. J Clin Endocrinol Metab 2007;92:3762-3.

63. El Fassi D, Banga JP, Gilbert JA, Padoa C, Hegedus L, Nielsen CH. Treatment of Graves' disease with rituximab specifically reduces the production of thyroid stimulating autoantibodies. Clin Immunol 2009;130:252-8.

64. Mitchell AL, Gan EH, Morris M, et al. The effect of B cell depletion therapy on anti-TSH receptor antibodies and clinical outcome in glucocorticoid-refractory Graves' orbitopathy. Clin Endocrinol 2013;79:437-42.

65. Salvi M, Vannucchi G, Campi I, et al. Treatment of Graves' disease and associated ophthalmopathy with the anti-CD20 monoclonal antibody rituximab: an open study. Eur J Endocrinol 2007;156:33-40.

66. Heemstra KA, Toes RE, Sepers J, et al. Rituximab in relapsing Graves' disease, a phase II study. Eur J Endocrinol 2008;159:609-15.

67. Nielsen JF, El Fassi D, Nielsen CH, et al. Evidence of orbital B and T cell depletion after rituximab therapy in Graves' ophthalmopathy. Acta Ophthalmol 2009;87:927-9.

68. Salvi M, Vannucchi G, Campi I, et al. Efficacy of rituximab treatment for thyroid-associated ophthalmopathy as a result of intraorbital B-cell depletion in one patient unresponsive to steroid immunosuppression. Eur J Endocrinol 2006;154:511-7.

69. El Fassi D, Nielsen CH, Hasselbalch HC, Hegedus L. Treatment-resistant severe, active Graves' ophthalmopathy successfully treated with B lymphocyte depletion. Thyroid 2006;16:709-10.

70. Khanna D, Chong KK, Afifiyan NF, et al. Rituximab treatment of patients with severe, corticosteroid-resistant thyroid-associated ophthalmopathy. Ophthalmology 2010;117:133-9 e2.

71. Silkiss RZ, Reier A, Coleman M, Lauer SA. Rituximab for thyroid eye disease. Ophthal Plast Recons 2010;26:310-4.

72. Minakaran N, Ezra DG. Rituximab for thyroid-associated ophthalmopathy. The Cochrane DB Syst Rev 2013;5:CD009226.

73. Kung AW. Life events, daily stresses and coping in patients with Graves' disease. Clin Endocrinol 1995;42:303-8.

74. Matos-Santos A, Nobre EL, Costa JG, et al. Relationship between the number and impact of stressful life events and the onset of Graves' disease and toxic nodular goitre. Clin Endocrinol 2001;55:15-9.

75. Coulter I, Frewin S, Krassas GE, Perros P. Psychological implications of Graves' orbitopathy. Eur J Endocrinol 2007;157:127-31.

76. Terwee CB, Gerding MN, Dekker FW, Prummel MF, Wiersinga WM. Development of a disease specific quality of life questionnaire for patients with Graves' ophthalmopathy: the GO-QOL. Br J Ophthalmol 1998;82:773-9.

77. Fayers T, Dolman PJ. Validity and reliability of the TED-QOL: a new three-item questionnaire to assess quality of life in thyroid eye disease. Br J Ophthalmol 2011;95:1670-4.

78. Streeten DH, Anderson GH, Jr., Reed GF, Woo P. Prevalence, natural history and surgical treatment of exophthalmos. Clin Endocrinol 1987;27:125-33.

79. Terwee C, Wakelkamp I, Tan S, Dekker F, Prummel MF, Wiersinga W. Long-term effects of Graves' ophthalmopathy on health-related quality of life. Eur J Endocrinol 2002;146:751-7.

80. Yeatts RP. Quality of life in patients with Graves ophthalmopathy. Trans Am Ophthalmol Soc 2005;103:368-411.

81. Ponto KA, Pitz S, Pfeiffer N, Hommel G, Weber MM, Kahaly GJ. Quality of life and occupational disability in endocrine orbitopathy. Deutsches Arzteblatt Int 2009;106:283-9.

82. Brix TH, Kyvik KO, Christensen K, Hegedus L. Evidence for a major role of heredity in Graves' disease: a population-based study of two Danish twin cohorts. J Clin Endocrinol Metab 2001;86:930-4.

83. Manji N, Carr-Smith JD, Boelaert K, et al. Influences of age, gender, smoking, and family history on autoimmune thyroid disease phenotype. J Clin Endocrinol Metab 2006;91:4873-80.

84. Ban Y, Davies TF, Greenberg DA, et al. Arginine at position 74 of the HLA-DR beta1 chain is associated with Graves' disease. Genes Immun 2004;5:203-8.

85. Simmonds MJ, Howson JM, Heward JM, et al. A novel and major association of HLA-C in Graves' disease that eclipses the classical HLA-DRB1 effect. Hum Mol Genet 2007;16:2149-53.

86. Jacobson EM, Tomer Y. The CD40, CTLA-4, thyroglobulin, TSH receptor, and PTPN22 gene quintet and its contribution to thyroid autoimmunity: back to the future. J Autoimmun 2007;28:85-98.

87. Vaidya B, Imrie H, Perros P, et al. Cytotoxic T lymphocyte antigen-4 (CTLA-4) gene polymorphism confers susceptibility to thyroid associated orbitopathy. Lancet 1999;354:743-4.

88. Smyth D, Cooper JD, Collins JE, et al. Replication of an association between the lymphoid tyrosine phosphatase locus (LYP/PTPN22) with type 1 diabetes, and evidence for its role as a general autoimmunity locus. Diabetes 2004;53:3020-3.

89. Inoue N, Watanabe M, Yamada H, et al. Associations between autoimmune thyroid disease prognosis and functional polymorphisms of susceptibility genes, CTLA4, PTPN22, CD40, FCRL3, and ZFAT, previously revealed in genome-wide association studies. J Clin Immunol 2012;32:1243-52.

90. Kamizono S, Hiromatsu Y, Seki N, et al. A polymorphism of the 5' flanking region of tumour necrosis factor alpha gene is associated with thyroid-associated ophthalmopathy in Japanese. Clin Endocrinol 2000;52:759-64.

91. Siegmund T, Usadel KH, Donner H, Braun J, Walfish PG, Badenhoop K. Interferon-gamma gene microsatellite polymorphisms in patients with Graves' disease. Thyroid 1998;8:1013-7.

92. Kretowski A, Wawrusiewicz N, Mironczuk K, Mysliwiec J, Kretowska M, Kinalska I. Intercellular adhesion molecule 1 gene polymorphisms in Graves' disease. J Clin Endocrinol Metab 2003;88:4945-9.

93. Brand OJ, Lowe CE, Heward JM, et al. Association of the interleukin-2 receptor alpha (IL-2Ralpha)/CD25 gene region with Graves' disease using a multilocus test and tag SNPs. Clin Endocrinol 2007;66:508-12.

94. Bahn RS, Dutton CM, Heufelder AE, Sarkar G. A genomic point mutation in the extracellular domain of the thyrotropin receptor in patients with Graves' ophthalmopathy. J Clin Endocrinol Metab 1994;78:256-60.

95. Bottini N, Musumeci L, Alonso A, et al. A functional variant of lymphoid tyrosine phosphatase is associated with type I diabetes. Nat Genet 2004;36:337-8.

96. Carlton VE, Hu X, Chokkalingam AP, et al. PTPN22 genetic variation: evidence for multiple variants associated with rheumatoid arthritis. Am J Hum Genet 2005;77:567-81.

97. Burn GL, Svensson L, Sanchez-Blanco C, Saini M, Cope AP. Why is PTPN22 a good candidate susceptibility gene for autoimmune disease? FEBS Letters 2011;585:3689-98.

98. Duerr RH, Taylor KD, Brant SR, et al. A genome-wide association study identifies IL23R as an inflammatory bowel disease gene. Science 2006;314:1461-3.

99. Farago B, Magyari L, Safrany E, et al. Functional variants of interleukin-23 receptor gene confer risk for rheumatoid arthritis but not for systemic sclerosis. Ann Rheum Dis 2008;67:248-50.

100. Huber AK, Jacobson EM, Jazdzewski K, Concepcion ES, Tomer Y. Interleukin (IL)-23 receptor is a major susceptibility gene for Graves' ophthalmopathy: the IL-23/T-helper 17 axis extends to thyroid autoimmunity. J Clin Endocrinol Metab 2008;93:1077-81.

101. Ban Y, Tozaki T, Tobe T, Jacobson EM, Concepcion ES, Tomer Y. The regulatory T cell gene FOXP3 and genetic susceptibility to thyroid autoimmunity: an association analysis in Caucasian and Japanese cohorts. J Autoimmun 2007;28:201-7.

102. Villanueva R, Inzerillo AM, Tomer Y, et al. Limited genetic susceptibility to severe Graves' ophthalmopathy: no role for CTLA-4 but evidence for an environmental etiology. Thyroid 2000;10:791-8.

103. Bednarczuk T, Gopinath B, Ploski R, Wall JR. Susceptibility genes in Graves' ophthalmopathy: searching for a needle in a haystack? Clin Endocrinol 2007;67:3-19.

104. Eckstein A, Quadbeck B, Mueller G, et al. Impact of smoking on the response to treatment of thyroid associated ophthalmopathy. Br J Ophthalmol 2003;87:773-6.

105. Cawood TJ, Moriarty P, O'Farrelly C, O'Shea D. Smoking and thyroid-associated ophthalmopathy: A novel explanation of the biological link. J Clin Endocrinol Metab 2007;92:59-64.

106. Bartalena L, Marcocci C, Bogazzi F, Panicucci M, Lepri A, Pinchera A. Use of corticosteroids to prevent progression of Graves' ophthalmopathy after radioiodine therapy for hyperthyroidism. N Engl J Med 1989;321:1349-52.

107. Bartalena L, Marcocci C, Bogazzi F, et al. Relation between therapy for hyperthyroidism and the course of Graves' ophthalmopathy. N Engl J Med 1998;338:73-8.

108. Tallstedt L, Lundell G, Torring O, et al. Occurrence of ophthalmopathy after treatment for Graves' hyperthyroidism. The Thyroid Study Group. N Engl J Med 1992;326:1733-8.

109. Perros P, Kendall-Taylor P. Natural history of thyroid eye disease. Thyroid 1998;8:423-5.

110. Weetman AP, Wiersinga WM. Current management of thyroid-associated ophthalmopathy in Europe. Results of an international survey. Clin Endocrinol 1998;49:21-8.

111. Bertelsen JB, Hegedus L. Cigarette smoking and the thyroid. Thyroid 1994;4:327-31.

112. Salvi M, Pedrazzoni M, Girasole G, et al. Serum concentrations of proinflammatory cytokines in Graves' disease: effect of treatment, thyroid function, ophthalmopathy and cigarette smoking. Eur J Endocrinol 2000;143:197-202.

113. Burch HB, Lahiri S, Bahn RS, Barnes S. Superoxide radical production stimulates retroocular fibroblast proliferation in Graves' ophthalmopathy. Exp Eye Res 1997;65:311-6.

114. Prummel MF, Wiersinga WM, Mourits MP, Koornneef L, Berghout A, van der Gaag R. Effect of abnormal thyroid function on the severity of Graves' ophthalmopathy. Arch Int Med 1990;150:1098-101.

115. Jarhult J, Rudberg C, Larsson E, et al. Graves' disease with moderate-severe endocrine ophthalmopathy-long term results of a prospective, randomized study of total or subtotal thyroid resection. Thyroid 2005;15:1157-64.

116. Marcocci C, Bartalena L, Bogazzi F, Bruno-Bossio G, Pinchera A. Relationship between Graves' ophthalmopathy and type of treatment of Graves' hyperthyroidism. Thyroid 1992;2:171-8.

117. Tallstedt L, Lundell G, Blomgren H, Bring J. Does early administration of thyroxine reduce the development of Graves' ophthalmopathy after radioiodine treatment? Eur J Endocrinol 1994;130:494-7.

118. Kung AW, Yau CC, Cheng A. The incidence of ophthalmopathy after radioiodine therapy for Graves' disease: prognostic factors and the role of methimazole. J Clin Endocrinol Metab 1994;79:542-6.

119. El-Kaissi S, Bowden J, Henry MJ, et al. Association between radioiodine therapy for Graves' hyperthyroidism and thyroid-associated ophthalmopathy. Int Ophthalmol 2010;30:397-405.

120. Träisk F, Tallstedt L, Abraham-Nordling M, et al. Thyroid-associated ophthalmopathy after treatment for Graves' hyperthyroidism with antithyroid drugs or iodine-131. J Clin Endocrinol Metab 2009;94:3700-7.

121. Ponto KA, Zang S, Kahaly GJ. The tale of radioiodine and Graves' orbitopathy. Thyroid 2010;20:785-93.

122. Wiersinga WM. Autoimmunity in Graves' ophthalmopathy: the result of an unfortunate marriage between TSH receptors and IGF-1 receptors? J Clin Endocrinol Metab 2011;96:2386-94.

123. Smith TJ, Padovani-Claudio DA, Lu Y, et al. Fibroblasts expressing the thyrotropin receptor overarch thyroid and orbit in Graves' disease. J Clin Endocrinol Metab 2011;96:3827-37.

124. Lehmann GM, Feldon SE, Smith TJ, Phipps RP. Immune mechanisms in thyroid eye disease. Thyroid 2008;18:959-65.

125. Smith TJ, Tsai CC, Shih M-J, et al. Unique attributes of orbital fibroblasts and global alterations in IGF-1 receptor signaling could explain thyroid-associated ophthalmopathy. Thyroid 2008;18:983-8.

126. Bahn RS. Thyrotropin receptor expression in orbital adipose/connective tissues from patients with thyroid-associated ophthalmopathy. Thyroid 2002;12:193-5.

127. Douglas RS, Gianoukakis AG, Goldberg RA, Kamat S, Smith TJ. Circulating mononuclear cells from euthyroid patients with thyroid-associated ophthalmopathy exhibit characteristic phenotypes. Clin Exp Immunol 2007;148:64-71.

128. Gerding MN, Prummel MF, Wiersinga WM. Assessment of disease activity in Graves' ophthalmopathy by orbital ultrasonography and clinical parameters. Clin Endocrinol 2000;52:641-6.

129. Eckstein AK, Finkenrath A, Heiligenhaus A, et al. Dry eye syndrome in thyroid-associated ophthalmopathy: lacrimal expression of TSH receptor suggests involvement of TSHR-specific autoantibodies. Acta Ophthalmol Scand 2004;82:291-7.

130. Bartalena L, Wiersinga WM, Pinchera A. Graves' ophthalmopathy: state of the art and perspectives. J Endocrinol Invest 2004;27:295-301.

131. Hansen C, Rouhi R, Forster G, Kahaly GJ. Increased sulfatation of orbital glycosaminoglycans in Graves' ophthalmopathy. J Clin Endocrinol Metab 1999;84:1409-13.

132. Garrity JA, Bahn RS. Pathogenesis of graves ophthalmopathy: implications for prediction, prevention, and treatment. Am J Ophthalmol 2006;142:147-53.

133. Sokol JA, Foulks GN, Haider A, Nunery WR. Ocular surface effects of thyroid disease. Ocul Surf 2010;8:29-39.

134. Tallstedt L, Norberg R. Immunohistochemical staining of normal and Graves' extraocular muscle. Invest Ophthalmol Vis Sci 1988;29:175-84.

135. Weetman AP, Cohen S, Gatter KC, Fells P, Shine B. Immunohistochemical analysis of the retrobulbar tissues in Graves' ophthalmopathy. Clin Exp Immunol 1989;75:222-7.

136. Marcocci C, Bartalena L. Role of oxidative stress and selenium in Graves' hyperthyroidism and orbitopathy. J Endocrinol Invest 2013;36:15-20.

137. Zarkovic M. The role of oxidative stress on the pathogenesis of graves' disease. J Thy Res 2012;2012:302537.

138. Venditti P, Di Meo S. Thyroid hormone-induced oxidative stress. Cell Molecular Life Sci 2006;63:414-34.

139. Asayama K, Dobashi K, Hayashibe H, Megata Y, Kato K. Lipid peroxidation and free radical scavengers in thyroid dysfunction in the rat: a possible mechanism of injury to heart and skeletal muscle in hyperthyroidism. Endocrinol 1987;121:2112-8.

140. Heufelder AE, Wenzel BE, Bahn RS. Methimazole and propylthiouracil inhibit the oxygen free radical-induced expression of a 72 kilodalton heat shock protein in Graves' retroocular fibroblasts. J Clin Endocrinol Metab 1992;74:737-42.

141. Ademoglu E, Ozbey N, Erbil Y, et al. Determination of oxidative stress in thyroid tissue and plasma of patients with Graves' disease. Eur J Int Med 2006;17:545-50.

142. Aslan M, Cosar N, Celik H, et al. Evaluation of oxidative status in patients with hyperthyroidism. Endocrine 2011;40:285-9.

143. Bianchi G, Solaroli E, Zaccheroni V, et al. Oxidative stress and anti-oxidant metabolites in patients with hyperthyroidism: effect of treatment. Horm Metab Res 1999;31:620-4.

144. Abalovich M, Llesuy S, Gutierrez S, Repetto M. Peripheral parameters of oxidative stress in Graves' disease: the effects of methimazole and 131 iodine treatments. Clin Endocrinol 2003;59:321-7.

145. Bednarek J, Wysocki H, Sowinski J. Peripheral parameters of oxidative stress in patients with infiltrative Graves' ophthalmopathy treated with corticosteroids. Immunol Lett 2004;93:227-32.

146. Bednarek J, Wysocki H, Sowinski J. Oxidative stress peripheral parameters in Graves' disease: the effect of methimazole treatment in patients with and without infiltrative ophthalmopathy. Clin Biochem 2005;38:13-8.

147. Chen MH, Liao SL, Tsou PL, Shih MJ, Chang TC, Chuang LM. Lysosome-related genes are regulated in the orbital fat of patients with graves' ophthalmopathy. Invest Ophthalmol Vis Sci 2008;49:4760-4.

148. Lantz M, Vondrichova T, Parikh H, et al. Overexpression of immediate early genes in active Graves' ophthalmopathy. J Clin Endocrinol Metab 2005;90:4784-91.

149. Kumar S, Leontovich A, Coenen MJ, Bahn RS. Gene expression profiling of orbital adipose tissue from patients with Graves' ophthalmopathy: a potential role for secreted frizzled-related protein-1 in orbital adipogenesis. J Clin Endocrinol Metab 2005;90:4730-5.

150. Ezra DG, Krell J, Rose GE, Bailly M, Stebbing J, Castellano L. Transcriptome-level microarray expression profiling implicates IGF-1 and Wnt signalling dysregulation in the pathogenesis of thyroid-associated orbitopathy. J Clin Pathol 2012;65:608-13.

151. Planck T, Parikh H, Brorson H, et al. Gene expression in Graves' ophthalmopathy and arm lymphedema: similarities and differences. Thyroid 2011;21:663-74.

152. Kahaly GJ. The thyrocyte-fibrocyte link: closing the loop in the pathogenesis of Graves' disease? J Clin Endocrinol Metab 2010;95:62-5.

153. Gopinath B, Musselman R, Beard N, et al. Antibodies targeting the calcium binding skeletal muscle protein calsequestrin are specific markers of ophthalmopathy and sensitive indicators of ocular myopathy in patients with Graves' disease. Clin Exp Immunol 2006;145:56-62.

154. Gopinath B, Musselman R, Adams CL, Tani J, Beard N, Wall JR. Study of serum antibodies against three eye muscle antigens and the connective tissue antigen collagen XIII in patients with Graves' disease with and without ophthalmopathy: correlation with clinical features. Thyroid 2006;16:967-74.

155. de Haan S, Lahooti H, Morris O, Wall JR. Epitopes, immunoglobulin classes and immunoglobulin G subclasses of calsequestrin antibodies in patients with thyroid eye disease. Autoimmunity 2010;43:698-703.

156. Iyer S, Bahn R. Immunopathogenesis of Graves' ophthalmopathy: the role of the TSH receptor. Best Pract Res Cl En 2012;26:281-9.

157. Douglas RS, Afifiyan NF, Hwang CJ, et al. Increased generation of fibrocytes in thyroid-associated ophthalmopathy. J Clin Endocrinol Metab 2010;95:430-8.

158. Chang TC, Huang KM, Chang TJ, Lin SL. Correlation of orbital computed tomography and antibodies in patients with hyperthyroid Graves' disease. Clin Endocrinol 1990;32:551-8.

159. Eckstein AK, Plicht M, Lax H, et al. Thyrotropin receptor autoantibodies are independent risk factors for Graves' ophthalmopathy and help to predict severity and outcome of the disease. J Clin Endocrinol Metab 2006;91:3464-70.

160. Dragan LR, Seiff SR, Lee DC. Longitudinal correlation of thyroid-stimulating immunoglobulin with clinical activity of disease in thyroid-associated orbitopathy. Ophthal Plast Recons 2006;22:13-9.

161. Vos XG, Smit N, Endert E, Tijssen JG, Wiersinga WM. Frequency and characteristics of TBII-seronegative patients in a population with untreated Graves' hyperthyroidism: a prospective study. Clin Endocrinol 2008;69:311-7.

162. Laurberg P, Wallin G, Tallstedt L, Abraham-Nordling M, Lundell G, Torring O. TSH-receptor autoimmunity in Graves' disease after therapy with anti-thyroid drugs, surgery, or radioiodine: a 5-year prospective randomized study. Eur J Endocrinol 2008;158:69-75.

163. Acharya SH, Avenell A, Philip S, Burr J, Bevan JS, Abraham P. Radioiodine therapy (RAI) for Graves' disease (GD) and the effect on ophthalmopathy: a systematic review. Clin Endocrinol 2008;69:943-50.

164. Moshkelgosha S, So PW, Deasy N, Diaz-Cano S, Banga JP. Cutting edge: retrobulbar inflammation, adipogenesis, and acute orbital congestion in a preclinical

female mouse model of Graves' orbitopathy induced by thyrotropin receptor plasmid-in vivo electroporation. Endocrinol 2013;154:3008-15.

165. Levy-Shraga Y, Tamir-Hostovsky L, Boyko V, Lerner-Geva L, Pinhas-Hamiel O. Follow-up of newborns of mothers with graves' disease. Thyroid 2014;24:1032-9.

166. Polak M. Hyperthyroidism in early infancy: pathogenesis, clinical features and diagnosis with a focus on neonatal hyperthyroidism. Thyroid 1998;8:1171-7.

167. Lee WY, Oh ES, Min CK, et al. Changes in autoimmune thyroid disease following allogeneic bone marrow transplantation. Bone Marrow Transpl 2001;28:63-6.

168. Davies T, Marians R, Latif R. The TSH receptor reveals itself. J Clin Invest 2002;110:161-4.

169. Morshed SA, Latif R, Davies TF. Characterization of thyrotropin receptor antibody-induced signaling cascades. Endocrinol 2009;150:519-29.

170. de Lloyd A, Bursell J, Gregory JW, Rees DA, Ludgate M. TSH receptor activation and body composition. J Endocrinol 2010;204:13-20.

171. Chistiakov DA. Thyroid-stimulating hormone receptor and its role in Graves' disease. Mol Genet Metab 2003;80:377-88.

172. Chazenbalk GD, Pichurin P, Chen CR, et al. Thyroid-stimulating autoantibodies in Graves disease preferentially recognize the free A subunit, not the thyrotropin holoreceptor. J Clin Invest 2002;110:209-17.

173. Latif R, Graves P, Davies TF. Oligomerization of the human thyrotropin receptor: fluorescent protein-tagged hTSHR reveals post-translational complexes. The Journal of biological chemistry 2001;276:45217-24.

174. Parmentier M, Libert F, Maenhaut C, et al. Molecular cloning of the thyrotropin receptor. Science 1989;246:1620-2.

175. Paschke R, Vassart G, Ludgate M. Current evidence for and against the TSH receptor being the common antigen in Graves' disease and thyroid associated ophthalmopathy. Clin Endocrinol 1995;42:565-9.

176. Cianfarani F, Baldini E, Cavalli A, et al. TSH receptor and thyroid-specific gene expression in human skin. J Invest Dermatol 2010;130:93-101.

177. Bell A, Gagnon A, Grunder L, Parikh SJ, Smith TJ, Sorisky A. Functional TSH receptor in human abdominal preadipocytes and orbital fibroblasts. Am J Physiol Cell Physiol 2000;279:C335-40.

178. Crisanti P, Omri B, Hughes E, et al. The expression of thyrotropin receptor in the brain. Endocrinol 2001;142:812-22.

179. Drvota V, Janson A, Norman C, et al. Evidence for the presence of functional thyrotropin receptor in cardiac muscle. Biochem Bioph Res Co 1995;211:426-31.

180. Inoue M, Tawata M, Yokomori N, Endo T, Onaya T. Expression of thyrotropin receptor on clonal osteoblast-like rat osteosarcoma cells. Thyroid 1998;8:1059-64.

181. Davies TF, Smith BR, Hall R. Binding of thyroid stimulators to guinea pig testis and thyroid. Endocrinol 1978;103:6-10.

182. Murakami M, Hosoi Y, Negishi T, et al. Thymic hyperplasia in patients with Graves' disease. Identification of thyrotropin receptors in human thymus. J Clin Invest 1996;98:2228-34.

183. Davies TF, Teng CS, McLachlan SM, Smith BR, Hall R. Thyrotropin receptors in adipose tissue, retro-orbital tissue and lymphocytes. Mol Cellular Endocrinol 1978;9:303-10.

184. Klein JR. Physiological relevance of thyroid stimulating hormone and thyroid stimulating hormone receptor in tissues other than the thyroid. Autoimmunity 2003;36:417-21.

185. Stadlmayr W, Spitzweg C, Bichlmair AM, Heufelder AE. TSH receptor transcripts and TSH receptor-like immunoreactivity in orbital and pretibial fibroblasts of patients with Graves' ophthalmopathy and pretibial myxedema. Thyroid 1997;7:3-12.

186. Daumerie C, Ludgate M, Costagliola S, Many MC. Evidence for thyrotropin receptor immunoreactivity in pretibial connective tissue from patients with thyroid-associated dermopathy. Eur J Endocrinol 2002;146:35-8.

187. Tsui S, Naik V, Hoa N, et al. Evidence for an association between thyroid-stimulating hormone and insulin-like growth factor 1 receptors: a tale of two antigens implicated in Graves' disease. J Immunol 2008;181:4397-405.

188. Valyasevi RW, Erickson DZ, Harteneck DA, et al. Differentiation of human orbital preadipocyte fibroblasts induces expression of functional thyrotropin receptor. J Clin Endocrinol Metab 1999;84:2557-62.

189. Bahn RS, Dutton CM, Joba W, Heufelder AE. Thyrotropin receptor expression in cultured Graves' orbital preadipocyte fibroblasts is stimulated by thyrotropin. Thyroid 1998;8:193-6.

190. Bahn RS, Dutton CM, Natt N, Joba W, Spitzweg C, Heufelder AE. Thyrotropin receptor expression in Graves' orbital adipose/connective tissues: potential autoantigen in Graves' ophthalmopathy. J Clin Endocrinol Metab 1998;83:998-1002.

191. Bahn RS. Thyrotropin receptor expression in orbital adipose/connective tissues from patients with thyroid-associated ophthalmopathy. Thyroid 2002;12:193-5.

192. Feliciello A, Porcellini A, Ciullo I, Bonavolonta G, Avvedimento EV, Fenzi G. Expression of thyrotropin-receptor mRNA in healthy and Graves' disease retro-orbital tissue. Lancet 1993;342:337-8.

193. Wakelkamp IM, Bakker O, Baldeschi L, Wiersinga WM, Prummel MF. TSH-R expression and cytokine profile in orbital tissue of active vs. inactive Graves' ophthalmopathy patients. Clin Endocrinol 2003;58:280-7.

194. Heufelder AE, Dutton CM, Sarkar G, Donovan KA, Bahn RS. Detection of TSH receptor RNA in cultured fibroblasts from patients with Graves' ophthalmopathy and pretibial dermopathy. Thyroid 1993;3:297-300.

195. Crisp MS, Lane C, Halliwell M, Wynford-Thomas D, Ludgate M. Thyrotropin receptor transcripts in human adipose tissue. J Clin Endocrinol Metab 1997;82:2003-5.

196. Bahn RS, Dutton CM, Joba W, Heufelder AE. Thyrotropin receptor expression in cultured Graves' orbital preadipocyte fibroblasts is stimulated by thyrotropin. Thyroid 1998;8:193-6.

197. Starkey KJ, Janezic A, Jones G, Jordan N, Baker G, Ludgate M. Adipose thyrotrophin receptor expression is elevated in Graves' and thyroid eye diseases ex vivo and indicates adipogenesis in progress in vivo. J Mol Endocrinol 2003;30:369-80.

198. Bahn RS, Dutton CM, Natt N, Joba W, Spitzweg C, Heufelder AE. Thyrotropin receptor expression in Graves' orbital adipose/connective tissues: potential autoantigen in Graves' ophthalmopathy. J Clin Endocrinol Metab 1998;83:998-1002.

199. Wakelkamp IM, Bakker O, Baldeschi L, Wiersinga WM, Prummel MF. TSH-R expression and cytokine profile in orbital tissue of active vs. inactive Graves' ophthalmopathy patients. Clin Endocrinol 2003;58:280-7.

200. Agretti P, De Marco G, De Servi M, et al. Evidence for protein and mRNA TSHr expression in fibroblasts from patients with thyroid-associated ophthalmopathy (TAO) after adipocytic differentiation. Eur J Endocrinol 2005;152:777-84.

201. van Zeijl CJ, Fliers E, van Koppen CJ, et al. Thyrotropin receptor-stimulating Graves' disease immunoglobulins induce hyaluronan synthesis by differentiated orbital fibroblasts from patients with Graves' ophthalmopathy not only via cyclic adenosine monophosphate signaling pathways. Thyroid 2011;21:169-76.

202. Wakelkamp IM, Gerding MN, Van Der Meer JW, Prummel MF, Wiersinga WM. Both Th1- and Th2-derived cytokines in serum are elevated in Graves' ophthalmopathy. Clin Exp Immunol 2000;121:453-7.

203. Hiromatsu Y, Yang D, Bednarczuk T, Miyake I, Nonaka K, Inoue Y. Cytokine profiles in eye muscle tissue and orbital fat tissue from patients with thyroid-associated ophthalmopathy. J Clin Endocrinol Metab 2000;85:1194-9.

204. Sempowski GD, Rozenblit J, Smith TJ, Phipps RP. Human orbital fibroblasts are activated through CD40 to induce proinflammatory cytokine production. Am J Physiol 1998;274:C707-14.

205. Cao HJ, Wang HS, Zhang Y, Lin HY, Phipps RP, Smith TJ. Activation of human orbital fibroblasts through CD40 engagement results in a dramatic induction of hyaluronan synthesis and prostaglandin endoperoxide H synthase-2 expression. Insights into potential pathogenic mechanisms of thyroid-associated ophthalmopathy. J Biol Chem 1998;273:29615-25.

206. Raychaudhuri N, Douglas RS, Smith TJ. PGE2 induces IL-6 in orbital fibroblasts through EP2 receptors and increased gene promoter activity: implications to thyroid-associated ophthalmopathy. PLoS One 2010;5:e15296.

207. Mitsiades CS, Mitsiades NS, McMullan CJ, et al. Inhibition of the insulin-like growth factor receptor-1 tyrosine kinase activity as a therapeutic strategy for multiple myeloma, other hematologic malignancies, and solid tumors. Cancer Cell 2004;5:221-30.

208. Yin KC, Chen D, Bakhtiar R, Verch T. Evaluation of two ELISA methods to detect therapeutic anti-IGF1R antibodies in clinical study samples of dalotuzumab. Bioanalysis 2011;3:2107-17.

209. Hoa N, Tsui S, Afifiyan NF, et al. Nuclear targeting of IGF-1 receptor in orbital fibroblasts from Graves' disease: apparent role of ADAM17. PLoS One 2012;7:e34173.

210. Delafontaine P, Song YH, Li Y. Expression, regulation, and function of IGF-1, IGF-1R, and IGF-1 binding proteins in blood vessels. Arterioscler Thromb Vasc Biol 2004;24:435-44.

211. Doern A, Cao X, Sereno A, et al. Characterization of inhibitory anti-insulin-like growth factor receptor antibodies with different epitope specificity and ligand-blocking properties: implications for mechanism of action in vivo. J Biol Chem 2009;284:10254-67.

212. Cohen BD, Baker DA, Soderstrom C, et al. Combination therapy enhances the inhibition of tumor growth with the fully human anti-type 1 insulin-like growth factor receptor monoclonal antibody CP-751,871. Clin Cancer Res 2005;11:2063-73.

213. Smith TJ. Insulin-like growth factor-I regulation of immune function: a potential therapeutic target in autoimmune diseases? Pharm Rev 2010;62:199-236.

214. Riedemann J, Macaulay VM. IGF1R signalling and its inhibition. Endocr-Relat Cancer 2006;13 Suppl 1:S33-43.

215. Dupont J, LeRoith D. Insulin and insulin-like growth factor I receptors: similarities and differences in signal transduction. Horm Res 2001;55 Suppl 2:22-6.

216. Douglas RS, Brix TH, Hwang CJ, Hegedus L, Smith TJ. Divergent frequencies of IGF-I receptor-expressing blood lymphocytes in monozygotic twin pairs discordant

for Graves' disease: evidence for a phenotypic signature ascribable to nongenetic factors. J Clin Endocrinol Metab 2009;94:1797-802.

217. Warshamana-Greene GS, Litz J, Buchdunger E, Garcia-Echeverria C, Hofmann F, Krystal GW. The insulin-like growth factor-I receptor kinase inhibitor, NVP-ADW742, sensitizes small cell lung cancer cell lines to the effects of chemotherapy. Clin Cancer Res 2005;11:1563-71.

218. Jones HE, Goddard L, Gee JM, et al. Insulin-like growth factor-I receptor signalling and acquired resistance to gefitinib (ZD1839; Iressa) in human breast and prostate cancer cells. Endocr Relat Cancer 2004;11:793-814.

219. Kurzrock R, Patnaik A, Aisner J, et al. A phase I study of weekly R1507, a human monoclonal antibody insulin-like growth factor-I receptor antagonist, in patients with advanced solid tumors. Clin Cancer Res 2010;16:2458-65.

220. Reidy DL, Vakiani E, Fakih MG, et al. Randomized, phase II study of the insulin-like growth factor-1 receptor inhibitor IMC-A12, with or without cetuximab, in patients with cetuximab- or panitumumab-refractory metastatic colorectal cancer. J Clin Oncol 2010;28:4240-6.

221. Tolcher AW, Sarantopoulos J, Patnaik A, et al. Phase I, pharmacokinetic, and pharmacodynamic study of AMG 479, a fully human monoclonal antibody to insulin-like growth factor receptor 1. J Clin Oncol 2009;27:5800-7.

222. Scartozzi M, Bianconi M, Maccaroni E, Giampieri R, Berardi R, Cascinu S. Dalotuzumab, a recombinant humanized mAb targeted against IGFR1 for the treatment of cancer. Curr Opin Mol Ther 2010;12:361-71.

223. Kooijman R, Scholtens LE, Rijkers GT, Zegers BJ. Type I insulin-like growth factor receptor expression in different developmental stages of human thymocytes. J Endocrinol 1995;147:203-9.

224. Kooijman R, Coppens A, Hooghe-Peters E. IGF-I stimulates IL-8 production in the promyelocytic cell line HL-60 through activation of extracellular signal-regulated protein kinase. Cell Signal 2003;15:1091-8.

225. Kooijman R, Coppens A. Insulin-like growth factor-I stimulates IL-10 production in human T cells. J Leuk Biol 2004;76:862-7.

226. Kimata H, Fujimoto M. Growth hormone and insulin-like growth factor I induce immunoglobulin (Ig)E and IgG4 production by human B cells. J Exp Med 1994;180:727-32.

227. Robbins K, McCabe S, Scheiner T, Strasser J, Clark R, Jardieu P. Immunological effects of insulin-like growth factor-I--enhancement of immunoglobulin synthesis. Clin Exp Immunol 1994;95:337-42.

228. Baxter RC, Twigg SM. Actions of IGF binding proteins and related proteins in adipose tissue. Trends Endocrin Met 2009;20:499-505.

229. Clemmons DR. The relative roles of growth hormone and IGF-1 in controlling insulin sensitivity. J Clin Invest 2004;113:25-7.

230. Brugts MP, Ranke MB, Hofland LJ, et al. Normal values of circulating insulin-like growth factor-I bioactivity in the healthy population: comparison with five widely used IGF-I immunoassays. J Clin Endocrinol Metab 2008;93:2539-45.

231. Brugts MP, van den Beld AW, Hofland LJ, et al. Low circulating insulin-like growth factor I bioactivity in elderly men is associated with increased mortality. J Clin Endocrinol Metab 2008;93:2515-22.

232. Minich WB, Dehina N, Welsink T, et al. Autoantibodies to the IGF1 receptor in Graves' orbitopathy. J Clin Endocrinol Metab 2013;98:752-60.

233. Firth SM, Baxter RC. Cellular actions of the insulin-like growth factor binding proteins. Endocrin Rev 2002;23:824-54.

234. Siddle K. The insulin receptor and type I IGF receptor: comparison of structure and function. Prog Growth Factor Res 1992;4:301-20.

235. Ni F, Sun R, Fu B, et al. IGF-1 promotes the development and cytotoxic activity of human NK cells. Nature Comm 2013;4:1479.

236. Johnson EW, Jones LA, Kozak RW. Expression and function of insulin-like growth factor receptors on anti-CD3-activated human T lymphocytes. J Immunol 1992;148:63-71.

237. Kooijman R, Willems M, De Haas CJ, et al. Expression of type I insulin-like growth factor receptors on human peripheral blood mononuclear cells. Endocrinol 1992;131:2244-50.

238. Pritchard J, Han R, Horst N, Cruikshank WW, Smith TJ. Immunoglobulin activation of T cell chemoattractant expression in fibroblasts from patients with Graves' disease is mediated through the insulin-like growth factor I receptor pathway. J Immunol 2003;170:6348-54.

239. Pritchard J, Horst N, Cruikshank W, Smith TJ. Igs from patients with Graves' disease induce the expression of T cell chemoattractants in their fibroblasts. J Immunol 2002;168:942-50.

240. Douglas RS, Gianoukakis AG, Kamat S, Smith TJ. Aberrant expression of the insulin-like growth factor-1 receptor by T cells from patients with Graves' disease may carry functional consequences for disease pathogenesis. J Immunol 2007;178:3281-7.

241. Furstenberger G, Senn HJ. Insulin-like growth factors and cancer. Lancet Oncol 2002;3:298-302.

242. Pollak MN, Perdue JF, Margolese RG, Baer K, Richard M. Presence of somatomedin receptors on primary human breast and colon carcinomas. Cancer Lett 1987;38:223-30.

243. Burtscher I, Christofori G. The IGF/IGF-1 receptor signaling pathway as a potential target for cancer therapy. Drug Resist Updates 1999;2:3-8.

244. Khandwala HM, McCutcheon IE, Flyvbjerg A, Friend KE. The effects of insulin-like growth factors on tumorigenesis and neoplastic growth. Endocrin Rev 2000;21:215-44.

245. Morrione A, DeAngelis T, Baserga R. Failure of the bovine papillomavirus to transform mouse embryo fibroblasts with a targeted disruption of the insulin-like growth factor I receptor genes. J Virol 1995;69:5300-3.

246. Stattin P, Bylund A, Rinaldi S, et al. Plasma insulin-like growth factor-I, insulin-like growth factor-binding proteins, and prostate cancer risk: a prospective study. J Natl Cancer I 2000;92:1910-7.

247. Sandhu MS, Dunger DB, Giovannucci EL. Insulin, insulin-like growth factor-I (IGF-I), IGF binding proteins, their biologic interactions, and colorectal cancer. J Natl Cancer I 2002;94:972-80.

248. Hankinson SE, Willett WC, Colditz GA, et al. Circulating concentrations of insulin-like growth factor-I and risk of breast cancer. Lancet 1998;351:1393-6.

249. Chan JM, Stampfer MJ, Giovannucci E, et al. Plasma insulin-like growth factor-I and prostate cancer risk: a prospective study. Science 1998;279:563-6.

250. Ma J, Pollak MN, Giovannucci E, et al. Prospective study of colorectal cancer risk in men and plasma levels of insulin-like growth factor (IGF)-I and IGF-binding protein-3. J Natl Cancer I 1999;91:620-5.

251. Wu X, Yu H, Amos CI, Hong WK, Spitz MR. Joint effect of insulin-like growth factors and mutagen sensitivity in lung cancer risk. J Natl Cancer I 2000;92:737-43.

252. Ferte C, Loriot Y, Clemenson C, et al. IGF-1R targeting increases the antitumor effects of DNA-damaging agents in SCLC model: an opportunity to increase the efficacy of standard therapy. Mol Cancer Ther 2013;12:1213-22.

253. Huang HJ, Angelo LS, Rodon J, et al. R1507, an anti-insulin-like growth factor-1 receptor (IGF-1R) antibody, and EWS/FLI-1 siRNA in Ewing's sarcoma: convergence at the IGF/IGFR/Akt axis. PLoS One 2011;6:e26060.

254. Tramontano D, Cushing GW, Moses AC, Ingbar SH. Insulin-like growth factor-I stimulates the growth of rat thyroid cells in culture and synergizes the stimulation of DNA synthesis induced by TSH and Graves'-IgG. Endocrinol 1986;119:940-2.

255. Clement S, Refetoff S, Robaye B, Dumont JE, Schurmans S. Low TSH requirement and goiter in transgenic mice overexpressing IGF-I and IGF-Ir receptor in the thyroid gland. Endocrinol 2001;142:5131-9.

256. van der Veeken J, Oliveira S, Schiffelers RM, Storm G, van Bergen En Henegouwen PM, Roovers RC. Crosstalk between epidermal growth factor receptor-

and insulin-like growth factor-1 receptor signaling: implications for cancer therapy. Curr Cancer Drug Tar 2009;9:748-60.

257. Kumar S, Nadeem S, Stan MN, Coenen M, Bahn RS. A stimulatory TSH receptor antibody enhances adipogenesis via phosphoinositide 3-kinase activation in orbital preadipocytes from patients with Graves' ophthalmopathy. J Mol Endocrinol 2011;46:155-63.

258. Kumar S, Iyer S, Bauer H, Coenen M, Bahn RS. A stimulatory thyrotropin receptor antibody enhances hyaluronic acid synthesis in graves' orbital fibroblasts: inhibition by an IGF-I receptor blocking antibody. J Clin Endocrinol Metab 2012;97:1681-7.

259. van Zeijl CJ, Fliers E, van Koppen CJ, et al. Effects of thyrotropin and thyrotropin-receptor-stimulating Graves' disease immunoglobulin G on cyclic adenosine monophosphate and hyaluronan production in nondifferentiated orbital fibroblasts of Graves' ophthalmopathy patients. Thyroid 2010;20:535-44.

260. Hansson HA, Petruson B, Skottner A. Somatomedin C in pathogenesis of malignant exophthalmos of endocrine origin. Lancet 1986;1:218-9.

261. Weightman DR, Perros P, Sherif IH, Kendall-Taylor P. Autoantibodies to IGF-1 binding sites in thyroid associated ophthalmopathy. Autoimmunity 1993;16:251-7.

262. Segretin ME, Galeano A, Roldan A, Schillaci R. Insulin-like growth factor-1 receptor regulation in activated human T lymphocytes. Horm Res 2003;59:276-80.

263. Dardalhon V, Korn T, Kuchroo VK, Anderson AC. Role of Th1 and Th17 cells in organ-specific autoimmunity. J Autoimmun 2008;31:252-6.

264. Germain RN. T-cell development and the CD4-CD8 lineage decision. Nat Rev Immunol 2002;2:309-22.

265. Mosmann TR, Coffman RL. TH1 and TH2 cells: different patterns of lymphokine secretion lead to different functional properties. Annu Rev Immunol 1989;7:145-73.

266. O'Shea JJ, Paul WE. Mechanisms underlying lineage commitment and plasticity of helper CD4+ T cells. Science 2010;327:1098-102.

267. Zhu J, Paul WE. Heterogeneity and plasticity of T helper cells. Cell Res 2010;20:4-12.

268. Moseley TA, Haudenschild DR, Rose L, Reddi AH. Interleukin-17 family and IL-17 receptors. Cytokine Growth F R 2003;14:155-74.

269. Cua DJ, Tato CM. Innate IL-17-producing cells: the sentinels of the immune system. Nat Rev Immunol 2010;10:479-89.

270. Corthay A. How do regulatory T cells work? Scand J Immunol 2009;70:326-36.

271. Vignali DA, Collison LW, Workman CJ. How regulatory T cells work. Nat Rev Immunol 2008;8:523-32.

272. Tchilian EZ, Beverley PC. CD45 in memory and disease. Arch Immunol Ther Exp (Warsz) 2002;50:85-93.

273. Sallusto F, Lenig D, Forster R, Lipp M, Lanzavecchia A. Two subsets of memory T lymphocytes with distinct homing potentials and effector functions. Nature 1999;401:708-12.

274. Faint JM, Annels NE, Curnow SJ, et al. Memory T cells constitute a subset of the human CD8+CD45RA+ pool with distinct phenotypic and migratory characteristics. J Immunol 2001;167:212-20.

275. Moss P, Khan N. CD8(+) T-cell immunity to cytomegalovirus. Hum Immunol 2004;65:456-64.

276. Wiken M, Grunewald J, Eklund A, Wahlstrom J. Multiparameter phenotyping of T-cell subsets in distinct subgroups of patients with pulmonary sarcoidosis. J Int Med 2012;271:90-103.

277. Vaidya B, Shenton BK, Stamp S, et al. Analysis of peripheral blood T-cell subsets in active thyroid-associated ophthalmopathy: absence of effect of octreotide-LAR on T-cell subsets in patients with thyroid-associated ophthalmopathy. Thyroid 2005;15:1073-8.

278. Ludgate ME, McGregor AM, Weetman AP, et al. Analysis of T cell subsets in Graves' disease: alterations associated with carbimazole. Br Med J 1984;288:526-30.

279. Ohashi H, Okugawa T, Itoh M. Circulating activated T cell subsets in autoimmune thyroid diseases: differences between untreated and treated patients. Acta Endocrinol 1991;125:502-9.

280. Tyutyunikov A, Raikow RB, Kennerdell JS, Kazim M, Dalbow MH, Scalise D. Re-examination of peripheral blood T cell subsets in dysthyroid orbitopathy. Invest Ophthalmol Vis Sci 1992;33:2299-303.

281. Aniszewski JP, Valyasevi RW, Bahn RS. Relationship between disease duration and predominant orbital T cell subset in Graves' ophthalmopathy. J Clin Endocrinol Metab 2000;85:776-80.

282. Otto EA, Ochs K, Hansen C, Wall JR, Kahaly GJ. Orbital tissue-derived T lymphocytes from patients with Graves' ophthalmopathy recognize autologous orbital antigens. J Clin Endocrinol Metab 1996;81:3045-50.

283. de Carli M, D'Elios MM, Mariotti S, et al. Cytolytic T cells with Th1-like cytokine profile predominate in retroorbital lymphocytic infiltrates of Graves' ophthalmopathy. J Clin Endocrinol Metab 1993;77:1120-4.

284. Yang D, Hiromatsu Y, Hoshino T, Inoue Y, Itoh K, Nonaka K. Dominant infiltration of T(H)1-type CD4+ T cells at the retrobulbar space of patients with thyroid-associated ophthalmopathy. Thyroid 1999;9:305-10.

285. Heufelder AE, Bahn RS. Detection and localization of cytokine immunoreactivity in retro-ocular connective tissue in Graves' ophthalmopathy. Eur J Clin Invest 1993;23:10-7.

286. Grubeck-Loebenstein B, Trieb K, Sztankay A, Holter W, Anderl H, Wick G. Retrobulbar T cells from patients with Graves' ophthalmopathy are CD8+ and specifically recognize autologous fibroblasts. J Clin Invest 1994;93:2738-43.

287. Natt N, Bahn RS. Cytokines in the evolution of Graves' ophthalmopathy. Autoimmunity 1997;26:129-36.

288. McLachlan SM, Prummel MF, Rapoport B. Cell-mediated or humoral immunity in Graves' ophthalmopathy? Profiles of T-cell cytokines amplified by polymerase chain reaction from orbital tissue. J Clin Endocrinol Metab 1994;78:1070-4.

289. Nunery WR, Martin RT, Heinz GW, Gavin TJ. The association of cigarette smoking with clinical subtypes of ophthalmic Graves' disease. Ophthal Plast Reconstr Surg 1993;9:77-82.

290. Boschi A, Daumerie C, Spiritus M, et al. Quantification of cells expressing the thyrotropin receptor in extraocular muscles in thyroid associated orbitopathy. Br J Ophthalmol 2005;89:724-9.

291. Hwang CJ, Afifiyan N, Sand D, et al. Orbital fibroblasts from patients with thyroid-associated ophthalmopathy overexpress CD40: CD154 hyperinduces IL-6, IL-8, and MCP-1. Invest Ophthalmol Vis Sci 2009;50:2262-8.

292. Koumas L, Smith TJ, Phipps RP. Fibroblast subsets in the human orbit: Thy-1+ and Thy-1- subpopulations exhibit distinct phenotypes. Eur J Immunol 2002;32:477-85.

293. Han R, Tsui S, Smith TJ. Up-regulation of prostaglandin E2 synthesis by interleukin-1beta in human orbital fibroblasts involves coordinate induction of prostaglandin-endoperoxide H synthase-2 and glutathione-dependent prostaglandin E2 synthase expression. J Biol Chem 2002;277:16355-64.

294. Korducki JM, Loftus SJ, Bahn RS. Stimulation of glycosaminoglycan production in cultured human retroocular fibroblasts. Invest Ophthalmol Vis Sci 1992;33:2037-42.

295. Smith TJ, Bahn RS, Gorman CA, Cheavens M. Stimulation of glycosaminoglycan accumulation by interferon gamma in cultured human retroocular fibroblasts. J Clin Endocrinol Metab 1991;72:1169-71.

296. Imai Y, Odajima R, Inoue Y, Shishiba Y. Effect of growth factors on hyaluronan and proteoglycan synthesis by retroocular tissue fibroblasts of Graves' ophthalmopathy in culture. Acta Endocrinol 1992;126:541-52.

297. Zhang L, Bowen T, Grennan-Jones F, et al. Thyrotropin receptor activation increases hyaluronan production in preadipocyte fibroblasts: contributory role in hyaluronan accumulation in thyroid dysfunction. J Biol Chem 2009;284:26447-55.

298. Kaback LA, Smith TJ. Expression of hyaluronan synthase messenger ribonucleic acids and their induction by interleukin-1beta in human orbital fibroblasts: potential insight into the molecular pathogenesis of thyroid-associated ophthalmopathy. J Clin Endocrinol Metab 1999;84:4079-84.

299. Betz M, Fox BS. Prostaglandin E2 inhibits production of Th1 lymphokines but not of Th2 lymphokines. J Immunol 1991;146:108-13.

300. Smith TJ, Koumas L, Gagnon A, et al. Orbital fibroblast heterogeneity may determine the clinical presentation of thyroid-associated ophthalmopathy. J Clin Endocrinol Metab 2002;87:385-92.

301. Gianoukakis AG, Douglas RS, King CS, Cruikshank WW, Smith TJ. Immunoglobulin G from patients with Graves' disease induces interleukin-16 and RANTES expression in cultured human thyrocytes: a putative mechanism for T-cell infiltration of the thyroid in autoimmune disease. Endocrinol 2006;147:1941-9.

302. Jyonouchi SC, Valyasevi RW, Harteneck DA, Dutton CM, Bahn RS. Interleukin-6 stimulates thyrotropin receptor expression in human orbital preadipocyte fibroblasts from patients with Graves' ophthalmopathy. Thyroid 2001;11:929-34.

303. Valyasevi RW, Jyonouchi SC, Dutton CM, Munsakul N, Bahn RS. Effect of tumor necrosis factor-alpha, interferon-gamma, and transforming growth factor-beta on adipogenesis and expression of thyrotropin receptor in human orbital preadipocyte fibroblasts. J Clin Endocrinol Metab 2001;86:903-8.

304. Feldon SE, Park DJ, O'Loughlin CW, et al. Autologous T-lymphocytes stimulate proliferation of orbital fibroblasts derived from patients with Graves' ophthalmopathy. Invest Ophthalmol Vis Sci 2005;46:3913-21.

305. Feldon SE, O'Loughlin C W, Ray DM, Landskroner-Eiger S, Seweryniak KE, Phipps RP. Activated human T lymphocytes express cyclooxygenase-2 and produce proadipogenic prostaglandins that drive human orbital fibroblast differentiation to adipocytes. Am J Pathol 2006;169:1183-93.

306. Koumas L, Smith TJ, Feldon S, Blumberg N, Phipps RP. Thy-1 expression in human fibroblast subsets defines myofibroblastic or lipofibroblastic phenotypes. Am J Pathol 2003;163:1291-300.

307. Dorkhan M, Lantz M, Frid A, Groop L, Hallengren B. Treatment with a thiazolidinedione increases eye protrusion in a subgroup of patients with type 2 diabetes. Clin Endocrinol 2006;65:35-9.

308. Lee S, Tsirbas A, Goldberg RA, McCann JD. Thiazolidinedione induced thyroid associated orbitopathy. BMC Ophthalmol 2007;7:8.

309. Starkey K, Heufelder A, Baker G, et al. Peroxisome proliferator-activated receptor-gamma in thyroid eye disease: contraindication for thiazolidinedione use? J Clin Endocrinol Metab 2003;88:55-9.

310. Crisp M, Starkey KJ, Lane C, Ham J, Ludgate M. Adipogenesis in thyroid eye disease. Invest Ophthalmol Vis Sci 2000;41:3249-55.

311. Turcu AF, Kumar S, Neumann S, et al. A small molecule antagonist inhibits thyrotropin receptor antibody-induced orbital fibroblast functions involved in the pathogenesis of Graves ophthalmopathy. J Clin Endocrinol Metab 2013;98:2153-9.

312. Zhang L, Grennan-Jones F, Lane C, Rees DA, Dayan CM, Ludgate M. Adipose tissue depot-specific differences in the regulation of hyaluronan production of relevance to Graves' orbitopathy. J Clin Endocrinol Metab 2012;97:653-62.

313. Herzog EL, Bucala R. Fibrocytes in health and disease. Exp Hematol 2010;38:548-56.

314. Gillespie EF, Papageorgiou KI, Fernando R, et al. Increased expression of TSH receptor by fibrocytes in thyroid-associated ophthalmopathy leads to chemokine production. J Clin Endocrinol Metab 2012;97:E740-6.

315. Abe R, Donnelly SC, Peng T, Bucala R, Metz CN. Peripheral blood fibrocytes: differentiation pathway and migration to wound sites. J Immunol 2001;166:7556-62.

316. Phillips RJ, Burdick MD, Hong K, et al. Circulating fibrocytes traffic to the lungs in response to CXCL12 and mediate fibrosis. J Clin Invest 2004;114:438-46.

317. Hartlapp I, Abe R, Saeed RW, et al. Fibrocytes induce an angiogenic phenotype in cultured endothelial cells and promote angiogenesis in vivo. FASEB J 2001;15:2215-24.

318. Yang L, Scott PG, Giuffre J, Shankowsky HA, Ghahary A, Tredget EE. Peripheral blood fibrocytes from burn patients: identification and quantification of fibrocytes in adherent cells cultured from peripheral blood mononuclear cells. Lab Invest 2002;82:1183-92.

319. Chesney J, Bucala R. Peripheral blood fibrocytes: mesenchymal precursor cells and the pathogenesis of fibrosis. Curr Rheum Report 2000;2:501-5.

320. Chesney J, Bacher M, Bender A, Bucala R. The peripheral blood fibrocyte is a potent antigen-presenting cell capable of priming naive T cells in situ. P Natl Acad Sci USA 1997;94:6307-12.

321. Quan TE, Cowper S, Wu SP, Bockenstedt LK, Bucala R. Circulating fibrocytes: collagen-secreting cells of the peripheral blood. Int J Biochem Cell Biol 2004;36:598-606.

322. Hong KM, Belperio JA, Keane MP, Burdick MD, Strieter RM. Differentiation of human circulating fibrocytes as mediated by transforming growth factor-beta and peroxisome proliferator-activated receptor gamma. J Biol Chem 2007;282:22910-20.

323. Gomperts BN, Strieter RM. Fibrocytes in lung disease. J Leuk Biol 2007;82:449-56.

324. Moeller A, Gilpin SE, Ask K, et al. Circulating fibrocytes are an indicator of poor prognosis in idiopathic pulmonary fibrosis. Am J Resp Crit Care 2009;179:588-94.

325. Scholten D, Reichart D, Paik YH, et al. Migration of fibrocytes in fibrogenic liver injury. Am J Pathol 2011;179:189-98.

326. Sakai N, Wada T, Matsushima K, et al. The renin-angiotensin system contributes to renal fibrosis through regulation of fibrocytes. J Hypertens 2008;26:780-90.

327. Galligan CL, Siminovitch KA, Keystone EC, Bykerk V, Perez OD, Fish EN. Fibrocyte activation in rheumatoid arthritis. Rheumatology 2010;49:640-51.

328. Fernando R, Atkins S, Raychaudhuri N, et al. Human fibrocytes coexpress thyroglobulin and thyrotropin receptor. P Natl Acad Sci USA 2012;109:7427-32.

329. Li B, Smith TJ. Regulation of IL-1 receptor antagonist by TSH in fibrocytes and orbital fibroblasts. J Clin Endocrinol Metab 2014;99:E625-33.

330. Cao HJ, Han R, Smith TJ. Robust induction of PGHS-2 by IL-1 in orbital fibroblasts results from low levels of IL-1 receptor antagonist expression. Am J Physiol Cell Physiol 2003;284:C1429-37.

331. Tsai LJ, Lan JL, Lin CY, Hsiao SH, Tsai LM, Tsai JJ. The different expression patterns of interleukin-1 receptor antagonist in systemic lupus erythematosus. Tissue Antigens 2006;68:493-501.

332. Li B, Smith TJ. Divergent expression of IL-1 receptor antagonists in CD34(+) fibrocytes and orbital fibroblasts in thyroid-associated ophthalmopathy: contribution of fibrocytes to orbital inflammation. J Clin Endocrinol Metab 2013;98:2783-90.

333. Gabay C, Arend WP. Treatment of rheumatoid arthritis with IL-1 inhibitors. Springer Sem Immun 1998;20:229-46.

334. Chen H, Mester T, Raychaudhuri N, et al. Teprotumumab, an IGF-1R Blocking Monoclonal Antibody Inhibits TSH and IGF-1 Action in Fibrocytes. J Clin Endocrinol Metab 2014;99:1635-40.

335. Tsui S, Naik V, Hoa N, et al. Evidence for an association between thyroid-stimulating hormone and insulin-like growth factor 1 receptors: a tale of two antigens implicated in Graves' disease. J Immunol 2008;181:4397-405.

336. Fernando R, Vonberg A, Atkins SJ, Pietropaolo S, Pietropaolo M, Smith TJ. Human fibrocytes express multiple antigens associated with autoimmune endocrine diseases. J Clin Endocrinol Metab 2014;99:E796-803.

337. Many MC, Costagliola S, Detrait M, Denef F, Vassart G, Ludgate MC. Development of an animal model of autoimmune thyroid eye disease. J Immunol 1999;162:4966-74.

338. Baker G, Mazziotti G, von Ruhland C, Ludgate M. Reevaluating thyrotropin receptor-induced mouse models of graves' disease and ophthalmopathy. Endocrinol 2005;146:835-44.

339. Johnson KT, Wiesweg B, Schott M, et al. Examination of orbital tissues in murine models of Graves' disease reveals expression of UCP-1 and the TSHR in retrobulbar adipose tissues. Horm Metab Res 2013;45:401-7.

340. Costagliola S, Many MC, Stalmans-Falys M, Tonacchera M, Vassart G, Ludgate M. Recombinant thyrotropin receptor and the induction of autoimmune thyroid disease in BALB/c mice: a new animal model. Endocrinol 1994;135:2150-9.

341. Costagliola S, Alcalde L, Tonacchera M, Ruf J, Vassart G, Ludgate M. Induction of thyrotropin receptor (TSH-R) autoantibodies and thyroiditis in mice immunised with the recombinant TSH-R. Biochem Biophys Res Commun 1994;199:1027-34.

342. Costagliola S, Many MC, Stalmans-Falys M, Vassart G, Ludgate M. Transfer of thyroiditis, with syngeneic spleen cells sensitized with the human thyrotropin receptor, to naive BALB/c and NOD mice. Endocrinol 1996;137:4637-43.

343. Zhao SX, Tsui S, Cheung A, Douglas RS, Smith TJ, Banga JP. Orbital fibrosis in a mouse model of Graves' disease induced by genetic immunization of thyrotropin receptor cDNA. J Endocrinol 2011;210:369-77.

344. Coles AJ, Wing M, Smith S, et al. Pulsed monoclonal antibody treatment and autoimmune thyroid disease in multiple sclerosis. Lancet 1999;354:1691-5.

345. Jones JL, Phuah CL, Cox AL, et al. IL-21 drives secondary autoimmunity in patients with multiple sclerosis, following therapeutic lymphocyte depletion with alemtuzumab (Campath-1H). J Clin Invest 2009;119:2052-61.

346. Weetman A. Immune reconstitution syndrome and the thyroid. Best Pract Res Clin Endocrinol Metab 2009;23:693-702.

347. Spolski R, Leonard WJ. IL-21 and T follicular helper cells. Int Immunol 2010;22:7-12.

348. Boelaert K, Torlinska B, Holder RL, Franklyn JA. Older subjects with hyperthyroidism present with a paucity of symptoms and signs: a large cross-sectional study. J Clin Endocrinol Metab 2010;95:2715-26.

349. Toms TE, Panoulas VF, Smith JP, et al. Rheumatoid arthritis susceptibility genes associate with lipid levels in patients with rheumatoid arthritis. Ann Rheum Dis 2011;70:1025-32.

350. McCoy AN, Kim DS, Gillespie E, Atkins S, Smith TJ, Douglas RS. Rituximab (Rituxan(R)) therapy for severe thyroid associated ophthalmopathy diminishes IGF-1R T cells. J Clin Endocrinol Metab 2014:jc20133207.

351. Smith TJ, Hoa N. Immunoglobulins from patients with Graves' disease induce hyaluronan synthesis in their orbital fibroblasts through the self-antigen, insulin-like growth factor-I receptor. J Clin Endocrinol Metab 2004;89:5076-80.

352. Chen JW, Ledet T, Orskov H, et al. A highly sensitive and specific assay for determination of IGF-I bioactivity in human serum. Am J Physiol-Endoc M 2003;284:E1149-55.

353. Varewijck AJ, Boelen A, Lamberts SW, et al. Circulating IgGs may modulate IGF-I receptor stimulating activity in a subset of patients with Graves' ophthalmopathy. J Clin Endocrinol Metab 2013;98:769-76.

354. Smith BR, Bolton J, Young S, et al. A new assay for thyrotropin receptor autoantibodies. Thyroid 2004;14:830-5.

355. Apiwattanakul M, Asawavichienjinda T, Pulkes T, et al. Diagnostic utility of NMO/AQP4-IgG in evaluating CNS inflammatory disease in Thai patients. J Neurol Sci 2012;320:118-20.

356. Krassas GE, Pontikides N, Kaltsas T, et al. Free and total insulin-like growth factor (IGF)-I, -II, and IGF binding protein-1, -2, and -3 serum levels in patients with active thyroid eye disease. J Clin Endocrinol Metab 2003;88:132-5.

357. Smith TJ. Is IGF-I receptor a target for autoantibody generation in Graves' disease? J Clin Endocrinol Metab 2013;98:515-8.

358. Lemmey A, Maddison P, Breslin A, et al. Association between insulin-like growth factor status and physical activity levels in rheumatoid arthritis. J Rheumatol 2001;28:29-34.

359. Toussirot E, Nguyen NU, Dumoulin G, Aubin F, Cedoz JP, Wendling D. Relationship between growth hormone-IGF-I-IGFBP-3 axis and serum leptin levels with bone mass and body composition in patients with rheumatoid arthritis. Rheumatol 2005;44:120-5.

360. Doi T, Kanatsu K, Mayumi M, Hamashima Y, Yoshida H. Analysis of IgG immune complexes in sera from patients with membranous nephropathy: role of IgG4 subclass and low-avidity antibodies. Nephron 1991;57:131-6.

361. van Es JH, Gmelig Meyling FH, van de Akker WR, Aanstoot H, Derksen RH, Logtenberg T. Somatic mutations in the variable regions of a human IgG anti-double-stranded DNA autoantibody suggest a role for antigen in the induction of systemic lupus erythematosus. J Exp Med 1991;173:461-70.

362. Carapancea M, Cosaceanu D, Budiu R, et al. Dual targeting of IGF-1R and PDGFR inhibits proliferation in high-grade gliomas cells and induces radiosensitivity in JNK-1 expressing cells. J Neuro-Oncology 2007;85:245-54.

363. Adams TE, McKern NM, Ward CW. Signalling by the type 1 insulin-like growth factor receptor: interplay with the epidermal growth factor receptor. Growth Factors 2004;22:89-95.

364. Clemmons DR, Sleevi M, Allan G, Sommer A. Effects of combined recombinant insulin-like growth factor (IGF)-I and IGF binding protein-3 in type 2 diabetic patients on glycemic control and distribution of IGF-I and IGF-II among serum binding protein complexes. J Clin Endocrinol Metab 2007;92:2652-8.

365. Casellas A, Salavert A, Agudo J, et al. Expression of IGF-I in pancreatic islets prevents lymphocytic infiltration and protects mice from type 1 diabetes. Diabetes 2006;55:3246-55.

366. Neidhart M, Fehr K, Pataki F, Michel BA. The levels of memory (CD45RA-, RO+) CD4+ and CD8+ peripheral blood T-lymphocytes correlate with IgM rheumatoid factors in rheumatoid arthritis. Rheum Int 1996;15:201-9.

367. Duarte-Rey C, Bogdanos DP, Leung PS, Anaya JM, Gershwin ME. IgM predominance in autoimmune disease: genetics and gender. Autoimmun Rev 2012;11:A404-12.

368. Jang SY, Shin DY, Lee EJ, Lee SY, Yoon JS. Relevance of TSH-receptor antibody levels in predicting disease course in Graves' orbitopathy: comparison of the third-generation TBII assay and Mc4-TSI bioassay. Eye 2013;27:964-71.

369. Jang SY, Shin DY, Lee EJ, Choi YJ, Lee SY, Yoon JS. Correlation between TSH receptor antibody assays and clinical manifestations of Graves' orbitopathy. Yonsei Med J 2013;54:1033-9.

370. Jang SY, Shin DY, Lee EJ, Yoon JS. Clinical characteristics of Graves' orbitopathy in patients showing discrepancy between levels from TBII assays and TSI bioassay. Clin Endocrinol 2014;80:591-7.

371. Laurberg TB, Ellingsen T, Thorsen J, et al. Insulin-like growth factor I receptor density on CD4+T-lymphocytes from active early steroid- and DMARD-naive rheumatoid arthritis patients is up-regulated and not influenced by 1 year of clinically effective treatment. Rheum Int 2012;32:501-4.

372. Pritchard J, Tsui S, Horst N, Cruikshank WW, Smith TJ. Synovial fibroblasts from patients with rheumatoid arthritis, like fibroblasts from Graves' disease, express high levels of IL-16 when treated with Igs against insulin-like growth factor-1 receptor. J Immunol 2004;173:3564-9.

373. Förster G, Otto E, Hansen C, Ochs K, Kahaly G. Analysis of orbital T cells in thyroid-associated ophthalmopathy. Clin Exp Immunol 1998;112:427-34.

374. Fekete A, Soos L, Szekanecz Z, et al. Disturbances in B- and T-cell homeostasis in rheumatoid arthritis: suggested relationships with antigen-driven immune responses. J Autoimmunity 2007;29:154-63.

375. Sommershof A, Aichinger H, Engler H, et al. Substantial reduction of naive and regulatory T cells following traumatic stress. Brain Behav Immun 2009;23:1117-24.

376. Monti P, Heninger AK, Bonifacio E. Differentiation, expansion, and homeostasis of autoreactive T cells in type 1 diabetes mellitus. Curr Diabetes Rep 2009;9:113-8.

377. Maldonado A, Mueller YM, Thomas P, Bojczuk P, O'Connors C, Katsikis PD. Decreased effector memory CD45RA+ CD62L- CD8+ T cells and increased central memory CD45RA- CD62L+ CD8+ T cells in peripheral blood of rheumatoid arthritis patients. Arthritis Res Ther 2003;5:91-6.

378. Sallusto F, Geginat J, Lanzavecchia A. Central memory and effector memory T cell subsets: function, generation, and maintenance. Ann Rev Immunol 2004;22:745-63.

379. Felberg NT, Sergott RC, Savino PJ, Blizzard JJ, Schatz NJ, Amsel J. Lymphocyte subpopulations in Graves' ophthalmopathy. Arch Ophthalmol 1985;103:656-9.

380. Rodien P, Madec AM, Ruf J, et al. Antibody-dependent cell-mediated cytotoxicity in autoimmune thyroid disease: relationship to antithyroperoxidase antibodies. J Clin Endocrinol Metab 1996;81:2595-600.

381. Bossowski A, Urban M, Stasiak-Barmuta A. Analysis of changes in the percentage of B (CD19) and T (CD3) lymphocytes, subsets CD4, CD8 and their memory (CD45RO), and naive (CD45RA) T cells in children with immune and non-immune thyroid diseases. J Pediatr Endocrinol Metab 2003;16:63-70.

382. Pawlowski P, Mysliwiec J, Stasiak-Barmuta A, Bakunowicz-Lazarczyk A, Gorska M. Increased percentage of L-selectin+ and ICAM-1+ peripheral blood CD4+/CD8+ T cells in active Graves' ophthalmopathy. Folia Histochem Cyto 2009;47:29-33.

383. Sun Z, Zhong W, Lu X, et al. Association of Graves' disease and prevalence of circulating IFN-gamma-producing CD28(-) T cells. J Clin Immunol 2008;28:464-72.

384. Xia N, Zhou S, Liang Y, et al. CD4+ T cells and the Th1/Th2 imbalance are implicated in the pathogenesis of Graves' ophthalmopathy. Int J Mol Med 2006;17:911-6.

385. Matteucci E, Ghimenti M, Di Beo S, Giampietro O. Altered proportions of naive, central memory and terminally differentiated central memory subsets among CD4+ and CD8 + T cells expressing CD26 in patients with type 1 diabetes. J Clin Immunol 2011;31:977-84.

386. Malaguarnera R, Frasca F, Garozzo A, et al. Insulin receptor isoforms and insulin-like growth factor receptor in human follicular cell precursors from papillary thyroid cancer and normal thyroid. J Clin Endocrinol Metab 2011;96:766-74.

387. Champagne P, Ogg GS, King AS, et al. Skewed maturation of memory HIV-specific CD8 T lymphocytes. Nature 2001;410:106-11.

388. Champagne P, Dumont AR, Sekaly RP. Learning to remember: generation and maintenance of T-cell memory. DNA Cell Biol 2001;20:745-60.

389. Kahaly GJ, Shimony O, Gellman YN, et al. Regulatory T-cells in Graves' orbitopathy: baseline findings and immunomodulation by anti-T lymphocyte globulin. J Clin Endocrinol Metab 2011;96:422-9.

390. Goronzy JJ, Weyand CM. T cell homeostasis and autoreactivity in rheumatoid arthritis. Curr Dir Autoimmunity 2001;3:112-32.

391. Hug A, Korporal M, Schroder I, et al. Thymic export function and T cell homeostasis in patients with relapsing remitting multiple sclerosis. J Immunol 2003;171:432-7.

392. Duszczyszyn DA, Beck JD, Antel J, et al. Altered naive CD4 and CD8 T cell homeostasis in patients with relapsing-remitting multiple sclerosis: thymic versus peripheral (non-thymic) mechanisms. Clin Exp Immunol 2006;143:305-13.

393. Mikulkova Z, Praksova P, Stourac P, Bednarik J, Michalek J. Imbalance in T-cell and cytokine profiles in patients with relapsing-remitting multiple sclerosis. J Neurol Sci 2011;300:135-41.

394. Leon MP, Spickett G, Jones DE, Bassendine MF. CD4+ T cell subsets defined by isoforms of CD45 in primary biliary cirrhosis. Clin Exp Immunol 1995;99:233-9.

395. Hedman M, Faresjo M, Axelsson S, Ludvigsson J, Casas R. Impaired CD4 and CD8 T cell phenotype and reduced chemokine secretion in recent-onset type 1 diabetic children. Clin Exp Immunol 2008;153:360-8.

396. Morimoto C, Hafler DA, Weiner HL, et al. Selective loss of the suppressor-inducer T-cell subset in progressive multiple sclerosis. Analysis with anti-2H4 monoclonal antibody. N Engl J Med 1987;316:67-72.

397. Morimoto C, Steinberg AD, Letvin NL, et al. A defect of immunoregulatory T cell subsets in systemic lupus erythematosus patients demonstrated with anti-2H4 antibody. J Clin Invest 1987;79:762-8.

398. Reiff A, Weinberg KI, Triche T, et al. T lymphocyte abnormalities in juvenile systemic sclerosis patients. Clin Immunol 2013;149:146-55.

399. Fritsch RD, Shen X, Illei GG, et al. Abnormal differentiation of memory T cells in systemic lupus erythematosus. Arthritis Rheum 2006;54:2184-97.

400. Neidhart M, Pataki F, Schonbachler J, Bruhlmann P. Flow cytometric characterisation of the "false naive" (CD45RA+, CD45RO-, CD29 bright+) peripheral blood T-lymphocytes in health and in rheumatoid arthritis. Rheum Int 1996;16:77-87.

401. Hofer J, Hofer S, Zlamy M, et al. Elevated proportions of recent thymic emigrants in children and adolescents with type 1 diabetes. Rejuv Res 2009;12:311-20.

402. Saule P, Trauet J, Dutriez V, Lekeux V, Dessaint JP, Labalette M. Accumulation of memory T cells from childhood to old age: central and effector memory cells in CD4(+) versus effector memory and terminally differentiated memory cells in CD8(+) compartment. Mech Age Develop 2006;127:274-81.

403. Utsuyama M, Hirokawa K, Kurashima C, et al. Differential age-change in the numbers of CD4+CD45RA+ and CD4+CD29+ T cell subsets in human peripheral blood. Mech Age Develop 1992;63:57-68.

404. Linton PJ, Dorshkind K. Age-related changes in lymphocyte development and function. Nat Immunol 2004;5:133-9.

405. Grubeck-Loebenstein B, Wick G. The aging of the immune system. Adv Immunol 2002;80:243-84.

406. Bandres E, Merino J, Vazquez B, et al. The increase of IFN-gamma production through aging correlates with the expanded CD8(+high)CD28(-)CD57(+) subpopulation. Clin Immunol 2000;96:230-5.

407. Hong MS, Dan JM, Choi JY, Kang I. Age-associated changes in the frequency of naive, memory and effector CD8+ T cells. Mech Age Develop 2004;125:615-8.

408. Schluns KS, Lefrancois L. Cytokine control of memory T-cell development and survival. Nat Rev Immunol 2003;3:269-79.

409. Lakatos P, Foldes J, Nagy Z, et al. Serum insulin-like growth factor-I, insulin-like growth factor binding proteins, and bone mineral content in hyperthyroidism. Thyroid 2000;10:417-23.

410. Stuart CA, Meehan RT, Neale LS, Cintron NM, Furlanetto RW. Insulin-like growth factor-I binds selectively to human peripheral blood monocytes and B-lymphocytes. J Clin Endocrinol Metab 1991;72:1117-22.

411. Reiss K, Porcu P, Sell C, Pietrzkowski Z, Baserga R. The insulin-like growth factor 1 receptor is required for the proliferation of hemopoietic cells. Oncogene 1992;7:2243-8.

412. Kooijman R, Willems M, Rijkers GT, et al. Effects of insulin-like growth factors and growth hormone on the in vitro proliferation of T lymphocytes. J Neuroimmunol 1992;38:95-104.

413. Heemskerk VH, Daemen MA, Buurman WA. Insulin-like growth factor-1 (IGF-1) and growth hormone (GH) in immunity and inflammation. Cytokine Growth F R 1999;10:5-14.

414. El Yafi F, Winkler R, Delvenne P, Boussif N, Belaiche J, Louis E. Altered expression of type I insulin-like growth factor receptor in Crohn's disease. Clin Exp Immunol 2005;139:526-33.

415. Sarup JC, Johnson RM, King KL, et al. Characterization of an anti-p185HER2 monoclonal antibody that stimulates receptor function and inhibits tumor cell growth. Growth Reg 1991;1:72-82.

416. Burtrum D, Zhu Z, Lu D, et al. A fully human monoclonal antibody to the insulin-like growth factor I receptor blocks ligand-dependent signaling and inhibits human tumor growth in vivo. Cancer Res 2003;63:8912-21.

417. Maloney EK, McLaughlin JL, Dagdigian NE, et al. An anti-insulin-like growth factor I receptor antibody that is a potent inhibitor of cancer cell proliferation. Cancer Res 2003;63:5073-83.

418. Reddy M, Eirikis E, Davis C, Davis HM, Prabhakar U. Comparative analysis of lymphocyte activation marker expression and cytokine secretion profile in stimulated human peripheral blood mononuclear cell cultures: an in vitro model to monitor cellular immune function. J Immunol Methods 2004;293:127-42.

419. Testi R, Phillips JH, Lanier LL. T cell activation via Leu-23 (CD69). J Immunol 1989;143:1123-8.

420. Laffon A, Garcia-Vicuna R, Humbria A, et al. Upregulated expression and function of VLA-4 fibronectin receptors on human activated T cells in rheumatoid arthritis. J Clin Invest 1991;88:546-52.

421. Gessl A, Waldhausl W. Increased CD69 and human leukocyte antigen-DR expression on T lymphocytes in insulin-dependent diabetes mellitus of long standing. J Clin Endocrinol Metab 1998;83:2204-9.

422. Watanabe M, Yamamoto N, Matsuzuka F, Miyauchi A, Iwatani Y. Decrease of CD154 intensity on peripheral CD4+ T cells in autoimmune thyroid disease. Clin Exp Immunol 2004;136:555-8.

423. Abbas AK, Lohr J, Knoechel B. Balancing autoaggressive and protective T cell responses. J Autoimmunity 2007;28:59-61.

424. Hiromatsu Y, Kaku H, Miyake I, Murayama S, Soejima E. Role of cytokines in the pathogenesis of thyroid-associated ophthalmopathy. Thyroid 2002;12:217-21.

425. Dalla Libera D, Di Mitri D, Bergami A, et al. T regulatory cells are markers of disease activity in multiple sclerosis patients. PLoS One 2011;6:e21386.

426. Idali F, Wahlstrom J, Muller-Suur C, Eklund A, Grunewald J. Analysis of regulatory T cell associated forkhead box P3 expression in the lungs of patients with sarcoidosis. Clin Exp Immunol 2008;152:127-37.

427. Huan J, Culbertson N, Spencer L, et al. Decreased FOXP3 levels in multiple sclerosis patients. J Neuro Res 2005;81:45-52.

428. Putheti P, Pettersson A, Soderstrom M, Link H, Huang YM. Circulating CD4+CD25+ T regulatory cells are not altered in multiple sclerosis and unaffected by disease-modulating drugs. J Clin Immunol 2004;24:155-61.

429. Venken K, Hellings N, Hensen K, et al. Secondary progressive in contrast to relapsing-remitting multiple sclerosis patients show a normal CD4+CD25+ regulatory T-cell function and FOXP3 expression. J Neuro Res 2006;83:1432-46.

430. Pan D, Shin YH, Gopalakrishnan G, Hennessey J, De Groot LJ. Regulatory T cells in Graves' disease. Clin Endocrinol 2009;71:587-93.

431. Wang H, Zhao S, Tang X, Li J, Zou P. Changes of regulatory T cells in Graves' disease. Journal of Huazhong University of Science and Technology Medical Sciences 2006;26:545-7.

432. Simpson N, Gatenby PA, Wilson A, et al. Expansion of circulating T cells resembling follicular helper T cells is a fixed phenotype that identifies a subset of severe systemic lupus erythematosus. Arthritis Rheum 2010;62:234-44.

433. Zhu C, Ma J, Liu Y, et al. Increased frequency of follicular helper T cells in patients with autoimmune thyroid disease. J Clin Endocrinol Metab 2012;97:943-50.

434. Morita R, Schmitt N, Bentebibel SE, et al. Human blood CXCR5(+)CD4(+) T cells are counterparts of T follicular cells and contain specific subsets that differentially support antibody secretion. Immunity 2011;34:108-21.

435. Jia HY, Zhang ZG, Gu XJ, et al. Association between interleukin 21 and Graves' disease. Genetic Mol Res 2011;10:3338-46.

436. Biomarkers and surrogate endpoints: preferred definitions and conceptual framework. Clin Pharm Ther 2001;69:89-95.

437. Vaidya B, Imrie H, Perros P, et al. The cytotoxic T lymphocyte antigen-4 is a major Graves' disease locus. Hum Mol Genet 1999;8:1195-9.

438. Fitzpatrick M, Young SP. Metabolomics - a novel window into inflammatory disease. Swiss Med Wkly 2013;143:w13743.

439. Tsai CC, Wu SB, Cheng CY, et al. Increased response to oxidative stress challenge in Graves' ophthalmopathy orbital fibroblasts. Mol Vis 2011;17:2782-8.

440. Wolak JE, Esther CR, Jr., O'Connell TM. Metabolomic analysis of bronchoalveolar lavage fluid from cystic fibrosis patients. Biomarkers 2009;14:55-60.

441. Brindle JT, Antti H, Holmes E, et al. Rapid and noninvasive diagnosis of the presence and severity of coronary heart disease using 1H-NMR-based metabonomics. Nat Med 2002;8:1439-44.

442. Marchesi JR, Holmes E, Khan F, et al. Rapid and noninvasive metabonomic characterization of inflammatory bowel disease. J Proteome Res 2007;6:546-51.

443. Lauridsen MB, Bliddal H, Christensen R, et al. 1H NMR spectroscopy-based interventional metabolic phenotyping: a cohort study of rheumatoid arthritis patients. J Proteome Res 2010;9:4545-53.

444. Griffin JL, Kauppinen RA. A metabolomics perspective of human brain tumours. FEBS J 2007;274:1132-9.

445. Kind T, Tolstikov V, Fiehn O, Weiss RH. A comprehensive urinary metabolomic approach for identifying kidney cancerr. Anal Biochem 2007;363:185-95.

446. Sinclair AJ, Viant MR, Ball AK, et al. NMR-based metabolomic analysis of cerebrospinal fluid and serum in neurological diseases - a diagnostic tool? NMR Biomed 2010;23:123-32.

447. Hassan-Smith G, Wallace GR, Douglas MR, Sinclair AJ. The role of metabolomics in neurological disease. J Neuroimmunol 2012;248:48-52.

448. Young SP, Nessim M, Falciani F, et al. Metabolomic analysis of human vitreous humor differentiates ocular inflammatory disease. Mol Vis 2009;15:1210-7.

449. Barba I, Garcia-Ramirez M, Hernandez C, et al. Metabolic fingerprints of proliferative diabetic retinopathy: an 1H-NMR-based metabonomic approach using vitreous humor. Invest Ophthalmol Vis Sci 2010;51:4416-21.

450. Viant MR. Improved methods for the acquisition and interpretation of NMR metabolomic data. Biochem Bioph Res Co 2003;310:943-8.

451. Lindon JC, Holmes E, Nicholson JK. Metabonomics in pharmaceutical R&D. FEBS J 2007;274:1140-51.

452. Lenz EM, Bright J, Wilson ID, Morgan SR, Nash AF. A 1H NMR-based metabonomic study of urine and plasma samples obtained from healthy human subjects. J Pharmaceut Biomed 2003;33:1103-15.

453. Floegel A, Drogan D, Wang-Sattler R, et al. Reliability of serum metabolite concentrations over a 4-month period using a targeted metabolomic approach. PLoS One 2011;6:e21103.

454. Psychogios N, Hau DD, Peng J, et al. The human serum metabolome. PLoS One 2011;6:e16957.

455. Probert CS, Ahmed I, Khalid T, Johnson E, Smith S, Ratcliffe N. Volatile organic compounds as diagnostic biomarkers in gastrointestinal and liver diseases. J Gastrointest Liver 2009;18:337-43.

456. Denery JR, Nunes AA, Dickerson TJ. Characterization of differences between blood sample matrices in untargeted metabolomics. Analyt Chem 2011;83:1040-7.

457. Sutton CD, White SA, Edwards R, Lewis MH. A prospective controlled trial of the efficacy of isopropyl alcohol wipes before venesection in surgical patients. Ann Roy Coll Surg 1999;81:183-6.

458. Zhang J, Wei S, Liu L, et al. NMR-based metabolomics study of canine bladder cancer. Biochim Biophys Acta 2012;1822:1807-14.

459. Yildiz G, Demiryurek AT, Sahin-Erdemli I, Kanzik I. Comparison of antioxidant activities of aminoguanidine, methylguanidine and guanidine by luminol-enhanced chemiluminescence. Br J Pharmacol 1998;124:905-10.

460. Autore G, Marzocco S, Sorrentino R, Mirone VG, Baydoun A, Pinto A. In vitro and in vivo TNFalpha synthesis modulation by methylguanidine, an uremic catabolyte. Life Sci 1999;65:PL121-7.

461. Marzocco S, Di Paola R, Ribecco MT, et al. Effect of methylguanidine in a model of septic shock induced by LPS. Free Radical Res 2004;38:1143-53.

462. Komosinska-Vassev K, Olczyk K, Kucharz EJ, Marcisz C, Winsz-Szczotka K, Kotulska A. Free radical activity and antioxidant defense mechanisms in patients with hyperthyroidism due to Graves' disease during therapy. Clin Chim Acta 2000;300:107-17.

463. Bednarek J, Wysocki H, Sowinski J. Oxidation products and antioxidant markers in plasma of patients with Graves' disease and toxic multinodular goiter: effect of methimazole treatment. Free Radical Res 2004;38:659-64.

464. Lu R, Wang P, Wartofsky L, et al. Oxygen free radicals in interleukin-1beta-induced glycosaminoglycan production by retro-ocular fibroblasts from normal subjects and Graves' ophthalmopathy patients. Thyroid 1999;9:297-303.

465. Hondur A, Konuk O, Dincel AS, Bilgihan A, Unal M, Hasanreisoglu B. Oxidative stress and antioxidant activity in orbital fibroadipose tissue in Graves' ophthalmopathy. Curr Eye Res 2008;33:421-7.

466. Fu YK, Arkins S, Wang BS, Kelley KW. A novel role of growth hormone and insulin-like growth factor-I. Priming neutrophils for superoxide anion secretion. J Immunol 1991;146:1602-8.

467. Seven A, Tasan E, Inci F, Hatemi H, Burcak G. Biochemical evaluation of oxidative stress in propylthiouracil treated hyperthyroid patients. Effects of vitamin C supplementation. Clin Chem Lab Med 1998;36:767-70.

468. Rieck M, Arechiga A, Onengut-Gumuscu S, Greenbaum C, Concannon P, Buckner JH. Genetic variation in PTPN22 corresponds to altered function of T and B lymphocytes. J Immunol 2007;179:4704-10.

469. Hiromatsu Y, Eguchi H, Tani J, Kasaoka M, Teshima Y. Graves' ophthalmopathy: epidemiology and natural history. Int Med 2014;53:353-60.

470. Teng CS, Yeo PP. Ophthalmic Graves's disease: natural history and detailed thyroid function studies. BMJ 1977;1:273-5.

471. Sjogren K, Liu JL, Blad K, et al. Liver-derived insulin-like growth factor I (IGF-I) is the principal source of IGF-I in blood but is not required for postnatal body growth in mice. P Natl Acad Sci USA 1999;96:7088-92.

472. Ohlsson C, Sjogren K, Jansson JO, Isaksson OG. The relative importance of endocrine versus autocrine/paracrine insulin-like growth factor-I in the regulation of body growth. Ped Nephrol 2000;14:541-3.

473. Auernhammer CJ, Fottner C, Engelhardt D, Bidlingmaier M, Strasburger CJ, Weber MM. Differential regulation of insulin-like growth factor-(IGF) I and IGF-binding protein (IGFBP) secretion by human peripheral blood mononuclear cells. Horm Res 2002;57:15-21.

474. Wynes MW, Riches DW. Induction of macrophage insulin-like growth factor-I expression by the Th2 cytokines IL-4 and IL-13. J Immunol 2003;171:3550-9.

475. Kirstein M, Aston C, Hintz R, Vlassara H. Receptor-specific induction of insulin-like growth factor I in human monocytes by advanced glycosylation end product-modified proteins. J Clin Invest 1992;90:439-46.

476. Kochi Y, Suzuki A, Yamada R, Yamamoto K. Genetics of rheumatoid arthritis: underlying evidence of ethnic differences. J Autoimmunity 2009;32:158-62.

477. Nielen MM, van Schaardenburg D, Reesink HW, et al. Specific autoantibodies precede the symptoms of rheumatoid arthritis: a study of serial measurements in blood donors. Arthritis Rheum 2004;50:380-6.

478. Rantapaa-Dahlqvist S, de Jong BA, Berglin E, et al. Antibodies against cyclic citrullinated peptide and IgA rheumatoid factor predict the development of rheumatoid arthritis. Arthritis Rheum 2003;48:2741-9.

479. Kang YM, Zhang X, Wagner UG, et al. CD8 T cells are required for the formation of ectopic germinal centers in rheumatoid synovitis. J Exp Med 2002;195:1325-36.

480. Koetz K, Bryl E, Spickschen K, O'Fallon WM, Goronzy JJ, Weyand CM. T cell homeostasis in patients with rheumatoid arthritis. P Natl Acad Sci USA 2000;97:9203-8.

481. Ayoglu B, Haggmark A, Khademi M, et al. Autoantibody profiling in multiple sclerosis using arrays of human protein fragments. Mol Cell Proteomic 2013;12:2657-72.

482. Wright C, Sibani S, Trudgian D, et al. Detection of multiple autoantibodies in patients with ankylosing spondylitis using nucleic acid programmable protein arrays. Mol Cell Proteomic 2012;11:9 00384.

483. Papp K, Vegh P, Hobor R, et al. Immune complex signatures of patients with active and inactive SLE revealed by multiplex protein binding analysis on antigen microarrays. PLoS One 2012;7:e44824.

484. Adamski J, Suhre K. Metabolomics platforms for genome wide association studies--linking the genome to the metabolome. Curr Opin Biotech 2013;24:39-47.

485. Kapoor SR, Filer A, Fitzpatrick MA, et al. Metabolic profiling predicts response to anti-tumor necrosis factor alpha therapy in patients with rheumatoid arthritis. Arthritis Rheum 2013;65:1448-56.

486. Orphanidou-Vlachou E, Auer D, Brundler MA, et al. (1)H magnetic resonance spectroscopy in the diagnosis of paediatric low grade brain tumours. Eur J Radiol 2013;82:e295-301.

487. Wilson M, Cummins CL, Macpherson L, et al. Magnetic resonance spectroscopy metabolite profiles predict survival in paediatric brain tumours. Eur J Cancer 2013;49:457-64.

488. Tachibana S, Murakami T, Noguchi H, et al. Orbital magnetic resonance imaging combined with clinical activity score can improve the sensitivity of detection of disease activity and prediction of response to immunosuppressive therapy for Graves' ophthalmopathy. Endocrine J 2010;57:853-61.

489. Chang TC, Hsiao YL, Liao SL. Application of digital infrared thermal imaging in determining inflammatory state and follow-up effect of methylprednisolone pulse therapy in patients with Graves' ophthalmopathy. Graef Arch Clin Exp 2008;246:45-9.

490. Shih SR, Li HY, Hsiao YL, Chang TC. The application of temperature measurement of the eyes by digital infrared thermal imaging as a prognostic factor of methylprednisolone pulse therapy for Graves' ophthalmopathy. Acta Ophthalmol 2010;88:154-9.

491. Goldberg JI, Borgen PI. Breast cancer susceptibility testing: past, present and future. Expert Rev Anticanc 2006;6:1205-14.